

https://dspace.org/

Dietary iron overload. the generation of reactive oxygen species and hepatocarcinogenesis in experimental rats (Part 1)

Asare, G. A.

2003

https://hdl.handle.net/10539/24947

Downloaded from a DSpace repository. https://dspace.org/

DIETARY IRON OVERLOAD, THE GENERATION OF REACTIVE OXYGEN SPECIES AND HEPATOCARCINGENESIS IN EXPERIMENTAL RATS

MAJOR (RTD) GEORGE AWUKU ASARE

2003

DIETARY IRON OVERLOAD, THE GENERATION OF REACTIVE OXYGEN SPECIES AND HEPATOCARCINOGENESIS IN EXPERIMENTAL RAT MODELS

(PART 1)

Major (Rtd) George Awuku Asare

A thesis submitted to the Faculty of Health Sciences, University of the Witwatersrand

In fulfilment of the requirements for the degree of

Doctor of Philosophy

Johannesburg, 2003

DECLARATION

I, Major (Rtd) George Awuku Asare, declare that this thesis is my own work. It is being submitted, for the degree of Doctor of Philosophy, to the University of the Witwatersrand, Johannesburg. It has not been submitted before, for a degree or examination, to this or any other University.

Signed: 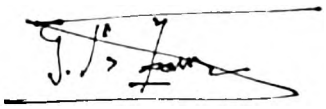 Date: 12/2003

Major (Rtd) George Awuku Asare Johannesburg

DEDICATION

This thesis is dedicated to my wife Betty

CONFERENCE PRESENTATION

1. Asare GA, Kew MC, Mossanda KSA, Siziba K (2003). A study of dietary iron overload in experimental rat models: generation of reactive oxygen species and immunohistochemical detection of DNA damage.

   Poster: 8. European meeting on liver carcinogenesis, Bad Kreuznach, Germany

ABSTRACT

Dietary iron (Fe) overload, originally referred to as Bantu Visceral Siderosis, is an Fe-loading condition that is still prevalent in rural populations of sub-Saharan Africa. The better known Fe loading disease, hereditary haemochromatosis (HH) is frequently complicated by hepatocellular carcinoma (HCC) and, in rare instances this occurs in the absence of cirrhosis. The latter, together with recent evidence that dietary Fe overload in the Black African carries an increased risk for HCC, suggests that excessive hepatic iron may itself be carcinogenic. The aim of the study was to determine if Fe alone could induce HCC in experimental rat models and, if so, to investigate possible mechanisms of hepatocarcinogenesis. 360 Wistar albino rats (*Rattus norvegicus*) were divided into 6 groups. The first group, the control animals, was designated C group. Groups 2 - 6 were Fe-fed alone or in combination with other chemicals: group 2 Fe alone (Fe group), group 3 (Fe + V) vitamins A & E supplementation [50 mg *all* trans-retinol (vitamin A) and 500 mg α-tocopherol (vitamin E) per kg diet], group 4 (Fe - V) received a diet totally devoid of vitamins A & E, group 5 (Fe + ASA) received 20 mg aspirin (ASA) per day, group 6 (Fe + Cu) received 300 mg/kg diet of copper sulphate (CuSO4) supplementation for 12 months followed by 3% copper hydroxide carbonate [$CuCO_3 \cdot Cu(OH)_2$]. Fe-fed rats were originally given 2% carbonyl iron (CI) up to 8 months. This was increased to 2.5% up to 12 months, followed by 0.5% ferrocene (dicyclopentadienyl iron) (*ad libitum*). The rats were monitored for 36 months and were sacrificed periodically and the blood and liver analysed. The following tests were performed: serum Fe, histological hepatic Fe grading, liver Fe concentration (LIC), Superoxide radical ($^{\bullet-}O_2$), Total Antioxidant Status (TAS), Glutathione peroxidase (GPx), Superoxide dismutase (SOD), Catalase (CAT), Vitamin C, Oxygen Radical Absorbance Capacity (ORAC), Malondialdehyde (MDA), FOX II assay for lipid hydroperoxides, 8-isoprostane (8-IP), 4-hydroxynonenal (4-HNE) immunohistochemistry, 8-hydroxy-2'-deoxyguanosine (8OHdG) immunohistochemistry, liver 8OHdG concentration (ELISA), Fluorimetric Analysis of DNA Unwinding (FADU), Ames mutagenicity test, Pulse Field Gel Electrophoresis (PFGE), AST, ALT,AFP and liver histology. Serum Fe reached a plateau after 16 months of Fe feeding. Serum Fe in the Fe-loading group was 2.5 times higher than the control group ($p<0.05$). At 12 months, hepatic Fe grading was 2+. When CI was substituted with ferrocene, Fe-loading was 4+ at

16 months. At 32 months LIC in the Fe groups was 19.8 ± 6.9 mg/g w.wt (33 times above the control group). Fe overload led to the generation of Reactive Oxygen Species (ROS). $^{\bullet-}O_2$ was 2-2.5 times higher in the Fe-fed groups than the control ($p>0.05$). Antioxidant levels (AO) were statistically significant but at different time-points. AO enzymes operated in a dynamic equilibrium and with a compensatory mechanism. The total lipid-soluble AO was 25% that of the total aqueous-soluble AO in the liver ($p<0.05$ at 12 months). The FOX II assay was found to be a better biomarker of lipid peroxidation (LPO) compared to MDA and 8-IP. LPO occurred as an early event of oxidative stress induced by Fe, and this was also detected immunohistochemically. Adducts of DNA oxidative damage i.e. 8OHdG were detected in the Fe-overloaded groups. Furthermore, liver 8OHdG concentration was significantly raised after 12 months ($p<0.05$). DNA strand-breaks were observed by PFGE in the early days of the study. In addition, DNA unwinding was observed and found to be significant between 12 and 20 months in the Fe-loaded groups ($p<0.05$). Mutagens were demonstrated in the liver in the Fe-loaded groups. The C group remained negative throughout with an average reversion frequency of 330 colonies. The Fe-loaded groups had twice this value between 20 and 24 months ($p<0.05$). Liver damage, assessed by AST and ALT levels, commenced after 16 months of Fe-overloading ($p<0.05$). 26% of Fe-overloaded livers examined histologically between 20 and 32 months had iron-free foci (IFF) that stained positive for GST-π. Histologically, neoplastic changes such as IFF were present in all the Fe-fed groups. Multiple IFF was detected in one liver from the Fe + V group. Inclusions resembling Mallory bodies were identified. Others, such as hamartomata, von Meyenburg complexes and Gandy-Gamma bodies, were observed. The presence of fat, focal fat and micro-steatosis was identified. In addition, hepatocellular adenoma was a borderline case in one liver from the Fe group. HCC was present in the liver of one rat in the Fe group. The tumour was 2 cm in diameter and arose in a liver without cirrhosis or fibrosis. AO vitamins and ASA were unable to prevent these histological events. Copper did not show any synergy histologically as a possible co-carcinogen. This study is the first to demonstrate the development of HCC in an animal model of haemochromatosis. Dietary Fe alone may be carcinogenic through a mechanism that involves the generation of reactive oxygen species, LPO, oxidative DNA damage, DNA strand breaks and unwinding, and mutagenesis.

ACKNOWLEDGEMENTS

This thesis would not have been carried out and completed without the invaluable guidance, encouragement and support of the Almighty God, my supervisors, colleagues and friends, whose contributions are gratefully acknowledged. In particular, I thank the following people:-

Professor MC Kew [Professor of Medicine and Director, Molecular Hepatology Research Unit (MHRU), Wits Medical School] my supervisor, Prof. KSA Mossanda (Department of Chemical Pathology, MEDUNSA) my co-supervisor, and Dr. A Kramvis (MHRU, Wits Medical School), for their expertise, critical appraisal and encouragement;

Professor AC Paterson (Head, Department of Anatomical Pathology, Wits Medical School), for the histological examination, consultations and editing of discussion on histological reports;

Dr. Ronnel Kahler (Department of Pharmacology and Therapeutics, MEDUNSA) for her assistance in chemiluminiscent studies;

Dr. K Siziba (Department of Biochemistry, University of the North), for teaching me immunohistochemistry;

Mr. Ronney (Histology technician, Department of Pathology, MEDUNSA), for his assistance in preparing histological slides for immunohistochemistry;

Mr. P Dawson (Director, Central Animal Services, Wits Medical School) and his team, for their technical support, care and maintenance of the animals;

Mr. N. Hartley (Department of Medicine, Wits Medical School) and his technical staff, for logistic support;

The Medical Research Council (MRC), The Cancer Association of South Africa (CANSA), The HE Griffin Cancer Research Trust and The Medical Faculty Research Endowment Fund, for funding this research;

My wife (Betty) and children for their forbearance during the years it has taken to complete this thesis.

TABLE OF CONTENTS

(PART 1)

		Page
DECLARATION		ii
DEDICATION		iii
PUBLICATIONS AND PRESENTATIONS		iv
ABSTRACT		v
ACKNOLDGEMENTS		vii
TABLE OF CONTENTS		ix
LIST OF FIGURES		xvii
LIST OF TABLES		xx

INTRODUCTION

1.0	**DIETARY IRON OVERLOAD AND HEPATOCELLULAR CARCINOMA**	1
1.1	Historical and Clinical Perspective	1
1.2	Putative Mechanisms of Iron-induced Carcinogenesis	5
2.0	**RESEARCH HYPOTHESIS**	7
2.1	AIMS AND OBJECTIVES	7
2.2	EXPERIMENTAL DESIGN	8
2.3	SUBJECTS AND DIET	9
2.3.1	Subjects	9
2.3.2	Diet	10
2.3.2.1	Carbonyl Iron (CI)	10
2.3.2.2	Ferrocene	11
2.4	METHODS	17

LITERATURE REVIEW

3.0	**TRACE ELEMENTS**	18
3.1	CHARACTERISTICS OF Fe AND Cu IN TRACE ELEMENT FUNCTION	18
3.1.1	Specificity	18
3.1.2	Homeostasis	19
3.1.3	Interactions	19
3.1.4	Amplification	20
3.2	FUNCTIONS AND METABOLISM OF IRON	20
3.2.1	Physiology	24
3.2.2	Iron Acquisition, Transport and Storage	25
3.2.3	Iron Overload	26

3.2.3.1 Iron overload in Experimental Animals 27
3.2.3.2 Iron Overload at the Ultrastructural Level 28
3.3 TRANSFERRIN 31
3.3.1 Molecular Properties 31
3.4 METAL-INDUCED HYPERTOXICITY 33
3.5 THE OXIDATIVE INJURY HYPOTHESIS 33
3.5.1 Oxyradicals Formation by Iron and Copper 33
3.5.2 Iron and Copper in Lipid Peroxidation and Oxidative Stress 34
3.6 SUBCELLULAR ORGANELLE DAMAGE 35
3.6.1 Lysosomal Injury Hypothesis 35
3.6.2 Mitochondria 36
3.6.3 Endoplasmic Reticulum 37
3.6.4 Plasma Membrane 38
3.6.5 Hepatic DNA Damage 39
3.6.6 Iron-Induced Hepatocellular Carcinogenesis 41
3.7 COPPER 43
3.7.1 BIOCHEMISTRY AND PHYSIOLOGY 43
3.7.1.1 Metabolism 43
3.7.1.2 Copper Homeostasis 45
3.7.1.3 Copper uptake and absorption 47
3.7.1.4 Post intestinal mucosal cell transport 47
3.7.1.5 Cu in Circulation 48
3.8 CLINICAL SIGNIFICANCE 49
3.8.1 Menkes' syndrome 50
3.8.2 Wilson disease 50

4.0 THE CHEMISTRY OF FREE RADICAL REACTIONS 51
4.0.1 The definition and reactions of Free Radicals 51
4.0.2 Radicals of molecular Oxygen: Physical and Chemical Properties 52
4.0.3 Reduction 52
4.0.4 Excitation 53
4.0.5 Reactions in which ROI's are formed 54
4.1 ROS INVOLVED IN IRON OVERLOAD 56
4.1.1 Superoxide radical 56
4.1.2 Hydrogen peroxide 57
4.1.3 Hydroxyl radical 58
4.1.4 Peroxyl radical 59
4.2 FREE RADICALS GIVE RISE TO FREE RADICALS – LPO 61
4.3 PATHOLOGICAL FREE RADICAL REACTIONS 65
4.4 FREE RADICAL DAMAGE 65
4.4.1 Damage to Enzymes and Proteins caused by Free Radicals 65
4.4.2 Damage to the cell Membrane and the Subcellular organelle 66
4.4.3 Fluorescent Molecular Damage and Lipofuscin Pigments 67
4.4.4 Free Radical Damage of Nucleic acids and their Components 67
4.4.5 Connection between LPO and tissue damage 67
4.5 FREE RADICAL REACTIONS AND MUTAGENESIS 68
4.6 FREE RADICAL REACTIONS AND CARCINOGENESIS 69

4.7	CELLULAR ENZYMATIC DEFENCE (AGAINST RADICALS OF MOLECULAR OXYGEN)	69
4.7.1	Antioxidant defence of the Intracellular Space	69
4.7.2	Antioxidant defence of the Extracellular Space	72
4.8	CONTROL OF FREE RADICAL REACTIONS	73
4.8.1	Control and Defence against Free Radical reactions in Biological Systems	73
4.8.2	Control by Membrane Structure	73
4.8.3	Control by Specific Molecular Structure	74
4.8.4	Control by Scavengers and Antioxidants	74
5.0	**VITAMINS**	76
5.0.1	Definition	76
5.1	VITAMIN A	76
5.1.1	Chemistry and Source	76
5.1.2	Requirement and Daily Allowance	77
5.1.3	Absorption, Transport and Metabolism	78
5.1.4	Functions	78
5.1.5	Deficiency	78
5.1.6	Excess	79
5.2	VITAMIN E	79
5.2.1	Chemistry and Source	79
5.2.2	Requirement and Allowance	80
5.2.3	Absorption, Transport and Metabolism	81
5.2.4	Functions	81
5.2.5	Deficiency and Excess	82
5.2.6	Vitamin E and Fibrogenesis	82
5.2.7	Vitamin E, Oxidative Stress and LPO	83
5.3	VITAMIN C	84
5.3.1	Chemistry and Source	84
5.3.2	Requirement and Allowance	84
5.3.3	Absorption, Transport and Metabolism	85
5.3.4	Iron and Vitamin C	85
5.3.5	Function	86
5.3.6	Deficiency and Excess	86
5.4	VITAMINS AND ANTIOXIDANTS	87
5.4.1	Water-soluble Radical Scavenging Antioxidants	88
5.4.2	Lipid-soluble Radical Scavenging Antioxidants	90
5.5	VITAMIN ANTIOXIDANTS IN CANCER PREVENTION	92
6.0	**SALICYLATES**	94
6.0.1	Distribution	94
6.0.2	Metabolism	95
6.0.3	Elimination	95
6.0.4	Excretion	95
6.0.5	Drug Interaction	96
6.0.6	Mechanism of Action	96

6.1 ASPIRIN ANTIOXIDANT ACTIVITY AND LPO 96
6.2 ASPIRIN AND LIVER PLASMA MEMBRANE 97
6.3 ASPIRIN AND LIVER 98
6.4 ASPIRIN AGAINST CANCER 98

7.0 BIOMARKERS OF OXIDATIVE STRESS 100
7.0.1 Introduction 100
7.1 BIOMARKERS OF LPO 100
7.1.1 Thiobarbituric acid-reactive substances (TBARs) 100
7.1.2 Breath Hydrocarbons 101
7.1.3 LDL Oxidation 101
7.1.4 F_2 Isoprostanes 102
7.1.5 Ferrous Oxidation of Xylenol orange (FOX) assay 103
7.1.6 Other Related Assays 103
7.2 BIOMARKERS OF DNA OXIDATION 103
7.2.1 8-hydroxydeoxyguanosine (8OHdG) 103
7.2.2 Antibodies to Oxidized DNA 105
7.2.3 Comet Assay 105
7.3 BIOMARKERS OF PROTEIN OXIDATION 106
7.3.1 Protein carbonyls 106

MATERIALS AND METHODS

8.0 MATERIALS AND METHODS 107
8.1 SERUM AND LIVER IRON (Fe) DETERMINATION 107
8.1.1 Principle 107
8.1.2 Reagents 107
8.1.3 Sample preparation for liver iron 107
8.1.4 Assay Procedure 108
8.1.5 Calculation 109
8.2 ASCORBIC ACID DETERMINATION 109
8.2.1 Introduction 109
8.2.2 Principle 109
8.2.3 Reagents and Preparation 109
8.2.4 Assay Procedure 112
8.2.5 Example of Spreadsheet and Calibration Curve 112
8.3 SUPEROXIDE DISMUTASE (SOD) DETERMINATION 113
8.3.1 Introduction 113
8.3.2 Principle 113
8.3.3 Reagents and Preparation 114
8.3.4 Assay Procedure 115
8.3.5 Calculation 116
8.3.6 Example of Spreadsheet and Calibration Curve 117
8.4 GLUTATHIONE PEROXIDASE (GPx) DETERMINATION 118
8.4.1 Principle 118
8.4.2 Reagents and Kit 118
8.4.3 Sample Preparation 119
8.4.4 Assay Procedure 119

8.4.5 Calculation 119
8.4.6 Example of Spreadsheet 120
8.5 CATALASE DETERMINATION 120
8.5.1 Introduction 120
8.5.2 Principle 121
8.5.3 Reagents and Preparation 122
8.5.4 Sample Preparation 122
8.5.5 Enzyme Stability 123
8.5.6 Assay Procedure 123
8.5.7 Calculation 123
8.5.8 Example of Spreadsheet 124
8.6 TOTAL ANTIOXIDANT STATUS (TAS) DETERMINATION 125
8.6.1 Principle 125
8.6.2 Reagents 125
8.6.3 Sample Preparation 125
8.6.4 Assay Procedure 126
8.6.5 Calculation 126
8.6.6 Example of Spreadsheet 126
8.7 OXYGEN RADICAL ABSORBANCE CAPACITY (ORAC) DETERMINATION 127
8.7.1 Introduction 127
8.7.2 Principle 127
8.7.3 Reagents and Preparation 127
8.7.4 Sample Preparation 128
8.7.5 Assay Procedure 129
8.7.6 Example of Spreadsheet 129
8.8 LIPID HYDROPEROXIDE (LOOH) DETERMINATION 130
8.8.1 Principle 130
8.8.2 Reagents and Preparation 131
8.8.3 Assay Procedure 132
8.8.4 Calculation 132
8.8.5 Example of Spreadsheet and Calibration Curve 133
8.9 MALONDIALDEHYDE (MDA) DETERMINATION 134
8.9.1 Introduction 134
8.9.2 Principle 134
8.9.3 Reagents and Preparation 135
8.9.4 Assay Procedure 135
8.9.5 Calculation 136
8.9.6 Example of Spreadsheet and Calibration Curve 136
8.10 8-ISOPROSTANE (8-IP) DETERMINATION 137
8.10.1 Introduction 137
8.10.2 Principle 137
8.10.3 Reagents 138
8.10.4 Assay Procedure 138
8.10.5 Example of Calibration Curve 139
8.11 DNA EXTRACTION 140
8.11.1 Principle 140

8.11.2 Reagents and Preparation 141
8.11.3 Assay Procedure 141
8.11.4 Verification of DNA 142
8.12 FLUORIMETRIC ANALYSIS OF DNA UNWINDING (FADU) 143
8.12.1 Introduction 143
8.12.2 Principle 143
8.12.3 Reagents and Preparation 144
8.12.4 Assay Procedure 145
8.12.5 Example of Spreadsheet 145
8.13 SUPEROXIDE RADICAL ($^{\bullet-}O_2$) DETERMINATION 146
8.13.1 Principle 146
8.13.2 Reagent Preparation 146
8.13.3 Assay Procedure 147
8.13.4 Example of Spreadsheet 148
8.14 PULSED FIELD GEL ELECTROPHORESIS (PFGE) 148
8.14.1 Introduction 148
8.14.2 Principle 148
8.14.3 Reagent preparation 150
8.14.4 Instrumentation 150
8.14.5 Assay Conditions 151
8.14.6 Assay Procedure 151
8.15 8-HYDROXYDEOXYGUANOSINE (8OHdG) DETERMINATION 151
8.15.1 Principle 151
8.15.2 Reagent Preparation 153
8.15.3 Assay Procedure 153
8.15.4 Example of Spreadsheet 155
8.16 AMES MUTAGENICITY TEST 156
8.16.1 Introduction 156
8.16.2 Principle 156
8.16.3 Bacteria Tester Strain 157
8.16.4 Reagents and Preparation 158
8.16.5 Characterization of TA97, TA98, TA100, TA102 162
8.16.5.1 Test for Histidine Requirement 162
8.16.5.2 Rfa (Permeability) Test 163
8.16.5.3 uvβ Mutation Test 164
8.16.5.4 R-factor Test 165
8.16.5.5 Spontaneous Reversion Test 170
8.16.5.6 Mutagenicity Test 171
8.17 DETECTION OF 8-HYDROXYDEOXYGUANOSINE (8OHdG) (IMMUNOHISTOCHEMICAL TECHNIQUES) 173
8.17.1 Introduction 173
8.17.2 Principle 173
8.17.3 Reagents 174
8.17.4 Assay Procedure 174
8.18 DETECTION OF 4-HYDROXY-2'-NONENAL (4-HNE) (IMMUNOHISTOCHEMICAL TECHNIQUES) 175
8.18.1 Introduction 175

8.18.2 Reagents and Equipment 176
8.18.3 Assay Procedure 177
8.19 LIVER IRON HISTOLOGY 177
8.20 ALPHA FETO PROTEIN (AFP) DETERMINATION 177
8.21 AST/ALT DETERMINATION 178
8.22 SERUM COPPER (Cu) DETERMINATION 178
8.22.1 Introduction 178
8.22.2 Principle 178
8.22.3 Assay Procedure 178
8.23 STATISTICAL ANALYSES 179

RESULTS

9.0 RESULTS 180
9.1 CORRELATION ANALYSIS OF GROUPS 192
9.2 CORRELATION ANALYSIS OF THE TEST PARAMETERS WITHIN GROUPS 192
9.3 ANALYSIS OF VARIANCE (ANOVA) 216
9.4 REGRESSION ANALYSIS 225
9.5 GRAPHS 226
9.6 IMMUNOHISTOCHEMISTRY PHOTOMICROGRAPHS 229
9.7 HISTOLOGY PHOTOMICROGRAPHS 239
9.8 PULSED FIELD GEL ELECTROPHORESIS 247

DISCUSSION AND CONCLUSION

10.0 DISCUSSION 248
10.1 AN ANIMAL MODEL FOR DIETARY IRON OVERLOAD 248
10.2 DIETARY IRON OVERLOAD AND HCC 252
10.3 DIETARY IRON OVERLOAD AND OXIDATIVE STRESS 261
10.4 DIETARY IRON OVERLOAD AND ANTIOXIDANTS 263
10.5 DIETARY IRON OVERLOAD AND BIOMARKERS OF LPO 274
10.6 DIETARY IRON OVERLOAD AND OXIDATIVE DNA DAMAGE 283
10.7 DIETARY IRON OVERLOAD AND MUTAGENESIS 290

11.0 CONCLUSION 296

ABBREVIATIONS 298

REFERENCES 301

(PART 2)

GRAPHS AND PHOTOMICROGRAPHS

GRAPHS	226
IMMUNOHISTOCHEMISTRY PHOTOMICROGRAPHS	229
HISTOLOGY PHOTOMICROGRAPHS	239

APPENDICES

A.	Correlation Analysis	Table 19x - 24x	*i - xii*
B.	ANOVA	Table 25x - 43x	*xiii - l*
C.	Regression Analysis	Table 44x	*li*
D.	Standard Deviation (SD)	Table 45x	*lii - lxvii*
E.	Histological Data	Table 46x	*lxviii - lxxiv*
F.	Raw Biochemical and Spotted Data	Table 1y – 8y	*lxxv - lxxxiii*
G.	Detailed Ames test results	Table z	*lxxxiv*
H.	Approval by Animal Ethics Screening Committee		*lxxxv*
I.	Drug Modification Approval by Animal Ethics Screening Committee		*lxxxvi*
J.	Certificate of Toxin-free diet by EPOL		*lxxxvii*
K.	Gelatine and Cu supplementation		*lxxxviii*
L.	Addendum (Decoding samples)		*xc*

LIST OF FIGURES

		Page
Figure 1	Growth curve of 3 types of commonly used experimental animals	9
Figure 2	Methods used for study	17
Figure 3	Pathway of iron metabolism	21
Figure 4	Changes in hepatic lysosomes after Fe or Cu overload	30
Figure 5	Mechanisms of hepatotoxicity induced by Fe or Cu overload	42
Figure 6	Phases of LPO	62
Figure 7	Free radical induced damage	64
Figure 8	Structure of Vitamin A	77
Figure 9	Structure of Vitamin E	80
Figure 10	Structure of Vitamin C	84
Figure 11	Molecular structure of aspirin	94
Figure 12	Structure of MDA	134
Figure 13	Metabolic Pathway of 8-IP	137
Figure 14	Structure of 8OHdG	152
Figure 15	Characterization of *Salmonella typhimurium* strains	166
Figure 16	Ames mutagenicity test	167
Figure 17	Summary of procedure for the Ames mutagenicity test	172
Figure 18	Interaction plot of Time and Group: serum iron levels	226
Figure 19	Interaction plot of Time and Group: superoxide radical generation	226
Figure 20	Interaction plot of Time and Group: GPx levels	226
Figure 21	Interaction plot of Time and Group: SOD levels	226

Figure 22	Interaction plot of Time and Group: Catalse levels	226
Figure 23	Interaction plot of Time and Group: Vitamin C levels	226
Figure 24	Interaction plot of Time and Group: TAS levels	227
Figure 25	Interaction plot of Time and Group: liver ORAC levels	227
Figure 26	Interaction plot of Time and Group: MDA levels	227
Figure 27	Interaction plot of Time and Group: liver 8-IP	227
Figure 28	Interaction plot of Time and Group: DNA Unwinding	227
Figure 29	Interaction plot of Time and Group: LPO FOX II assay	227
Figure 30	Interaction plot of Time and Group: Liver 8OHdG levels	228
Figure 31	Interaction plot of Time and Group: Ames mutagenicity test	228
Figure 32	Interaction plot of Time and Group: AST levels	228
Figure 33	Interaction plot of Time and Group: ALT levels	228
Figure 34	Interaction plot of Time and Group: Serum Cu levels	228
Figure 35	Liver 8OHdG immunohistochemistry of the Fe group	229
Figure 36	Liver 8OHdG immunohistochemistry of the Fe + V group	230
Figure 37	Liver 8OHdG immunohistochemistry of the Fe – V group	231
Figure 38	Liver 8OHdG immunohistochemistry of the Fe + ASA group	232
Figure 39	Liver 8OHdG immunohistochemistry of the Fe + Cu group	233
Figure 40	Liver 4-HNE immunohistochemistry of the Fe group	234
Figure 41	Liver 4-HNE immunohistochemistry of the Fe + V group	235
Figure 42	Liver 4-HNE immunohistochemistry of the Fe – V group	236
Figure 43	Liver 4-HNE immunohistochemistry of the Fe + ASA group	237
Figure 44	Liver 4-HNE immunohistochemistry of the Fe + Cu group	238
Figure 45	Histology of Hepatic Iron Overload	239

Figure 46	Iron-free focus in Iron Overloaded Liver	240
Figure 47	Iron-free focus at 28 months	241
Figure 48	GST-π stain, Positive for Iron-free foci	241
Figure 49	Mallory Bodies in Iron-free focus	242
Figure 50	Globules in Iron-free focus	243
Figure 51	HCC Wholemount	244
Figure 52	'Blocked' area of Figure 51	245
Figure 53	Pseudoglandular HCC (H&E stain)	246
Figure 54	Pseudoglandular HCC (Perls' Prussian blue stain)	246
Figure 55	Pulsed Field Gel Electrophoresis	247

LIST OF TABLES

			Page
Table 1	Effect of iron and copper overload *in vivo* on hepatic mitochondria		36
Table 2	Disease status or pathological conditions associated with copper		46
Table 3	Serum and Liver Iron Determination		108
Table 4	Vitamin C Determination		112
Table 5	SOD Determination		116
Table 6	GPx Determination		119
Table 7	Blood Catalase Determination		123
Table 8	Serum Total Antioxidant Status (TAS) Determination		126
Table 9	ORAC Determination		129
Table 10	Serum LPO Determination		132
Table 11	MDA Determination		135
Table 12	Determination of FADU		145
Table 13	Superoxide Radical Determination		147
Table 1x – 24x	Correlation analysis	(Appendix A)	*i - xii*
Table 25x – 43x	ANOVA	(Appendix B)	*xiii - l*
Table 44x	Regression analysis	(Appendix C)	*li*
Table 45x	Standard deviation (SD)	(Appendix D)	*lii - lxvii*
Table 46x	Histological data	(Appendix E)	*lxviii - lxxiv*
Table 1y – 8y	Raw Biochemical /Spotted data	(Appendix F)	*lxxv - lxxxiii*
Table z	Detailed Ames test results	(Appendix G)	*lxxxiv*

1.0 DIETARY IRON OVERLOAD AND HEPATOCELLULAR CARCINOMA

1.1 Historical and Clinical perspectives

Dietary iron overload was first described by Strachan in 1929 (Strachan, 1929). This iron loading condition occurs in parts of sub-Saharan Africa (where as many as 10% of the adult population may be affected) and was previously referred to as Bantu visceral siderosis. Following necropsy analysis of 876 Blacks from southern and central Africa, Strachan concluded that haemochromatosis (a disorder that interferes with iron metabolism and results in excess iron deposits throughout the body) was a common disease in Black Africans and that the major cause of the iron overload was the diet. Although these findings were greeted with scepticism, the high prevalence of this condition and its cause was later confirmed in a number of studies (Higginson *et al.*, 1953; Walker, 1953; Bothwell *et al.*, 1960, 1962, 1964; Buchanan 1966, 1967, 1969; MacPhail *et al.*, 1979a, 1979b; Gordeuk *et al.*, 1986; Friedman *et al.*, 1990; Gordeuk 1992b; Moyo *et al.*, 1998; Mandishona *et al.*, 1998).

Iron overload in southern African blacks was later thought to result from some metabolic defect caused by chronic malnutrition (Gillman and Gillman, 1951). However, very high dietary intake of iron was subsequently confirmed to be the reason, with most of the iron being derived from the iron drums and pots used in brewing traditional alcoholic beverages, which were consumed in large quantities by the blacks (Bothwell *et al.*, 1964). The bulk of the iron was deposited in the liver and the mononuclear-macrophage system (Bothwell *et al.*, 1965). Consequences of this iron deposition are micronodular cirrhosis, ascorbic acid deficiency, and osteoporosis (Bothwell *et al.*,1960). Recent evidence has

suggested the possibility that dietary iron overload may be caused by an interaction between the increased dietary iron and a gene distant from the HLA linked iron-loading locus responsible for the hereditary iron loading disease, hereditary haemochromatosis (HH). There is as yet no evidence to support this hypothesis, however (Gordeuk, 1992a).

A revision of the South African Liquor Laws in 1963 was followed by far reaching changes in the drinking habits of urban black South Africans that eventually led to a considerable decline in the prevalence and severity of iron overload in urban dwellers, and hence a lessening of interest in research into this condition (MacPhail *et al.*, 1979a). However, interest in dietary iron overload was revived when this disease was shown to be still prevalent in rural populations in sub-Saharan Africa (Gordeuk *et al.*, 1986).

The recognition that dietary iron overload is an important public health problem in sub-Saharan Africa raised the question of its possible association with other common diseases in Black Africans, including hepatocellular carcinoma (HCC). Although this malignancy occurs frequently throughout sub-Saharan Africa (Kew, 1992), no causal association between iron overload and HCC in Black Africans has previously been proved (Paterson *et al.*, 1985). However, an association between the two conditions was reported in a number of earlier publications (Kew, 1981; Gordeuk *et al.*, 1996; Moyo *et al.*, 1998). Furthermore, in 1998 Mandishona *et al.* reported a statistically significant association between dietary iron overload and HCC, giving a relative risk for developing HCC of 10.6 and a population attributable risk of 29%, and suggesting a significant role for this disorder in the aetiology and pathogenesis of HCC (Mandishona *et al.*, 1998).

HCC is regarded as one of the major malignant diseases in the word today. Among the reasons for this are its high incidence in several of the world's most populous regions, its grave prognosis, and the fact that a number of potentially preventable risk factors for the tumour have been identified. The peculiar geographical distribution of HCC, as well as time trends in its occurrence and the effects of migration on its incidence, implicated environmental carcinogens in the aetiology and pathogenesis of the tumour. Men are more likely than are women to develop HCC, and its prevalence generally increases with increasing age, except in black Africans where there is a shift towards younger age groups (Kew, 1994). Major risk factors for the tumour are persistent infection with hepatitis B or C viruses, repeated exposure to the mycotoxin, aflatoxin, and cirrhosis, whatever its cause. In addition, dietary iron overload is an important risk factor in sub-Saharan Africa. The risk posed by dietary iron overload should be seen in the context that most of the conventionally recognised toxic effects of alcohol on the liver are uncommon in Black Africans with dietary iron overload (the home brewed beer has an alcohol content of 3%) and with HCC (Friedman *et al.*, 1990). Friedman (1990) and others have, however, found portal fibrosis or cirrhosis in a higher proportion of subjects with hepatocellular iron grades 3+ or 4+ than in subjects with lower iron grades. This observation is consistent with the belief that iron overload is a cause or a co-factor in the development of portal fibrosis and cirrhosis in black Africans.

The best known of the iron loading diseases is hereditary haemochromatosis (HH). In patients with HH an inborn error of metabolism leads to the absorption of excessive quantities of iron from diets with normal iron content. The condition occurs predominantly

in populations of Northern European origin. The mutant gene mainly responsible for this condition is closely linked to the HLA-A locus on chromosome 6. A candidate gene originally called HLA-H, but now renamed *HFE*, encodes a 343 amino acid HMC class 1 protein, and 83% of subjects affected with HH are homozygous for two mutations in the gene, C282Y (substitution of tyrosine for cysteine at position 282) and H63D (the substitution of aspartate for histidine at position 63)(Feder *et al.*, 1996). The C282Y mutation is closely related to HH, with between 83% (Feder *et al.*, 1996) and 100% of clinically affected individuals being homozygous (C282Y/C282Y) for this mutation (Jazwinska *et al.*, 1996). However, the implication of the H63D mutation is less clear. A small number of patients with HH have been identified as either compound heterozygotes (C282Y/H63D) or as homozygotes for H63D (H63D/H63D). H63D heterozygotes have hepatic iron concentrations significantly higher than control subjects, but lower than C282Y homozygotes. Most importantly, there is no biochemical or histological evidence of liver disease, and there are no clinical manifestations in the H63D heterozygotes. The exact mechanisms by which mutations in the *HFE* gene lead to increased intestinal iron absorption in the face of an elevated body iron content are unknown. Recent studies have shown that *HFE* associates with the transferrin receptor (TfR) and may thus play some role in regulating the entry of iron into cells (Anderson, 2001). This capability is lost in C282Y mutant *HFE*. Powell (2002) has speculated that the ability of intestinal crypt cells to take up iron from plasma transferrin (Tf) (a means of signalling the intestine of the body iron levels and hence body iron requirement) may be defective in HH patients. Consistent with this belief is the observation that the mucosal epithelium in HH contains remarkably little iron in comparison with patients having other forms of iron overload, despite comparable

degrees of systemic iron loading in all of these iron loading diseases. Furthermore, in HH the excess iron is preferentially deposited in the hepatocytes. In contrast, iron deposition in dietary iron overload is in the Kupffer cells and macrophages, as well as hepatocytes.

HH is frequently complicated by HCC formation, with relative risks of between 100 and over 200 being calculated (Niederau *et al.*, 1985). The longer the patient survives the more likely is this complication. The vast majority of patients with HH who develop HCC have cirrhosis, and it was originally believed that cirrhosis, and not iron *per se,* was the cause of the malignant transformation. However, about 30 patients have recently been reported to develop HCC in the absence of cirrhosis (Blumberg *et al.*, 1988; Leone *et al.*, 2000; Pellise *et al.*, 2001), suggesting that excessive iron itself may be hepatocarcinogenic.

1.2 Putative mechanisms of iron-induced carcinogenesis

The putative mechanisms of iron-related carcinogenesis involve iron's role in oxidative injury and in cell growth. Iron has been shown to cause lipid peroxidation (LPO) and oxidant stress in experimental dietary overload and patients with HH. This observation is supported by a growing number of studies showing increased products of LPO in the liver of iron-overloaded animals (Houglum *et al.*, 1990; Paradis *et al.*, 1997a; Marmunti *et al.*, 1998). The formation of sufficient reactive oxygen species (ROS) leads to an impairment of basic immune defences, such as antigen-specific immune responses, cytotoxic T-cell proliferation and function, and enhancement of suppressor T-cell activity. These alterations in T-cell function may lead to impaired immune surveillance against cancer.

One possible argument against iron's role as a carcinogen has been the few reports of cancers arising after iron depletion (Fracanzani *et al.*, 2001). However, the carcinogenic effects of most toxins are known to occur as long as 20 years after exposure. It can therefore be hypothesized that the generation of ROS, lysosomal and DNA damage, or other mechanisms are irreversibly underway before iron depletion occurs, and that the eventual toxin removal does not stop what is already an inevitable process (Mallory and Kowdley, 2001).

Many questions about the role of iron in hepatocarcinogenesis remain to be answered. Moreover, laboratory evidence supporting iron's role as a carcinogen has yet to be conclusively shown. The purpose of this study is to develop an animal model of dietary iron overload and to investigate the putative mechanisms of iron-induced HCC, including whether iron is directly carcinogenic or induces HCC only indirectly by causing chronic necroinflammatory hepatic disease in the form of cirrhosis or fibrosis.

2.0 RESEARCH HYPOTHESIS

It is believed that iron (Fe) overloaded individuals may be susceptible to LPO, mediated by Fe according to the "Fenton" or "Haber-Weiss" reaction, with the resultant effect being the production of excessive quantities of ROS. These oxygen species induce DNA strand breaks and may increase the rate of DNA unwinding, with consequent mutagenic and carcinogenic activity.

The suggested hypothesis is that the generation of ROS as a result of Fe overload, LPO, oxidative DNA damage including strand breaks, unwinding, and mutagenesis, are major steps in the pathogenesis of Fe induced HCC.

2.1 AIMS OF THE STUDY

The aims of the study were to ascertain:

i. if HCC develops in Fe overloaded rats, and to investigate the mechanism(s) of this occurrence, including whether excess hepatic iron was directly or indirectly carcinogenic.

ii. if Fe overload leads to an increased generation of ROS and, if so, their involvement in hepatocarcinogenesis.

iii. the involvement of LPO and oxidative DNA damage in mutagenesis.

iv. if DNA strand breaks and DNA unwinding are part of the hepatocarcinogenic process.

In order to elucidate the mechanism(s) by which dietary Fe overload causes HCC in an experimental animal model, the following criteria were adhered to in this study: (1) iron exposure leading to iron overload was planned to occur over at least half the animals life span, (2) the route of exposure was analogous to that in humans (i.e. *per os* by diet, gavage, water-drinking), (3) exposure was directed to the whole body rather than specific sites, and (4) appropriate controls were included in the experiment.

2.2 EXPERIMENTAL DESIGN

In the study, 6 groups each made up of 60 Wistar albino rats were established. The first group, the control group, was designated C group. Groups 2 to 6 were fed Fe as described below. Group 2 was designated Fe group. Group 3 (Fe + V group) received vitamins A and E supplementation [50 mg *all* trans-retinol (vitamin A) and 500 mg α-tocopherol (vitamin E) per kg diet], in addition to iron. Group 4 (Fe - V group) received a diet totally devoid of vitamins A and E (but supplemented with iron). Group 5 (Fe + ASA group) received 20 mg acetyl salicylic acid (aspirin) per day in addition to the iron diet. Group 6 (Fe + Cu) received 300 mg/kg wt $CuSO_4$ for 12 months, followed by 3% copper hydroxide carbonate [$CuCO_3 \cdot Cu(OH)_2$] together with iron supplementation.

The rats were studied for 3 years. Five rats from each group were sacrificed every 4 mo for 2 years. Thereafter, sacrifice depended on the health status of the animal. Rats were initially anaesthetized with 0.1 ml/100 g wt Anaket and Chinazin (4:1). Blood was sampled by cardiac puncture. Blood sampling was always done between 0700 hr and 0900 hr. Rats were then euthanased and their livers harvested under aseptic conditions. One portion of

the liver was snap frozen in liquid nitrogen (and then stored at -70°C) and the other placed in 10% buffered formalin. In cases of unexpected death, the liver was harvested.

2.3 SUBJECTS AND DIET

2.3.1 Subjects

The Wistar albino rat (*Rattus norvegicus*) was selected for the study based on its higher growth and survival rate compared to the Fischer 344 and the Sprague Dawley rats (Figure 1).

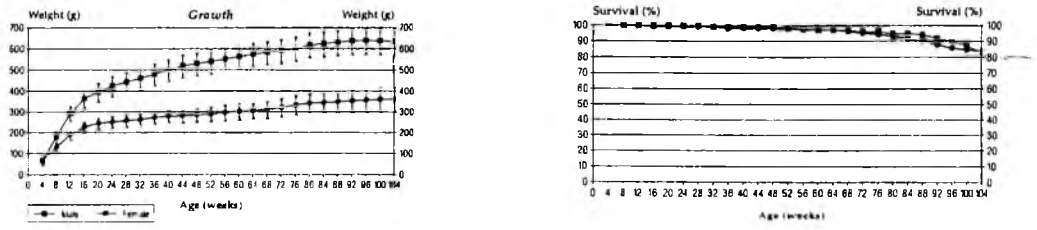

Wistar albino: Growth and Survival Curves

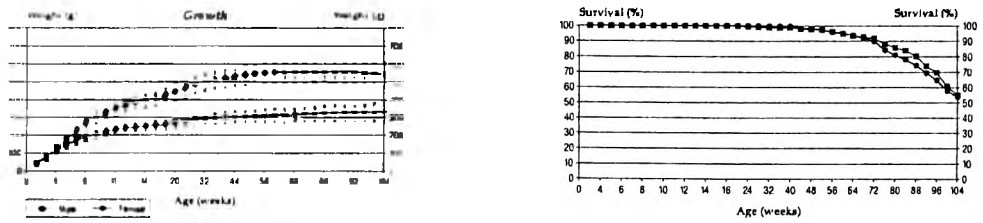

Sprague Dawley: Growth and Survival Curves

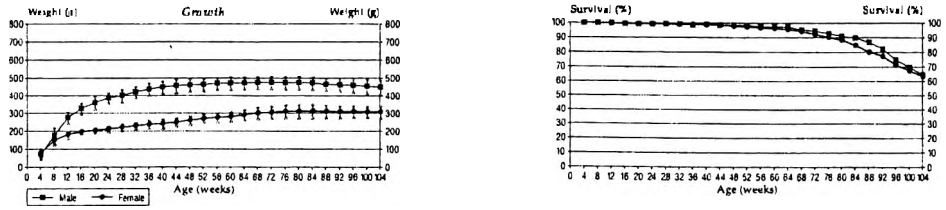

Fischer 344: Growth and Survival Curves

Figure 1 Growth Curves of 3 types of commonly used experimental rats (Harlan, 2000).

Eighty female and 40 male Wistar albino rats weighing 120-140 g were crossed to raise 360, largely male pups. Wistar albino rats received humane care in accordance with the guidelines of the Animal Ethics Committee of the University of the Witwatersrand. Rats were housed in plastic cages with stainless steel tops in the animal unit of the Medical School of the University of the Witwatersrand where room temperature, humidity and ventilation were controlled according to international standards. Animals were maintained at a 12-hour light-cycle. Ethical approval was obtained from the Animal Ethics Screening Committee of the University of the Witwatersrand for this study (AESC No. 2000/90/3 & AESC No. 2002/54/3). Rats were purchased from Harlan Olac Ltd, Bicester, UK.

2.3.2 Diet

Weanling rats were fed (*ad libitum*) the standard chow diet (AIN-93G Formulation, manufactured by EPOL, South Africa), supplemented initially with 2% pentacarbonyl iron (CI) according to the protocol of Plummer *et al.* (1997). CI and the subsequently used ferrocene were obtained from Sigma (Germany). The control group (C) received the standard chow diet. Pups were weaned at 6 weeks and continued to receive the iron supplementation or control diet. Because of the relatively ineffective iron loading at 8 months CI was increased to 2.5%. However, hepatic Fe loading was still poor at 12 months and the 2.5% CI supplementation was finally replaced with 0.5% dicyclopentadienyl iron (ferrocene) at this point.

2.3.2.1 CI

CI ($C_9Fe_2O_9$) is commonly referred to as iron powder. It is manufactured using the

carbonyl decomposition process, with the resultant iron appearing as uniform microscopic spheres with only traces of carbon, oxygen and nitrogen. CI is of high purity with superior electromagnetic properties. Typically, CI is used as a catalyst, radar absorbing material, precision electronic component, animal feed, multivitamin complexes and iron supplements.

2.3.2.2 Ferrocene

Ferrocene was first synthesized in 1951. The sandwich structure of ferrocene (shown below) was first predicted from its image resonance (IR) and nuclear magnetic resonance (NMR), and confirmed by X-ray crystallography.

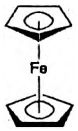

The uses of ferrocene range from being a biochemical and analytical chemical to other industrial applications such as diesel oil improvement, gasoline anti-knocking agent, fertilizers etc. It is also used as an ingredient of antibiotics and blood tonic preparations (Madinaveitta, 1965) and for anticancer treatment [investigated in animals (Kovjazin *et al.*, 2003)]. Furthermore, some ferrocene analogues have been postulated to totally restore the activity of chloroquine against chloroquine-resistant parasites (Domarle *et al.*, 1998). Finally, its potential use in human anti-malarial therapy has also been investigated (Domarle *et al.*, 1998). Twelve types of novel ferrocenyl sugars with anti-malaria properties towards *P. falciparum* and anti-cancer properties in mouse cancer cell FM3A have been synthesized (Itoh *et al.*, 2000).

Ferrocene metabolism

The mechanisms present in the intestine which regulate the absorption of iron are apparently arranged to deal only with ions of this metal. They fail to operate when presented with compounds containing ferrocene nucleus from which the iron cannot be ionized without disrupting the very stable molecule. The physical and chemical properties of ferrocene are more akin to those of aromatic hydrocarbons, such as benzene and naphthalene, than to those of ion salts, however chelated these salts may be. This is reflected in the behaviour of the ferrocenes in the animal body. Like the lower homologues of benzene, the ferrocenes with small aliphatic substitutes are well absorbed when given by mouth. The higher homologues of ferrocene, like those of benzene, fail to be absorbed (Madinaveitia, 1965). Once ferrocenes are absorbed in the body they continue to behave as benzoid compounds. Like benzoic acid and benzene sulphonic acids, the sulphonated ferrocenes and the ferrocene carboxylic acids are eliminated in the urine, presumably un-degraded, though perhaps conjugated. The mechanisms present in the kidney which normally prevent iron passing into the urine do not recognise the metal as such when it is presented to them as a ferrocene derivative (Madinaveitia, 1965).

The fate of the absorbed iron has been examined in detail in ferrocene itself, and in some less-toxic and well absorbed ferrocarbnons, especially in dineopentyl ferrocene (Madinaveitia, 1965). In mice and rats the yellow ferrocenes could be seen in the stomach and duodenum during the first few hours after ingestion. The intestine was stained yellow until just below the point at which it is joined to the bile duct. This may indicate that, like many other water-insoluble substances, the ferrocenes are absorbed with the help of the

bile acids. Ferrocene was not present in the bile of guinea-pigs dosed with dineopentyl ferrocene.

Toxicity of ferrocenes

The toxicity of ferrocenes is of a different type from that of iron salts, and it is thought to be the result of the ferrocene nucleus and not to the iron they contain. The toxicity of some ferrocenes to mice increased when they were given by mouth as solutions in oils. These ferrocenes are yellow compounds in fat. The fat of mice that received a single dose of dineopentyl ferrocene corresponding to 1g/kg of iron was discoloured. The benzene extractable iron of the homogenized carcass of the animals increased reaching a maximum of 2.3 mg of iron per 20 g mouse the day after dosing and then decreased. The toxicity of dineopentyl and probably of other ferrocenes also depends both on the amount of fat and ferrocene given. The mechanism by which the fats increase the toxicity of ferrocenes has not been elucidated. Animals receiving lethal doses of water-soluble ferrocenes die in convulsions after dosing. It is possible that some insoluble ferrocenes are metabolised to toxic water-soluble compounds still containing the intact ferrocene nucleus. Water-insoluble ferrocenes act more slowly, but with similar symptoms (Madinaveitia, 1965).

Mutagenicity and genotoxicity of ferrocene

Ferrocene was negative in a bacterial mutation assay (pre-incubation), using *S. typhimurium* strains TA98, TA100, TA1535, and TA1537 with and without metabolic activation systems from induced rat and hamster livers (Haworth S *et al.*, 1983). It was also negative for the plate incorporation test using *S. typhimurium* strains TA 97, TA98,

TA100, TA102, TA1535, TA 1537 and TA1538 (Dunkel *et al.*, 1999). Ferrocene was further found to be negative in a sex-linked recessive lethal *D. melanogaster* assay after feeding (Zimmering *et al.*, 1985). In a mouse lymphoma L5178Y TK $^{+/-}$ mutation assay in the presence of liver S9 mix, ferrocene was found negative (Dunkel *et al.*, 1999). Lastly, ferrocene was negative for a chromosome aberration assay using Chinese Hamster ovary (CHO)(Galloway *et al.*, 1985). However, ferrocene was positive in the following assays: (a) a sex-linked recessive lethal assay in *D. melanogaster* after injection (Zimmering *et al.*, 1985), (b) a heritable translocation assay in *D. melanogaster* after injection (Zimmering *et al.*, 1985), (c) a mouse lymphoma L5178Y TK $^{+/-}$ mutation assay in the absence of liver S9 mix (Dunkel *et al.*, 1999 and (d) a sister chromatid exchange (SCE) assay in CHO cells, with and without metabolic activation (Galloway *et al.*, 1985). No data from genotoxicity studies in intact mammals has been found.

Yeary *et al.* (1969) showed that oral doses of 300 and 1000 mg/kg b.wt for 3 months resulted in a high level of haemosiderosis in dogs. However, cirrhosis observed in dogs, was considered by the authors to be the effect of the hydrocarbon moiety. Cirrhosis has so far not been reported in any rat study using ferrocene.

Nielsen and Heinrich (1993) studied the metabolism of 3,5,5-trimethylhaxanoyl-ferrocene (TMH-ferrocene), an analogue of ferrocene, in experimental rats. The bioavailability of iron from TMH-ferrocene (48% whole body retention from a 5mg Fe dose) was twice as high as ferrocene and 6 times higher than $(TMH)_2$-ferrocene and ferrous sulphate. In contrast to well-known iron salts, the intestinal absorption of TMH-ferrocene iron was

independent of the dose (1 or 5 mg Fe) and similar in iron deficient and iron-loaded rats, indicating that the body's iron stores do not regulate the intestinal absorption of TMH-ferrocene. After intestinal absorption, TMH-ferrocene iron in the portal blood is transported to the liver independently from transferrin. The iron is released from the hydrocarbon moiety within the liver. Depending on the body's iron stores, TMH-ferrocene iron is then incorporated preferentially into haemoglobin (iron-deficient state) or added to iron stores in the liver. A transient storage of ferrocene iron in fat tissues has been observed after oral administration of ferrocene but not TMH-ferrocene. As a result of the high bioavailability of ferrocene, chronic feeding of this compound results in a rapid and progressive iron overloading in rats. For example Nielsen *et al.* (1993) obtained hepatic iron of 16.9 mg/g w.w after 10 weeks of feeding rats a diet containing 0.5% TMH-ferrocene.

The biochemical and the biophysical properties of ferrocene were investigated by Ward *et al.* (1991) using experimental animals. Male Wistar rats were fed a chow diet with total iron intake of 5 mg/day for 6 weeks. High hepatic iron was predominantly located in the lysosomes. Hepatic iron loading was 7.24 ± 1.97 mg Fe/g tissue. Ferritin and haemosiderin were isolated from the livers of the ferrocene-loaded rats and their iron stores consisted mainly of ferrihydrite. Free-radical-mediated damage in the iron-loaded livers was inferred from the significant depletion of α-tocopherol in both the livers and subcellular hepatic

lysosomal fraction, which inversely correlated with the increasing iron content and was associated with increased fragility of the lysosomal membranes. In addition, male

C57BL/6lbg mice fed a diet containing 0.04-0.2% w/w ferrocene (less than half the amount used in the present study) for 115 days developed severe hepatic siderosis accompanied by a 15-fold induction of non-haem iron content, compared with control mice receiving a diet with normal amounts of iron. The ferrocene treatment led to significant increases in hepatocellular necrosis as measured by plasma alanine aminotransferase (ALT) levels. Histological assessment of hepatic fibrosis revealed mild increases in collagen deposition localized with accumulations of hemosiderin, primarily in centrilobular hepatocytes. Hepatic fibrosis was confirmed by measurement of hepatic hydroxyproline content that was increased 4-fold in ferrocene-fed mice compared to the controls. Hepatic siderosis was accompanied by significant increases in hepatic malondialdehyde (MDA) content, suggesting the ferrocene-induced iron burden initiated LPO *in vivo* (Valerio and Petersen, 2000).

Dullman *et al.* (1992) fed female Wistar rats with 0.5%TMH-ferrocene for 56 weeks. First signs of liver damage, such as necrosis of single hepatocytes and mild fibrosis, began at a liver iron concentration of 14.7 ± 1.4 mg/g w.w. With increasing iron loading, focal necrosis of hepatocytes and iron-burdened macrophages occurred, and significant perisinusoidal as well as portal fibrosis developed. Cirrhosis could not be induced in this animal model, however. In the present study 0.5% ferrocene was added to the chow diet. This corresponds to 39 mg Fe per day (calculated on an average of 20 g chow diet consumption per rat) and is well below the LD_{50} value of 440mg. In addition, ferrocene has 88.7% absorption and 27.4% whole body retention (Nielsen and Heinrich, 1993).

2.4 METHODS

A battery of assays was employed to cover iron overload, ROS, antioxidants, LPO, DNA changes, liver disease, tumour markers and HCC. Methods are outlined below.

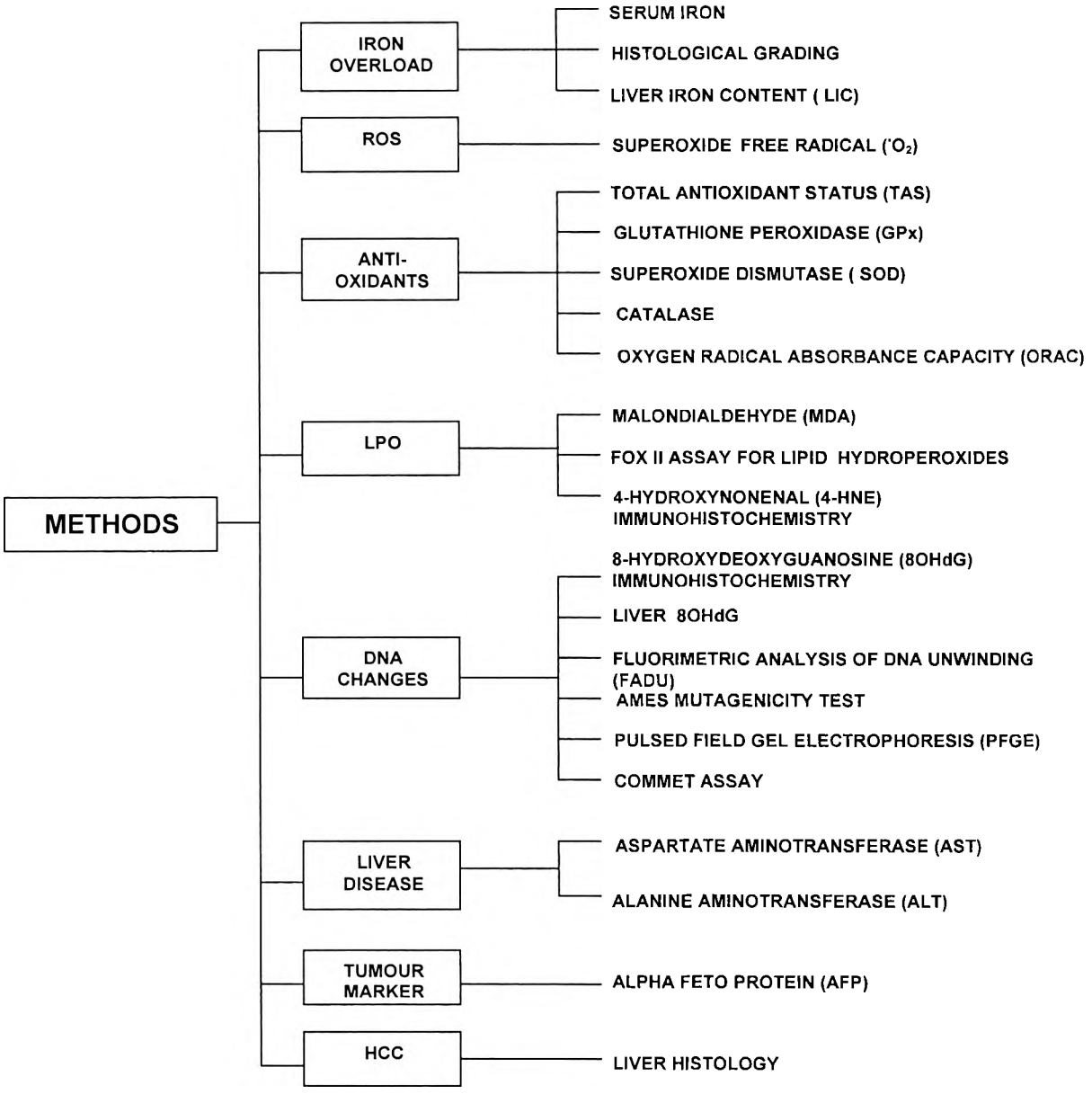

Figure 2 METHODS USED FOR THIS STUDY

3.0 TRACE ELEMENTS

Trace elements are those that occur in human and animal tissues in milligram per kilogram amounts. Similarly, requirement is expressed in milligrams per day. An element is considered essential when a deficiency produces impairment of function and when restoration of physiological amounts of that element alone prevents or alleviates the impairment. In absolute deficiency, death occurs. In excess, a marginal toxic response occurs, followed in severe instances by a fatal toxic response. Biochemical functions of iron and other trace metals and signs of deficiencies in humans are known.

3.1 CHARACTERISTICS OF IRON AND COPPER IN TRACE ELEMENT FUNCTION

Four main characteristics of trace element function are well understood. These are: specificity, homeostasis, interactions and amplification.

3.1.1 Specificity

Trace elements are essential and specific in their functions *in vivo*. They cannot be replaced by chemically similar elements. The essential trace elements interact with electron donor atoms such as nitrogen, sulphur, and oxygen, the types of interaction depending on bond types and configurational preferences. Certain trace elements (e.g., Fe, Cu, Mo) are stable in more than one valance state, which allows for biological oxidation-reduction functions, whereas others (e.g., Zn^{2+}) are stable in a single state only, which allows for more of a conformation or substrate-binding role (Stadtman, 1990).

3.1.2 Homeostasis

Mechanisms that ensure optimal body distribution of an element over a range of intakes constitute a system of homeostatic regulation of the element. The amount of trace element absorbed generally decreases with increasing concentration in the intestinal lumen and associated tissues. Active transport mechanisms involving absorption by specific metal binders and feedback inhibition have been postulated for iron, zinc and copper (Pena *et al.*, 1999).

The principal excretory route for elimination of most trace metals is in the faeces. Faecal excretion reflects dietary intake, homeostatic regulatory mechanisms, gastrointestinal absorption and endogenous metal secretion into the intestines. Relatively small amounts of trace metals are excreted through urine. Other minor routes include loss through hair, nails, skin cell desquamation and sweat. Menstrual iron loss and seminal zinc loss are also minor but can be significant in certain circumstances.

3.1.3 Interactions

A high concentration of one trace element can interfere with the metabolism of other trace elements present in normal or marginal amounts. Alternatively, the effect of a toxic trace element may be ameliorated by another "protective" trace element. Large amounts of zinc in diet interfere with intestinal Cu absorption, and result in Cu deficiency despite otherwise adequate Cu intake. Cu deficiency, in turn, is known to provoke iron deficiency and anaemia (Owen, 1973).

3.1.4 Amplification

Very small amounts of trace elements are required for optimal performance of the whole organism. The absence of small amounts of trace elements (e.g., Fe) can result in overt clinical abnormalities (e.g., anaemia). The basis of this amplification of trace element action is that trace elements are constituents of, or interact with, enzymes and hormones that regulate the metabolism of much larger amounts of biochemical substrates.

3.2 FUNCTIONS AND METABOLISM OF IRON (Fe)

Fe, the most important essential trace element, represents 55 and 45 mg/kg of the body weight in adult healthy men and women, respectively. Normally about 60-70% of total body Fe is present in haemoglobin in circulating erythrocytes. Myoglobin, cytochrome, and other Fe-containing enzymes comprise a further 10%, and the remaining 20-30% is stored as ferritin. Although Fe bound to transferrin (Tf) is less than 0.1% (~ 3mg) of the total body Fe, it is dynamically the most important Fe pool with the highest rate of turnover (Finch *et al.*, 1982). The metabolism of Fe resembles in many aspects that of other trace elements. Normally, very small quantities are present in most cells of the body, in plasma, or in other extracellular fluids. The body rigorously conserves its Fe stores.

Figure 3 illustrates the pathways of Fe metabolism and the daily rates of exchange between the various Fe compartments. Approximately 2.5g of Fe are contained within erythrocytes (RBCs) or their precursors in the bone marrow. A plasma Fe transport protein called apotransferrin, which has two Fe-binding sites per molecule, accomplishes transport of Fe from one organ to another. Each of these sites can bind one Fe^{3+} together with one ion of

HCO_3^-. The apotransferrin-Fe^{3+} complex is called Tf. Approximately 2.5 mg of Fe are normally present in plasma.

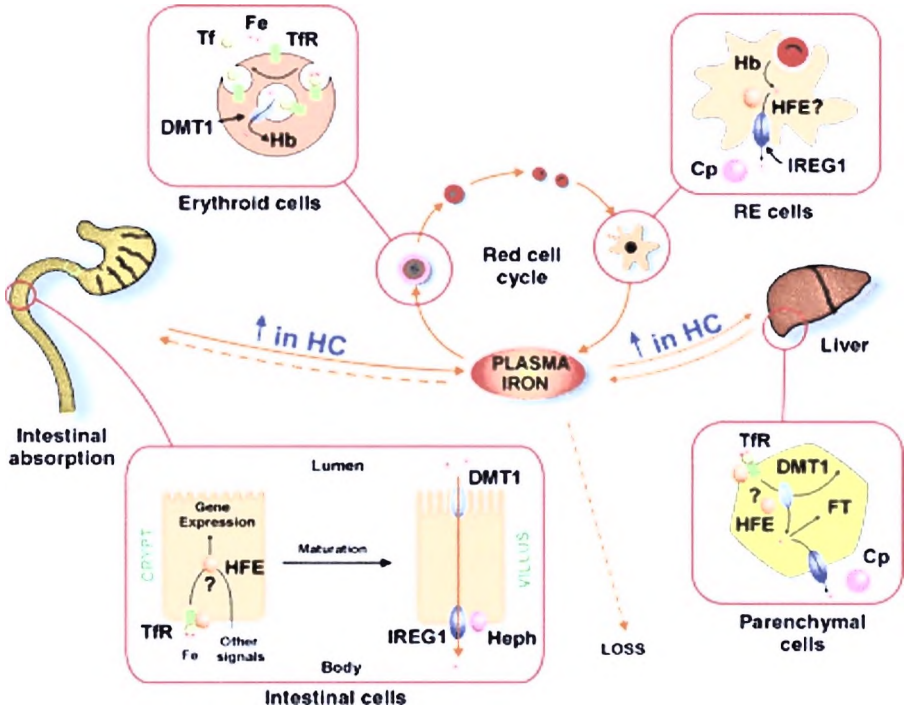

Figure 3 Pathway of iron metabolism showing sites where *HFE* may play a role. The basic components of iron influx and efflux are shown in intestinal, erythroid, reticuloendothelial (RE), and parenchymal cells. Tf, transferrin; Cp, ceruloplasmin; Fe, iron; Heph, hephaestin; FT, ferritin; Hb, haemoglobin; HC, haemochromatosis. (Anderson and Powell, 2000).

A major pathophysiological feature of haemochromatosis is an increase in intestinal iron absorption. It is predicted that mutations in genes important for intestinal iron transit would ameliorate the haemochromatosis phenotype. This is indeed the case, and *HFE* knockout mice carrying mutations in the gene for the brush border iron transporter DMT1 show reduced levels of hepatic iron accumulation. DMT1 is the major molecule facilitating the

uptake of dietary iron by the epithelial cells of the proximal small intestine (Figure 3)(Fleming *et al.*, 1997). Mice defective in DMT1 (*mk*) have a profound microcytic, hypochromic anaemia. The demonstration by Levy and colleagues (Levy *et al.*, 2000) that deletion of the *HFE* gene cannot correct the *mk* phenotype shows that DMT1 is the major route of entry into intestinal epithelial cells in haemochromatosis.

The intestinal epithelial cell is a polarized cell and iron must traverse not only the apical membrane but the basolateral membrane as well. Insight into this iron efflux step, have come from the cloning of the gene mutant in *sla* mice (Vulpe *et al.*, 1999), another mouse strain with an inherited anaemia. The affected gene has been named *Hephaestin* and it bears significant homology to the copper-containing plasma protein ceruloplasmin, which has been known to play a role in iron release from tissues. *HFE* knockout mice carrying the *sla* mutation show considerably reduced hepatic iron levels, indicating that hephaestin plays an important role in iron loading. However, since the block of absorption is not complete, alternative basolateral iron transfer pathways appear to be operating. It would be expected that disruption of the newly identified basolateral iron transporter IREG1 (or ferroprotein 1) (McKie *et al.*, 2000) would also ameliorate the iron overloading phenotype of *HFE* knockout mice (Anderson and Powell, 2000).

Ferritin is the major Fe storage compound. It is a spherical molecule consisting of an apoferritin shell and an interior ferric oxyhydroxide (FeOOH)x crystalline core. The apoferritin shell is composed of 24 subunits or monomers. Pores on the surface permit ingress and egress of molecules such as Fe^{2+}, ascorbic acid, and flavin mononucleotide.

The FeOOH core crystal may contain as many as 4000 Fe atoms, although it usually contains 2000 or less. Release of Fe from ferritin is probably non-enzymatic and may involve rapid reduction by reduced flavin mononucleotide or other reducing substances. The resultant Fe^{2+} leaves the crystal and diffuses out through a pore of the ferritin shell. Thus, ferritin is both a very efficient Fe trap and a readily available source of Fe for metabolic requirements.

Ferritin is found in nearly all cells of the body. In hepatocytes and in the macrophage system of the bone marrow and other organs, ferritin provides a reserve of Fe readily available for the formation of haemoglobin and other haem proteins. In healthy men, the total body content of stored Fe, mostly as ferritin, is approximately 800mg; in healthy women it ranges from 0-200mg. Minute quantities of ferritin are also present in serum in concentrations proportional to the total body stored Fe. Liver injury results in release of relatively large amounts of ferritin into plasma.

Haemosiderin, the other form of stored Fe, is aggregated, partially deproteinized ferritin. In contrast to ferritin, haemosiderin is insoluble in aqueous solutions. Fe is only slowly released from haemosiderin. Like ferritin, haemosiderin normally is found predominantly in cells of liver, spleen, and bone marrow. Tissue Fe normally amounts to approximately 8 mg. Tissue Fe diminishes early in the course of Fe deficiency. Numerous cellular enzymes and coenzymes require Fe, either as an integral part of the molecular structure or as a co-factor.

3.2.1 Physiology

A well balanced diet provides 10-15 mg of Fe daily, mostly in the form of haemoglobin and myoglobin in meat. About 1 mg of Fe is absorbed each day. Absorption occurs principally in the duodenum. Haem is absorbed directly; inorganic Fe is absorbed in the ferrous state.

Both ferritin and Tf are present in the absorptive cells of the intestinal mucosa, and it is believed that they operate to regulate Fe absorption. When body Fe stores are high, the ferritin content of mucosal epithelium is also high and the Tf content is low. Fe that enters mucosal cells is trapped in ferritin and lost when the mucosa cell is sloughed into the intestinal lumen. This mechanism reduces Fe absorption when body stores of Fe are already increased. Conversely, with Fe deficiency, the mucosal cell content of apoferritin is diminished, the Tf (and apotransferrin) content is increased, and Fe absorption is accelerated.

The major pathway of Fe metabolism (Figure 3) is a virtually closed cycle in which Fe passes from the plasma Tf to the RBC precursors in the bone marrow, where it is incorporated into haemoglobin. These cells then enter the circulation as mature RBCs, where they remain for about 120 days before they are metabolically "worn out" and are engulfed by phagocytes, particularly in the spleen. The Fe is released from the haemoglobin and returns to the plasma Tf, thus completing one cycle and beginning another.

Each day about 1-2 mg of Fe absorbed from the intestinal tract enters this cycle to compensate for the 1-2 mg of Fe lost each day from the body. With each menstrual cycle women lose about 40 - 80 ml of blood, which is equivalent to 20 - 40 mg of Fe. This loss must be made up by increased absorption of Fe by intestinal mucosa. Similarly, about 600-900 mg of Fe is lost as a consequence of each pregnancy.

3.2.2 Fe acquisition, transport and storage

Because of Fe's virtual insolubility and potential toxicity under physiological conditions, specialized molecules for the acquisition, transport and storage of Fe in a soluble, nontoxic forms have evolved to meet the cellular and organismal Fe requirements. Thus, under normal circumstances these physiological Fe-complexing agents leave body fluids and cells with extremely low concentrations of "free Fe". Nevertheless, the existence of a short-lived Fe-containing intermediate within the cell is a possibility. Although the nature of this intermediate pool of chelatable or transient Fe remains elusive, the size of this pool is maintained by sophisticated control mechanisms that co-ordinately regulate cellular Fe uptake and storage.

In vertebrates Fe is transported within the body between sites of absorption, storage and use by the plasma glycoprotein, Tf, which binds Fe tightly but reversibly. Tf is recognised by specific cell membrane receptors that are crucial for cellular Fe acquisition. After its intracellular release from Tf-receptor complexes, Fe enters functional compartments or is stored in ferritin. The daily turnover of Tf Fe is of the order of 30 mg. Normally about 80% of this Fe is transported to the bone marrow in humans (and also to the spleen in

rodents), for haemoglobin synthesis, in developing erythroid cells (Figure 3). From these sites, reticulocytes are released into the circulation where, within 24 hrs, they lose Tf receptors, mitochondria, ribosomes, and all the other components of haemoglobin synthesis and develop into mature erythrocytes that circulate in the blood for about 120 days (in humans). Senescent erythrocytes are phagocytized by the cells of the monocyte-macrophage (reticuloendothelial) system, where the haem moiety is split from haemoglobin and catabolized. The liberated Fe is released back to plasma Tf at a rate that normally matches the rate of Fe transport for erythropoiesis. Although this well-maintained dynamic equilibrium of Tf Fe is reasonably well understood, all of the mechanisms and controls involved in the release of Fe from reticuloendothelial cells have not been defined. The remaining 5 mg of the daily plasma Fe turnover is exchanged with the nonerythroid tissue i.e. the liver. About 1 mg of dietary Fe is absorbed per 24 hrs and net organismal Fe balance is maintained by a daily loss of approximately 1 mg through nonspecific mechanisms (mostly cell desquamation). In summary, there are two important features of organismal Fe metabolism. First, Fe turnover is virtually an internal event in the body; and second, most of the Fe turnover is used for the synthesis of haem by erythroid cell.

3.2.3 Iron Overload

Traditionally, haemosiderosis indicated Fe overload without overt associated tissue injury and haemochromatosis implied Fe overload with injury to involved organs as manifested by cellular degradation and fibrosis. In current usage, however, haemochromatosis is a generic term for Fe overload, irrespective of evidence of tissue injury. Fe overload most commonly results from chronic excessive absorption of Fe from diet. HH is a disorder of

Fe overload as a result of an inborn error of Fe metabolism. The precise mechanism is unknown. Iron overload is rarely the result of repeated blood transfusions or protracted ingestion of Fe supplements. Sideroblastic anaemia is a group of Fe-loading disorders of unknown cause. In a hereditary type of this disorder, there is deficiency of δ-amino-levulinic acid synthetase in RBC precursors. Fe accumulates in mitochondria because of this metabolic bottleneck.

3.2.3.1 Fe overload in experimental animals

The development of methods for producing Fe overload in rats has provided a valuable tool for the investigation of the role of Fe in disease processes, such as hepatic fibrosis and cirrhosis (Roberts *et al.*, 1993; Mackinnon *et al.*, 1995). One of the simplest of these methods is the addition of CI to the diet (Bacon *et al.*, 1983; Pietrangelo *et al.*, 1990; Britton *et al.*, 1990; Britton *et al.*, 1994; Tector *et al.*, 1995). Effective Fe loading is achieved quickly by adding 3% CI to the diet of mother rats shortly after they give birth, and to the diet of the offspring after weaning. By the age of 10 weeks, offspring have Fe deposition in 75 - 100 % of hepatocytes (grade III -IV siderosis). However, during the loading period rats suffer from diarrhoea and their growth rate is severely retarded, so that at age 10 weeks they weigh approximately 35% less than controls. Various modifications of the feeding regimen have been used, such as addition of 2% or 2.5% CI to the diet, or addition of 3% for the first month, then reducing this to 2.5%. However, there are no published reports demonstrating any advantages of one regimen over another.

In a study by Plummer *et al.* (1997), four pregnant Porton rats were assigned to receive

0, 0.5, 1.0, or 2.0% by weight of CI. The allocated diets were commenced 2 days after the rats gave birth, thereby initiating Fe supplementation to the offspring via breast milk. When the offspring were 3 weeks old, they were separated from their mothers and caged according to sex. They continued to receive the Fe supplementation until they were 32 weeks old. At weeks 8, 16, 24, and 32, liver biopsies were performed on all rats. Rats not receiving supplementation showed only a small (approx. 2 fold) increase in hepatic Fe content from the age of 8-32 weeks, and none of the livers showed excess stainable Fe. Male rats tend to reach a plateau of hepatic Fe content by 8-16 weeks, whereas female rats continued to load over the whole 32 weeks period. Females had a higher hepatic Fe content than males by a factor of 2.8. Fe loading scores in the biopsies taken suggested that rats tend to reach their maximum loading by 16 weeks. No fibrosis was apparent in any of the livers. At the highest dose of Fe, the weight of female rats was lower by an average of 14%, and of males by 19%, compared with the corresponding controls. The researchers were of the opinion that levels of 2% CI in the diet gives grade III-IV Fe loading, while having only a moderate effect on growth rate. The gastrointestinal toxicity of Fe is presumably less with 2% dietary Fe than with 3%, which caused a greater degree of growth retardation. In conclusion, 2% CI supplementation was suitable for maximum Fe loading within 16-32 weeks with little adverse effects.

rload at the ultrastructural level

load is examined at the ultrastructural level, Fe-loaded cells have abundant lysosomes that contain Fe stored in the form of ferritin and haemosiderin 994). Peters and co-workers (Peters *et al.*, 1976; Seymour *et al.*, 1978) have

proposed that Fe overload results in an acquired lysosomal storage disease. The accumulation of Fe in lysosomes increases their fragility and damages the cell. These investigators observed that the activities of several lysosomal enzymes, including N-acetyl-glucosaminidase (NAGA) and acid phosphatase (ACP), are increased in liver biopsies of patients with Fe-overload (Peters *et al.,* 1976). These increases may result from lysosomal proliferation and distension (Peters *et al.,* 1985). When lysosomal fragility was determined in homogenates of these biopsies, there was a reduction in latent (membrane-enclosed) NAGA activity without a change in latent ACP activity, suggesting that there may be two populations of lysosomes in the Fe-loaded livers: one population rich in NAGA, which becomes more fragile, and the other rich in ACP, which is relatively unaffected. In patients with HH who had their Fe stores normalized by phlebotomy, the NAGA latency returned to normal, indicating that the increased lysosomal fragility was Fe-dependent (Seymour *et al.,* 1978). Although it is not known if the lysosomal fragility observed *in vitro* reflects the situation *in vivo*, suggestive evidence is provided by a study in thalassaemic patients in which elevated serum NAGA levels were correlated with the degree of Fe overload (as assessed by serum ferritin levels) (Frigerio *et al.*, 1984). Stal *et al.* (1990) performed ultrastructural studies on liver biopsies from patients with HH and observed that the lysosomal volume density in hepatocytes is increased and is correlated with the degree of Fe overload. Lysosomal volume density normalized following Fe removal by phlebotomy.

One mechanism that may contribute to the increased lysosomal fragility found in Fe overload is LPO. It has been shown that ferritin, and especially haemosiderin, are increased in liver biopsies from patients with Fe overload (about 10- to 100-fold, respectively) (O' Connell *et al.,* 1986).

Both ferritin and haemosiderin can stimulate LPO *in vitro* at acidic pH without the need for a reducing element (O' Connell *et al.*, 1985). Since lysosomes are an acid organelle compartment, it is possible that intra-lysosomal LPO initiated by ferritin occurs in Fe overload. Haemosiderin is about 20% as potent as ferritin in stimulating LPO *in vitro*. On this basis, it has been suggested that conversion of ferritin to haemosiderin may have a relatively cytoprotective effect by reducing the ability of Fe to stimulate LPO (O' Connell *et al.*, 1986). However, in Fe overload, because the total amount of haemosiderin increases disproportionately, its potential role in toxicity cannot be ruled out.

Myers *et al.* (1991) studied the structure, physicochemical properties, and pH of hepatic lysosomes in rats with dietary Fe overload (Figure 4). Lysosomal Fe content was increased drastically, and the lysosomes were enlarged, and more fragile. Lysosomal membrane from the Fe-loaded group had evidence of increased LPO [measured as thiobarbituric acid reactive substance (TBARs)], and their fluidity was decreased. It was concluded that iron-catalyzed peroxidation of lysosomal membrane lipids is likely the mechanism of these structural, physicochemical, and functional disturbances.

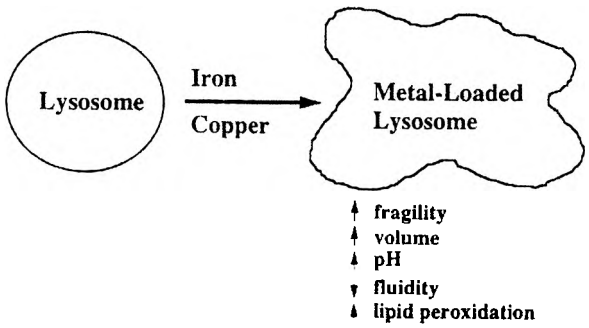

Figure 4. Changes in hepatic lysosomes after iron or copper overload

3.3 TRANSFERRIN (Tf)

Plasma Tf belongs to a family of related Fe-binding proteins including lactoferrin (Lf), which is found both intracellularly and in secretions such as milk, tears, and semen. These proteins have a molecular weight of 80 kDa and share a high degree of sequence homology. Tf functions to transport Fe between sites of absorption, storage and use. Immature erythroid cells are major consumers of Tf-Fe. The membrane-bound Tf homologue, melanotransferrin, can transport Fe 'complexed' to low-molecular-weight ligands into the cell (Beer *et al.*, 1997). The physiological relevance of this process is unknown. Although Tf has bacteriostatic activity (Linder and Hazegh-Azam, 1996), the physiological significance of this antibacterial activity is unclear.

3.3.1 Molecular properties

The Tfs are monometric glycoproteins (~ 6% carbohydrate) consisting of two homologous domains, each of which contains one high-affinity Fe(III)-binding site. Although the carbohydrate moiety does not seem to be required for Tf function, a partial loss of terminal sialic residues is a distinctive finding in alcoholism. Tf binds two atoms of Fe(III) with high affinity. The binding of Tf to Fe is a pH dependent process, a property that is involved in the physiological mechanism of Fe release from the protein. X-ray crystallographic studies of both human Lf and rabbit Tf indicate that the Fe atom is surrounded by four protein ligands, the phenolate oxygen of two tyrosine residues, an imidazole nitrogen of a histidine residue, and a carboxylate oxygen of an aspartic acid residue. These protein ligands occupy four of the six octahedral sites around each Fe atom, leaving two *cis* positions to be filled by water and or an anion (Borjigin *et al.*, 1999).

The anion is bicarbonate and is bound in a bidentate mode, occupying a pocket between the Fe atom, an arginine side chain, and the N-terminus of helix 5 (Bull *et al.*, 1993a). Serum Tf is a bilobular molecule (Casareno *et al.*, 1998), the two lobes having a high degree of internal homology. These bilobular molecules have one Fe-binding site per lobe and a pseudo two-fold axis linking the two lobes of the molecule. A similar folding pattern is observed in each lobe, consistent with duplication of a primordial gene coding for a 40 kDa monoferric Tf. Binding and release of Fe by Tf are accompanied by dramatic conformational changes in the protein. In the absence of Fe, the two domains involved in binding are widely separated and assume an "open" configuration. On the other hand, insertion of Fe brings the two domains of the binding cleft close towards the metal, and Tf assumes a "closed" configurational state.

Although it has long been believed that the two Fe binding sites of Tf are equivalent and independent, this is not the case. Electron spin resonance and absorption spectroscopy studies comparing the two binding sites of the N- and C- terminal domains provide convincing evidence that the two sites are not identical. Furthermore, the two sites exhibit differences with respect to the effect of pH on the stability of Fe binding and their affinity for Fe at a constant pH. Fe binding to the site in the N-terminal domain is both more acid-labile and of a lower affinity than the binding to the site in the C-terminal domain (association constants of 6.8×10^{19} and 4×10^{20}, respectively, for the 2 sites of human Tf at pH 7.4). Tf in plasma is only about 30% saturated with Fe. It is therefore predicted from the thermodynamics and kinetics of Fe binding that all four species of Tf will be present i.e. Fe-free apotransferrin, fully saturated diferric Tf, and the two monoferric Tfs

containing Fe in either the N-terminal or C-terminal domain binding sites. Chelly *et al.* (1993) found that all four species of Tf in normal human serum elicit a redistribution of iron to the C-terminal site, suggesting that a low molecular weight serum substance causes the preferential binding of Fe to the N-terminal site. There is no evidence that would suggest a functional significance for the difference in the two Fe binding sites of Tf or for the distribution of Fe between the sites in normal human plasma. Reticulocytes and hepatocytes *in vitro* remove Fe equally well from either of the Tf Fe-binding sites.

3.4 METAL-INDUCED TOXICITY

The liver is an important organ of Fe and Cu deposition in overload conditions, and elevated hepatic concentrations of these metals can result in hepatocellular injury. Two main hypotheses have been postulated: the oxidative injury hypothesis and the lysosomal injury hypothesis. A third hypothesis involving lipocytes activation and cytokine expression has recently evolved (Arezzini *et al.*, 2003).

3.5 THE OXIDATIVE INJURY HYPOTHESIS

The oxidative injury hypothesis postulates that Fe and Cu overload can result in the formation of oxyradicals in the liver, with resultant damage to cellular constituents and impairment of hepatocellular function.

3.5.1 Oxyradicals formation by Fe and Cu

Abundant evidence now exists from *in vitro* experiments that both Fe and Cu can, when these metals are available in a redox-active form, catalyze the production of oxyradicals

(Halliwell *et al.*, 1989). Two important radicals that can result from these reactions are lipid radicals and $^{\bullet}OH$. One type of reaction promoted by Fe and Cu that leads to the formation of lipid radicals is the decomposition of preformed lipid hydroperoxides (LOOH). Ferrous (Fe^{2+}) ions or cuprous (Cu^{+}) ions can react with LOOH to form alkoxyl radicals ($LOO^{\bullet}$). Details of this are discussed under the section on ROS. However, the net reaction is:

$$
\begin{array}{llll}
* \; M^{n} + H_2O_2 & \text{------>} & M^{(n+1)} + {}^{\bullet}OH + OH^{-} \\
M^{(n+1)} + {}^{-}{}^{\bullet}O_2 & \text{------>} & M^{n} + O_2 \\
\hline
H_2O_2 + {}^{-}{}^{\bullet}O_2 & \text{------>} & {}^{\bullet}OH + OH^{-} + O_2 \\
 & \text{M catalyst} &
\end{array}
$$

* *Where Mn is a transition metal i.e. Fe or Cu.*

Spin-trapping experiments have confirmed that $^{\bullet}OH$ radicals are produced in the livers of experimental animals after administration of Fe or Cu (Burkitt *et al.*, 1991; Kadiiska *et al.*, 1992; Kadiiska *et al.*, 1995). The $^{\bullet}OH$ is extremely reactive and can attack many cell constituents, including lipids, nucleic acids, carbohydrates and proteins. Furthermore, the polyunsaturated fatty acids (PUFAs) of membrane phospholipids are particularly susceptible to oxidative attack.

3.5.2 Fe and Cu in LPO and oxidative stress

After the initiation of LPO by $^{\bullet}OH$, a number of by-products, including conjugated dienes, LOOH, thiobabituric acid-reactants (TBA-reactants), malondialdehyde (MDA), and 4-hydroxynonenal (HNE) are formed. MDA and HNE, which are reactive aldehydes, can react with proteins and the resulting adducts then serve as markers of LPO. In recent times

isoprostanes have been recognized as suitable markers of oxidative stress (Delanty *et al.*, 1996; Reilly *et al.*, 1997). High concentrations of the metals in the liver seem to be required to produce LPO, suggesting that the normal storage and excretion pathways have to be overwhelmed before Fe or Cu is available to catalyze oxyradical production.

Although oxyradicals have the potential to cause damage to lipids, proteins, carbohydrates, and DNA, cells contain protective mechanisms in the form of antioxidants (including vitamins), scavenging enzymes, and repair processes that counteract the effects of oxyradical production. The net effect of this cellular function depends on the balance between radical production and cytoprotective agent response.

3.6 SUBCELLULAR ORGANELLE DAMAGE

3.6.1 Lysosomal Injury Hypothesis

Accumulation of Fe and Cu in lysosomes is a common feature of Fe and Cu overload. It is generally considered that sequestration of Fe or Cu within lysosomes serves a protective role by removing the redox-active metal from the cytoplasm and by providing a route for removal from the liver through lysosome-mediated biliary excretion (La Russo, 1989). The lysosomal injury hypothesis proposes that excess accumulation of Fe or Cu within the lysosomes can lead to lysosomal fragility, impaired lysosomal function, and eventually cellular injury through the release of hydrolytic enzymes and stored metals into the cytoplasm.

3.6.2 Mitochondria

Table 1 The effect of Iron or Copper Overload *In Vivo* on hepatic mitochondria.

Metal	Observation
Iron Overload	Lipid peroxidation
	Impaired oxidative metabolism
	Decreased cytochrome c oxidase
	Decreased Ca^{2+} sequestration
	Decreased Ca^{2+} release
	Decreased content of reduced pyrimidine nucleotides
Copper Overload	
	Lipid peroxidation
	Impaired oxidative metabolism
	Decreased cytochrome oxidase

Table 1 summarizes the effects of Fe and Cu overload on hepatic mitochondria in experimental animals. Mitochondrial oxidative metabolism is susceptible to metal-induced impairment. In normal mitochondria, electron transport is tightly coupled to the phosphorylation of adenosine diphosphate (ADP). Thus, in the absence of ADP, the rate of oxygen consumption is low, while with ADP present the rate of oxygen consumption is increased. Normal mitochondria, therefore, have a high respiratory control ratio (RCR). Hepatic mitochondria from Fe-loaded rats show significant decreases in the state 3 respiratory rate and in the RCR at moderate degrees of hepatic Fe overload. At hepatic Fe concentrations at which oxidative metabolism is decreased, evidence of conjugated diene formation indicative of mitochondrial LPO is evident. Similar damage to the mitochondrial respiration chain in association with LPO has been observed in rats with Cu overload (Sokol *et al.*, 1993). These studies suggest that chronic hepatic Fe or Cu overload *in vivo* results in an inhibitory defect in the mitochondrial electron transport chain. Similar defects in oxidation are produced *in vitro* by metal-induced peroxidation of normal mitochondria.

The effect of both Fe and Cu overload on mitochondrial respiration results primarily from a decrease in cytochrome c oxidase activity. Cytochrome oxidase is functionally dependent on intact cardiolipin, a mitochondrial phospholipid that contains a high percentage of PUFA. Thus, it is likely that LPO damages cardiolipin, which may impair cytochrome oxidase activity. Alternatively, direct peroxidative injury to the protein subunits of cytochrome oxidase might occur concomitantly with mitochondrial LPO in Fe overload. The impairment in mitochondrial oxidative capacity caused by Fe or Cu overload could have a deleterious effect on the energy state of the liver. Consistent with this possibility, chronic dietary Fe-overload in rats results in a substantial decrease in hepatic ATP concentrations (Pietrangelo *et al.*, 1995b). This decrease in hepatic ATP levels may disturb hepatocellular function and compromise cellular integrity.

Chronic Fe overload in rats also results in impaired calcium sequestration by hepatic mitochondria (Britton *et al.,* 1991), which occurs in parallel with a decrease in substrate oxidation. Since mitochondrial calcium sequestration depends on the maintenance of the mitochondrial transmembrane potential, it is likely that the defect in substrate oxidation is at least in part responsible for the altered mitochondrial calcium sequestration. Furthermore, an increase in mitochondrial permeability may play a role in decreasing calcium sequestration (Britton, 1996).

3.6.3 Endoplasmic Reticulum (ER)

Hepatic microsomal LPO has been found *in vivo* in rats with chronic dietary Fe overload, when the hepatic content exceeded a certain threshold (Bacon *et al.*, 1986). In addition,

decreases in mitochondrial cytochrome P-450, aminopyrine demethylase activity, and cytochrome b5 were associated with microsomal LPO in the model. Although this finding does not prove direct causality, it seems likely that the loss of these cytochromes was the result of peroxidative damage. It has been demonstrated *in vitro* that Fe-induced peroxidation in hepatic microsomes causes a reduction in cytochrome P-450 (Waller *et al.*, 1983). Bonkovsky *et al.* (1984) measured antipyrine clearance and hepatic cytochrome P-450 concentrations in patients with various types of Fe overload. Although the number of patients studied was very small and some variations existed between the groups, no differences were found between Fe-loaded patients and controls. Another microsomal function that is sensitive to the damaging effects of peroxidation is calcium sequestration (Waller *et al.*, 1983). Chronic Fe overload in rats results in an impairment in hepatic microsomal calcium sequestration, and this may alter calcium homeostasis and contribute to cell injury.

3.6.4 Plasma membrane

Little data are available concerning the effects of Fe or Cu overload on liver plasma membrane. At a mild degree of Fe overload in rats, there is a decrease in the content of unsaturated fatty acids in the phospholipids of the plasma membrane fraction. Similar changes are also seen in the mitochondrial membranes, and these changes in membrane composition are consistent with the occurrence of LPO. It is possible that some enzymes in the plasma membrane of the hepatocytes may be inhibited by Fe or Cu overload, since it has been shown that some thiol-rich enzymes (such as Na^+, K^+- ATPase) in plasma membranes of heart cells are sensitive to Fe (Link *et al.*, 1994).

3.6.5 Hepatic DNA damage

Patients with long-standing HH with cirrhosis are at increased risk of developing HCC. Accordingly, it has been proposed that HCC in these patients may be a consequence of Fe-induced oxidative damage to hepatic DNA, combined with the replicative stimulus provided by the nodular regeneration of cirrhosis. Fe salts have been shown to produce DNA strand breaks when incubated *in vitro* with purified DNA or with isolated rat liver mitochondria or nuclei (Imlay *et al.*, 1988; Hruszkewycz, 1988). In addition, it has been demonstrated that endogenous Fe plays a key role in the DNA damage produced by hydrogen peroxide in mammalian cells, because pre-treatment with Fe chelating agents diminishes this damage (Mello *et al.*, 1984). It is thought that some Fe is bound to DNA *in vivo* and that this Fe, in the presence of $^{\bullet-}O_2$ and H_2O_2, can catalyze the formation of "site-directed" $^{\bullet}OH$ radicals that cause DNA damage (Halliwell *et al.*, 1990). LPO products in the presence of Fe can also produce DNA damage *in vitro* through a mechanism that may also involve $^{\bullet}OH$ radicals (Park *et al.*, 1992).

The first evidence that chronic Fe overload *in vivo* results in damage to hepatic DNA was provided by studies that showed an increased number of strand breaks in hepatic DNA from Fe-loaded rats (Edling *et al.*, 1990). The induction of strand breaks in DNA has been associated with both initiation and promotion events in chemically induced carcinogenesis (Walles *et al.*, 1984; Hartley *et al.*, 1985). Increased oxidative damage in hepatic DNA has been demonstrated in acyl hydrocarbon (*Ah*) - responsive mice after a single subcutaneous injection of Fe dextran (Faux *et al.*, 1992). Oxidative DNA was evaluated using 8-hydroxydeoxyguanosine (8OHdG) as a marker. It has been demonstrated that DNA

templates containing 8OHdG are misread both at the modified base and at adjacent residues, which could result in oxidative mutagenesis (Kuchino *et al.*, 1987; Wood *et al.*, 1990). In addition to producing DNA damage, Fe can cause the transformation of cells. Repeated intraperitoneal injections of rats with the Fe chelate ferric nitrilotriacetate (FeNTA) resulted in renal adenocarcinoma with metastasis to the liver and lung (Okada *et al.*, 1983). Exposure of cultured rat epithelial cells to a high concentration of iron nitrilotriacetate (FeNTA) resulted in the appearance of some cells that showed morphological transformation, grew in soft agar, and induced metastatic carcinoma when injected in newborn rats. This suggests that oxidative damage to DNA catalyzed by FeNTA may play a key role in the rapid neoplastic transformation of these cells (Yamada *et al.*, 1990).

Little information is available concerning DNA damage in patients with Fe overload. In a study on hepatic DNA samples from 6 patients with HH, "bulky" DNA lesions were detected that contained 2 to 50 base modifications per 100 million nucleotides. Surprisingly, the levels of 8OHdG were not raised in these samples, suggesting that these "bulky" DNA lesions may be a more sensitive indicator of Fe-induced DNA damage (Carmichael *et al.*, 1995).

Ionic Cu in the presence of H_2O_2 or reducing agents can cause DNA damage *in vitro* (Aruoma *et al.*, 1991). Cu overload in rats results in increased levels of 8OHdG in hepatic DNA, indicative of oxidative damage. In Long Evans Cinnamon (LEC) rats, long-term administration of Cu could lead to chronic hepatitis, increased levels of 8OHdG in hepatic

DNA, and HCC (Masuda *et al.*, 1988). Administration of penicillamine (Cu-chelating agent) to LEC rats could prevent these effects. This suggests that the development of HCC in these animals might be related to Cu-induced oxidative DNA damage. In patients with Wilson disease (WD), "bulky" lesions of hepatic DNA have been reported, without increase in 8OHdG content (Carmichael *et al.,* 1995). HCC is rarely seen in WD, perhaps because the usual clinical course of the disease does not allow sufficient time for it to develop.

Evidence exists of oxidative injury to hepatic DNA in animals with Fe and Cu overload. This damage might be an important step leading to carcinogenesis, especially when coupled with a regenerative stimulus provided by cirrhosis. Although hepatic DNA damage has been detected in patients with HH or WD, it is not known if this is the result of an oxidative process.

3.6.6 Iron Induced Hepatocarcinogenesis

The main clinical, biologic, and pathologic features of HCC complicating haemochromatosis are similar to those of other HCCs (Deugnier *et al.*, 1993b). Iron free foci (IFF) defined as clear-cut sublobular nodules of hepatocytes free of iron or either significantly less iron than the surrounding parenchyma were found in 7.6% of 185 patients with uncomplicated haemochromatosis and in 83% of haemochromatosis patients with HCC (Deugnier *et al.*, 1992, 1993a). Evidence from experimental (Hirota and Williams, 1979) and clinical (Deugnier *et al.*, 1993a) data, points to the possible involvement of IFF as an early step toward HCC. Cirrhosis is no longer thought to be a prerequisite for the

development of HCC in haemochromatosis livers and therefore, iron could be a (co) carcinogenic factor. Although there is some evidence of the promoting effect of iron on tumour cell growth *in vivo* (Thompson *et al.*, 1991) and *in vitro* (Bergeron *et al.*, 1985), a direct carcinogenic effect of iron has not been documented in rats. Oxidative stress has been suggested as a possible mechanism of iron-induced HCC. Excessive oxidative stress as seen in iron overload may cause DNA alterations including point mutations, deletion, additions or chromosomal translocations. Moreover, environmental toxins such as iron may alter the methylation status of DNA. These events may lead to potential mutagenic effects (Pogribny *et al.*, 1995) and activation of oncogenes and inactivation of tumour suppressor genes. The mutation frequency of the p53 tumour suppressor gene in HH was 60% A:T to G:C and 40% A:T to T:A mutations in one study (Vautier *et al.*, 1999). This mutation spectrum suggests that etheno-deoxyguanine or etheno-deoxyadenine DNA adducts may be responsible for the DNA damage. These DNA modifications are produced by the reaction with LPO products in the livers of HH patients (Nair *et al.*, 1998).

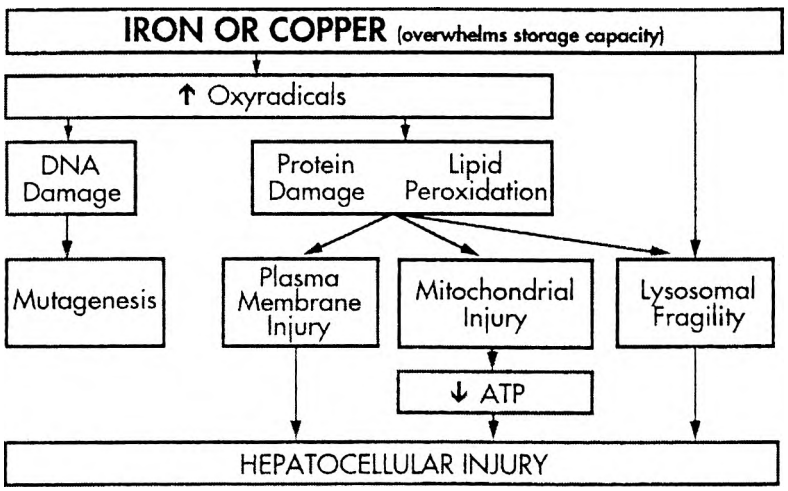

Figure 5 Mechanisms of hepatotoxicity induced by Fe or Cu overload.

3.7 COPPER (Cu)

3.7.1 BIOCHEMISTRY AND PHYSIOLOGY

The major functions of Cu metalloproteins involve oxidative-reduction reactions. Most known Cu-containing enzymes bind and react directly with molecular oxygen. Cu is an integral component of many metalloenzymes, including ceruloplasmin, cytochrome c oxidase, superoxide dismutase, dopamine-β-hydroxylase, ascorbate oxidase, lysyl oxidase and tyrosinase (Linder and Hazegh-Azam, 1996).

A number of pathological conditions have been attributed to the loss of cuproenzyme activity. Failure of pigmentation has been attributed to depressed tyrosinase activity required in the first step in the biosynthesis of melanin. A variety of connective tissue cross-linking defects (cardiac, vascular, and skeletal) may be caused by a loss of lysyl oxidase activity (Owen, 1982; Strain, 1994). Ataxia may result from depressed cytochrome c oxidase activity of motor neurons. Depressed dopamine-9-hydroxylase activity can result in abnormal catecholamine conversions. Furthermore, Cu plays an important role in Fe metabolism. Cu deficiency impairs Fe absorption, and anaemia accompanies severe Cu deficiency. Ceruloplasmin, the major Cu-containing protein in plasma, has a ferroxidase activity that oxidizes ferrous Fe to the ferric state prior to its binding by plasma Tf (Owen,1973).

3.7.1.1 Metabolism

Cu absorption is maximal in the duodenum and may be absorbed from the stomach. Within the intestinal mucosa cells, Cu can react with metallothionein, a sulfhydryl-rich protein

group that binds Cu through the formation of mercaptide bonds. Other metal ions, particularly zinc and cadmium, compete with Cu for sulfhydryl-binding sites, which explain the antagonism of these metals toward Cu absorption (Rojas *et al.,* 1996). The amount of Cu absorbed from the intestine is between 50% and 80% of ingested Cu (Johnson and Milne, 1991). Factors affecting Cu levels include gender (women absorb a greater percentage than men), the amount ingested, the chemical form, and certain dietary constituents. The latter include other trace elements, sulfate, various amino acids, fibre, and phytates. Cu absorption may be impaired in patients with diffuse diseases affecting the small bowel such as sprue, lymphosarcoma, and scleroderma. Absorbed Cu is rapidly transported to the liver where it is stored, mostly as metallothionein-like cuproprotein. Cu is released from the liver, mainly as ceruloplasmin, a multifunctional cuproprotein that accounts for 60% to more than 80% of the total Cu in the plasma. Cu may be transported to cells for incorporation into Cu-containing enzymes by several identified transport mechanisms. These include ceruloplasmin, transcuprein, Cu-albumin, and Cu-amino acid complexes. The movement of Cu within the cell and its incorporation into cuproproteins may be regulated by both glutathione and metallothionein (Anon, 1991). The liver is the key organ in the homeostatic regulation of Cu metabolism. Cu is stored in the liver and incorporated and released as ceruloplasmin to maintain blood levels. Intestinal absorption mechanisms and regulation of biliary excretion also have major roles in regulating of Cu homeostasis (Sternlieb, 1980).

Cu is excreted primarily in the faeces as unabsorbed dietary Cu and from the biliary and gastrointestinal secretions. Biliary Cu excretion ranges from 0.5 to 1.3 mg/day. Cu losses

in the urine and sweat amount to less than 3% of dietary intake. Menstrual losses of Cu are minor: 0.1 to 0.8 mg per menstrual period. Estrogens increase serum Cu concentrations, probably by increasing hepatic ceruloplasmin synthesis. Serum Cu concentration is normally higher in women than men. Testosterone and progesterone administration has also been reported to increase plasma Cu levels (Mehta *et al.*, 1989).

During infections or inflammatory stress, serum Cu concentrations rise because of the acute-phase action of interleukin-1 (Rafter, 1994). Elevated serum Cu concentrations are seen in portal cirrhosis, biliary tract disease, and hepatitis, probably because excess Cu, which would normally be excreted in the bile, is retained in the circulation. Hypocupraemia has been observed in haemolytic jaundice, haemochromatosis, and some types of cirrhosis because of the inability of the damaged liver to synthesize ceruloplasmin.

3.7.1.2 Cu Homeostasis

Cu ions are involved in a unique chemistry as a result of their ability to adopt distinct redox states, either oxidized [Cu(II)] or in the reduced state [Cu(I)]. Consequently, Cu ions serve as important catalytic cofactors in redox chemistry for proteins that carry out fundamental biological functions that are required for growth and development. Cu-requiring proteins are involved in a variety of biological processes and deficiencies in these enzymes, or alterations in their activities, often cause disease states or pathophysiological conditions as shown in Table 2.

Table 2 Disease states or pathophysiological conditions associated with copper.

Common Name (Cu containing substances)	Biological Function	Consequence of Deficiency or Defects
Cu/Zn SOD	Free radical detoxification	Oxidative damage of cell components
Cytochrome c oxidase	Electron transport in the mitochondria	Symptoms of deficiency of ATP:myopathy, ataxia, seizures
Lysyl oxidase	Cross linking of collagen and elastin	Connective tissue symptoms: vascular rapture and torsion, Loose skin and joints, emphysema,
Dopamin-9-hyroxylase	Catecholoamine production	Hypothalamic imbalance: hypothermia, Hypotension, dehydration, somnolence
Tyrosinase,	Melanin production	Depigmentation
Peptidylglycine Monooxygenase	Bioactivation of Peptide hormones	Probable widespread effects through malfunction of several peptide hormones
Ceruloplasmin	Ferroxidase, Cu transport	Anemia
Clotting Factor, V, VIII	Blood clotting	Bleeding tendency
Angiogenin,	Induction of blood vessel	Defective blood vessel development
Metallothionein	Cu – sequestration	Cu toxicity
Prion protein	Normal function currently unknown; Cu binding properties suggest potential role in Cu uptake	Altered sleep pattern and circadian rhythm in mice, Creutzfeld Jacob disease, Kuru, Gerstmann-Straussler-Scheinker disease Fatal familial insomnia
β-amyloid precursor protein	Normal function currently unknown	Familial Alzheimer's disease,
Hephaestin,	Iron egress from intestines	Sex-linked anaemia

Cu is also a potent cytotoxin when allowed to accumulate in excess of cellular needs. In addition to the generation of ROS, Cu may manifest its toxicity by displacing other metal cofactors from their natural ligands in key cellular signalling proteins. For example, the replacement of Zn(II) by Cu(II) in the zinc-finger DNA binding domain of the human

oestrogen receptor renders this protein defective in binding to its cognate target DNA sequences *in vitro*, thereby potentially interfering with its role in hormone-dependent signal transduction *in vivo* (Predki and Sarkar 1992).

3.7.1.3 Cu uptake and absorption

Organisms must have uptake mechanisms to absorb Cu from nutrients, transport Cu across biological membranes, and deliver it to Cu-requiring proteins. However, precise regulatory mechanisms must be in place to prevent the accumulation of Cu ions to toxic levels. The importance of maintaining this critical balance is underscored by the existence of two well-characterised human genetic diseases in Cu transport, Menkes and Wilson Disease (WD) (Bull and Cox, 1993b). In mammals, dietary Cu is absorbed across the mucosal membrane in cells that line the stomach and the small intestines. Exactly how this occurs is currently unknown. It has been proposed that Cu diffuses through the mucous layer that covers the intestinal wall (Linder, 1991). However, given the exquisite care with which copper is guided into and within yeast cells it seems unlikely that diffusion alone will account for this process.

3.7.1.4 Post intestinal mucosal cell transport

The pathway of Cu through the baso-lateral membrane has been identified through studying Menkes disease. Menkes disease is characterized by progressive neurological impairment and death in infancy. The entrapment of Cu in intestinal cells, kidney and vascular endothelial cells in the blood-brain barrier in Menkes patients leads to Cu deficiency, as ascertained by defects in the activities of many Cu-dependant proteins. The

isolation of the Menkes disease gene (ATP7A) showed that this gene encodes a membrane associated P-type ATPase (Chelly *et al.*, 1993).

3.7.1.5 Cu in circulation

In the portal blood and systemic circulation Cu is bound to albumin and histidine. Exactly how albumin and histidine relinquish Cu to organs and tissues is currently unclear. However, it is possible that the bound Cu is handed off to the hCtr1 Cu transporter, either directly or indirectly. The predominant Cu-containing protein in mammalian serum is ceruloplasmin, a glycosylated multi-Cu ferroxidase synthesized primarily in the liver and that carries >95% of the total serum Cu. Ceruloplasmin coordinates 7 Cu atoms that are incorporated during its biosynthesis and maturation in the secretory pathway (Sato and Gitlin, 1991). Although it is not yet established whether ceruloplasmin is involved in Cu mobilization from the serum, the absence of ceruloplasmin in patients in aceruloplasminemia, a genetic disorder of ceruloplasmin deficiency, has not yet been shown to alter Cu levels in the peripheral tissues examined (Harris *et al.*, 1998).

It has been proposed that excess Cu is stored in the vacuoles to prevent toxicity. The role of putative Cu chaperones for targeting Cu to the vacuole and their mechanism of action is unknown. Furthermore, the mechanism by which Cu ions are delivered from the plasma membrane transporters to the Cu chaperones without releasing free Cu ions into the cytosol remains unclear.

3.8 CLINICAL SIGNIFICANCE

Cu deficiency in infants has been observed in prematurity, malnutrition, malabsorption, chronic diarrhoea, hyperalimentation, and prolonged feeding with low-Cu total-milk diets. The susceptibility of premature infants to Cu deficiency is related to their low stores of liver and spleen Cu (which accumulates rapidly during the last trimester of gestation) and the probability of longer feeding exclusively on milk formulae. A deficit in protein nutrition is sufficient to impair Cu transport and storage and may also be a causal factor. Signs of Cu deficiency include (1) neutropenia and hypochromic anaemia in the early stages, both of which are responsive to oral Cu but not iron; (2) osteoporosis and various bone and joint abnormalities that reflect deficient Cu-dependent cross-linking of bone collagen and connective tissue; (3) decreased pigmentation of the skin and general pallor, which are attributed to tyrosine-required melanin synthesis; and (4) in the later stage, possible neurological abnormalities (hypotonia, apnea, psychomotor retardation), probably caused by cytochrome c oxidase deficit. Long-term hyperalimentation with infusates deficient in trace minerals has been shown to produce Cu deficiency in both infants and adults. Observed signs are those usually associated with Cu deficiency, including lowered plasma Cu and ceruloplasmin, anaemia, etc. Cu deficiency has also been associated with Zn therapy for sickle cell disease and treatment with Cu-chelating agents such as penicillamine. Low levels of serum Cu contribute to an increased risk of coronary heart disease through instability of heart rhythm and hyperlipidemia. Experimental animals fed Cu-deficient diets and human subjects fed diets believed to be marginal in Cu have exhibited many signs closely related to coronary heart disease. These include abnormal electrocardiograms, hypercholesterolaemia, glucose intolerance, and hypertension.

3.8.1 Menkes' syndrome

An extreme form of Cu deficiency is seen in Menkes' syndrome, an X-linked genetic defect in Cu transport and storage. Clinical manifestations occur early in life and include kinky or twisted, brittle steely hair (attributed to loss of Cu-catalyzed disulfide bond formation), depigmentation, and vascular defects. The affected infants are Cu-deficient, and have low serum, hepatic, and cerebral Cu concentrations, low ceruloplasmin levels, and little or no cytochrome c oxidase activity in nerve tissues. Symptoms usually appear by three months of age, with death occurring by five years of age. Affected infants exhibit a build up of copper in the duodenal mucosal tissue as a result of defective Cu absorption. Red cell Cu is not decreased, and neutropenia and anaemia, two usual signs of Cu deficiency, do not appear.

3.8.2 Wilson disease (WD)

WD (hepatolenticular degeneration) is a genetically determined Cu accumulation disease that usually presents between 6 and 40 years of age. Disease symptoms include neurological disorders, cirrhosis, and Kayser-Fleischer rings (green-brown discoloration) in the cornea caused by Cu deposition. Cu accumulates in the liver, brain, kidney, and cornea. The haemolysis, necrosis, and other cellular damage that occur may be caused by LPO, a known effect of Cu toxicity. Urinary Cu excretion is increased. The hepatic synthesis of ceruloplasmin is decreased, which results in a low serum concentration of this enzyme (<20 mg/dl). Serum Cu is generally decreased because of low ceruloplasmin concentrations. Thus, the simultaneous measurements of serum Cu, ceruloplasmin, and urinary Cu are useful in the diagnosis of this disease.

4.0 THE CHEMISTRY OF FREE RADICAL REACTIONS

4.0.1 The Definition and Reactions of Free Radicals

Free radicals are formed from molecules by breaking a bond such that each fragment keeps one electron. Free radicals may also be formed by collision of the non-radical species by a reaction between a radical and a molecule, which must then produce a radical since the total number of electrons is odd (Aruoma, 1998). Radical ions are positively or negatively charged free radicals, e.g. a protonated amine radical (H_3N^+), or the superoxide radical anion ($^{\bullet-}O_2$).

Even though a species is an ion depending on the number of its electrons in relation to the number of protons, all species with unpaired electrons in their outer orbital are free radicals, independent of the number of protons. Several chemical reactions are inhibited by the fission of the two-electron bond. The bond may be cleaved symmetrically, producing free radicals (Eq.1), or asymmetrically, when ions are formed (Eq.2).

$$A{:}B \text{ -----> } A\cdot + B_+ \qquad (1)$$

$$A{:}B \text{ -----> } A{:}^- + B^+ \qquad (2)$$

Chemical substances may be converted into free radicals by irradiation (i.e. X-ray or UV), or by additives called inhibitors. It has long been known that ionizing radiation produces free radicals in biological systems, and these play a major role in the aetiology of radiation injuries. In addition, free radicals may be formed in aerobic organisms, including humans, in the course of physiological and pathological processes or by exogenous agents (Del Maestro, 1980).

Free radical reactions are, in general, chain reactions. In the course of these reactions, free radicals are formed during the initiation step(s). These enter into reactions in the course of several propagation steps, during which the number of free radicals is conserved until they are eventually destroyed in a termination process.

Free radicals of importance in living organisms include hydroxyl ($^{\bullet}OH$), superoxide ($^{\bullet-}O_2$), nitric oxide ($NO^{\bullet}$), thyl ($RS^{\bullet}$) and peroxyl ($ROO^{\bullet}$). Peroxynitrite ($ONOO^{-}$), hypochlorous acid (HOCl), hydrogen peroxide (H_2O_2), singlet oxygen ($^1\Delta g$) (often written as $^1O_2$) and ozone (O_3) are not free radicals, but can easily lead to a free radical reaction.

4.0.2 Radicals of Molecular Oxygen: Physical and Chemical Properties.

Radicals formed from molecular oxygen are a serious hazard for both living and nonliving matter. The biradical property of oxygen allows it to act as an initiator and to participate in additive reactions. Nevertheless, it is basically a weak oxidant as a result of its free electron with parallel spin. Reactive intermediates of oxygen are generated by reduction or excitation. Reactive intermediates formed in the course of excitation and reduction, are not invariably free radicals (e.g. delta singlet oxygen or H_2O_2). Nevertheless, they resemble free radicals in their reactivity and importance. These are called "reactive oxygen intermediates" (ROI's).

4.0.3 Reduction

In the course of the complete tetravalent (four-electron) reduction of oxygen, water is formed. If it undergoes sequential univalent (one-electron) reduction, reactive

intermediates are formed. The $^{\bullet}O_2$, H_2O_2 and the $^{\bullet}OH$ are such intermediates. These may damage biological systems. According to the quantum reduction mechanical concept of spin restriction, univalent reduction is more likely to occur *in vivo*. In living organisms therefore, oxidative enzymes (i.e. cytochrome oxidase) have developed, which circumvent the law of spin restriction and catalyze divalent and tetravalent reduction of oxygen, so that only small amounts of ROIs are formed. Cytochrome oxidase catalyzes the tetravalent reduction of oxygen and it is responsible for the bulk of the total oxygen consumption in the course of cellular metabolism. Nevertheless, ROIs are formed in small amounts during cellular metabolism, but the defence systems are able to neutralize them under normal conditions. Additionally, ROI's are formed during autooxidation of different chemical compounds, more readily via univalent reduction of O_2 (Miller *et al.,* 1990). For example, during autooxidation of hydroquinones, leukoflavins, catecholamines, thiols, tetrahydropterins, or oxyhaemoglobin, $^{\bullet-}O_2$ are formed. Furthermore, ROI's are generated during enzymatic processes (e.g. of xanthine oxidase), in subcellular organelles (i.e. mitochondria, chloroplast), or during cell functions of phagocytes or thrombocytes.

4.0.4 Excitation

$^1O_2$ is formed if one of the unpaired electrons of molecular oxygen is transferred via energy absorption to a higher energy orbital and its spin is inverted. $^1O_2$ exists in two states, i.e. as delta singlet oxygen $\Delta\ ^1O_2$ in which the newly paired electrons occupy the same orbital, and sigma singlet $\Sigma\ ^1O_2$ in which the electrons of opposite spins are in different orbitals. The excess energy of $^1O_2$ may be spent through thermal decomposition, light emission, or chemical reaction (as indicated by chemiluminescence) (Klebanoff, 1980; McCord *et al.,* 1978).

4.0.5 Reactions in which ROI's are Formed

$^{\bullet-}O_2$ may be found during autooxidation of various compounds, in the mitochondrial respiratory pathway, if the members of the cycle are reduced and react with oxygen, in chloroplast, and in connection with phagocyte function and reduced nicotinamide adenine dinucleotide phosphate (NADPH) oxidase function (Rossi *et al.,* 1985). The reactivity of $^{\bullet-}O_2$ is limited. Its importance lies in its ability to oxidize transition metal complexes and organic substrates, to bind to metals, and to be transformed into other ROIs. In acid media, such as the vacuole of the phagocyte or the micro-environment of cell membranes, $^{\bullet-}O_2$ is protonated into the perhydroxy radical ($H\,O_2^{-\bullet}$). The cell surface, containing polyanions, attract H^+ ions. $H\,O_2^{-\bullet}$ is a stronger oxidant than $^{\bullet-}O_2$ and is cytotoxic.

H_2O_2 is formed either by the divalent reduction of molecular oxygen catalysed, for example, by glucose oxidase or from $^{\bullet-}O_2$ catalyzed by the enzyme superoxide dismutase (SOD) (Fridovich, 1989). During the Harber Weiss reaction of $^{\bullet-}O_2$ and H_2O_2 the extremely reactive $^{\bullet}OH$ radical is produced.

$$^{\bullet-}O_2 + H_2O_2 \text{ --------> } O_2 + {}^{\bullet}OH + OH^-$$

This reaction, however, proceeds very slowly in living organisms and thus significant amounts of $^{\bullet}OH$ are not formed. The reactions are accelerated by metal catalysis, resulting in a Fenton-type reaction where significant amounts of $^{\bullet}OH$ may be produced.

$$\begin{array}{llllllll} ^{\bullet-}O_2 & + & * M^{n+1} & \text{-------}> & M^n & + & O_2 & \\ M^n & + & H_2O_2 & \text{-------}> & M^{n+1} & + & {}^{\bullet}OH & + \quad OH^- \\ \hline H_2O_2 & + & H_2O_2 & \text{-------}> & O_2 & + & {}^{\bullet}OH & + \quad OH \end{array}$$

* *Where M is a transition metal, i.e. Fe or Cu.*

By analogy with the Fenton reaction, hydroperoxide may participate in the reaction instead of H_2O_2.

$$Fe^{2+} + ROOH \text{ -------> } Fe^{3+} + RO^{\bullet} + OH^{-}$$

The alkoxy radical $RO^{\bullet}$ is only slightly less reactive than the $^{\bullet}OH$ radical, and may damage biological systems excessively, either itself or the $^{\bullet}OH$ produced as a result of internal hydrogen atom transfer. $^1O_2$ may be formed in the following reactions:

$$H_2O_2 + {}^{\bullet-}O_2 + H^{+} \text{ --------> } {}^1O_2 + H_2O_2 \quad (1)$$

$$^{\bullet-}O_2 + H_2O_2 \xrightarrow{\text{metal}} {}^1O_2 + {}^{\bullet}OH + OH^{-} \quad (2)$$

$$OCl^{-} + H_2O_2 \text{ --------> } {}^1O_2 + Cl^{-} + H_2O_2 \quad (3)$$

$$^{\bullet}O_2 + {}^{\bullet}OH \text{ --------> } {}^1O_2 + OH^{-} \quad (4)$$

$$2\,{}^{\bullet-}O_2 + R-\overset{O}{\overset{\|}{C}}-O-O-\overset{O}{\overset{\|}{C}}-R \text{ --------> } 2\,{}^1O_2 + 2RCO_2^{-\bullet} \quad (5)$$

Reaction (1) is an analogue of the spontaneous dismutation of $^{\bullet-}O_2$. Spontaneous dismutation is the same as the SOD-catalyzed reaction, but is a nonenzymatic reaction and is much slower. Reaction (2) is a variant of the Fenton reaction. Reaction (3) occurs in the course of the function of the granulocyte myeloperoxidase – H_2O_2 – halide system. $^1O_2$ may be formed during the interaction of $^{\bullet-}O_2 + {}^{\bullet}OH$ (reaction 4) and of $^{\bullet-}O_2$ and diacyl peroxides (reaction 5) (Badway and Karnovsky, 1980; Fantone *et al.*, 1982).

4.1 REACTIVE OXYGEN SPECIES (ROS) INVOLVED IN IRON OVER - LOAD

4.1.1 Superoxide radical ($^{\bullet-}O_2$)

The $^{\bullet}O_2$ is an oxygen-centered radical with selective reactivity. This species is produced by a number of enzyme systems, by autooxidation reactions, and by non-enzymatic electron transfers that univalently reduce molecular oxygen. In aqueous solution, $^{\bullet-}O_2$ can oxidize ascorbic acid. It can also reduce certain iron complexes, such as cytochrome c and ferric-ethylenediaminetetraacidic acid (Fe^{3+}-EDTA). SOD accelerates the dismutation of $^{\bullet-}O_2$, converting it to H_2O_2 and O_2 (Fridovich, 1989; Richter *et al.,* 1977). Some $^{\bullet-}O_2$ is made deliberately. For example, the phagocytes (neutrophils, monocytes, macrophages, eosinophils) generate large amounts of $^{\bullet-}O_2$ as part of their killing mechanism (Babior and Woodman 1990; Weiss 1989). When this essential defence mechanism goes wrong, several diseases are accompanied by excessive phagocyte activation, leading to tissue damage, to which ROS and reactive nitrite species (RNS) are contributory factors (Babior and Woodman 1990; Eze, 1993). Neutrophils have the function of recognizing foreign particles such as bacteria, either because bacteria have an unusual surface or, more often, because antibodies are bound to them. Enzymes like SOD seem to have specifically evolved to make $^{\bullet-}O_2$ exist in the plasma membrane of neutrophils. Although normally inactive, this enzyme is activated when neutrophils encounter a foreign particle. The enzyme takes NADPH from the neutrophil cytosol, oxidizes it to $NADP^+$, and passes electron onto O_2, hence reducing O_2 to $^{\bullet-}O_2$ outside the cell (Rossi *et al.*, 1985; Klebanoff, 1980). Activation of the enzyme occurs at the point of contact particle, and this piece of membrane is then used to engulf the particle, forming a phagocytic vacuole. The

importance of the production of $^{\bullet}O_2$ in humans is shown by chronic granulomateous disease (CGD) (Curnutte and Babior, 1987), a collective name given to inborn disorders in which the membrane-bound NADPH oxidase is inactive.

$^{\bullet-}O_2$ production is activated when foreign particles touch the neutrophil surface and some $^{\bullet-}O_2$ escapes into the extracellular fluid. Yet extracellular fluids have little superoxide dismutase activity. Thus, excessive production of $^{\bullet-}O_2$ and HOCl by activated phagocytes can impose an oxidative stress on the surrounding tissues, and this happens in several human diseases.

4.1.2 Hydrogen peroxide (H_2O_2)

H_2O_2 is not a free radical. It can cross membranes and slowly oxidize a number of compounds. H_2O_2 can be formed *in vivo* when $^{\bullet-}O_2$ dismutates and also by many oxidase enzymes, including monamine and amino acid oxidases. Xanthine oxidase converts hypoxanthine to xanthine and xanthine to urate, O_2 being simultaneously reduced to both $^{\bullet-}O_2$ and H_2O_2 (Granger, 1988). Levels of xanthine oxidase are normally low in human tissues, but they may increase after injury, such as trauma or ischaemia (Buckley, 1994).

Some metabolic roles of H_2O_2 are known, and others have been proposed. H_2O_2 can regulate gene expression: one mechanism is by (directly or indirectly) displacing an inhibitory subunit from the cytoplasmic gene transcription factor NF-κB (Schreck *et al.*, 1992), at least in some cell types (Brennan and O'Neill, 1995). The activated factor then migrates to the nucleus and causes expression of multiple genes. Other peroxides (such as

lipid peroxides) do the same (Collins, 1993). H_2O_2 at low (micromolar) levels also seems to be poorly reactive. However, higher levels of H_2O_2 can attack several cellular energy-producing systems. For example, it inactivates the glycolytic enzyme glyceraldehyde-3-phosphate dehydrogenase. H_2O_2 also forms the $^{\bullet}OH$ in the presence of transition metal ions and O_2, and can facilitate this reaction (Miller *et al.*, 1990).

4.1.3 Hydroxyl radical ($^{\bullet}OH$)

Much of the toxicity of $^{\bullet-}O_2$ and H_2O_2 involves formation of $^{\bullet}OH$. The $^{\bullet}OH$ radical is a highly reactive oxygen-centered radical with an estimated half-life in cells of only 10^{-9} seconds. One feature of the $^{\bullet}OH$ (and other radicals) is that it gives rise to another radical. Thus, when it reacts with a molecule, the result is the formation of another radical species. The resulting species usually has lower reactivity than the $^{\bullet}OH$. $^{\bullet}OH$ radicals attack all proteins, DNA, PUFAs in membranes and many other biological molecules. In the case of $^{\bullet}OH$ generation by Fenton type chemistry, the extent of $^{\bullet}OH$ formation is largely determined by the availability and location of the metal ion catalyst. In an *in vitro* study in which the technique of gas chromatography with selected ion monitoring (GC/MS/SIM) was used to compare the role of Cu and Fe ions in promoting damage to DNA by H_2O_2, Cu ions were significantly more reactive in causing DNA damage in the presence of H_2O_2 than were equimolar Fe ions (Aruoma *et al.*, 1991).

The availability of "free" Fe and Cu *in vivo* is controlled. Fe ions are absorbed from the gut and are transported to iron-requiring cells by the protein Tf in an attempt to keep the Fe pool as small as possible. $^{\bullet}OH$ generation can take place when the homeostasis is altered.

For example Cu and Fe ions released into perfusates can cause ischaemia / reperfusion injury (Chevion *et al.*, 1993). Using electron spin resonance (ESR) spin trapping system, Ramos *et al.* (1992) detected $^{\bullet}OH$ as the α-hydroxyethyl spin trapping adduct of 4-pyridyl-1-oxide-n-terbutylnitrone formed from phorbol-12-myristate-13-acetate-stimulated human neutrophils and monocytes without the addition of supplemental Fe. In systems that lacked myeloperoxidase, it was necessary to add Fe to detect $^{\bullet}OH$ adduct. Thus, human neutrophils and monocytes can generate $^{\bullet}OH$ through a myeloperoxidase-dependent mechanism (Ramos *et al.*, 1995) that could have microbicidal implications.

4.1.4 Peroxyl radicals ($ROO^{\bullet}$)

These radicals are formed during LPO chain reactions, such as the oxidation of polyunsaturated fats and unsaturated fatty acids. LPO may be initiated by any species that has sufficient reactivity to abstract a hydrogen atom from a PUFA side chain (such as those of arachidonic acid and linolenic acid) in membrane lipids. Arachidonic acid is a precursor of prostaglandins and leukotriens. It contains a number of methylene-interrupted double bonds that are particularly prone to hydrogen atom abstraction. Although the mechanism and the biological significance of LPO have been extensively reviewed (Dix and Aitkens 1993; Esterbauer *et al.*, 1993), delineation of LPO as a major pathway in most degenerative diseases would depend on adequate standardization and control of measurement conditions (Auroma, 1996). The link between DNA damage, faulty repair of DNA, protooncogene activation, and the ability of some of the end products of LPO to act as promoters of carcinogenesis has been widely discussed (Cheeseman, 1993).

The end products of LPO could have profound effects on vascular function because of their ability to mimic or antagonize the actions of some of the stereospecific products formed by cyclooxygenase and lipoxygenase enzymes. For example, the F_2-isoprostanes are generated by peroxidation of arachidonic acid via the generation of $ROO^{\bullet}$ isomers that undergo endoxyclization to prostaglandin-like compounds. Their formation *in vivo* appears to be enhanced under conditions of oxidative stress (Nourooz-Zadeh *et al.*, 1995; Morrow and Roberts, 1996).

Oxidation of low density lipoprotein (LDL) is a free-radical-mediated process that results in numerous structural and functional changes (Esterbuaer *et al.*, 1993). The initiation of LDL oxidation occurs by the peroxidation of the PUFA in LDL. Oxidation of LDL is initiated by ROS that abstract $H^{\bullet}$ from a double bond in PUFA, followed by molecular rearrangement that leads to the formation of conjugated double bonds that are commonly referred to as conjugated dienes (CD) (Esterbauer H *et al.*, 1993). Cholesterol in LDL can be oxidized to oxysterols, such as 7-keto cholesterol. The propagation phase is followed by a decomposition phase, in which there is cleavage of double bonds resulting in the formation of aldehydes such as MDA and 4-HNE, and hexanol, that can crosslink with amino groups on *apo* B-100.

Changes in the protein moiety of LDL also occur during oxidation (Parthasarathy and Rankin, 1992). The aldehydic products of LDL oxidation are diffusible cytotoxins (Chisolm, 1991). Oxidation is followed by an increase in the negative charge of LDL, possibly resulting from derivatization of positively charged amino groups through the

formation of Schiffs base with aldehydes. Furthermore, the *apo*-B protein undergoes oxidative scission leading to fragmentation.

4.2 FREE RADICALS GIVE RISE TO FREE RADICALS – LPO

Lipids are readily oxidized both *in vivo* and *in vitro*, for example, by the peroxidized lipids present in age pigments. The parallel spin of molecular oxygen prevents the direct addition of the electron pair to another molecule and thus prevents chemical bond formation. For a bond to be formed, spin reversal must occur. Since spin reversal takes a long time in comparison to the half-life of activated complexes, molecular oxygen is a relatively weak oxidant, and autooxidation of lipids in living organisms is a relatively slow process. Nevertheless, if lipids are activated to free radicals $R^{\bullet}$ via removal of hydrogen (mediated by a free radical initiator), they enter into reactions with molecular oxygen more readily. A $ROO^{\bullet}$ is formed during the reaction and this process is called LPO. PUFA are especially liable to peroxidation since the C–H bond of their so- called α-methylene carbon next to the double bond is weak, and thus they may be regarded as partially activated. Therefore, as the initial step of LPO, hydrogen is removed from this carbon atom (the hydrogen of α–methylene carbon atom is also called allylic hydrogen) (Del Maestro, 1980).

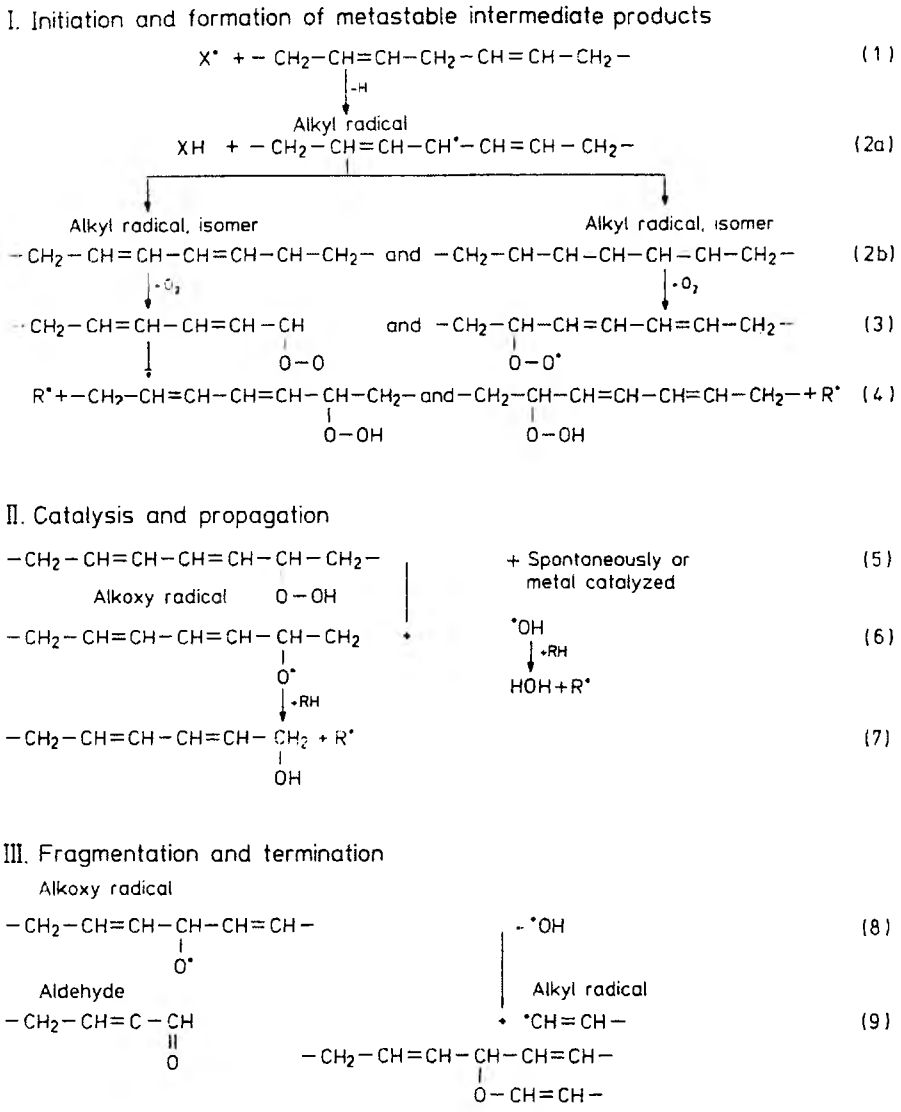

Figure 6 Phases of Lipid Peroxidation (After Demopoulos *et al.*, 1980).

Figure 6 shows the process of LPO:

1. During initiation a free radical substance ($X^{\bullet}$ in Figure 6) reacts with a fatty acid chain containing one or more multiple bonds (R with two multiple bonds). 2. (a) A radical centre is formed next to the double bond (α-methylene carbon) after the free radical initiator has abstracted a hydrogen atom and thereby ceased to be a free radical (XH). At the same time an alkyl radical $R^{\bullet}$ is formed from the lipid. (b) Several configurational changes follow the initiation almost immediately and massive electron transfers occur: (i) transfer of the free electron to other C atoms; (ii) this moves the double bonds closer, leading to the formation of conjugated double bonds. (iii) Some double bonds adopt the *trans* configuration, instead of the *cis* configuration characteristic of fatty acids.

3. The oxygen is added to the $R^{\bullet}$ and a $ROO^{\bullet}$ is formed.

4. $ROO^{\bullet}$s abstract hydrogen from the nearby molecules (RH, which may be other unsaturated fatty acids, proteins, antioxidants, or nucleic acids) and thus the metastable hydroperoxides (ROOH) are formed.

5–6. ROOH are capable of spontaneous decomposition to $^{\bullet}OH$ and alkoxyl radicals $RO^{\bullet}$. As a result of metal catalysis, $RO^{\bullet}$, $ROO^{\bullet}$ and $^{\bullet}OH$ or hydrogen ions are formed.

7. With the abstraction of hydrogen from neighbouring molecules RH, the $RO^{\bullet}$ and $^{\bullet}OH$ are terminated, but further radicals are formed from the molecules losing their hydrogens.

8. $RO^{\bullet}$ may undergo further oxidation or may be fragmented by continuous free radical attack on their α-methylene carbon atoms. In this way bis-hydroperoxides (i.e. two OOH groups on single fatty acids) may be formed and the fatty acid is decomposed into aldehydes and alkyl radical fragments.

9. Alkyl radicals may react with the surrounding radicals, e.g. $RO^{\bullet}$, and thus the process is terminated as a result of the formation of O-bonded bridges between the molecules, or C–C bonds may be formed with another alkyl radical.

Initiation may thus start a chain reaction that, if uncontrolled by defence mechanisms, may lead to extensive damage to surrounding molecules. Autooxidation of lipids eventually leads to the formation of new C–C bonds. Since lipids are membrane constituents, it is easy to see what extent to which cross-linking may damage the membranes (Figure 7).

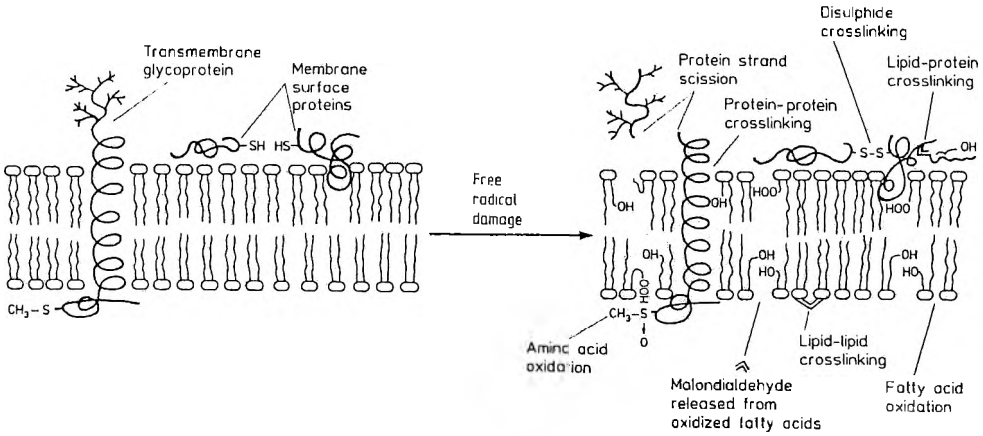

Figure 7 Free radical induced damage. MDA, one of the products of LPO, facilitates cross-linking. Free radical may also produce protein-protein cross-links, amino acid oxidation, a fissure of protein fibres. (Freeman and Crapo, 1982)

Autooxidation is considerably accelerated by the presence of transition metals (i.e. Fe and Cu) that enhance the degradation of metastable hydroperoxides (Figure 6, Eqs. 5,6). Lipids that are readily oxidized promote the metal-catalyzed oxidation, in the presence of O_2 or more inert cellular components like proteins or nucleic acids (Figure 6, Eqs. 7,9). Autooxidation is a very slow circumscribed process under physiological conditions.

Under pathological conditions, however, it is accelerated, becomes more extensive, and may damage all basic biomolecules (Demopoulos *et al.,* 1980; Slater, 1984). The meta-stable lipid peroxides formed during LPO, MDA, and other stable end products of LPO, e.g. 2-alkenals and 4-hydroxyl-2-alkenals, may reach more distant parts of the cell or other cells and tissues as a result of their relative stability. Thus, LPO may also damage cells or tissues that are not directly exposed to peroxidative damage (Petkai, 1980; Pryor, 1982).

Previous studies using much higher amounts of dietary Fe in male rats, formed a strong correlation between Fe intake and LPO (Dresow *et al.*, 1995; Inan *et al.*, 1998; Dougherty *et al.*, 1981). In a study on Fe overload that compared 200 and 30,000 μg/g dietary Fe as CI in male rats, Dabbagh AJ *et al.* (1994) reported substantial hepatic LPO, and depletion of endogenous antioxidants, including vitamin E.

4.3 PATHOLOGICAL FREE RADICAL REACTIONS

Uncontrolled, abnormal radical reactions occurring in the cell are called pathological free radical reactions. Radicals generated under physiological conditions, when control mechanisms fail for some reason, may also elicit such reactions. In addition, exogenous agents and physical interactions with ionizing radiation, UV, or plastic implants may cause these reactions.

4.4 FREE RADICAL DAMAGE

4.4.1 Damage of Enzymes and Proteins Caused By Free Radicals

Polymerization, breakage of polypeptide chains, and changes in the amino acid structure

may occur in proteins and enzymes exposed to LPO in aqueous solutions. Proteins containing unsaturated fatty acid and sulphur containing amino acids (tryptophan, tyrosine, phenylalanine, histidine, methionine, cysteine) are mostly sensitive to the modification of the amino acid structure (Freeman *et al.*, 1982). Because proteins are membrane constituents, their damage explains the membrane-damaging effect of free radicals, while the loss of the specific activity of the enzymes may also have severe consequences.

Some of the important membrane proteins are phospholipid dependent. Their active configuration is generated via interaction of the hydrophobic parts of the polypeptide chain and the fatty acid parts of the special membrane phospholipids. Na^+,K^+ -ATPase, succinyl dehydrogenase and cytochrome oxidase are among these enzymes that are damaged. Understandably, LPO triggered by free radical reactions, inactivates these enzymes, (Demopoulos, 1980).

4.4.2 Damage of the Cell Membrane and the Subcellular Organelle

Biomembranes and subcellular organelles are the chief targets of LPO-induced damage. Mitochondrial and microsomal membranes contain relatively more PUFA in their phospholipids than the plasma membrane and are, therefore, more susceptible to peroxidation. Substances generating free radicals damage various subcellular structures selectively. Damage of the lysosome membranes may lead to intracellular catabolism. Lysosomes contain relatively less PUFA compared with the mitochondria and microsomes, and therefore, they are less susceptible to oxidative injury (Tappel, 1973).

4.4.3 Fluorescent Molecular Damage and Lipofuscin Pigments

Lipofuscin pigments accumulate in human and animal tissue as a result of aging. These are lipid-protein complexes resulting from the peroxidation of the PUFAs of subcellular membranes and correspond to the so-called residual body, the end product of lysosomal digestion. This conjugated imine structure (RN=CH–CH=CH–NH–R), having fluorescent chromophore properties, is an indictor of the cross-linking reactions of LPO (Freeman *et al.,* 1982: Holland *et al.,* 1982). MDA may be present in lipofuscin either in the Schiff base form, or in the polymerized form. Ceroid, having a structure similar to lipofuscin also accumulates during normal aging, as a result of pathological processes (Vistnes *et al.,* 1983).

4.4.4 Free Radical Damage of Nucleic acids and Their Components

Free radical damage to the DNA of living organisms may be the result of breakage of the main chains or of a strand, degradation of bases, or cleavage of hydrogen bonds. All components of nucleic acids may be exposed to free radical damage, which either becomes permanent or may be repaired by special mechanisms. Unrepaired damage in bases may lead to mutation, while damage in the pentose part may result in chain breakage. Histones with high arginine and lysine content have been found to be good $^{\bullet}OH$ radical scavengers with a possible role of protecting DNA against pathological free radical reactions (Nakayama *et al.,* 1984; Zs-Nagy and Floyd, 1984).

4.4.5 Connection Between LPO and Tissue Damage

LPO may proceed in a controlled form without causing total cell damage. But it may also

lead to tissue damage, either reversible or irreversible. In the latter case it causes the death of the cells. Reversibility is the result of cellular antioxidant protection. Lysosomal enzyme release invariably causes cell damage, but cell death is the result of intracellular Ca^{2+} accumulation caused by the failure of the microsomal Ca^{2+} pump. LPO may not only be the cause of cell damage, but may also be the result of tissue damage caused by some other factors. It is thus hard to judge in some disease states whether cell damage as a result of LPO is primary, or whether LPO is secondary to cellular damage. Antioxidants are inactivated in the damaged tissue, and metals stored in the cells (mostly Fe and Cu) are released. These may then promote LPO (Younes and Siegers, 1984).

4.5 FREE RADICAL REACTIONS AND MUTAGENESIS

Free radical reactions can induce mutation of DNA either directly or indirectly. Mutagenesis, however, is not always harmful. Deficiency in the repair mechanism may be secondary to DNA damage caused by free radicals. The mutagenic effect of free radicals on bacteria has been proved experimentally, and a similar effect of activated phagocytes has been found in cell cultures (Moody and Hassan, 1982). Three types of antimutagens have been distinguished, depending upon their mechanism.

1. Desmutagens, that inactivate or kill mutagens.
2. Inhibitors of the metabolism of substances needing metabolic activation for their mutagenic action.
3. Antimutagens proper, which inhibit the mutagenic effect at the cellular level.

Although the antimutagenic effects of antioxidants have been repeatedly described, the results have been contradictory.

4.6 FREE RADICAL REACTIONS AND CARCINOGENESIS

The majority of tumours are caused by environmental factors. Although environmental chemical carcinogens are of diverse structure, they act almost without exception by way of free radical mechanisms: they are either free radicals themselves, or are converted to free radicals when activated, or they induce pathological free radicals reactions indirectly. Three types of anticarcinogenic protective mechanisms are known: (a) prevention of the formation of active forms; (b) stimulation of carcinogen detoxifying systems; and (c) mechanisms acting after interaction with targets.

Endogenous carcinogens and mutagens (i.e. MDA) are produced in aging as a result of LPO. Some stable diffusible products of LPO can damage the genetic material, thus playing a role in the initiation and promotion of tumours. Chemicals can also cause chromosomal damage (similarly to membrane active substances) in an indirect way by activating the respiratory burst of phagocytes and by inducing peroxisome proliferation leading to LPO (Cerutti, 1985). Mitochondrial univalent leakage and the disturbed balance of the protective mechanisms acting against it may constitute another link between aging, mutagenesis and carcinogenesis.

4.7 CELLULAR ENZYMATIC DEFENCE (AGAINST RADICALS OF MOLECULAR OXYGEN)

4.7.1 Antioxidant defence of the Intracellular Space

The chief mechanism protecting cells *in vivo* against oxygen toxicity and LPO is the maintenance of low oxygen tension in the tissues (approx. 26Mm Hg). Thus, the formation

of $^{\bullet-}O_2$ and other LPO-inducing ROIs is kept under control (Hornby and Crivello, 1983) and SOD enzymes mediate the removal of $^{\bullet-}O_2$. The therapeutic potential of SOD has stimulated the production of an authentic human SOD (HSOD) by gene technology (Wheeler *et al.*, 2001).

SODs are metalloproteins containing Mn, Fe or Cu + Zn (MnSOD, FeSOD, CuZnSOD) and are ubiquitous in the cells of aerobic organisms. All subunits are composed of 151 amino acids and contain an atom of Cu and Zn each. Both subunits are bound by a disulphide bridge, and lose their enzyme activity through its dissolution. The molecule has a bullet-shaped spatial structure and the external Cu atoms form the active catalytical centre. Zn plays no role in the enzyme activity. FeSOD is found in prokaryotes, MnSOD in both eukaryotes and prokaryotes, while CuZnSOD in eukaryotes. The mitochondria of eukaryotes contain only MnSOD, whereas the cytosol also contains MnSOD, in addition to CuZnSOD. SOD catalyses the reaction

$$^{\bullet-}O_2 \quad + \quad 2H^+ \quad \text{--------}> \quad H_2O_2 \quad + \quad O_2$$

H_2O_2 may thus be formed not only during the divalent reduction of O_2 but by SOD activity. For instance, MnSOD may transform $^{\bullet-}O_2$ produced during mitochondrial metabolism into H_2O_2, which means that permanent production of small amounts of H_2O_2 in cells is removed by catalase (CAT), a haem enzyme, and by various peroxidases [i.e. selenium glutathione peroxidase (SeGPx)]. CAT is found in peroxisomes and catalyses the reaction

$$H_2O_2 \quad \text{--------}> \quad H_2O \quad + \quad ½\ O_2$$

At low molecular H_2O_2 concentrations, CAT is relatively unreactive. Its peroxisomal

localization also suggests that other defence systems may also be responsible for the removal of H_2O_2. Thus peroxidases catalyze the reaction and thereby decompose H_2O_2 utilizing reducing agents.

SeGPx can remove not only H_2O_2 but also LOOH. Thus, it functions later than vitamin E. It does not prevent the formation of hydroperoxides, but degrades them once they are formed. At low H_2O_2 concentration SeGPx provides the main line of defence, whereas at higher toxic levels of H_2O_2, CAT also starts functioning. SOD and peroxidase or SOD and CAT may jointly fulfil the role of a terminal oxidase, catalyzing the reduction of $^{\bullet-}O_2$ to water (McCord and Fridovich, 1978). A selenium-independent glutathione peroxidase (SeiGPx) has been isolated, which cannot metabolise H_2O_2 but only organic peroxides. The role of SeGPx is probably in protection against LPO (Holland *et al.*, 1982).

The cellular enzymes described (with the exception of SeGPx and SeiGPx, which attack lipid peroxides) remove ROIs directly, thereby inhibiting LPO, which is kept at a minimum level. The cellular vitamin antioxidants (C,A,E,K) and thiol-containing compounds, ubiquinone, urates, glucose etc. constitute the second line of defence, in addition to their participation in the first line via their scavenger activity.

The third line of cellular defence is the decomposition of the end products of LPO (i.e. the alkenes, alcohols, epoxides and aldehydes) produced in the degradation of lipid peroxides. It has been shown that enzymes that have so far been thought to have the primary function of metabolizing xenobiotics, have the capability of metabolizing LPO products. Possibly

this activity also belongs to their primary functions. For instance, epoxide hydrolase and aldehyde reductase have been shown to metabolize peroxidation products, while cytochrome P-450 monooxidases have been found to metabolize endogenous lipids and prostaglandins. Cytochrome P-450 has multiple functions. It may participate in the defence mechanisms against LPO; it may be damaged during LPO, and it may be the source of $^{\bullet-}O_2$ formation. The protective enzymes are mutually interdependent. For example, $^{\bullet-}O_2$ inhibits CAT and other haeme-containing peroxidases, and SOD provides protection against this inhibitory effect. Similarly, two of the three SODs are inactivated by H_2O_2, while CAT and peroxidase provide protection against this inactivation (Fridovich, 1983).

4.7.2 Antioxidant Defence of the Extracellular Space

A very low level of the enzymes participating in cellular defence can be detected in the extracellular space. They probably get there by passive diffusion from the interior of the cells. Therefore, the defence of the extracellular space against free radical reactions is much weaker. In addition only a small fraction of the low serum SOD activity is the result of CuZnSOD. Its greatest part is accounted for by a high molecular weight tetrameric SOD (CuZnSOD - a dimer) that also contains Cu (four atoms) and probably the same amount of Zn. It was believed earlier that this tetrameric SOD only occurs in the extracellular space, as indicated by its glycoprotein structure characteristic of most plasma proteins, but not found intracellularly. It was, therefore called, extracellular SOD (EC-SOD). However, EC-SOD has also been detected in cells. Apart from a few exceptions, it occurs in much smaller amounts intracellularly than CuZnSOD and MnSOD. The SOD activity in the extracellular space is low in spite of the presence of EC-SOD. This probably reflects a

"compromise" between the necessary defence of the extracellular space against destructive ROIs (e.g. the microbicidal and cytolytic function of phagocytes) and the chemotactic activity triggered by $^{\bullet-}O_2$ (Marklund, 1984). Ceruloplasmin is a ferroxidase; it oxidizes Fe (II) to Fe (III), thereby inhibiting the metal catalysis of LPO. It probably also acts as a direct scavenger of $^{\bullet-}O_2$. These properties make ceruloplasmin one of the antioxidants of the extracellular space. Tf is also believed to be another circulatory antioxidant. As opposed to ceruloplasmin, which is invariably saturated with Cu, Tf is saturated with Fe only in pathological states. Its antioxidant activity depends on its Fe-free fraction only because it is an Fe chelator. An antioxidant action has been attributed to urate and glucose in the extracellular space (Sagone Jr *et al.*, 1983).

4.8 CONTROL OF FREE RADICAL REACTIONS

4.8.1 Control and Defence against Free Radical Reactions in Biological Systems

Molecular structures of vital importance, like the cell membrane, DNA and proteins, have constituents that are very sensitive to radical reactions, such as the α–methylene carbon atom of PUFAs, as well as the allylic hydrogen and the thymidine base.

4.8.2 Control by Membrane Structure

Free radicals formed during electron transport are kept under control by the enzymes and carriers of the transport chain, which are bound to the membrane and are closely packed together. The PUFAs of the membrane are localized in its hydrophobic region, far from the site of electron transport, which takes place in the hydrophillic region. Thus, the protection of PUFA is inherent in the membrane structure. This defence may be damaged if the cell

membrane or mitochondria are injured, giving rise to pathological free radical reactions. PUFAs of the membrane phospholipids are "packed" by cholesterol. Hydrogen bonds in membranes also provide protection against free radicals. However, hydrophobic chemical pathogens (e.g. CCl, DDT, halothane and some carcinogenic substances) can penetrate the hydrophobic region and initiate free radical reactions.

4.8.3 Control by Specific Molecular Structure

Some normally occurring free radicals are under control because they are intermediates formed during reactions of enzyme-substrate complexes. As a result of their fixed localization and short half-life, they have little chance to interact with other substances. The rate of radical reactions is influenced by the amount of membrane unsaturated fatty acids and the degree of their unsaturation. These in turn, depend to a lesser extent on the fat content of the diet and, predominantly, on genetic factors (Demopoulos, 1973).

4.8.4 Control by Scavengers and Antioxidants

Substances interacting with free radicals and thereby inhibiting free radical reactions are called scavengers. These must reach their target at the right time and in the right concentrations. Synthetic scavengers used for therapy must be of low toxicity. Also, the scavenger radical formed during the interaction of the scavenger with the toxic radical intermediates should be less reactive or have a longer half-life than the radical they attack. Scavengers show a high degree of selectivity in their reactions with free radicals, which are stoichiometric reactions. They should therefore be applied in proper doses (Slater, 1984). Scavengers and antioxidants may be enzymes or vitamins.

Lately, antioxidants have been reported to have a tumour promoter and mutagenic effect and radiosensitizing ability. These opposing effects of antioxidants (i.e. carcinogen-anticarcinogen) may be accounted for by the dose as well as endogenous factors (i.e. lipid peroxides, which have a role in the control of cell division). For example PUFAs in low concentrations stimulate mitosis. However, at higher concentrations they produce larger amounts of lipid peroxides and have an antimitotic effect. The balance between ROIs and the protective systems such as enzyme / vitamin antioxidants acting against them, play an important role in carcinogenesis.

5.0 VITAMINS

5.0.1 Definition

Vitamins are organic compounds required in trace amounts (microgram or milligram quantities per day) in the diet, of humans and other animals and are needed for health and reproduction. They can be synthesized chemically or isolated from certain plants. Some synthetic analogues and derivatives of vitamins have been designed to serve as inhibitors (e.g. methotrexate as an antifolate), as have others that substitute part of the natural vitamin (e.g. 8-ethylriboflavin and riboflavin). Only small amounts of vitamins are required for their function: they often have catalytic (coenzymatic) roles, in contrast to the relatively large amounts of such macronutrients as protein, lipid and carbohydrate.

Vitamins are one of the most essential factors that affect the health and development of humans. The deficiency of a single vitamin is relatively uncommon. However, it can occur as a result of an inborn error of metabolism or as a result of unusual restriction of dietary intake. More frequently seen are complex deficiencies that arise as a result of food fads, as complications of certain diseases, especially those affecting food absorption, as a result of massive loss of blood or haemodialysis, or as a consequence of the use of certain drugs. On the other hand, excessive use of vitamins is sometimes encountered.

5.1 VITAMIN A

5.1.1 Chemistry and Source

The two natural forms of vitamin A, *retinal* and *3-hydroretinol* (A_2) are C15- isoprenoid alcohols that have a substituted β-ionone and 3-dehydro-β-ionone ring, respectively, as shown in Figure 8.

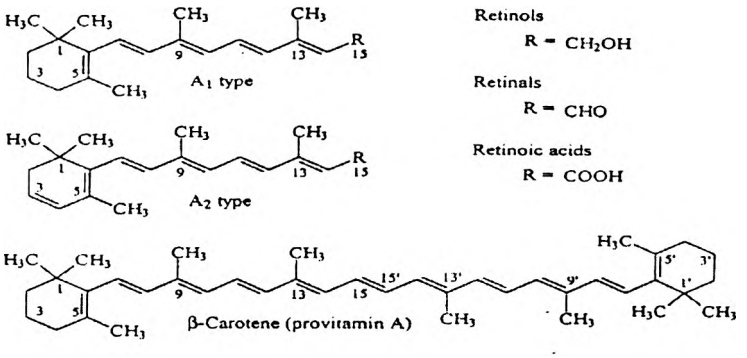

Figure 8 Vitaminic forms of A_1, A_2 and β-carotene. R=CH_2OH for retinol, CHO for retinals and CO_2H for retinoic acids.

Vitamin A is sensitive to oxygen and UV light. Vitamin A_1 predominates, especially as long chain fatty acid esters, in the liver of mammals and saltwater fish (e.g., in cod liver), whereas the biologically less active vitamin A_2 is found in fresh water fish oils. The structure of the most common and effective provitamin A, *β*-carotene, is given in Figure 8.

5.1.2 Requirement and Daily Allowance

Studies in humans indicate that 500 to 600 μg of retinol, or considerably more *β*-carotene, is the minimum requirement for adults to maintain an adequate blood concentration and to prevent deficiency symptoms (National Research Council, 1989). Greater intakes are necessary to produce significant liver storage. The recommended daily allowance (RDA) is 1000 R.E. (retinol equivalents) for adult males and 800 R.E. for females. Based on animal studies, the American Institute of Nutrition-93 (AIN-93) fixed vitamin A for laboratory rodents at 4000 IU (≡ 400 R.E) (Reeves PG *et al.*, 1993).

5.1.3 Absorption, Transport and Metabolism

The emulsification to micelles by bile salts enhances the uptake of various forms of vitamin A and provitamin A by mucosal cells of the small intestine. Absorption of the free retinol is followed by re-esterification with long-chain fatty acids within the mucosal cells. Retinyl esters, in association with chylomicrons, then pass via the lymphatic system to the liver and are stored in a lipoglycoprotein complex. Retinol associated with plasma retinol-binding protein is released from hepatocytes to form, with circulating pre-albumin, a molecular aggregate of sufficient size to avoid loss through glomerular filtration. Small amounts are stored in the kidney and lung tissues. However, storage of vitamin A is mainly hepatic, and the liver can store requirements for approximately 2 years for an adult.

5.1.4 Functions

The best-understood physiological function of vitamin A is its participation as retinal in vision. Other forms (retinol and retinoic acid) are necessary for growth of bones, testicular and ovarian functions, embryonic development and for regulation of growth and differentiation of epithelial tissues. Retinol and retinoic acid may act as cofactors in biochemical reactions.

5.1.5 Deficiency

Degenerative changes in the eye or skin are commonly observed in vitamin A deficiency (Wilson, 1991). Poor dark adaptation or "night blindness (nyctalopia)" is an early symptom, followed by degenerative changes in the retina. Associated skin changes include dryness, roughness, papular eruptions and follicular hyperkeratosis.

5.1.6 Excess

Toxic effects occur with hypervitaminosis A, either as a result of ingestion of excess vitamin or as a side effect of inappropriate therapy (Campbell *et al.*, 1980; Wilson, 1991). One of the most important factors affecting the toxicity of vitamin A is the form in which it is administered, and symptoms can appear more readily after administrating aqueous emulsions rather than oily solutions. Hypervitaminosis can occur when the liver storage of retinol and its esters exceeds 10,000 IU/g of tissue, a level 10 times the estimated RDA for adult males, or if plasma vitamin A levels exceed 140 μg/dl. Moderately high doses taken for protracted periods result in chronic toxic effects which can lead to a fatty liver. Administration of doses up to three-fold the RDA for several years result in hepatotoxicity (Geubel *et al.*, 1991). However, no mutagenicity was found with the Ames test (Bagdon *et al.*, 1960; Heywood *et al.*, 1985). In addition, tumorigenicity of *β*-carotene was not found during a 2-year study period in animals, and in carcinogenicity studies in mice, vitamin A was without discernible tumorigenicity (Diplock, 1995).

5.2 VITAMIN E

5.2.1 Chemistry and Source

δ-*α*-tocopherol is the most biologically active form of vitamin E. Units of vitamin E are based on this. This group is made up of 8 related natural compounds that are biosynthesized in plants and are abundant in vegetable oils. The chemical structure of vitamin E and its related compounds are shown in Figure 9.

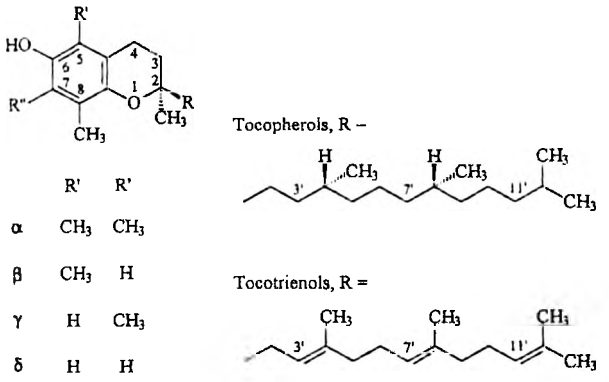

	R'	R'
α	CH_3	CH_3
β	CH_3	H
γ	H	CH_3
δ	H	H

Figure 9 Vitaminic forms of E

At room temperature, members of this group are viscous oils. They are soluble in lipid solvents and insoluble in water, stable in acid and heat in the absence of oxygen, but are degraded in alkaline solutions and by UV light.

5.2.2 Requirement and Allowance

The requirement for vitamin E is related to the PUFA content of cellular structures, and this depends on the nature and amount of dietary fat, which affects such structures. Hence, the minimum adult requirement for vitamin E is uncertain but is probably not more than 3-4 mg (4.5-6 IU) for δ-α-tocopherol per day (National Research Council, 1989). When vitamin E activity of tocopherols and tocotrienols in mixed diets is calculated, an estimated range of 7-13 mg of α-tocopherol equivalents (10-20 IU) can be expected. This intake maintains plasma concentrations of total tocopherols within the reference interval of 0.5-1.2 mg/dl, which also ensures an adequate concentration in all tissues. The requirement for rodents is 75 IU/kg diet as indicated in the AIN-93G report (Reeves *et al.*, 1993).

5.2.3 Absorption, Transport and Metabolism

Twenty to 80 percent of dietary vitamin E absorbed from the gastrointestinal tract (duodenum) requires the presence of dietary fat, bile salts and normal pancreatic function for effective absorption. Most tocopherols enter the blood stream through the lymph, where the tocopherol is associated with chylomicrons and very low-density lipoproteins. The vitamin is stored in most tissues, with the largest amount stored in adipose tissues. Up to 4 years' requirement can be stored. The rapid exchange of tocopherols occurs between the erythrocyte membranes and plasma lipoproteins. Only a small fraction of physiological amounts administered appear in urine. Large doses of Fe may increase the daily requirement of vitamin E. Vitamin E may facilitate absorption, hepatic storage, utilization and reduction of toxicity of vitamin A. Even though it is thought that large doses of vitamin A may even deplete vitamin E stores, evidence from 2319 participants in the "Carotene and Retinol Efficiency Trial" given 30 mg β-carotene/day (50-60 times the RDA) and 25,000 IU retinol/day (25 times the RDA) for up to 6 years showed no evidence of decreased vitamin E (Goodman *et al.*, 1994). In the present study 10 times the vitamin E RDA for rodents was given.

5.2.4 Functions

Vitamin E is considered an essential nutritional element, although its exact function is unknown. Vitamin E best serves as an antioxidant for unsaturated fatty acyl moieties of lipids within membranes. Oxidative damage of polyunsaturated fatty acyl parts of membrane phospholipids can occur as a result of H_2O_2 production by flavoprotein oxidases. Concurrently, this can lead to free radical damage and vitamin E can serve as an

antioxidant interrupting the initiation step of the LPO reaction. It may also act as a co-factor in some enzyme systems. A potential role for vitamin E in the prevention or treatment of cancer has been suggested. However, efficacy has not been proven.

5.2.5 Deficiency and Excess

Signs of deficiency include irritability, oedema, and haemolytic anaemia. Deficiency symptoms rarely occur in children or adults except in cases of severe malabsorption, for example, in cystic fibrosis. Toxic responses to high intake of vitamin E in which competition for absorption may increase requirements for other fat-soluble vitamins, notably D and K, have been recognised in animals. This problem appears to occur in humans who already have limited quantities of vitamin K. In general, relatively high doses of vitamin E (e.g., 300 mg/day) appear to be tolerated. The toxicity of vitamin E is low, and animal studies have shown that vitamin E is not mutagenic, carcinogenic, or teratogenic (Diplock, 1995).

5.2.6 Vitamin E and Fibrogenesis

The effect of vitamin E supplementation on hepatic fibrogenesis in chronic dietary Fe overload was investigated by Brown *et al.* (1997). Dietary supplementation with α-tocopherol acetate resulted in 1.2 – 2 and 2–2.5 fold increases in both hepatic and plasma α-tocopherol levels in the vitamin supplemented group compared to the control. Vitamin E supplementation caused a significant reduction of TBARs. Histologically, fibrosis was mild in the Fe group and no bridging fibrosis was observed. The results demonstrate dissociation between LPO and collagen production and suggest that the profibrogenic

action of the Fe in this model is mediated through effects that cannot be completely suppressed by vitamin E.

5.2.7 Vitamin E, Oxidative Stress and LPO

MDA and cytosolic aldehyde dehydrogenase (ALDH) levels were examined in rat liver tissues after feeding different levels of vitamin E and or selenium and PUFAs for 12-38 weeks. MDA production was significantly increased by vitamin E deficiency or by high levels of polyunsaturated fat intake, but not selenium deficiency. ALDH increased upon increased production of MDA after 12-16 weeks. However, ALDH activity was suppressed after 38 weeks of feeding on the vitamin E deficient diet. The results indicate that hepatic cytosolic ALDH may be involved in the metabolism of MDA during a relatively short-term *in vivo* LPO increase, but that ALDH activity becomes suppressed after more severe *in vivo* LPO has been produced (Hye-Sung, 1994).

The protective effect of vitamin E and cobalt was examined by Inan *et al.* (1998). Results of the 3-week study on 38 male Wistar rats showed that *in vivo* cobalt, in addition to vitamin E (100 mg/kg b.wt 3x weekly), could function as a potent antioxidant in the amelioration of Fe-induced LPO. In the liver, cobalt and vitamin E reduced LPO levels by 50%. Fe overload however, caused a 70% decrease in cytochrome *c* oxidase activity, leading to reduced ATP synthesis. Accordingly, increased ATP demand caused ATP degradation to hypoxanthine and the formation of several new ROS. The concentration of hypoxanthine in the liver was found to be 3-4 fold higher than in the controls. However, because vitamin E is an inhibitor of LPO, its action as an antioxidant resulted in a decrease

of hypoxanthine. Furthermore, vitamin E protected the liver tissue from the presence of extensive granuloma formation in Fe- overloaded liver tissue more efficiently than cobalt.

5.3 VITAMIN C

5.3.1 Chemistry and Source

L-Ascorbic acid (vitamin C), shown in Figure 10, is a white crystalline solid that is readily soluble in water. It is reversibly oxidized to dehydroascorbic acid (ascorbone) (Figure 10), and the *dehydro* form is more readily degraded than the reduced form. Some mammals, including humans lack L-gulonolactone oxidase, the enzyme that catalyzes the formation of 2-keto-L-gulonolactone, which spontaneously tautomerizes to L-ascorbic acid. The best source of vitamin C is in citrus fruits, berries, melons, tomatoes, green pepper, raw cabbage, and leafy green vegetables. Losses during processing, especially with heat and aerobic conditions, can be considerable.

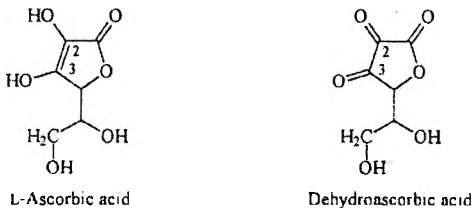

Figure 10 L-Ascorbic and dehydroascorbic acids

5.3.2 Requirement and Allowance

An RDA of 60 mg seems adequate to maintain near saturation of tissues in the adult male, with a body pool of about 1.5 g. An RDA of 40 to 45 mg is suggested for children.

5.3.3 Absorption, Transport and Metabolism

Absorption of vitamin C occurs readily, mostly from the stomach, where some of the ascorbic acid is converted to the *dehydro* form. At physiological pH, the uncharged dehydroascorbic acid passes across cell membranes faster than the monoanionic L-ascorbate. Passive diffusion of vitamin C may largely account for entry into some cells such as leukocytes and erythrocytes, but an active transport mechanism may also be operative. The half-life for vitamin C in humans is about 16 days. Ascorbate, dehydroascorbic acid, and lesser amounts of a number of catabolites are present in the urine.

5.3.4 Iron and Vitamin C

Ascorbic acid is known to enhance the availability and absorption of iron from non-heme iron sources (Hallberg L, 1981). Vitamin C achieves this effect in the small intestine by helping to convert dietary iron from the ferric state (Fe^{3+}) to the more soluble ferrous state (Fe^{2+}), and by binding to ferric iron (Fe^{3+}) to form soluble complexes (Bendich & Cohen, 1990). When body iron stores are low, the enhancing effect of vitamin C on non-haem iron absorption is markedly higher than when iron stores are high. It is well known that in the presence of redox-active iron, ascorbic acid acts as a pro-oxidant *in vitro* and might contribute to the formation of hydroxyl radical, which eventually may lead to lipid, DNA or protein oxidation (Samuni *et al.*, 1983). Thus, ascorbic acid supplementation in individuals with high iron and or bleomycin-detectable iron (BDI) in some preterm infants could be deleterious because it may cause oxidative damage to biomolecules (Minetti *et al.*, 1992; Berger *et al.*, 1995; Halliwell, 1996; Herber *et al.*, 1996). However, no pro-

oxidant effect was observed on ascorbic acid supplementation on DNA damage in presence or absence of iron (Herbert *et al.*, 2000).

5.3.5 Functions

The most clearly established and critical functional role for ascorbic acid is that of a cofactor for protocollagen hydroxylase, the enzyme responsible for hydroxylation of prolyl and lysyl residues within nascent peptides in connective tissue protein. Absorption of Fe^{2+} is enhanced by simultaneous ingestion of the vitamin.

5.3.6 Deficiency and excess

Protracted deficiency of vitamin C leads to scurvy. Infantile scurvy, also known as Barlow's disease, exhibits a bayonet-rib syndrome. Some scorbutic patients may develop anaemia, display radiological changes characteristic of osteoporosis, or die suddenly from heart failure. Large doses of ascorbic acid have generally been considered to be non-toxic and free of adverse effects except for gastrointestinal symptoms that are experienced by some subjects (Dallman, 1990; Campbell *et al.*, 1980). However, more serious adverse effects have been observed and are suspected to be potential hazards. Acute, sub-acute, chronic, and sub-chronic toxicity of vitamin C is infrequent and is well tolerated without side effects (Hanck, 1982). High ascorbic acid intake has no effect on Fe absorption in healthy Fe-replete subjects, which repudiates suggestions that Fe overload could be a consequence of high ascorbate intake (Cook, 1984). It appears that the regulation of body Fe stores is unaffected by any increased availability of Fe from the diet that might be caused by the effect of excess ascorbate on Fe. Vitamin C has virtually no adverse effect even in patients with hemochromatosis.

Many reports indicate that ascorbic acid added to cells in culture increases the rate of mutagenesis (Rivers, 1989). Detailed reports exist of increased DNA repair, and chromosome aberrations in cells cultured in media that included ascorbate (Driscoll *et al.*, 1999; Mure and Rossman, 2001). However, these effects were shown only in cultures that contained Fe^{3+} or Cu^{2+}, and when steps were taken to ensure low concentrations of these metals in the culture medium, no detrimental effect on DNA was observed. In such *in vitro* systems, the mutagenic effect of ascorbate can probably be attributed to the generation of oxygen-derived free radicals driven by ascorbate and metal ions. Efficient free radical-scavenging systems protect DNA *in vivo* from such effects, and intracellular concentrations of ascorbate, and metals (that are efficiently sequestrated on binding proteins), are so low and unlikely to be harmful.

5.4 VITAMINS AS ANTIOXIDANTS

Antioxidants may act at different phases of LPO. They may: (a) inhibit the initiation process by abstracting the allylic hydrogen from the α-methylene carbon atom (e.g. vitamin E); (b) inhibit the formation of hydroperoxides by chain breakers (e.g. vitamins E & C); (c) degrade the hydroperoxides formed without producing radicals by inhibiting the metal catalysis and accelerating the decomposition of hydroperoxides (e.g. penicillamine); (d) and remove the free radical by scavenger activity (e.g. vitamins E & A) (Hornsby *et al.*, 1983). Individual antioxidants may act by one or more of the above-mentioned mechanisms. Whether a substance behaves as an antioxidant or prooxidant (facilitating peroxidation) depends on its concentration and on the environment in which it acts. Suppose that a free radical $X^{\bullet}$ is formed in a cell and attacks cell constituent A:

A's hydrogen atom is abstracted and paired with X's single electron. This leads to further damaging reactions. Alternatively, antioxidant Z with a scavenger action may capture the unpaired electron of $X^{\bullet}$ and the resultant molecule XZ may become reactive. The same scavenger molecule Z may, under different conditions, be activated to $Z^{\bullet}$ after having accepted the single electron of $X^{\bullet}$ and may even be more reactive than $X^{\bullet}$, causing even greater damage. Therefore, in using synthetic scavengers it is an important requirement that the scavenger radical product of the reaction should be less reactive than the radical to be removed. At the same time, reactions in complex *in vivo* systems are not completely predictable. For example, Cu if added to PUFA, facilitates autooxidation. However, Cu-complexes in tissues generally but not invariably, behave as antioxidants. Vitamin C is a prooxidant at low concentrations in the presence of trace amounts of transition metals (Cu/ Fe) (either free or chelates) and reduces the metals, thereby promoting the metal catalysis of LPO. At high concentrations, however, when there are sufficient binding sites, vitamin C is an antioxidant.

5.4.1 Water-soluble Radical Scavenging Antioxidants

Vitamin C acts as a water-soluble antioxidant, acting against aqueous radicals formed in whole blood. In a study by Niki *et al.* (1990), when whole blood alone was incubated at 37°C in air, neither antioxidants were consumed nor did oxidation proceed appreciably. However, as soon as the water soluble-radical initiator, 2,2'-azobis(amidinopropane) dihydrochloride was added, the consumption of water-soluble antioxidants was observed. Vitamin C was consumed most rapidly, followed by bilirubin, uric acid and plasma vitamin E. As plasma antioxidants were consumed, LOOH formation was observed.

Vitamin E on the other hand was only slowly consumed at the initial stage (Frei *et al.*, 1989). These results suggest that vitamin C operates as the first line of the plasma antioxidant defence system against ROS. Water-soluble antioxidants are capable of scavenging only free, aqueous radicals and cannot scavenge lipophilic radicals within the membranes or the lipoproteins. Therefore, once the aqueous radicals attack lipids, for example, and the oxidation proceeds within the lipid layer, or when the oxidation is induced by the lipophilic radicals formed initially within the lipophilic interior, the water soluble antioxidants can no longer suppress the oxidation efficiently.

Vitamin C can act synergistically with vitamin E (McCay, 1985; Niki, 1987). It has been observed in fact that vitamin C acts as an efficient antioxidant with vitamin E in the oxidation of LDL and phospholipid liposomal membranes induced by lipophilic radicals (Sato *et al.*, 1990), although vitamin C by itself is not a good antioxidant in the absence of vitamin E. Vitamin C reduces nitroxide radical almost instantaneously in homogenous solutions. However, the rate of their interactions becomes less as the nitoxide radical goes deeper into the interior of the membrane (Takahashi *et al.*, 1988). These results suggest that vitamin E is located near the surface of LDL and membranes.

Vitamin C is a strong reducing agent. It is unstable, readily losing its hydrogen atoms. It may act as an antioxidant by interrupting the LPO chain reaction and losing a hydrogen atom as it reacts with the $ROO^{\bullet}$ and produces the more stable monodehydroascobate. Additionally, it may also have a direct $^{\bullet-}O_2$ and $^{\bullet}OH$ scavenger action. When vitamin C interacts with ROIs, the product is a mixture of monodehydroascobate and

dehydroascobinic acid, depending on whether one or two hydrogen atoms are removed (Dormandy, 1983; Pottathil *et al.,* 1981).

5.4.2 Lipid–Soluble Radical Scavenging Antioxidants

Vitamin E is known to be an important, lipophilic radical scavenging antioxidant (Burton *et al.,* 1985). It scavenges not only lipophilic radicals within the lipid compartment but also aqueous radicals attacking membranes from outside. Antioxidant activities of lipophilic radical scavengers depend not only on their chemical activities toward oxygen radicals, but also on physical factors such as the local concentration and the mobility of antioxidants within the specific microenvironment. Furthermore, the antioxidant activity of α-tocopherol in membranes is much less than that in solutions, and it decreases as the oxygen radical goes deeper into the membrane interior (Takahashi *et al.*, 1989). Apparently, the mobility of α-tocopherol is markedly restricted, at least vertically, in membranes. The main lipid phase antioxidant activity of vitamin E in the cell membrane occurs through hydrogen donation to hydroperoxides. Thus, the formation of hydroperoxides is prevented, the chain reaction is terminated, and the extension of the pathological free reaction is prevented. In addition, it also scavenges $^1O_2$. The phytyl side chain of vitamin E is not involved in its antioxidant action (Hornsby *et al.,* 1983).

In a study done by Ibrahim *et al.* (1997), male Swiss-Webster mice fed on vitamin E-deficient fish oil diet for 4 weeks had significantly higher levels of TBARs, conjugated dienes, and protein carbonyls. The levels of TBARs were further increased by Fe supplementation. Significantly lower concentrations of α-tocopherol and higher

glutathione (GSH) were found in the liver of mice fed on fish oil and vitamin E, than the other groups. Dietary fat or vitamin E and Fe did not alter the activities of Se-GSH peroxidase, non-Se-GSH peroxidase, catalase, and glutathione reductase. In addition, dietary fat or vitamin E and Fe did not affect the level of ascorbic acid. These results suggest that vitamin E protects not only lipid-soluble compounds, but also water-soluble constituents, against oxidative damage.

High levels of dietary vitamin E, however, do not replace cellular glutathione peroxidase (GPX1) protection from acute oxidative stress. In a study with GPX1 knockout mice and wild type mice, dietary vitamin E levels had no apparent effect on the histopathology. High levels of vitamin E intake, up to 100-fold daily nutritional needs, could not prevent the GPX1 or the wild type mice from paraquat lethality or substantially prolong their survival time. Supplementing α-tocopherol acetate at 7500 mg/kg resulted in a decrease in the survival of the wild type mice after the paraquat injection. Although vitamin E is considered safe at large oral dosages, megavitamin E doses may act as a prooxidant when free radicals are continuously generated, as under these experimental conditions. Despite the potent inhibition of hepatic LPO, high levels of dietary vitamin E did not replace the protection of GPX1 against the paraquat-induced lethality or the diquat-induced plasma ALT level increase in mice (Cheng *et al.*, 1999).

Vitamin A plays a role in the differentiation of the epithelial tissue and in growth, and may have anticarcinogenic action. Its anticarcinogenic and antioxidant actions may be related to its unsaturated fatty acid content, which provides an alternative pathway for LPO. It is also

a $^1O_2$ scavenger, and its metal chelating property contributes to its potential antioxidant and anticarcinogenic actions.

5.5 VITAMIN ANTIOXIDANTS IN CANCER PREVENTION

Early epidemiological studies indicated that a diet rich in yellow vegetables is associated with decreased risk of cancer (MacLennan *et al.*, 1977; Hirayama, 1979). Peto *et al.* (1981) hypothesized that the beta-carotene present in these vegetables might be responsible for the observed decreased in cancer rates. Since then, more than 100 case-control and cohort studies have examined the association between the intake of vitamins and the risk of developing cancer.

The Chinese Cancer Prevention Study tested the effects of four combinations of vitamins, using one-half replicate of a 2x4 factorial experimental design, among 29,548 adults aged 40-69 years residing in Linxian, China. During the follow-up 2127 deaths occurred, including 792 cancer deaths, and 1298 incident cases of cancer. Only one of the combinations resulted in a slightly lower incidence of cancer (Blot *et al.*, 1993). In the Alpha-Tocopherol, Beta-Carotene Cancer Prevention Study, 29,133 Finnish male smokers, aged 50-69 yrs, were given 20 mg β-carotene daily. β-carotene had little or no effect on the incidence of cancers (ABCPS, 1994). The Physicians' Health Study randomly assigned 22,071 healthy US male physicians, aged 40-84 yrs, to β-carotene (50 mg on alternate days) or placebo. After treatment and follow-up of 12 yrs, 2566 incident cases of cancer occurred. Supplementation with β-carotene had no effect on cancer incidence (Hennekens *et al.*, 1996). Similar results were obtained in the β-Carotene and Retinol Efficiency Trial

(CARET) testing a combination of β-carotene (30 mg daily) and vitamin A (25,000 IU daily) (Omenn *et al.*, 1996; Greenburg *et al.*, 1994).

Adverse effects of β-carotene in cancer prevention studies have been reported (DeLuca and Ross, 1996; Albanes, 1999; ABCPS Group, 1994). The conundrum here is that β-carotene itself may act as an anticarcinogen, but its oxidized products at high concentrations may facilitate carcinogenesis (Wang and Russell, 1999). In a recent study, researchers found that vitamins A and E appeared to prevent cancer cells from self-destruction through apoptosis (Salganik, 1999; Greenburg *et al.*, 1994). Twenty studies examined the relation between blood levels of vitamin E or α-tocopherol and cancer risk (Knekt, 1991; Knekt *et al.*, 1991). About one-third of the blood-based studies observed significantly lower levels of vitamin E in prediagnostic specimens of subjects who eventually went on to develop cancer (total cancer, as well as various site-specific cancers), as compared with controls.

As data in support of or against the use of vitamins as antioxidants continue to increase, it may be worthwhile investigating the antioxidant properties of other chemical compounds that are capable of trapping ROIs and equally safe for medication. One such compound is acetylsalicylic acid (aspirin). The unsaturated double bonds in the benzene ring, does suggest that aspirin may have antioxidant properties.

6.0 SALICYLATES

Salicylates are classified into two groups; acetylated and nonacetylated. Acetylsalicylic acid (ASA) or aspirin is the most important salicylic acid of ester derivatives. Salicylic acid and its derivatives are absorbed rapidly from the stomach and intestines by passive diffusion of undissociated molecules (Cohen, 1976). In addition, food significantly prolongs the mean gastric residence time of aspirin as well as the time to reach peak salicylate concentrations.

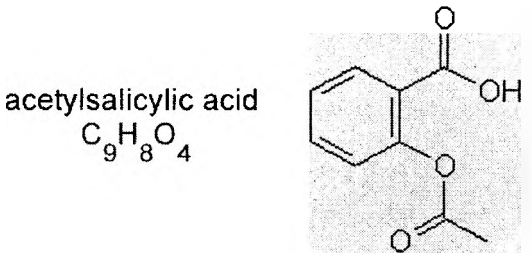

Figure 11 Molecular structure of aspirin

6.0.1 Distribution

The distribution of the acetyl group of aspirin is different from that of the salicyl moiety. The labile acetyl group is bound to a variety of proteins, glycoproteins, and lipids of the liver and other organs (Rainsford *et al.*,1983). With salicylates the fraction bound to albumin decreases with increasing total salicylate concentration (Windorfer *et al.*, 1978). At low therapeutic salicylate concentrations in plasma (100 µg/ml), about 90% is bound, while at higher concentrations (400 µg/ml), only about 76% of the salicylate is bound (Wosilait, 1976). The protein binding of salicylates is also influenced by age and disease. Salicylates are present in breast milk and the peak concentration of salicylate in milk is 2% to 5% of the peak maternal plasma salicylate concentrations.

6.0.2 Metabolism

Aspirin is absorbed and rapidly hydrolysed (in the bowel wall and liver) to salicylic acid. Salicylic acid is eliminated from the body by: 1) renal excretion of salicylic acid; 2) conjugation with glycine to form salicyluric acid (SU); 3) conjugation with glucuronic acid to form salicyl phenolic glucuronide (SPG), salicyl acyl glucuronide (SAG), salicyluric acid phenolic glucuronide (SUPG); 4) oxidation to gentisic acid (GA) and 5) the formation of gentisuric acid from either SU (through microsomal oxidation) or GA (via glycine conjugation). 2,3-dihydrobenzoic acid has been identified in urine and plasma following the ingestion of aspirin.

6.0.3 Elimination

After a small dose of aspirin (i.e., 300 mg or less) about 90% is excreted as SU and SPG (Tsuchiya and Levy, 1972). However, after moderate doses, when the amount of salicylates in the body is more than about 600 mg, the maximum rate of formation of SU, SUPG, and SPG are reached. The amount of salicylic acid in the body increases non-linearly with increasing dosage. When the amount of salicylate increases from 250 mg (equivalent of one aspirin tablet) to 10 g, the time required for the first 50% of the dose to be removed from the body increases from 3 to 20 hours.

6.0.4 Excretion

Renal excretion of salicylate is through a balance of glomerular filtration, active proximal tubular secretion, passive tubular secretion, and passive tubular absorption. The excretion of salicylic acid is markedly pH-dependant: as the urinary pH changes from 5 to 8, the

amount of free ionized salicylate excreted increases from 2% to 3% of the total salicylate dose to more than 80% (Smith *et al.*, 1946). There are several reports of circadian rhythms in the urinary excretion of salicylate, with excretion being faster after the drug is ingested between 7:00 and 11:00pm (Reinberg *et al.*, 1975). This increase may in part be related to the circadian changes in urinary pH or the increased clearance of salicylate during bed rest or prolonged supination (Levy, 1967).

6.0.5 Drug Interactions

Published drug interactions with aspirin do not include an interaction with Fe and its products, although gastrointestinal bleeding may have a negative effect on Fe absorption. In addition, reduced Fe levels may be the result of haemoglobin loss.

6.0.6 Mechanism of action

Injury triggers the production of prostaglandins, hormone-like molecules that causes fever and inflammation. Because of the prostaglandins, the nerve endings that are involved amplify and bring about recognition of pain. Prostaglandins H2 synthetase (PGHS) is the enzyme that synthesizes prostaglandins, and aspirin blocks the production of prostaglandins.

6.1 ASPIRIN – ANTIOXIDANT ACTIVITY AND LPO.

The hydroxylation of aromatic compounds such as aspirin by ROS has been demonstrated by Richmond *et al.* (1981). *In vitro* studies have also shown that the effect of aspirin on free radical reactions is metal dependent. Aspirin is able to form metal complexes similar

to SA, which are able to react with highly reactive $^{\bullet}OH$ radicals (Grootveld and Halliwell, 1986). The efficiency of this aspirin-$^{\bullet}OH$-radical-scavenger depends on its binding affinity for metal ions (Gutteridge, 1984; Kirkova *et al.*, 1992).

Studies carried out on Wistar rats with varying aspirin doses of 300 mg/kg/d - 500 mg/kg/d (Kirkova *et al.*, 1995) showed that LPO, measured by MDA production in aspirin-treated rats, was not significantly different from the control. This is contrary to the possible antioxidant capacity demonstrated by Gutteridge (1984). However, against the background knowledge of significant MDA production in liver homogenates after Fe(II)-induction, the effects of aspirin may have been hidden. The lack of significant changes in the H_2O_2-induced MDA production in the erythrocytes of aspirin-treated rats could also be ascribed to the high endogenous Fe level in these preparations. Gunther *et al.* (1991), reported after a 5-day oral treatment with 700 mg/kg salicylic acid, that the endogenous MDA level was not changed in the erythrocyte but slightly increased in the liver. On the contrary, it is known that MDA is one of the products of the enzymic oxidation of arachidonic acid, particularly of thromboxane biosynthesis (Hamberg *et al.*, 1975) and that aspirin leads to irreversible inactivation of cyclooxygenase. Hence a decrease in MDA could be expected after aspirin treatment (Rang and Dale, 1987).

6.2 ASPIRIN AND LIVER PLASMA MEMBRANE

The lipid composition in the cell membrane primarily defines its fluidity, and modifications affect important cellular functions such as ion-transport, neurotransmitter release and the activity of membrane-bound enzymes (Spector and Yosek, 1985). Although

some studies suggest that ASA stabilizes lysosomal membranes, others found ASA ineffective in stabilizing rat liver lysosomes. Omer *et al.* (1990) studied the effect of ASA on liver membranes, and membrane-bound enzymes. Their results showed that chronic oral administration of ASA at 50 mg/kg had no effect on cholesterol and phospholipid levels. However, significantly higher cholesterol and phospholipid levels were obtained in the group that received 200 mg/kg. Furthermore, raised levels of liver membrane phospholipids and cholesterol may be involved in the development of liver injury through the peroxidation of PUFAs.

6.3 ASPIRIN AND LIVER

High serum levels of ASA cause liver cell damage. However, the mechanisms remain obscure. Takashi *et al.* (1998) studied the effect of ASA on rat liver tissue. AST, ALT and direct bilirubin (D-bil) were not significantly increased at low doses. However, at a higher dose of 150mg/kg body wt. *per o.s.* daily for 3 weeks, the level of γ-glutamyltranspeptidase (γ-GTP) was significantly higher than that of the controls and liver damage was observed. In addition, mitochondria isolated (after 7 days) had a larger diameter than the controls. Although the mitochondrial change was not significant, it may be linked to the uncoupling of oxidative phosphorylation observed in the mitochondria isolated from ASA-treated rats (Tomoda *et al.*, 1992).

6.4 ASPIRIN AGAINST CANCER

Most studies done on the anti-cancer potential of aspirin relate to colorectal cancer. However, few or no studies have been done in relation to aspirin and liver cancer. It is

believed that the explanation for aspirin's anti-tumour effect is that it blocks production of substances that may be required for tumour growth (Marcus, 1995) and this may be explored in this study.

7.0 BIOMARKERS OF OXIDATIVE STRESS

7.0.1 Introduction

Epidemiological studies focusing on chronic diseases and antioxidants have in the past relied primarily on antioxidant nutrients. This approach, however, is in essence using estimates from exposure to a selected group of nutrients for actual oxidative status. Emphasis is now being placed on developing functional biomarkers of oxidative stress status that integrate the effect of exposure to oxidants with the full range of oxidant protective mechanisms *in vivo*. Such biomarkers being studied include lipids, DNA and protein oxidative products.

7.1 BIOMARKERS OF LPO

Oxidation of lipids has been extensively studied and there are more biomarkers available for lipid oxidation than for DNA and protein combined.

7.1.1 Thiobarbituric acid-reactive substances (TBARs)

TBARs are one of the earliest markers used in human and animal studies (Buege and Aust, 1978). The assay of TBARs is a simple spectrophotometric assay that measures the chromogen produced by the reaction of thiobarbituric acid (TBA) with MDA, an end product of LPO. This is an easy method but non-specific because of other substances such as aldehydes reacting with TBA (Handelman and Pryor, 1999). The latter has rendered this approach obsolete. A modified version of this method uses HPLC to separate the MDA-TBA adduct from other interfering chromogens. This improves the specificity, sensitivity and reproducibility (Wong *et al.*, 1987). TBARs can be measured in tissue but are

generally measured in plasma. Plasma MDA has been reported to respond to alterations in antioxidant nutrients (Dixon *et al.*, 1998).

7.1.2 Breath hydrocarbons

The measurement of breath hydrocarbons is another commonly used non-invasive approach for investigating LPO *in vivo* (Knutson *et al.*, 2000). Pentane and ethane, which are formed from peroxidation of (n-6) and (n-3) fatty acids, respectively, are volatile compounds released into the breath. Potential errors involve contamination with ambient-air pentane and ethane (Knutson *et al.*, 2000). In a recent study (Allard *et al.*, 1994), levels of breath pentane were higher in smokers (an oxidatively stressed group) than in non-smokers. Breath hydrocarbon levels were reduced in smokers on β-carotene supplementation.

7.1.3 LDL oxidation

The oxidative modification of LDL is thought to enhance atherogenicity. For this reason, susceptibility of LDL to induce oxidative stress *ex vivo* has been used as a possible bio-marker of oxidative defence, at least in the LDL particle itself. Lipid-soluble antioxidants are known to be located in LDL *in vivo*. LDL susceptibility should therefore reflect the antioxidant defence system, particularly as it related to lipid substrates and lipid-soluble antioxidant compounds. This assay involves challenge to exogenous oxidants. For example, Cu is commonly used to induce oxidation and is followed by measuring of lag time before oxidation. Consistency of vitamin E to resistance to oxidation has been shown (Jialal *et al.*, 1995). In interpreting results based on LDL oxidation, antioxidant efficacy

and the choice of inducing agents used for both metal ion-dependent (i.e.. cupric ions) oxidation and metal ion-independent [e.g. 2,2'-azobis(2-amidinopropane)dihydrochloride or AAPH] oxidation should be taken into account (Gaziano *et al.*, 1995).

7.1.4 F_2 isoprostanes

F_2 isoprostanes are produced by free-radical induced peroxidation of arachidonic acid (Morrow *et al.*, 1990). These compounds are formed in phospholipids and are cleaved and released into the circulation, before excretion into urine as free isoprostanes (Roberts and Morrow, 1997). The most abundant F_2 isoprostane is 8-isoprostaglandin $F_{2\alpha}$ (8-iso-$PGF_{2\alpha}$), which has been suggested to be a promising marker of oxidative injury (Sodergren *et al.*, 2000).

Urine is often considered a better matrix than serum for quantifying isoprostane status. Aspirin, for example, suppresses 8-isoprostane in serum (Reilly *et al.*, 1996) but not in urine samples stored for any length of time, and such samples are generally considered inappropriate for isoprostane analysis. For urine samples, standardization of isoprostane concentration by creatinine should be considered.

One possible limitation to the use of isoprostanes in epidemiologic studies is that typical laboratory analysis depends on gas chromatography /mass spectroscopy (GC/MS) methods that are time consuming and therefore expensive for a large sample size. However, GC/MS methods have excellent specificity and sensitivity (Handelman and Pryor, 1999). Immunological assays, although available, may sacrifice specificity because of possible

cross-reactions with other prostanoids. Studies of the modulation of isoprostanes are available. For example, Reilly *et al.* (1996) reported that vitamin C administration for 5 days at 2 g daily to heavy smokers significantly reduced 8-iso-$PGF_{2\alpha}$ in urine. However, vitamin E had no effect at either 100 or 800 IU/day.

7.1.5 Ferrous Xylenol orange (FOX) assay

This method is simple and sensitive. Additionally, it is said to give highly reproducible results for biological samples. It is reported to outperform the iodometric assay, and other assays in terms of simplicity and reproducibility. Finally, very small quantities only of samples are required for this assay (Wolff, 1994).

7.1.6 Other related assays

Oxygen radical absorbance capacity (ORAC)(Cao *et al.*, 1993) and total $ROO^{\bullet}$-trapping (TRAP)(Wayner *et al.*, 1985) take into account the total antioxidant capacity of a system to scavenge or trap oxygen radicals. Assays such as ORAC allow investigators to use different reactive oxygen species generators to measure total antioxidant capacity of a sample under different conditions.

7.2 BIOMARKERS OF DNA OXIDATION

7.2.1 8OHdG

This is one of the most common markers used in assessing oxidative DNA damage. This compound is sometimes referred to as 8-oxy-7-hydrodeoxyguanosine (8-oxodG). DNA can be oxidized to produce many oxidative products. However, oxidation of the C-8 of guanine

is one of the more common oxidative events, and results in a mutagenic lesion that produces predominantly G-to-T transversion mutations. It has been suggested that 8OHdG could be used as a possible approach to the assessment of the individual's cancer risk as a result of oxidative stress (Kasai, 1997). 8OHdG can be measured in human DNA samples (i.e. lymphocyte DNA, placental DNA etc) and urine. Several methods for quantifying this marker are available. High performance liquid chromatography (HPLC) with electrochemical detectors (HPLC/ECD) and CG/MS methods are the most widely used, although enzyme-linked immunosorbent assays (ELISA) techniques are also being employed (Santella, 1999). HPLC and ELISA methods were compared using placental tissue DNA. Values by both methods correlated well, but the ELISA values were higher than those determined by HPLC (Loft *et al.*, 1994). This is possibly the result of cross-reactivity with other compounds other than 8OHdG.

The ready availability of urine makes it the preferred sample for epidemiological studies. Although convenient, urinary 8OHdG also has limitations. 8OHdG in the urine is a function not only of DNA oxidation (Loft *et al.*, 1994), but also of excision repair. Urinary 8OHdG may be influenced by metabolic rate as well as renal integrity. These factors must be taken into consideration especially in intervention studies. Haegele *et al.* (2000), measured lymphocyte 8OHdG by HPLC/ECD and urinary 8OHdG by ELISA in a 14-day fruit and vegetable intervention trial. Results indicated that plasma lutein and β-cryptoxanthin, both of which are xanthophyll carotenoids, were significantly inversely correlated with urinary isoprostane excretion (8-iso-$PGF_{2\alpha}$) and with 8OHdG in lymphocyte DNA but not with urinary 8OHdG. The authors noted the shortcomings

with the ELISA as extreme variability in the pre-intervention urinary 8OHdG values.

7.2.2 Antibodies to oxidized DNA

Serum antibodies to 5-hydroxymethyl-2'-deoxyuridine (HMdU), a product of thymine oxidation has been proposed as a possible biomarker of oxidized DNA. Frenkel *et al.* (1998) found that humans produce antibodies to this compound, and titres of anti-HMdU can be measured in a simple ELISA assay. This marker was evaluated in blood samples from 169 women with samples obtained 0.5- 6 years before diagnosis of breast, colon or rectal cancer. Anti-HMdU antibody level was significantly higher in the cases as compared to age-matched controls. Limited evidence suggests that dietary supplementation with α-tocopherol (60 or 200 mg/d) can reduce levels of this biomarker (Hu *et al.*, 1999).

7.2.3 Comet assay

The Comet assay, also referred to as the single-cell microgel electrophoresis or SCGE assay, was developed to detect DNA strand breaks. Breaks in the DNA allow supercoiled loops of DNA to relax and move out to form what looks under the conditions of the assay like a Comet with a tail. The proportion of the DNA in the tail is indicative of the extent of breaks. Modifications to the Comet assay have been developed that allow for the detection of oxidized DNA bases. An intermediate step has been introduced using edonuclease III, which induces breaks in the DNA at sites of oxidized pyrimidines (Collins *et al.*, 1993). Pool-Zobel *et al.* (1997) used this modified Comet assay to demonstrate that supplementation of the diet with tomato, carrot or spinach products significantly reduced endogenous levels of strand breaks in lymphocyte DNA.

7.3 BIOMARKERS OF PROTEIN OXIDATION

Biomarkers of protein oxidation are often applied when a battery of markers of oxidative stress status are being studied. Increased markers of protein oxidation have been associated with diseases such as Alzheimer's disease, Parkinson's disease, Duchenne muscular dystrophy, amyotrophic lateral sclerosis, rheumatoid arthritis and progeria (Stadtman and Berlett, 1998).

7.3.1 Protein carbonyls

The biomarker that is generally used to estimate protein oxidation is protein carbonyl. The conventional assay is a colorimetric procedure that involves dinitrophenylhydrazine (Levine *et al.*, 1990). More recently an ELISA method has been developed (Winterbourn and Buss, 1999) that correlates well with the colorimetric assay.

Marangon *et al.* (1999) investigated the effects of oral supplementation with α-tocopherol and lipoic acid on various parameters of oxidative stress in 31 healthy subjects. Lipoic acid significantly decreased plasma carbonyl levels after 2,2'-azobis-(2-methylpropion-amidine)-dihydrochloride (AAPH) induced oxidation, whereas α-tocopherol had no effect on plasma carbonyls. Both lipoic acid and α-tocopherol prolonged LDL lag time and decreased urinary F_2 isoprostanes in their study.

8.0 METHODS

8.1 SERUM / LIVER IRON DETERMINATION

8.1.1 Principle

Ferric Fe is dissociated from its carrier protein transferrin in an acid medium and simultaneously reduced to the ferrous form. The ferrous Fe is then complexed with a chromogen, to produce a blue chromophore that absorbs maximally at 595 nm (Ceriotti and Ceriotti, 1980).

i. Transferrin $(Fe^{3+})_2$ $\xrightarrow{\text{buffer}}$ $2\ Fe^{3+}$ + Transferrin

ii. $2\ Fe^{3+}$ $\xrightarrow{\text{Reducing agent}}$ $2\ Fe^{2+}$

iii. $2\ Fe^{2+}$ + Chromogenous compound ----------> Ligand (blue chromophore)

8.1.2 Reagents

Sigma Serum Iron Kit was used that contained the following reagents:

A. Iron buffer reagent: hydroxylamine hydrochloride, 1.5% (w/v), in acetate buffer, pH 4.5 with surfactant added.

B. Iron colour reagent: ferrozine, 0.85% (w/v), in hydroxylamine hydrochloride solution with stabilizer added.

C. Fe standard: Fe, 500 µg/dl (89 µmol/l) in hydroxylamine hydrochloride solution.

8.1.3 Sample Preparation for Liver Iron. [The method of Torrance and Bothwell (1968) was used].

- An acid solution was prepared as follows:

  50 g TCA was dissolved in 200 ml ddH_2O (iron-free) in a 500 ml volumetric flask. 148.5 ml conc. HCl was gently added and the volume made up to 500 ml. (The solution was stored in a dark bottle and was stable for 2 mo).

- 0.1g of tissue was weighed accurately and divided into 4 or more pieces. This was transferred into a test tube and 1.0 ml of acid solution was added. The tube was sealed with parafilm and incubated at 65°C for 20 hrs.

- A 1:100 dilution of the supernatant (using the iron buffer reagent- hydroxylamine hydrochloride, from kit) was made and the tissue iron determined as described below. The concentration of tissue iron was corrected for dilution and weight. Results were expressed as µg/g wet wt.

8.1.4 Assay Procedure

The procedure was followed according to the manufacturer's instructions. However, the sample and reagent volumes were modified as shown below.

Table 3 Serum and liver iron determination

Sample and Reagents	Volume	Remarks
Buffer	1000µl	
Sample / Standard / Blank	100µl	ddH_2O was used for blank
		Mixed and incubated at 37°C for 5 min
		The initial absorbance of the sample/standard was read at 560 nm against the blank
Chromogen	40µl	
Mixed and incubated for 5min at 37°C. The final absorbance was read against blank. The initial absorbance was subtracted from final absorbance to give δA for sample and standard.		

8.1.5 Calculation

$$\text{Fe conc. of sample} = \frac{\delta A_{\text{sample}}}{\delta A_{\text{standard}}} \times \text{Conc.}_{\text{standard}}$$

8.2 ASCORBIC ACID DETERMINATION

8.2.1 Introduction

Ascorbic acid can be determined colorimetrically with 2,4-dinitrophenylhydrazine to form the red bis-hydrozone or with 2,4-dichlorophenolo-indophenol that is reduced to a colourless form. Assessment of vitamin C status is generally done by measuring serum (plasma) and leukocyte levels of the vitamin. Urinary excretion and red cell concentrations have been found to be specific and useful indices of vitamin C status.

8.2.2 Principle

Ascorbic acid in plasma is oxidized by Cu (II) to form dehydroascorbic acid, which reacts with acidic 2,4-dinitrophenylhydrazine to form a red bis-hydrazone, which is measured at A_{520}.

8.2.3 Reagents and Preparation

- Metaphosphoric acid - H_3PO_4
- H_2SO_4
- 2,4-dinitrophenylhydrazine
- Thiourea
- $CuSO_4$

1. Metaphosphoric acid (HPO_3) sol^n : 6.0g/dl (freshly prepared)
   - 30.0g of HPO_3 in 500ml of dH_2O.
2. H_2SO_4 : 4.5 mol/l
   - 250 ml H_2SO_4 was added slowly to 500ml cold water and made up to 1L
     Because considerable heat was generated, the flask was placed on ice.
3. H_2SO_4 : 12 mol/l
   - 650 ml H_2SO_4 was added slowly to 300ml cold water and made up to a volume of 1L and refrigerated.
4. 2,4-Dinitrophenylhydrazine (2,4-DNPH) 2.0 g/dl in 4.5 mol H_2SO_4
   - 10 g of 2,4-DNPH in H_2SO_4 was made up to a volume of 500 ml.
     This was allowed to stand in a refrigerator overnight and then filtered.
5. Thiourea sol^n. 5.0 g/dl
   - 5 g thiourea was added to a volume of 100 ml (Stable at 4°C for 1 min).
6. $CuSO_4$ sol^n: 0.6 g/dl
   - 0.6 g of anhydrous $CuSO_4$ in dH_2O was made up to a volume of 100 ml.
7. Dinitrophenylhydrazine -thiourea-copper sulfate reagent (DTCS)
   - 5 ml Thiourea sol^n.]
   - 5 ml $CuSO_4$ sol^n.] } 4°C (stable for 1 wk.)
   - 100 ml 2,4-DNPH]
8. Standards : - All ascorbic acid standards were prepared daily.

   A) Ascorbic acid stock standard, 2.0 mmol/l (In 6.0 g/dl freshly prepared HPO_3)

$$2.0 \text{ mmol/l} = \frac{g}{176.13}$$

$$2.0 \times 10^{-3} \text{ M} = \frac{g}{176.13}$$

$$g = 176.13 \times 2.0 \times 10^{-3}$$

$$= 352.26 \times 10^{-3}$$

$$= 0.35g$$

$$\equiv 0.035g / dl$$

B) Working standard.

$$V_1 = \frac{M_2 V_2}{M_1}$$

$$V_1 = M_2 \times \frac{10}{2} \quad ml$$

In seven 10 ml volumetric flasks, the following were pipetted:

0.0200	mmol/l	=	100.0	µl	] *Stock ascorbic*
0.0175	mmol/l	=	87.5	µl	] *acid was used,*
0.0150	mmol/l	=	75.0	µl	] *and made*
0.0100	mmol/l	=	50.0	µl	] *up to 10.0 ml*
0.0050	mmol/l	=	25.0	µl	] *with freshly*
0.0025	mmol/l	=	12.5	µl	] *prepared HPO_3*
0.0010	mmol/l	=	5.0	µl	] *sol^n.*

8.2.4 Assay Procedure

Table 4 Vitamin C determination

Sample and Reagents	Volume	Remarks
Freshly prepared H_3PO_4	500 µl	
Sample / Standard / Blank	25 µl	ddH_2O was used for blank Vortexed and centrifuged at 2500g for 10 min
Clear supernatant was pipetted into screw-capped tubes	480 µl	
DTCS	160 µl	*Tubes were incubated at 37°C for 3hrs*
		Tubes were removed and chilled on ice for 10 min.
Cold 12M H_2SO_4	800µl	*Tubes were capped and mixed by vortexing.*
The final absorbance against blank was read at 520 nm.		

8.2.5 Example of Spreadsheet and Calibration Curve

To correct for the dilution of plasma by HPO_3, the concentration of vitamin C in the samples obtained from the standard curve was multiplied by 21 (dilution factor).

Srl.	Abs.	Conc. y=3.5383x-0.0026	Mean Conc (mmol/l)	µmol/l
S1	**0.005**	**0.0021**		
S2	**0.005**	**0.0021**		
S3	**0.010**	**0.0036**		
S4	**0.022**	**0.0070**		
S5	**0.036**	**0.0109**		
S6	**0.038**	**0.0115**		
S7	**0.041**	**0.0123**		
C1	0.020	0.0064	0.00418	4.18
C3	0.006	0.0024		
C5	0.019	0.0061		
C4	0.002	0.0013		
C5	0.014	0.0047		

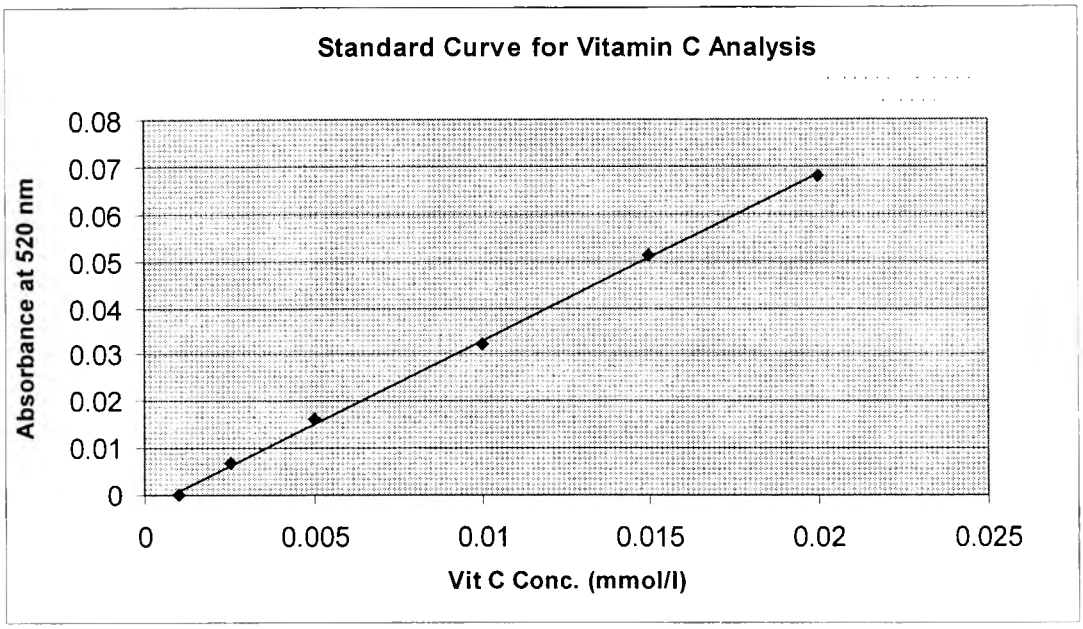

8.3 SUPEROXIDE DISMUTASE (SOD) DETERMINATION

8.3.1 Introduction

The role of SOD is to accelerate the dismutation of the toxic superoxide ($^{\bullet-}O_2$) radicals produced during oxidative energy processes to hydrogen peroxide and molecular oxygen.

$$(^{\bullet-}O_2)_2 \quad + \quad 2H^+ \quad \text{-------}> \quad H_2O_2 \quad + \quad O_2$$

8.3.2 Principle

This method employs xanthine and xanthine oxidase (XOD) to generate $^{\bullet-}O_2$ radicals that react with 2-(4-Iodophenyl)-3-(4-nitrophenol)-5-phenyltetrazolium chloride (I.N.T.) to form a red formazan dye. SOD activity is then measured by the degree of inhibition of this reaction.

$$\text{Xanthine} \xrightarrow{\text{XOD}} \text{Uric acid} + {}^{\bullet-}O_2 \quad \ldots\ldots\ldots\ldots\ldots\ldots(1)$$

$$\text{I.N.T.} \xrightarrow{{}^{\bullet}O_2} \text{Formazan dye} \quad \ldots\ldots\ldots\ldots\ldots\ldots\ldots\ldots(2)$$

OR

$$O_2^{-\bullet} + {}^{\bullet-}O_2 + 2H^+ \xrightarrow{\text{SOD}} O_2 + H_2O_2 \quad \ldots\ldots\ldots\ldots\ldots(3)$$

SOD promotes reaction (3). Therefore reaction (2) is inhibited as a result of insufficient ${}^{\bullet-}O_2$. The degree of inhibition is directly proportional to the amount of SOD, and inversely proportional to the amount of formazan produced.

8.3.3 Reagents and Preparation

Randox Laboratories Ltd. SOD kit was used and the procedure followed according to the manufacturer's instructions. The kit consisted of the following:

A. Mixed substrate made up of xanthine (0.05 mmol/l) and I.N.T. (0.025 mmol/l).

B. CAPS 40 mmol/l; pH 10.2 and EDTA 0.94 mmol/l

C. Xanthine oxidase (80 U/l)

D. SOD standard (5.3 mmol/l)

E. Sample diluent (0.01 mol/l phosphate buffer, pH 7.0)

Preparation of Various Standards

The lyophilized standard (Std) was reconstituted to 10 ml and serial dilutions were prepared as follows:

	Vol. of Std. Sol^{n}	Vol. of sample diluent
S6	Undiluted Std.	-
S5	5ml of S6	5ml
S4	5ml of S5	5ml
S3	5ml of S4	5ml
S2	3ml of S3	6ml
S1	---	5ml

Preparation of Sample

180 µl of heparinized whole blood was used. Erythrocytes were washed 4 times using 1ml normal saline (0.9%) each time. Each wash was centrifuged at 3000 rpm for 10 min and the plasma aspirated off.

400 µl of cold ddH_2O was then added to the washed cells. This was vortexed and allowed to stand for 15 min at 4°C. 10 µl of the lysate was then added to 490 µl of the phosphate buffer to achieve a 50-fold dilution factor (df) and a 30% - 60% inhibition of equation (2).

8.3.4 Assay Procedure.

The procedure was followed according to the manufacturer's instructions with slight modifications. The reaction was carried out at 37°C. The absorbance was read against air blank at 505 nm.

Table 5 SOD determination.

Sample and Reagents	Volume	Remarks
Diluted Sample / Control/ Sample diluent (blank)	25 µl	
Mixed Substrate (Xanthine /I.N.T.)	850 µl	
		It was mixed well.
Xanthine Oxidase	125µl	
This was well mixed, and the timer started simultaneously. The initial absorbance (A_1) was read at 30 sec. The reaction was allowed to proceed for 3 min before reading the final absorbance (A_2) at 3:30 min.		

8.3.5 Calculation

$$\frac{A2 - A1}{3} = \delta A / \text{min (standard or sample)}$$

Sample diluent rate (S1 rate) = rate of uninhibited reaction = 100%

Rates of all standard and diluted samples were converted into percentages of the sample diluent rate, and subtracted from 100% to give the percentage inhibition.

$$100 - \frac{(\delta A_{std/min} \times 100)}{(\delta A_{s1/min})} = \% \text{ inhibition} \quad \ldots\ldots\ldots\ldots(4)$$

A curve of percentage inhibition for each standard against Log_{10} standard concentration of SOD U/ml was plotted. Using the percentage inhibition of the sample from equation (4), SOD concentration was obtained from the standard curve.

SOD units/ml of whole blood = SOD units/ml from standard curve x 50 (df)

Finally, SOD units /g haemoglobin was calculated using equation (5).

$$\frac{\text{SOD units / ml}}{\text{g haemoglobin}} = \text{SOD units / g haemoglobin} \quad \text{.....(5)}$$

8.3.6 Example of Spreadsheet and Calibration Curve

Srl.	Final Abs A2	Initial Abs A1	δA=A2-A1	δA/min (d)	% Inhibition 100-(δStd x 100 ./ (δAS1/min)	Log10 Conc.	Anti-Log	Mean x 200(Df)= z	Hb g/dl	SOD/g Hb (z / Hb/ml)	Mean SOD
S1	0.057	-0.016	0.073	0.024	21.51						
S2	0.048	-0.01	0.058	0.019	37.63	-0.655	0.22				
S3	0.018	-0.018	0.036	0.012	61.29	-0.178	0.66				
S4	0.001	-0.023	0.024	0.008	74.19	0.122	1.33				
S5	-0.011	-0.024	0.013	0.004	86.02	0.423	2.65				
S6	-0.022	-0.028	0.006	0.002	93.55	0.724	5.30				
C1	0.02	0.009	0.011	0.004	88.17	0.045	1.11	221.8	13.9	1596	
C2	0.031	-0.009	0.04	0.013	56.99	-0.243	0.57	114.4	12.5	915	
C3	0.022	-0.012	0.034	0.011	63.44	-0.086	0.82	164.3	13.2	1244	
C4	0.025	-0.01	0.035	0.012	62.37	-0.112	0.77	154.6	13.8	1121	
C5	0.021	-0.01	0.031	0.010	66.67	-0.007	0.98	196.8	14.4	1367	1249

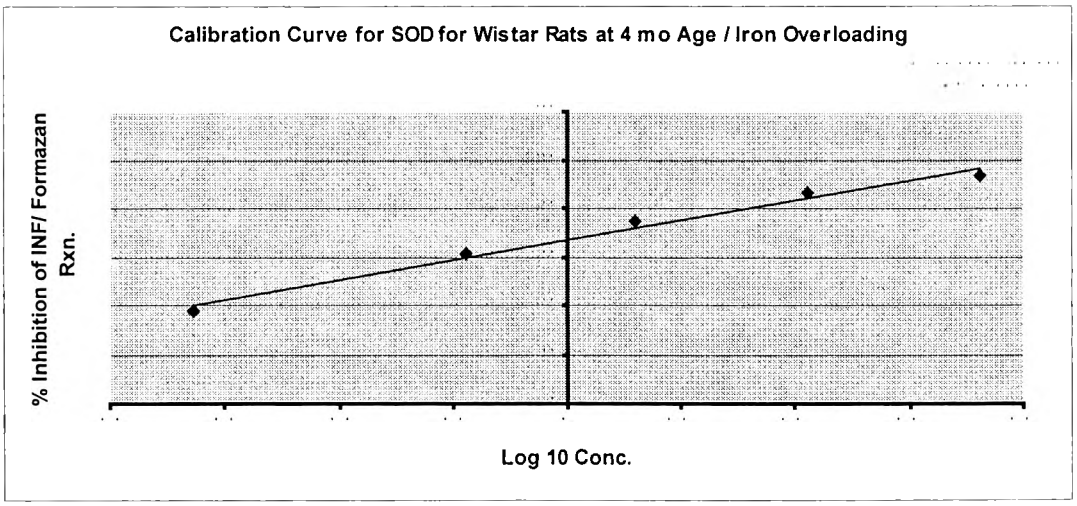

8.4 GLUTATHIONE PEROXIDASE (GPx) DETERMINATION

8.4.1 Principle

Glutathione Peroxide (GPx) catalyses the oxidation of glutathione (GSH) by cumene hydroperoxide. In the presence of glutathione reductase (GR) and NADPH the oxidized glutathione (GSSG) is immediately converted to the reduced form with a concomitant oxidation of NADPH to $NADP^+$. The decrease in absorbance as a result of the reaction is measured at 340 nm [Paglia and Valentine (1967); Kraus and Ganther (1980)].

$$2GSH + ROOH \xrightarrow{GPx} ROH + GSSG + H_20$$

$$GSSG + NADP + H^+ \xrightarrow{GR} NADP^+ + 2GSH$$

Randox Laboratories Ltd. commercial kit was used and the procedure followed according to the manufacturer's instruction.

8.4.2 Reagents in Kit

A. Glutathione (4.0 mmol/l)

B. Glutathione reductase (> 0.5 U/l)

C. NADPH (0.34 mmol/l)

D. Phosphate buffer (0.05 mol/l; pH 7.2)

E. EDTA (4.3 mmol/l)

F. Cumene hydroperoxide (0.18 mmol/l)

F. Diluting agent

8.4.3 Sample Preparation

Heparinized whole blood (25 µl) was diluted with 625µl of the diluting agent. The assay was slightly modified for the rat's blood sample, because the absorbance of the final reaction mixture could not be read on the Cobas Mira autoanalyzer. GPx was subsequently determined manually.

8.4.4 Assay Procedure

Table 6 GPx determination

Sample and Reagents	Volume	Remarks
Diluted sample / Blank / Control	200 µl	ddH_2O was used as blank
ddH_20	500 µl	*The ddH_2O and glutathione/ glutathione reductase reagent were mixed together before being added to the diluted blood sample.*
Glutathione / glutathione reductase reagent	500 µl	
Cumene hydroperoxide	40 µl	
This was mixed and the timer started simultaneously. The initial absorbance (A1) at 340 *nm* was read after 1 min and the final absorbance (A2) read at 4 min.		

8.4.5 Calculation

GPx concentration was calculated from the following formula:

U/l of haemolysate (diluted sample) = 8412 x δA 340 nm / min (where δA = A2-A1).

8.4.6 Example of Spreadsheet and Calculations

Srl.	In Abs A1	Final Abs A2	δA A2 – A1	δAb -δAbsBlk	δAbs/min	[GPx]= 8412 x δAbs/min	x 26 Df	U/dl	Hb g/dl	GPx U/g Hb	Mean GPx
Contr	0.738	0.683	0.055	0.034	0.01133	95.3	2479	248			
Std	0.764	0.700	0.064	0.043	0.01433	120.6	3135	313			
Blk	0.671	0.657	0.014								
C1	0.645	0.245	0.400	0.386	0.12867	1082.3	28141	2814	14.0	201.0	
C2	0.650	0.266	0.384	0.370	0.12333	1037.5	26974	2697	13.0	207.5	
C3	0.644	0.177	0.467	0.453	0.15100	1270.2	33026	3303	14.3	230.9	
C4	0.566	0.179	0.387	0.373	0.12433	1045.9	27193	2719	14.9	182.5	
C5	0.584	0.162	0.422	0.408	0.13600	1144.0	29745	2974	15.4	193.1	203.0

8.5 CATALASE DETERMINATION

8.5.1 Introduction

Catalase exhibits a dual function. Decomposition of H_2O_2 to give H_2O and O_2 [(catalytic activity eq. (1)], and oxidation of H donor eg. methanol, ethanol, fomic acid, phenol, with consumption of peroxide [peroxidic activity, eq.(2)].

$$2H_2O_2 \xrightarrow{\text{catalase}} 2H_2O + O_2 \qquad (1)$$

$$ROOH + AH_2 \xrightarrow{\text{catalase}} H_2O + ROH + A \qquad (2)$$

H_2O_2 and other ROS are increasingly recognized as toxic intermediates in a wide variety of pathological conditions. H_2O_2 is considered a key metabolite because of its relatively high stability, diffusion and involvement in cell signaling cascades. Safe disposal of H_2O_2 in cells is carried out by catalases and peroxidases. H_2O_2 being unmodified and passive can diffuse between cell compartments. Its toxicity is traced to the formation of $^{\bullet}OH$ upon

capture of an electron for instance, from Fe (II) or Cu (II). The $^{\bullet}OH$ reacts immediately with almost all cellular compounds giving rise to alterations such as modified or disrupted proteins or nucleic acids. Thus, it is understandable why catalases are one of the most efficient enzymes known. It is so efficient that it cannot be saturated by H_2O_2 at any concentration.

8.5.2 Principle

The decomposition of H_2O_2 can be followed directly by the decrease in absorbance at 240 nm ($\varepsilon_{240} = 0.00394 \pm 0.0002$ liters mmol^{-1} mm^{-1}). The difference in absorbance (δA_{240}) per unit time is a measure of catalase activity.

To avoid inactivation of the enzyme during the assay (usually 30 sec), or formation of bubbles in the cuvette resulting from liberated O_2, it is necessary to use a relatively low H_2O_2 concentration (10 mM). The H_2O_2 concentration is critical in as much as there is direct proportionality between the substrate concentration and the rate of decomposition. The dependence of the H_2O_2 decomposition on the temperature is small, hence that measurements can be carried out between 0°C and 37°C. However, 20°C is recommended. The pH activity curve relative to *V*o has a fairly broad pH optimum (pH 6.8 - 7.5): measurements were made at pH 7.0.

8.5.3 Reagents and Preparation

A. Phosphate buffer, pH 7.0

a) 6.81 g K_2PO_4 ..... 1L (solution '*a*')

b) 8.90 g $Na_2HPO_4.2H_2O$..... 1L (solution '*b*')

c) '*a*' + '*b*' in ratio of 1:1.5 (v/v).....(solution '*c*')

B. Preparation of 30 mM H_2O_2

0.170 ml 30 % H_2O_2, was added to sol^{n}. '*c*' and made up to 50 ml.

8.5.4 Sample Preparation

Venous blood in heparin, or citrate, was centrifuged at 800 g in 4 vol. of normal saline. The supernatant, buffy coats and upper 15% of the packed cells were removed by aspiration after each washing. Washing was done 4 times. A stock haemolysate was prepared containing ≈ 5g Hb/100 ml by adding 4 parts by vol. of cold ddH_2O to the blood sample. A 1:500 dilution of the concentrated haemolysate was prepared with phosphate buffer immediately before the assay was performed.

100 µl blood was washed with 400 µl normal saline (4 times).

- 40 µl (packed cells) + 160 µl cold H_2O = 200 µl hemolysate
- 1:500 dilution of the haemolysate was made as ff:
- 10 µl (haemolysate) + 5 ml PO_4 buffer solution '*c*'.

8.5.5 Enzyme Stability

Catalase in intact erythrocytes and in concentrated haemolysates is stable for up to 6 days when kept at 2°C. However, there is a relatively rapid decline of activity in dilute haemolysate, which is more likely the result of decomposition of the enzyme into subunits, than to proteolytic changes. At a concentration of 1.2 mg Hb/ml the activity decreases by 10-15% within 24 hrs; at a concentration of 0.06 mg Hb/ml the loss of activity is 10% after 1 hr and 80-90% after 24 hr. Consequently, haemolysate samples should be analyzed within 5-10 min after dilution.

8.5.6 Assay Procedure

Table 7 Blood Catalase determination

Sample and Reagents	Volume	Remarks
		λ = 240 nm; Light path 10 mm. Spectrophotometer was zeroed with air blank
Haemolysate	2000 µl	*In UV cuvette*
30% H_2O_2 in PO_4 buffer	1000 µl	The solution was mixed with a plastic paddle. The stopwatch was started immediately and the initial (A1) reading taken at 5 sec. The final reading (A2) was made at 35 sec.
		Test was repeated

8.5.7 Calculation

The decomposition of H_2O_2 initially takes about 30 sec. It follows that of a first order reaction with H_2O_2 concentration between 0.01 and 0.05 M. The rate constant (k) for the overall reaction is as follows:

$k = (1/\Delta t)(\text{In } S_1/S_2) = (2.3/\Delta t)\log S_1/S_2$

For a time interval of 15 sec, the following relationship is obtained:

$k = (2.3/15)(\log A_1/A_2)\ (\text{sec}^{-1})$

To calculate *k*/ml or *k*/g Hb the following equation was used:

k / ml = ka

k/g Hb = k/ml (1000/b)

= (2.3 /15) (a/b) ($\log A_1/A_2$) (sec^{-1})

A_1 = A_{240} at $t = 0$, $A_2 = A_{240}$ at $t = 15$

a = dilution factor $\frac{\textit{Hb conc. in blood or erythrocyte sediment (mg Hb/ml)}}{\textit{Hb conc. in cuvette mg Hb/ml.}}$

b = *Hb content of the blood (g/l)*

i.e. $\Delta A = 0.450 - 4.00\ (\log \frac{0.450}{0.400}) = 0.05115$

the following relationship holds:

$k = (2.3/\Delta t)(\log A_1/A_2)$

$= 0.1175/\Delta t\ (\text{sec}^{-1})$

8.5.8 Example of Spreadsheet and Calculation

Srl	In. Ab1	Fi. Ab2	Ab1/Ab2	b=Log10 Ab1/Ab2	(2.3/30)*b / 10-3	Cat. x 10-3=y	Hb=c	Df (500) x c=z	[Cat]=zy	Mean [Cat] x 10^ -3	Mean [Cat]
C1	0.537	0.419	1.282	0.108	0.00826	8.262	13.9	6950	57418.3		
C2	0.545	0.429	1.270	0.104	0.00797	7.969	12.5	6250	49804.2		
C3	0.553	0.434	1.274	0.105	0.00807	8.068	13.2	6600	53249.1		
C4	0.519	0.435	1.193	0.077	0.00588	5.879	13.8	6900	40562.7		
C5	0.511	0.432	1.183	0.073	0.00559	5.592	14.4	7200	40261.3	48259	48.3

8.6 TOTAL ANTIOXIDANT STATUS

8.6.1. Principle

2,2'-Azino-di-(3-ethylbenzthiazoline sulphonate) (ABTS®), when incubated with a peroxidase (metmyoglobin) and H_2O_2, produces the radical cation ABTS® $^+$. The radical cation is a relatively stable blue-green colour that can be measured at 600 nm. However, antioxidants present in the sample will react with the cation free radical, thereby reducing its concentration and colour development. The level of antioxidants present in the sample is therefore proportional to the chromogen produced.

$HX\text{-}Fe^{III} + H_2O_2 \text{ -------> } X-[Fe^{IV}=O] + H_20$

$ABTS® + X-[Fe^{IV}=O] \text{ --------> } ABTS®^{+} + HX\text{-}Fe^{III}$

$HX\text{-}Fe^{iii}$ = metmyoglobin

$X-[Fe^{IV}=O]$ = ferrylmyoglobin

8.6.2 Reagents in Kit

A. Phosphate buffered saline (80 mmol/l, pH 7.4)

B. Metmyoglobin (6.1 µmol/l)

C. ABTS® (610 6.1 µmol/l)

D. H_2O_2 (250 µmol/l)

E. 6-Hydroxy-2,5,7,8-tetramethylchroman-2-carboxylic acid (Trolox)

Randox Laboratories Ltd. TAS commercial kit was used and the test was carried out according to the manufacturer's instructions.

8.6.3 Sample Preparation

Freshly drawn heparinized plasma was used. Haemolysis was avoided.

8.6.3 Assay Procedure

Table 8 Serum Total Antioxidant Status

Sample and Reagents	Volume	Remarks
Diluted Sample / Blank / Control	20 µl	*ddH_2O was used as blank*
HX-Fe^{III} / ABTS®	1000 µl	
		Well mixed and initial absorbance(A1) read at 600 nm.
H_2O_2	200 µl	
This was mixed and the timer started simultaneously. The final absorbance (A2) was read after 3 min. This reaction was performed at 37°C.		

8.6.5 Calculation

TAS (mmol/l) = Factor x (δA Blk - δA Sample), where δA = A2 – A1

Factor = $\frac{\text{Standard concentration}}{(\delta A \text{ Blk} - \delta A \text{ Standard})}$

8.6.6 Example of Spreadsheet

Srl.	Final Abs	Initial Abs	δAbs	δBlk - δAbs	TAS (mmol/l) (1.65/δBlk-δAbstd)xδBlk-δAbT	Mean TAS (mmol/l)
Control	0.132	0.015				
Std.	0.002	0.002	0.000	0.297	1.885	
Blk	0.297	0.000	0.297	0.000	0.000	
C1	0.163	0.005	0.158	0.139	0.772	
C2	0.176	0.001	0.175	0.122	0.678	
C3	0.152	0.003	0.149	0.148	0.822	
C4	0.186	0.010	0.176	0.121	0.672	
C5	0.206	0.012	0.194	0.103	0.572	0.703

8.7 OXYGEN RADICAL ABSORBANCE CAPACITY (ORAC)

8.7.1 Introduction

Several methods have been developed to assess the total antioxidant capacities of various biological samples. However, these methods have their shortcomings. The ORAC assay depends on the properties of B- or R-phycoerythrin (PE). This assay is to date the only method that takes the reactive species (RS) reaction to completion and uses an "area under the curve" (AUC) technique for quantification, thus, combining both inhibition time and inhibition percentage of the RS action by antioxidants into a single quantity (Cao and Prior, 1999).

8.7.2 Principle

The ORAC assay depends on the detection of chemical damage to R-PE through the decrease in its fluorescence emission. Under appropriate conditions, the loss of PE fluorescence in the presence of RS is an index of oxidative damage of the protein. The inhibition against the loss of PE fluorescence in the ORAC assay is a measure of its antioxidant capacity against the RS.

8.7.3 Reagents and Preparation

- Potassium hydrogen phosphate (K_2HPO_4)
- Sodium dihydrogen phosphate (NaH_2PO_4)
- B-Phycoerythrin (B-PE)
- 2.2'-Azobis-(2-amidinopropane) dihydrochloride (AAPH)
- 6-Hydroxy-2,5,7,8-tetramethylchroman-2-carboxylic acid (Trolox)

A. 75 mM Phosphate buffer was prepared by dissolving 130.65 g K_2HPO_4 in 1L ddH_2O (0.75 M), and 98.99 g NaH_2PO_4 in another liter of ddH_2O (0.75 M) separately. The 0.75 M K_2HPO_4 and 0.75 M NaH_2PO_4 were mixed in a ratio of 1:9 to give a final concentration of 75 mM. The pH was adjusted to 7.0 and all solutions were stored at 4°C.

B. 68.0 mg/l PE was prepared by dissolving 1 mg of PE in 14.7 ml ddH_2O.

C. 160 mM AAPH was prepared by dissolving 43.39 g AAPH in 1L ddH_2O.

D. 20 µM, 40 µM, 80 µM and 160 µM trolox standards were prepared by dissolving 0.005 g/L, 0.01 g/L, 0.02 g/L and 0.04 g/L ddH_2O respectively. Standards were aliquot into small vials and stored at -70°C.

8.7.4 Sample Preparation

a. Protein fraction: crude liver tissue extract was prepared by homogenizing liver tissue in phosphate buffer (1:4 w/v). The soluble fraction was obtained by a-two step centrifugation; first at 12,000 g for 10 min, followed by 100,000 g for 15 min. The supernatant, (approximately 0.5% w/v protein), was further diluted (1:25) to obtain 0.02% protein for the ORAC assay.

b. Non-protein fraction: the crude liver extract of 1:4 w/v was adjusted to 0.5% (5 g/l) protein concentration. Acetone was added at the ratio of 1:4 (liver extract : acetone). This was centrifuged at 4°C for 10 min and the supernatant was recovered for the ORAC assay.

c. Phosphate buffer and Trolox were used for blank and standard, respectively.

8.7.5 Assay Procedure

Table 9 ORAC determination

Sample and Reagents	Volume	Remarks
Phosphate buffer	1750 µl	
PE	100 µl	*The phosphate buffer and PE were preincubated at 37°C for 15min.*
AAPH	50 µl	
Sample / Standard / blank	100 µl	The solution was vortexed.
Fluorescence was measured at: Ex=540; Em=565		Sample was read every 10 min until fluorescence of the last reading was 5% that of the first.

8.7.6 Example of Spreadsheet and Calculation

A sample table, showing the calculation of trolox equivalent of the absorbance capacity of the antioxidants in the sample homogenate is shown below.

	30min	60 min	90 min	120 min	140 min	160 min	180 min	200 min	f140/ 120	f160/ 120	f180/ 120	f200/ 120	β= (0.5+Σf)x5	([Std] / βs)xβtxDf	Mean(uM Trolox Units)	mM Trolox Units
C1	13.1	8.1	5.8	4.5	3.6	2.9	2.5	2.2	0.800	0.644	0.556	0.489	14.94	10675		
C2	13.1	11.0	8.4	6.7	5.6	4.8	4.3	3.8	0.836	0.716	0.642	0.567	16.31	11647		
C3	14.2	9.0	6.7	5.3	4.4	3.8	3.3	3.0	0.830	0.717	0.623	0.566	16.18	11557	11293	11.29
160 uM	90.0	72.8	69.3	69.1	69.0	68.8	68.7	68.5	0.999	0.996	0.994	0.991	22.40			

Where:

f = A fraction of the previous and current time point

Df = Dilution factor

[Std] = Standard concentration

βs = β of standard

βt = β of test

8.8 LIPID HYDROPEROXIDE (LOOH) DETERMINATION

8.8.1 Principle

Ferrous oxidation with xylenol orange (FOX *VERSION II*) is based on the principle of the rapid peroxide-mediated oxidation of the Fe^{2+} to Fe^{3+} under acidic conditions. The latter in the presence of xylenol orange, forms an Fe-xylenol orange complex that can be measured spectrophotometrically at 560 nm (Nourooz-Zadeh *et al.,* 1994).

In this method, alkoxyl radicals generated in the ferrous oxidation step react rapidly with native lipid, generating further hydroperoxide in a chain reaction (Eqs. 1-4).

$$ROOH + Fe2+ \longrightarrow Fe3+ + RO^{\bullet} + OH^{-} \quad (1)$$

$$RO^{\bullet} + RH \longrightarrow ROH + R^{\bullet} \quad (2)$$

$$R^{\bullet} + O_2 \longrightarrow ROO^{\bullet} \quad (3)$$

$$ROO^{\bullet} + RH \longrightarrow ROOH + R^{\bullet} \quad (4)$$

$$R^{\bullet} + BHT \longrightarrow RH + BT \quad (5)$$

Inclusion of the chain-breaking antioxidant butylated hydroxytoluene (BHT) terminates the chain reaction. As shown in Eq.(5), BHT presumably repairs alkyl radicals produced by the reaction of alkoxyl radicals with unsaturated lipids [Eq. (2)]. Experimentally, BHT at a concentration of 4 mM was found to provide a firm endpoint when measuring phosphatidyl-choline and low-density lipoprotein peroxide content. The FOX reagent was further adopted for the measurement of LOOH by the addition of methanol (90%, v/v) in order to solubilize the lipid and BHT. Sorbitol was omitted in the FOX reagent as the high

concentration of methanol (>25 M) in the revised method made the presence of sorbitol as an oxyl radical scavenger superfluous.

8.8.2 Reagents and Preparation

- Xylenol orange (XO)
- Ferrous ammonium sulfate $[Fe(NH_4)_2(SO_4)_2]$
- Butylated hydroxytoluene (BHT)
- Sulphuric acid (H_2SO_4)
- Methanol. HPLC grade. (MeOH)

A. 250 mM H_2SO_4 was prepared by diluting 13.88 ml conc. H_2SO_4 (18 M) with ddH_2O to 1L.

B. 4.4 mM BHT /MeOH was prepared by dissolving 0.97 g BHT in 1L HPLC grade MeOH.

C. Stock FOX solution: 1 mM XO / 2.5mM $Fe(NH_4)_2(SO_4)_2$ in 250 mM H_2SO_4 was prepared by dissolving 0.76 g XO and 0.98 g $Fe(NH_4)_2(SO_4)_2$ in 1L 250 mM H_2SO_4.

D. Working FOX II solution: 1 ml stock FOX II solution was added to 9 ml BHT/MeOH solution. This was freshly prepared before use.

E. The following concentrations of H_2O_2 were prepared using 30% Sigma H_2O_2 which is equivalent to 8.82 M:

- Stock standard 8.82 mM H_2O_2 was prepared by diluting 1ml 30% H_2O_2 (8.82 M) to 1L. Thereafter, the following standards were prepared:

- 4.4 µl of stock standard was made up to 10 ml = 3.9 µM

  8.8 µl " = 7.81 µM

  17.5 µl " = 15.62 µM

  35.0 µl " = 31.25 µM

  70.0 µl " = 62.50 µM

8.8.3 Assay Procedure

Table 10 Serum LPO determination

Sample and Reagents	Volume	Remarks
Plasma / Blank (H_2O)/ Std	50 µl	1.5 ml microfuge vials were used and work done in duplicate
Working FOX II reagent	950 µl	*The solution was vortexed*
		It was then incubated at room temp. for 30 min
		Microfuge vials were centrifuged at 12,000 g for 5 min. to remove all flocculated materials
Absorbance of supernatant was read at 560 nm.		

8.8.4 Calculation

The concentrations of the samples were calculated from the calibration curve.

8.8.5 Example of Spreadsheet and Calibration Curve

	Mean Ab	Conc. µM	Mean Conc. µM
S1	0.009	3.9	
S2	0.025	7.8	
S3	0.052	15.6	
S4	0.113	31.3	
S5	0.260	62.5	
C1	0.173	43.0	
C2	0.197	48.5	
C3	0.279	37.6	
C4	0.211	31.8	
C5	0.118	30.2	38.2

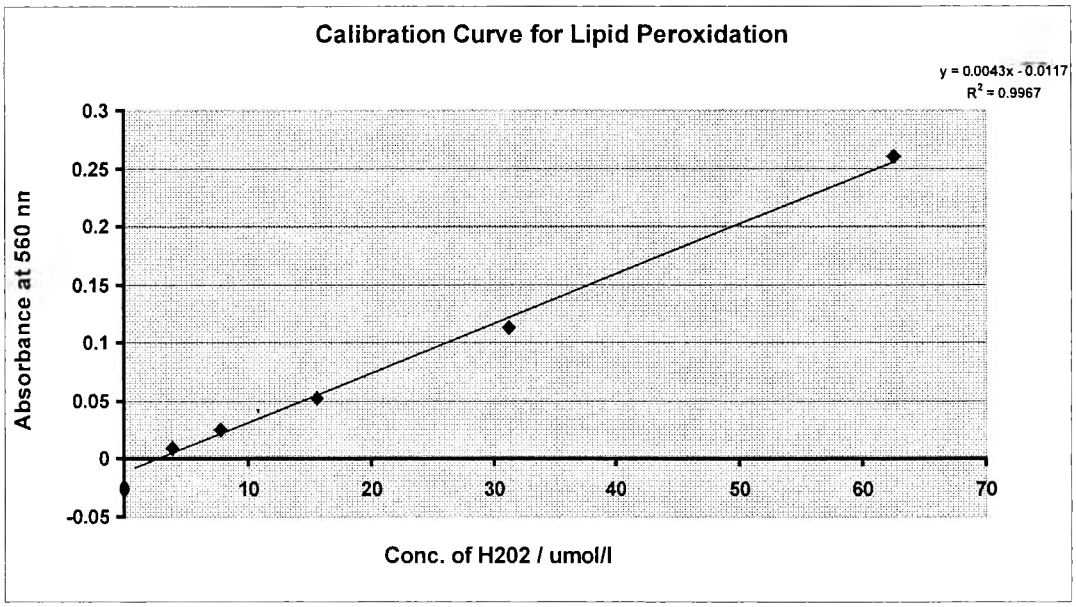

8.9 MALONDIALDEHYDE (MDA) DETERMINATION

8.9.1 Introduction

LPO is a well-established mechanism of cellular injury in both plants and animals, and used as an indicator of oxidative stress in cells and tissues. Lipid peroxides are unstable, and they decompose to form a complex series of compounds, including reactive carbonyl compounds. PUFA peroxides generate MDA and 4-HNE upon decomposition. The measurement of MDA and 4-HNE has been used as an indicator of LPO.

8.9.2 Principle

BIOXYTECH® LPO-586™ (OXIS, USA) kit was used and the manufacturer's instruction followed accordingly.

This assay is based on the reaction of a chromogenic reagent, N-methyl-2-phenylindole with MDA and 4-hydroxy-alkenals at 45°C. One molecule of MDA reacts with two molecules of N-methyl-2-phenylindole to yield a stable chromophore with maximal absorbance at 586 nm.

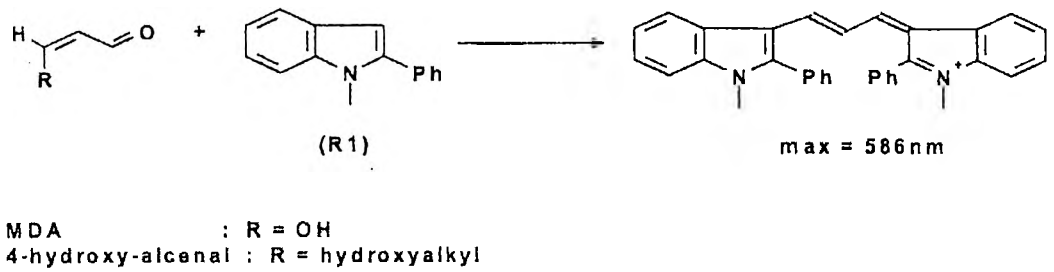

Figure 12 Structure of MDA

8.9.3. Reagents and Preparation

A. 10.3 mM N-methyl-2-phenylindole, in acetonitrile

B. 10 mM 1,1,3,3-Tetramethoxypropane in 20mM Tris-HCL, pH 7.4 (MDA Standard)

C. Methanol, 100% HPLC grade

D. 37% HCl

E. Standard preparation:

The standard concentration of 10 mM stock was diluted 1/100 (v/v) with ddH_2O before further dilutions as indicated below.

Final concentration of standard (μM)	0.5	1.0	1.5	2.0	2.5	3.0
Volume of 100 μM standard (μl)	0	5.0	10	15	20	25
Volume of ddH_2O (μl)	200	195	190	185	180	175

8.9.4 Assay Procedure

The procedure was followed according to the manufacturer's instructions as shown below. ddH_2O was used as a blank.

Table 11 MDA determination.

Sample and Reagent	Volume	Remarks
Sample / Standard / Blank	200 μl	*Microfuge tubes were used*
N-methyl-2-phenylindole, in acetonitrile	650 μl	*The solution was gently vortexed*
37% HCl	150 μl	*The solution was mixed well and 'stoppered'.*
		Tubes were incubated at 45°C for 60 min
Turbid samples were centrifuged at 15,000 g for 10 min to obtain a clear supernatant. Supernatant was transferred into a cuvette and the absorbance read at 586 nm.		

8.9.5 Calculation

A calibration curve of absorbance of standards against standard concentration was plotted. The concentrations of the various samples were read from the standard curve.

8.9.6 Example of Spreadsheet and Calibration Curve

Srl.	Abs.	Blk	Abs - Blk	Conc. µM	Mean Conc. µM	Conc x5
S1	0			0.0		
S2	0.068			0.5		
S3	0.131			1.0		
S4	0.189			1.5		
S5	0.252			2.0		
S6	0.351			2.5		
C1	0.118	0.106	0.012	0.117		
C2	0.091	0.030	0.061	0.480		
C3	0.081	0.037	0.044	0.354		
C4	0.096	0.027	0.069	0.539		
C5	0.099	0.036	0.063	0.494	0.397	1 984

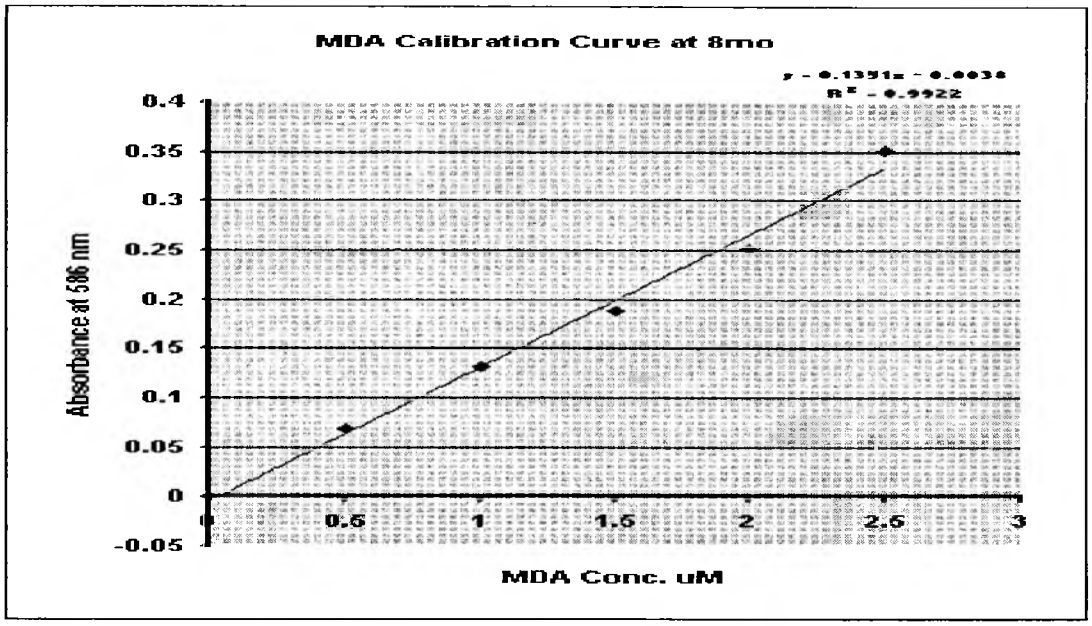

8.10 8-ISOPROSTANE (8-IP)

8.10.1 Introduction

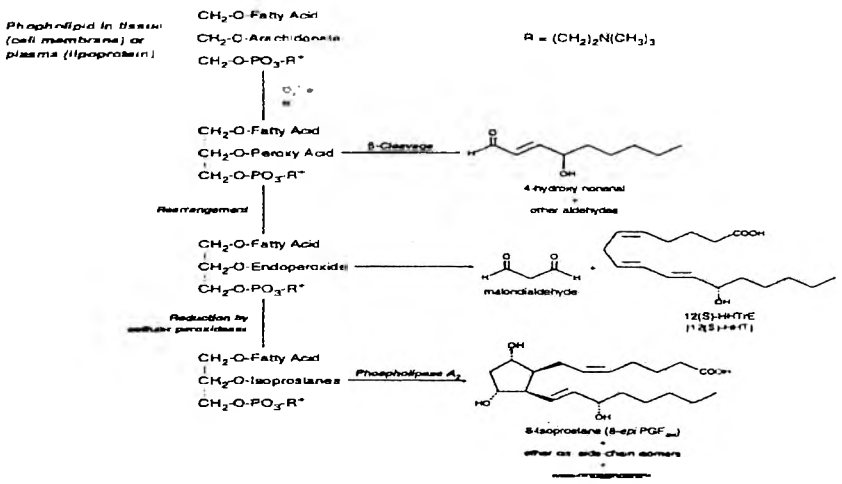

Figure 13 The metabolic pathway for the formation of 8-IP.

8.10.2 Principle

This ELISA procedure is based on the competition between 8-IP in the sample and an 8-IP-acetylcholinesterase (AChE) conjugate (8-IP tracer) for a limited number of 8-IP-specific rabbit antiserum binding sites. Because the concentration of the 8-IP tracer is held constant while the concentration of 8-IP varies, the amount of the 8-IP tracer that is able to bind to the rabbit antiserum will be inversely proportional to the concentration of 8-IP in the well. The rabbit antiserum-8-IP complex (either free or tracer) binds to the mouse monoclonal anti-rabbit IgG antibody that has been previously attached to the well. The plate is then washed to remove all unbound reagents and the Ellman's reagent (which contains the substrate to AChE) is added to the well. The product of this enzymatic

reaction has a distinct yellow colour that is measured spectrophotometrically at 412 nm. The absorbance is directly proportional to the [bound 8-IP Tracer] and inversely proportional to [8-IP].

8.10.3 Reagents in Kit

8-IP kit (Cayman Chemicals, USA) was used and the manufacturer's instructions followed accordingly. The kit contained the following:

1. Mouse anti-rabbit IgG coated plate
2. 8-IP EIA antisera
3. 8-IP AChE tracer
4. 8-IP EIA standard
5. EIA buffer concentrate
6. Wash buffer concentrate
7. Tween 20
8. Ellman's Reagent

8.10.4 Assay Procedure

- Reconstitution of reagents was done according to the manufacturer's instructions using Ultra Pure water (from Cayman). In addition, mapping of the plate was designed as recommended by the manufacturer. Wells to cater for blanks, "Non-specific binding" (NSB), "minimum binding" (B_0) and "total activity or maximum binding" (TA) were incorporated. Assay was performed in triplicates.

- 50 µl of standards and samples were added to the appropriate wells.
- 50 µl of 8-IP AChE Tracer was again added to each well except the TA and the blank wells.
- 50 µl 8-IP antiserum was added to each well except the TA, NSB and blank wells.
- The plate was covered with a plastic film and incubated for 18 hrs at room temp.
- Wells were emptied and washed 5x with the wash solution.
- 200 µl of Ellman's solution was added to each well.
- 5 µl of Tracer was then added to the TA wells.
- Plate was again covered with a plastic film and kept in the dark for 60 to 90 min for the colour to develop.
- The colour typically developed when B_0 read 0.3 to 0.8 A.U at 405 nm.

8.10.5 Example of Calibration Curve and Spreadsheet

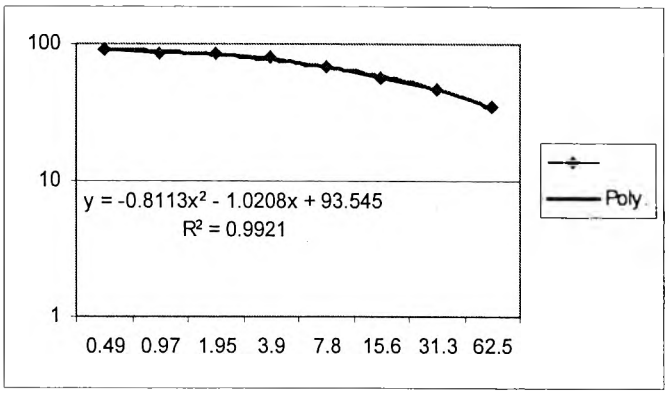

	Raw Data mU	Raw Data mU	Raw Data	Average		Corrected
Blk	0.003	-0.003		0		
NSB	0.009	0.012		0.0115		
Bo	650	665		657.5		
TA	313	331			A	B

	Abs1(mU) mU	Abs2(mU) mU	Corrected (-Av.NSB) (-0.005)	Corrected	%Abs/Abs(max) [%B/Bo]	[%B/Bo]	Mean A&B (%B/Bo)	8-IP Conc.	Dose (pg/ml)	x DF 0.9	x2 = 8-IP /g liver
S1	118	115	129.5	126.5	19.7	19.2	19.5		62.50		
S2	140	144	151.5	155.5	23.0	23.7	23.3		31.30		
S3	206	197	217.5	208.5	33.1	31.7	32.4		15.60		
S4	274	287	285.5	298.5	43.4	45.4	44.4		7.80		
S5	334	333	345.5	344.5	52.5	52.4	52.5		3.90		
S6	443	431	454.5	442.5	69.1	67.3	68.2		1.95		
S7	540	484	551.5	495.5	83.9	75.4	79.6		0.97		
S8	562	584	573.5	595.5	87.2	90.6	88.9		0.49		
F1	36	26	47.5	37.5	7.2	5.7	6.5	*800*		720	2397.60
F2	49	33	60.5	44.5	9.2	6.8	8.0	*550*		495	1648.35
F3	57	68	68.5	79.5	10.4	12.1	11.3	*390*		351	1168.83
F4	32	30	43.5	41.5	6.6	6.3	6.5	*800*		720	2397.60
F5	36	90	47.5	101.5	7.2	15.4	11.3	*390*		351	1168.83

8.11 DNA EXTRACTION FROM TISSUE BY SALTING OUT METHOD (Miller *et al.*, 1988)

8.11.1 Principle

This method involves the use of a high salt concentration to dehydrate and precipitate cellular proteins, while DNA remains soluble. The DNA obtained from this simple technique yield quantities comparable to those obtained from the phenol chloroform method and is suitable for most procedures.

8.11.2 Reagents and Preparation

A. Buffer A (pH 8.0)

10 mmol/l Tris	1.21 g/l	}
100 mmol/l NaCl	5.84 g/l	} autoclaved
10 mmol/l EDTA	3.72 g/l	}

B Rnase: 20 mg/ml (added fresh before every extraction).

C. Proteinase K: 20 mg/ml Buffer A.

D. 10% SDS: 10g SDS was dissolved in 100 ml ddH_2O (not autoclaved).

E. NaCl (6 mol/l): 35 g NaCl was dissolved in 100 ml ddH_2O.

F. Chloroform / Isoamyl alcohol. This was mixed in the ratio of 24:1

G. Chloroform (MERCK).

H. 70% Ethanol: 70 ml absolute ethanol was made up to 100 ml with ddH_20 and kept ice cold.

I. TE Buffer (pH 7.4): 10 mmol/l Tris (1.21 g/l), plus 1 mmol/l EDTA (0.273 g/l)

8.11.3 Assay Procedure

1. 100 mg of tissue, was sliced very thinly with a scalpel blade and added to 5 ml buffer A in a 50 ml NUNC tube.
2. 100 µl proteinase K and 20 µl RNase were added to the tissue / buffer A solution. 4 ml 10% SDS was finally added. The NUNC tube was tightly screwed and incubated at 37°C overnight with gently swirling. Where tissue was not well digested a little more proteinase K was added and temperature raised to 50°C.

3. 2 - 3 ml 6 mol/l NaCl was added. (Although 1.5 ml had been recommended to give a final concentration of 1 mol/l).
4. This was gently shaken by continuous inversion for 10 min at 22°C (room temp). Where solution was not milky, a little more of the 6 mol/l NaCl was added.
5. The mixture was centrifuged at 3500 rpm for 15 min at 22°C. The supernatant was then transferred into a polypropylene tube.
6. An equal volume of the chloroform/isoamyl alcohol mixture was added to the supernatant and mixed gently by inversion for 5 min.
7. This was centrifuged at 3500 rpm for 10 min at 8°C. The supernatant was transferred to another polypropylene tube.
8. An equal volume of chloroform was added and mixed gently by inversion for 5 min.
9. This was centrifuged at 3500 rpm for 10 min at 8°C. The supernatant was then transferred into a sterile polypropylene test tube.
10. Small quantities of isopropanol were added and inverted gently until DNA strands precipitated out of the solution. (Approximately 1 to1.5 ml was added).
11. The DNA was hooked out with a sealed hooked Pasteur pipette. The DNA was washed for 2 minutes in cold 70% ethanol by dipping the hooked DNA into it. This was then transferred to 200 µl TE buffer.

8.11.4 Verification of DNA

1. 50 ml 1% agarose gel was prepared.
2. 3 µl ethidium bromide was added to the molten gel at about 50°C.

3. The gel was run in 1% TBE buffer. 5 µl DNA and bromophenol blue dye were used alongside a 50 kb ladder.
4. A voltage of 85 V and 56 mA current was applied for about 2 hrs.
5. The gel was viewed under UV to ascertain the presence of the rat liver DNA.

8.12 FLUORIMETRIC ANALYSIS of DNA UNWINDING (FADU)

8.12.1 Introduction

The technique adopted was a combination of the following:

a. Fluorimetric method for rapid detection of DNA strand breaks in human WBC produced by low doses of radiation (Birnboim and Jevcak, 1981).
b. Increased unwinding of hepatic double-stranded DNA (dsDNA) in rats with chronic dietary iron overload (Edling *et al.,* 1990).
c. Assessment of DNA damage and repair in human peripheral blood mononuclear cells (PBMC) using a novel unwinding technique (Kristina Elmendorff-Dreikorn, 1999).

8.12.2 Principle

When DNA is exposed to moderate alkali solutions, breaks occur in the phosphodiester backbone and the two strands unwind. Ethidium bromide (or PicoGreen) will selectively bind to the double-stranded DNA (dsDNA) in the presence of single-stranded DNA (ssDNA) when short duplex regions in the ssDNA molecules are solubilized by alkali.

It has been observed that the rate of unwinding of large DNA molecules in alkali is increased by prior exposure of cells to ionizing radiation. This is interpreted to mean that radiation induced DNA strand breaks are responsible for the increase in the rate of unwinding and, conversely, that increase in the rate of unwinding is a sensitive measure of strand breaks.

0.5 g Liver was pressed into 1.5 ml EDTA buffer and gently homogenized. Following sedimentation on ice, aliquots of the supernatant were mixed with lysis buffer containing PicoGreen and incubated with NaOH to induce unwinding of the DNA. After 1 hr the rate of fluorescence was measured at Ex: 480 nm and Em: 520 nm.

8.12.3 Reagents and Preparation

A. TE Buffer: Tris-HCL + EDTA, pH 7.4.

10 mM Tris-HCL and 1 mM EDTA was prepared by weighing the following and dissolving into 1L ddH_20: 1.576 g Tris-HCL and 0.292 g EDTA (pH = 10.0).

B. Stock lysis solution, pH 10.0

The 9.0 M Urea stock lysis solution was prepared by weighing the following and dissolving into 1L double distilled water:

540.54 g Urea

1 g SDS (0.1% SDS)

58.44 g EDTA (0.2M EDTA)

C. 0.025 M NaOH. This was prepared by dissolving 1 g NaOH in 1L dH_20

D. Lysis-PicoGreen solution:

This was freshly prepared by adding 200 µl of PicoGreen to 10 ml of Stock lysis solution. The resulting solution was protected from bright light.

E. Liver homogenate:

0.5 g fresh liver was gently homogenized in 1.5 ml TE buffer using the lowest speed (1) of Ultra Turax T8 homogenizer for 30 sec. Samples were allowed to sediment for 1 hr on ice.

8.12.4 Assay Procedure

Table 12 Determination of FADU

Sample and Reagents	Micro	Macro	Remarks
Liver Extract / Blank (TE buffer)	25 µl	250 µl	
Lysis-PicoGreen Solution	25 µl	250 µl	*Added very slowly without mixing or shaking*
			Incubated on ice / in the dark for 1 hr
0.025 M NaOH Solution	25 µl	2500 µl	
Fluorescence Measured at: Ex=480 nm; Em=520 nm			*Fluorescence was measured every* 5 min for 1 hr.

8.12.5 Example of Spreadsheet and Calculation

Srl	10min f1	25min f2	δf	δf/min	Mean δf/min
C1	64.7	63.7	1.0	0.067	
C2	87.4	86.1	1.3	0.087	
C3	84	82.5	1.5	0.100	
C4	76.9	75.7	1.2	0.080	
C5	69.1	67.9	1.2	0.080	0.083

8.13 SUPEROXIDE RADICAL ($^{\cdot}O_2$) DETERMINATION BY CHEMI-LUMINISCENT TECHNIQUES

8.13.1 Principle

Luminescence is the emission of light by non-thermal processes. In the case of luminescence analysis, the light is produced by chemical reactions. Molecules responsible for emitting the light absorb free energy released by the chemical reaction and become 'excited'. In this state some of the peripheral electrons of the molecule are raised to a higher energy level. When these electrons lose energy, they return to a lower energy level and the energy lost during this transition is emitted as photons. When the electrons have lost all their absorbed energy, the molecule then returns to its stable ground state.

The chemiluminophore used for this research is luminol.

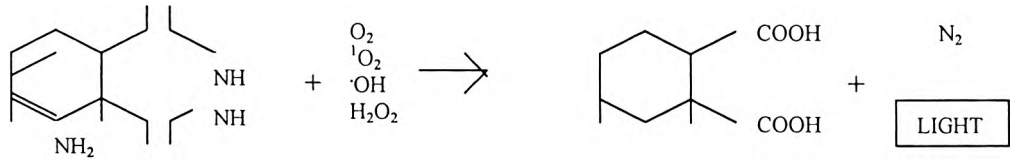

LUMINOL OXIDANT α–AMINOPHTHALATE

The luminol interacts with the oxidizing species to produce larger, more measurable amounts of light at a peak wavelength of approximately 425 nm. This was measured by a four-channel luminometer interfaced with a computer.

8.13.2 Reagent Preparation

A. 10^{-4} M luminol stock solution was prepared by dissolving 0.177 g luminol in 100 mL of 0.1 M borate buffer.

B. Borate buffer: 0.1 M, pH 9.0 was prepared by dissolving 9.5 g / 250 ml dH_20. The pH was adjusted to 9.0.

C. 10^{-3} M N-formylmethionylleucinylphenylalanine (fMLP) (stock 10 mM in DMSO).

D. Phenol-free Hank's balanced salt solution (HBSS) (Sigma).

E. Heparinized whole blood was diluted 1:9 with phenol-free HBSS.

8.13.3 Assay Procedure

Table 13 Superoxide radical determination

Sample and Reagents	Volume	Remarks
1:9 diluted blood sample	500 µl	*In luminometer cuvette*
10 mM luminol solution	200 µl	*Resultant solution was loaded onto luminometer*
fMLP	300 µl	*Commencement of reaction*

- Graph: 15 sec / division was used.
- Temperature setting: 37°C
- Graph was displayed on the screen and ensured that baseline had stabilized halfway across the first square.
- Gain was adjusted as required so that the luminescence curves were within the range on the displayed graph.
- Once the gain was established, the test was performed at that particular gain setting.
- The peak luminescence was recorded in mV from the point of fMLP addition to the end of the graph.
- The results were computerized.

8.13.4 Example of Spreadsheet and Calculation

Srl.	Neutrophil Count x10^9	T (max)	Tmax/ Neutr	Mean Tmax/Neutr	Integral	Integr/ Neutr	Mean Integr/Neutr.	Max. O2 (mV)	Max. O2 (mV) / Neutr.	Mean Max. O2(mV)/Neutr
A1	0.97	169.00	174		1182.80	1219		1.843	1.90	
A2	0.90	169.00	188		1204.29	1338		1.631	1.81	
A3	3.07	169.00	55		2580.03	840		4.858	1.58	
A4	1.13	169.00	150		3832.83	3392		7.998	7.08	
A5	1.05	338.00	322	178	1854.43	1766	1711	2.445	2.33	2.94

8.14 PULSED FIELD GEL ELECTROPHORESIS (PFGE)

8.14.1 Introduction

Pulse Field Gel Electrophoresis (PFGE) is a technique for resolving chromosome-sized DNA molecules. By alternating the electric field between spatially distinct pairs of electrodes, megabase (mb) sized molecules are able to reorient and move at different speeds through the pores of an agarose gel. PFGE is used to estimate the number of DNA double-strand breaks induced by ionizing radiation and other external agencies. It is believed that iron overload leads to oxidative stress, which in-turn induces DNA strand-breaks through complex processes.

8.14.2 Principle

The CHEF-DR II system (Clamped Homogenous Electric Fields) provides highly uniform, or homogenous, electric fields within the gel. This is accomplished using an array of 24 electrodes that are "clamped," or held to intermediate potentials to eliminate lane distortion.

Additionally, CHEF generates a 120° reorientation (field) angle because of the hexagonal geometry of the electrode array, which is the optimal angle for separating DNA molecules ranging from 100 kb to 6 mb in size. Finally the CHEF-DR II system maintains homogenous electric fields using patented dynamic regulation (DR). With DR, the electrodes not only generate the electric field, but also sense changes in local buffer conductivity as a result of buffer breakdown, change in buffer type, gel thickness, or temperature. Voltage potentials are readjusted immediately to maintain uniform fields, thus ensuring high-resolution separations during runs and between runs.

In this method, pulsed, alternating orthogonal electrical fields are applied to the gel. Large DNA molecules become trapped in their reptation tubes every time the direction of the electric field is altered and can make no further progress through the gel until they have reoriented themselves along the new axis of the electrical field. The larger the DNA molecule, the longer the time required for this alignment. Molecules of DNA whose reorientation times are less than the period of the electrical pulse will therefore be fractionated according to size. The limit of resolution of PFGE depends on several factors including the:

* degree of uniformity of the two electric fields
* absolute lengths of the electrical pulses
* ratio of the lengths of the electric pulses used to generate the two electric fields
* angles of the two electric fields
* relative strengths of the two electric fields

8.14.3 Reagents and Preparation

- Tris
- Boric acid
- EDTA
- Ethidium bromide

1. 150 ml 0.9% agarose gel was prepared by the addition of 150 ml ddH_20 to 13.5 g agarose and heated in a microwave the resultant mixture. 5 µl of ethidium bromide was added to the molten gel at 60°C.
2. Stock 1X TBE buffer (pH 7.0) was prepared as follows: Tris-base 21.6 g/l, EDTA 1.86 g/l, Boric acid 11.0 g/l. This was diluted to obtain 2L 0.5X TBE (1X TBE is 89 mM Tris pH = 7.0, 89 mM boric acid, and 2 mM EDTA) running buffer.

8.14.4 Instrumentation

The basic component of a pulsed field gel system consist of:

- gel box with temp. regulation
- switch unit for controlling the electrical fields
- power supply

8.14.5 Assay Conditions:

a. CHEF-DR II parameters

- Block used = b-1
- Voltage = 4.5 V
- Time = 17 hrs
- Initial switch time = 0.1 s
- Final switch time = 200 s
- Current = 180 mA
- Pump rate = 75
- Temperature = 17-22°C

8.14.6 Assay procedure

Gel was run for 17 hrs on the CHEF-DR II using DNA extracted from the various groups. Two from each group was loaded together with a 50 kb marker (marker XV, Boehringer Mannhem, USA). A photograph of the gel was then taken after the run.

8.15 8-HYDROXY-2'DEOXYGUANOSINE (8OHdG) DETERMINATION

8.15.1 Principle

The 8OHdG test is a competitive *in vitro* ELISA for the quantitative measurements of the DNA adduct, 8-hydroxy-2'-deoxyguanosine (8OHdG) in tissue, serum and plasma. 8OHdG monoclonal antibody and the sample (liver tissue homogenate) are added to a microtiter plate that has been pre-coated with 8OHdG. The 8OHdG monoclonal antibody

reacts competitively with the 8OHdG in the tissue and 8OHdG immobilized on the microtiter plate. Therefore, higher concentrations of 8OHdG in the tissue sample will lead to a reduced binding of the antibody to the 8OHdG on the plate. Antibodies that are bound to the 8OHdG in the tissue sample are washed away from the antibodies that are bound to the 8OHdG on the microtiter plate.

An enzyme-labeled secondary antibody that is added to the plate, binds to the monoclonal antibody that is bound to the 8OHdG coated on the plate. Unbound enzyme-labeled secondary antibody is removed by a wash step and the addition of a chromatic substrate results in colour development in proportion to the amount of antibody bound to the plate. Finally, the reaction is terminated by the addition of 1M phosphoric acid and the absorbance read at 450 nm on a microplate plate reader.

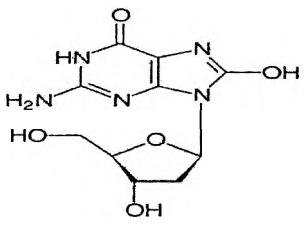

Figure 14 Structure of 8-hydroxy-2'-deoxyguanosine

8.15.2 Reagent Preparation

8-OHdG kit (Genox USA) was used. The kit contained the following:

1. 8-OHdG Microtiter plate : precoated with 8-OHdG (8x12 wells, split type).
2. Primary antibody : monoclonal antibody specific for 8-OHdG.
3. Primary antibody solution : phosphate buffered saline.
4. Secondary antibody : horseradish peroxidase-conjugated antibody
5. Secondary antibody solution : phosphate buffered saline.
6. Chromatic solution : 3,3',5,5'-Tetramethylbenzidine.
7. Diluting solution : H_2O_2 / citrate-phosphate-buffered saline.
8. Wash solution (5 times) : 5 times concentrated phosphate buffered saline.
9. Reaction terminating solution : 1M phosphoric acid
10. 8-OHdG standards : 0.5, 2.0, 8.0, 20.0, 80.0, 200.0 ng/ml

8.15.3 Assay Procedure:

The assay procedure is represented by a flow chart on the next page.

Well A1 was designated blank. The primary antibody was not added to this well.

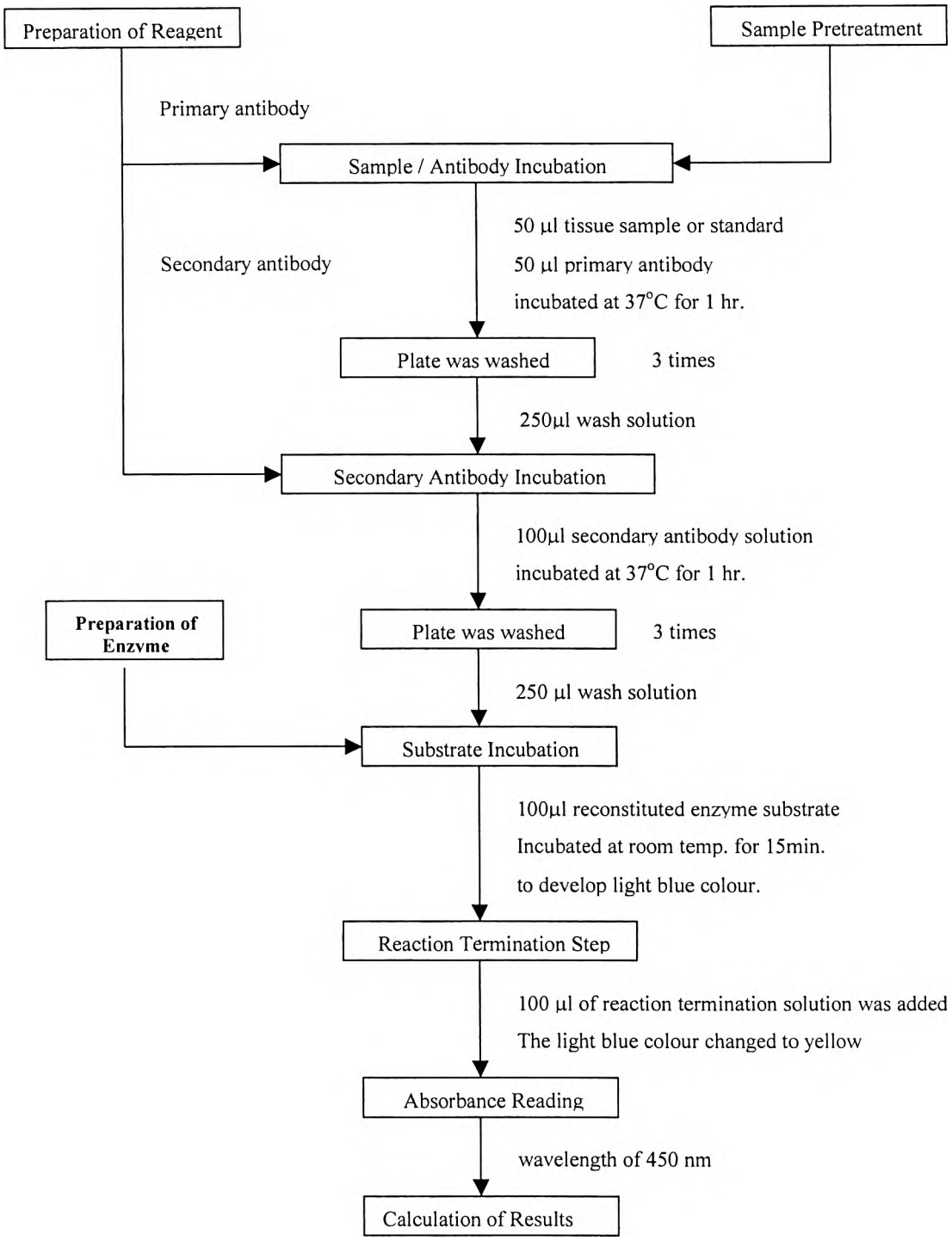
Preparation of Reagent
Sample Pretreatment
Primary antibody
Sample / Antibody Incubation
50 µl tissue sample or standard
50 µl primary antibody
incubated at 37°C for 1 hr.
Secondary antibody
Plate was washed
3 times
250µl wash solution
Secondary Antibody Incubation
100µl secondary antibody solution
incubated at 37°C for 1 hr.
Preparation of Enzyme
Plate was washed
3 times
250 µl wash solution
Substrate Incubation
100µl reconstituted enzyme substrate
Incubated at room temp. for 15min.
to develop light blue colour.
Reaction Termination Step
100 µl of reaction termination solution was added
The light blue colour changed to yellow
Absorbance Reading
wavelength of 450 nm
Calculation of Results

8.15.4 Example of Spreadsheet and Calculation

A standard curve of absorbance against Log_{10} concentration was plotted as shown below.

Pubs 8OHdG levels at 20 months age / Iron overloading

Srl	Abs	Log 10 Conc	Anti-L	x 1.5 (DF)	Conc/g Liver	Mean 8-OHdG (ng/g)
S1	2.200	-0.301	0.500			
S2	2.210	0.301	2.000			
S3	1.980	0.903	7.998			
S4	1.570	1.301	19.999			
S5	0.850	1.903	79.983			
S6	0.470	2.301	199.986			
F1	0.749	1.942	87.506	131	263	
F2	0.677	2.017	104.032	156	312	
F3	0.814	1.884	76.644	115	230	
F4	0.701	1.991	97.875	147	294	
F5	0.740	1.951	89.276	134	268	273

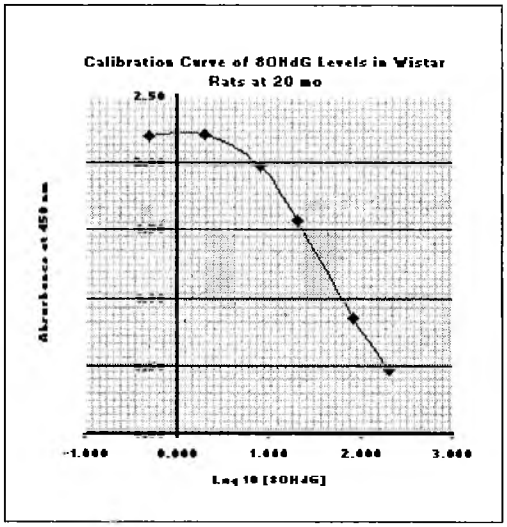

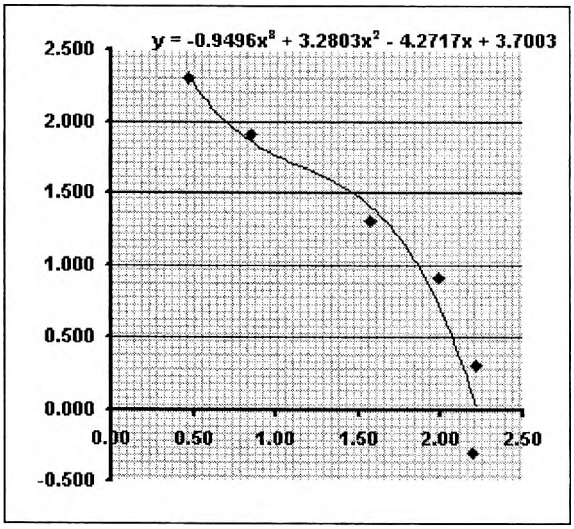

Calibration Curve A **Calibration Curve B**

In order to make 'y' the subject of the equation for easy calculation of 'x' values from calibration curve A, log_{10} values were plotted on the on the y-axis and absorbance on the x-axis (calibration curve B).

8.16 AMES MUTAGENICITY TEST (Maron and Ames, 1983).

8.16.1 Introduction

Normal metabolism produces oxidants that are by-products. These oxidants such as $^{\bullet-}O_2$ and H_2O_2, are the same mutagens produced by irradiation that cause damage to DNA, proteins and lipids. Two factors are critical for the formation of these mutagens: lesions in DNA, formed when DNA is damaged, and cell division that converts DNA lesions to mutagens.

8.16.2 Principle

A test for determining if a chemical is a mutagen is the *Ames Mutagenicity Test* named after Bruce N Ames. The Ames test is based on the assumption that any substance that is mutagenic (for the bacteria used in this test) may also turn out to be a carcinogen. However, some substances that cause cancer in laboratory animals do not give a positive Ames test (and vice-versa). The low cost of the test makes it invaluable for screening substances.

The bacterium used in the test is a strain of *Salmonella typhimurium* that carries a defective (mutant) gene, making it unable to synthesize the amino acid histidine (His) from the ingredient in its culture medium. However, some types of mutations (including this one) can be reversed, (a back mutation) with the gene regaining its function. These 'revertants' are able to grow in a medium lacking histidine. Many chemicals are not mutagenic (or carcinogenic) by themselves, but become converted to mutagens (and carcinogens) as they are metabolized in the body. For this reason, the Ames test incorporates a mixture of liver enzymes.

8.16.3 The Bacteria Tester Strain

A set of histidine-requiring strains is used for mutagenicity testing. Each tester strain contains a different type of mutation in the histidine operon. In addition to the histidine mutation, the standard tester strains contain other mutations that greatly increase their ability to detect mutagens. One mutation *(rfa)* causes partial loss of the lipopolysaccharide barrier that coats the bacteria and increases permeability to large molecules that do not penetrate the normal cell wall. The other mutation (*uvr*B) is a deletion of a gene coding for the DNA excision repair system, resulting in greatly increased sensitivity in detecting many mutagens. The deletion excising the *uvrB* gene extends through the bio-gene and consequently, these bacteria also require biotin for growth. The standard tester strains mostly used are TA97, TA98, TA100 and TA102. TA97, TA98 and TA100 contain R-factor plasmid, pKM 101. This increases chemical and spontaneous mutagenesis by enhancing an error-prone DNA repair system. TA102 contains multicopy plasmid pAQ1 that carries the *his*G428 mutation and the tetracycline resistant gene. In addition, TA100 contains the *his*G46 mutation. The normal gene *his*G gene codes for the first enzyme of histidine biosynthesis. This mutation substitutes proline $\overset{-GGG-}{-CCC-}$ for leucine $\overset{-GAG-}{-CTC-}$. Therefore TA100, detects mutagens that cause base-pair substitutions primarily at one of these G-C pairs.

TA98 contains the *his*D3052 mutation. The normal gene *his*D gene codes for histidinol dehydrogenase and detects various frame-shift (FS) mutations. These FS mutations can stabilize the shifted pairing that often occurs in repetitive sequences or 'hot spots' of the DNA, resulting in a frame-shift mutation that restores the correct reading frame for

histidine synthesis. The *his* D3052 has the sequence -CGCGCGCG-/-GCGCGCGC-, 8 repetitive –GC-residues near the site of a FS mutation in the *his*D gene. The mutation is reverted by i.e. 2-nitrosofluorene, daunomycin. TA97 contains the *his*D6610 mutation, plus a second 'hot spot' of alternating -GC- base pairs near the run of the cytosines. It is sensitive to some of the mutagens that revert TA98. TA102 contains the *his*G gene that contains the ochre mutation TAA. This strain detects efficiently a variety of mutagens such as formaldehyde, glyoxal, hydroperoxides, bleomycin, X-rays, UV light.

8.16.4 Reagent List and Preparation

Oxoid Nutrient Broth No. 2

Bacto Difco Agar

NaCl

L-Histidine

D-Biotin

KCl

$MgCl_2.6H_2O$

NaH_2PO_4

Na_2HPO_4

NADP

G-6-PO_4

$MgSO_4.7H_2O$

K_2HPO_4

$NaHNH_4PO_4.4H_2O$

Citric acid monohydrate

Glucose

Daunomycin

Ampicillin

Crystal Violet

Aroclor -1254

DMSO

Nutrient broth (*autoclaved*)

- Oxoid nutrient broth - 1.25 g
- ddH_2O - 50 ml

Nutrient agar plates (contains histidine) (*autoclaved*)

- Oxoid nutrient broth - 4.8 g
- Bacto agar - 9.0 g
- ddH_2O - 600 ml

Top agar (*autoclaved*)

- Bacto agar - 0.6 g
- NaCl - 0.5 g
- ddH_2O - 100 ml

Vogel-Bonner medium E (VB medium) (*autoclaved*)

- ddH_2O - 670 ml
- $MgSO_4.7H_2O$ - 5 g

- Citric acid monohydrate - 50 g
- K_2HPO_4 or $K_2HPO_4.5H_2O$ - 250 g or 327.59 g
- $NaHNH_4PO_4.4H_2O$ - 78.5 g

were added in the above order.

were added after each compound had dissolved.

Minimum glucose plates

- Bacto agar - 15 g
- ddH_2O - 910 ml

The above-mentioned was autoclaved.

added 25X VB medium E - 40 ml

added 40% glucose - 50 ml

Histidine / Biotine Sol^n (*autoclaved*)

Per 250 ml

- D-Biotin (FW 247.3) - 30.9 mg
- L-Histidine - 24.0 mg

0.1 M Hitidine sol^n (*autoclaved*)

- L-Histidine - 1.55 g/ 100 ml

0.5 mM Biotin sol^n (*autoclaved*)

- D-Biotin - 0.012 g/ 100 ml

0.1% Crystal violet sol^n

- Crystal violet - 0.01 g
- ddH_2O - 10 ml

Daunomycin (daunorubicin hydrchloride)

- Daunomycin - 1 mg / ml

Glucose-6-phosphate (G-6-P)

- G-6-P - 2.82 g/ 10 ml

Nicotinamide adenine dinucleotide phosphate (NADP) sol^{n}

- NADP (FW 765.4) - 383 mg / 5 ml

1.65 M KCl / 0.4 M $MgCl_2$ salt sol^{n} (Per 100 ml)

- KCl - 12.3 g
- $MgCl_2.6H_2O$ - 8.14 g

0.2 M Sodium phosphate buffer (60 ml A + 440 ml B)

- 0.2M $NaH_2PO_4.H_2O$ - 13.8 g / 500 ml.....A
- 0.2M Na_2HPO_4 - 14.2 g / 500 ml.....B

S9 Mix (rat liver microsomal enzymes + co-factors) for 50 ml

- Rat liver S9 (Aroclor-1254-induced) 2.0 ml
- KCl / $MgCl_2$ Salt sol^{n} - 1.0 ml
- 1 M G-6-P - 0.25 ml
- 0.1 M NADP - 2.0 ml
- 0.2 M phosphate buffer - 25.0 ml (pH 7.4)
- ddH_2O - 19.75ml

S9 was donated by MRC Unit, Tygerberg, Cape Town.

8.16.5 Characterization of TA97, TA98, TA100, TA102 strains (donated by Ames Lab, USA).

A. Upon receipt of discs impregnated with the *Salmonella* strains, each disc was dropped into separate tubes containing 10 ml nutrient broth. This was incubated at 37°C overnight with shaking.

B. The overnight culture was plated on nutrient agar plates to obtain single colonies and incubated at 37°C overnight. *(This is referred to as the master plate.)*

C. Six culture tubes were filled with 10 ml nutrient broth. Single colonies were transferred into each of the tubes and incubated overnight at 37°C with shaking.

D The various markers were performed on each of the tubes and the tube that satisfied all criteria was selected. Where none was suitable, a repeat was carried out using single colonies from step B.

8.16.5.1 Test for Histidine Requirement

- Requirement
  - Minimum glucose plates
  - 0.1 M Histidine
  - 0.5 M Biotin
  - ddH_2O (autoclaved)
- Two circles were marked on the bottom of the culture plates and labeled H_2O & H/B. (Figures 15 and 16*a-d*, pages 162-165).

- A sterile loop was dipped into autoclaved ddH_2O and plated within the H_2O circle. Similarly, a loop-full of 0.1 M Histidine was plated within the H/B circle followed *by a loop-full of 0.5 M Biotin.*
- *Finally, a loop-full i.e. TA97 from one of the 6 tubes was plated within the ddH_2O circle and another within the H/B circle.*
- *The a/m procedure was repeated for two other minimum glucose plates. Thus,* triplicates were produced for each of the 6 tubes.
- The whole procedure for each of the 6 tubes of TA98, TA100 & TA102 was repeated.
- The minimum glucose plates were incubated at 37°C overnight.

8.16.5.2 rfa (Permeability) Test

- Requirement
  - Nutrient agar plates (NA)
  - Top agar
  - 0.1% Crystal violet sol^n
- The Top agar was placed in a water bath at 45°C.
- 2.5 ml of Top agar was dispensed into culture tubes and capped.
- 0.1 ml i.e. TA98 was added to each tube and vortexed for about 5 sec.
- This was quickly poured onto the NA plate. The plate was gently swirled to allow even distribution.
- Work was done in triplicate.
- The above procedure was repeated for the other *Salmonella* strains.

- An HPLC syringe was rinsed with HPLC MeOH. Using the syringe, 10 µl of the crystal violet solution was drawn onto an autoclaved filter paper disc.
- The crystal violet-soaked disc was placed in the center of the plate (i.e. TA98 plate).
- For all 6 tubes of TA97, TA98, TA100, TA102, the above-mentioned procedure was repeated. Flamed forceps was used to handle sterile filter paper discs.
- The Nutrient agar plates were incubated at 37°C for 24 hr. (Figures 15 and 16*e-h*, pages 162-165).

8.16.5.3 *uvβ* Mutation Test

- Requirement - NA plates.
- Work was done in triplicates and plates labeled TA98, TA100 etc.
- A line was drawn under each plate (demarcating it into two halves).
- A loop-full of i.e. TA 97 from tube 1 was streaked across the plate. In all, 4-6 parallel streaks were made. Two streaks were made from each tube. In addition, streaks were made at right angles to the dividing line. Samples from all 6 tubes of i.e. TA97 were treated in a similar manner.
- A piece of sterile cardboard or paper towel (sprayed with 70% EtOH) was placed across the plate along the vertical line that divided the plate.
- The plates were irradiated by a 15W UV lamp for 6 sec at a vertical distance of about 33 cm from above (Figures 15 and 16*n-p*, pages 162-165).
- Finally, the plates were incubated at 37°C for 12-24 hrs.

8.16.5.4 R-factor Test

- Requirement
  - Minimum glucose plates
  - Top agar
  - 0.5 mM His/Bio sol^{n}
- 10 ml of His/Bio Sol^{n} was added to the Top agar held at 45°C.
- 2.0 ml of the Top agar (with His/Bio) was added to culture tubes (incubating at 37°C).
- 0.1 ml of i.e. TA98 (tube 1) was then added to each of the tubes containing the Top agar.
- This was vortexed for 3 sec and quickly poured onto the Minimum glucose plate. The plate was swirled gently and the Top agar allowed settling.
- Ampicillin discs (Bacto - sensitivity disc 10 µg 6363-33 DIFCO) was gently dropped onto the plates.
- The procedure was repeated for all 6 tubes of i.e. TA98, TA100, TA102 & TA97.
- Plates were incubated at 37°C for 48 hr (Figures 15 and 16*i-l*, pages 162-165).

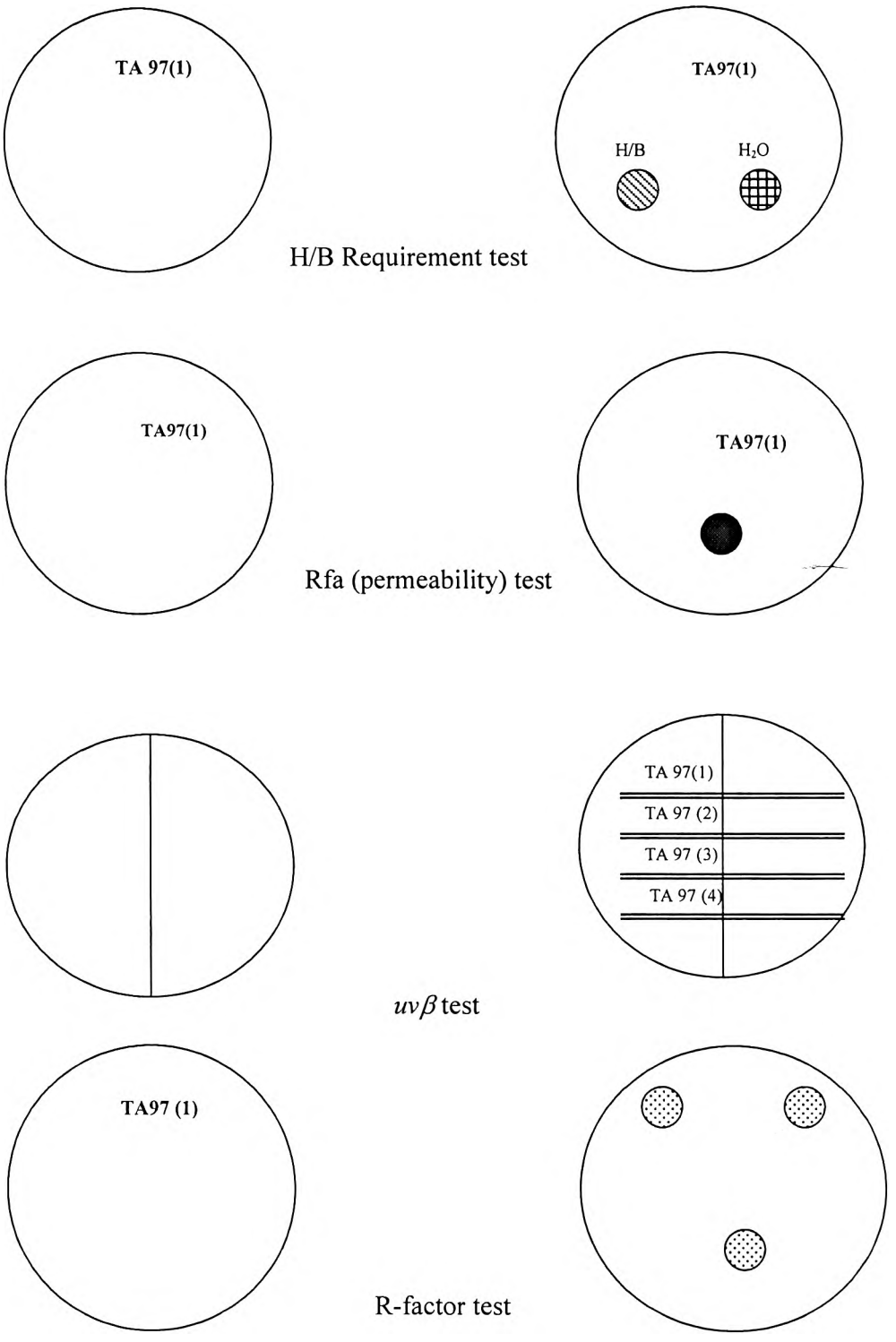

Figure 15 Characterization of *Salmonella typhimurium* strains using the various markers.



Figure 16*a*. Positive Histidine / Biotine requirement test.



Figure 16*b* Positive Histidine / Biotine requirement test.

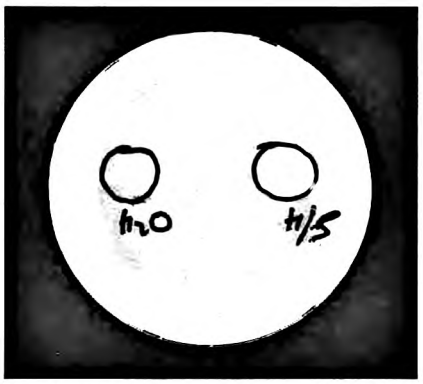

Figure 16*c* Positive Histidine / Biotine requirement test.



Figure 16*d* Negative Histidine / Biotine requirement test. Growth is present in the H_2O control.



Figure 16*e* Positive Rfa (permeability) test (TA97).



Figure 16*f* Positive Rfa (permeability) test (TA 98).



Figure 16*g* Positive Rfa (permeability) test (TA100).

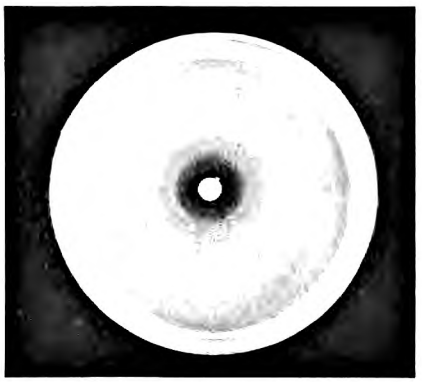

Figure 16*h* Positive Rfa (permeability) test (TA102).



Figure 16*i* Positive R-Factor test (TA 97).



Figure 16*j* Negative R-Factor test (TA 98).

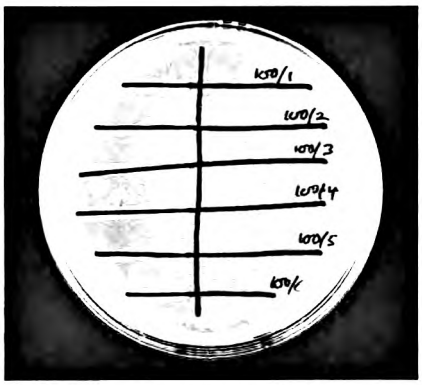

Figure 16*k* Positive uvrβ test (Mutation) TA 100.

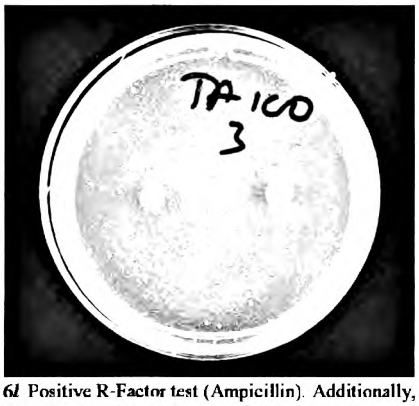

Figure 16*l* Positive R-Factor test (Ampicillin). Additionally, spontaneous 'revertants' can be seen as bright spots (colonies).



Figure 16*m* Positive R-factor test (Ampicillin) TA 102.

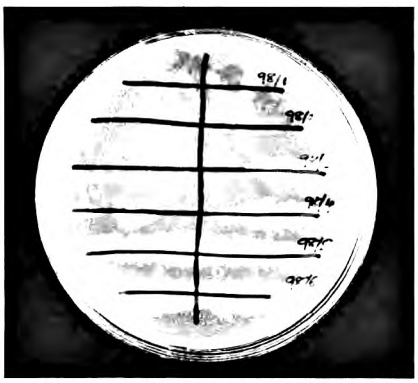

Figure 16*n* Negative uvrβ test (Mutation). Wild type *Salmonella typhimurium* growth (TA102).

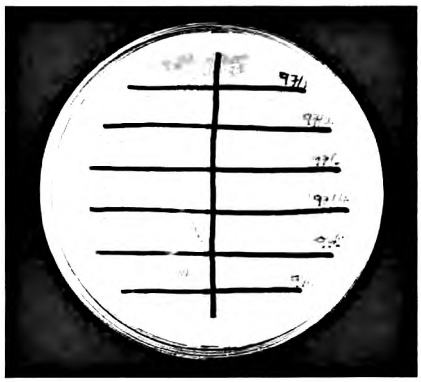

Figure 16*o* Positive uvrβ test (TA 97).

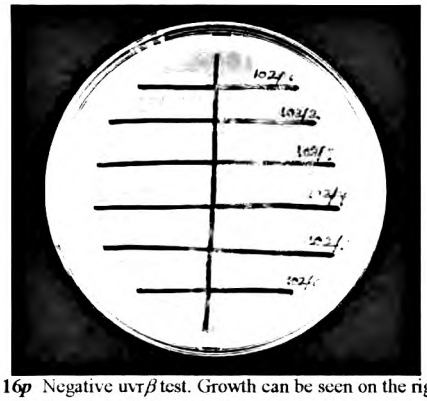

Figure 16*p* Negative uvrβ test. Growth can be seen on the right side (*UV* irradiated section).

8.16.5.5 Spontaneous Revertant Test

- Requirement - Nutrient agar plates
  - Top agar
  - 0.5 mM Histidine/Biotin Sol^{n}
- Five plates were prepared for each of the 6 tubes from a particular strain i.e. TA97(1), TA97(2).....TA97(6).
- The Top agar was incubated at 45°C and the culture tubes at 37°C.
- 2.5 ml Top agar was dispensed into each (cupped) culture tube under sterile conditions.
- 0.6 ml of the tester strain i.e. TA97(1) was quickly pipetted and 0.1 ml was dispensed into the 5 culture tubes.
- The culture tube was vortexed for 3 sec and quickly poured onto the Nutrient agar plate.
- The labeled culture plate was gently swirled on a flat top and allowed to settle.
- The above procedure was repeated for all samples and culture plates were incubated at 37°C for 48 hrs undisturbed.
- Colonies ('revertants' against the background lawn) were counted (i.e. Figure 16*l*, page 164).
- For TA97, the acceptable range is: 90-180 colonies

  TA98, " 30-50 "

  TA100, " 120-200 "

  TA102, " 240-360 "

Finally, one sample tube from each *Salmonella typhimurium* strain that strictly passed all 5 conditions was selected. The selected tube was referred to as "master copies". Master copies were stored at 4°C and used over the next few days. Master plates however, (first culture, see 8.16.5 section B) were stored at -70°C for some few months. For long term storage the following procedure was followed:

- 50 ml of Nutrient broth was prepared and autoclaved for each strain.
- The Nutrient broth was allowed to partially cool down. This was incubated for 30 min with continuous shaking at 37°C.
- The 50 ml Nutrient broth was inoculated with 1ml of the cultured bacteria from the selected tube and incubated for 12 hrs, with continuous shaking at 37°C.
- 0.09 ml DMSO (filtered through a 0.22 μm filter) was added per 1 ml of culture and gently mixed. 1 ml was then aliquot into 'Nunc' tubes. This was stored at -70°C for years.

8.15.5.6 Mutagenicity Test

- The same procedure as that described for the *Spontaneous revertant test* was used. However, 0.1 ml of the suspected mutagenic substance was first added to the 2.0 ml Top agar, followed by 0.1 ml of the tester strain i.e. TA97.
- Test samples were challenged with 0.1 ml S9 mix. This was added to the Top agar. However, in the present study, the addition of S9 mix did not make any significant change.

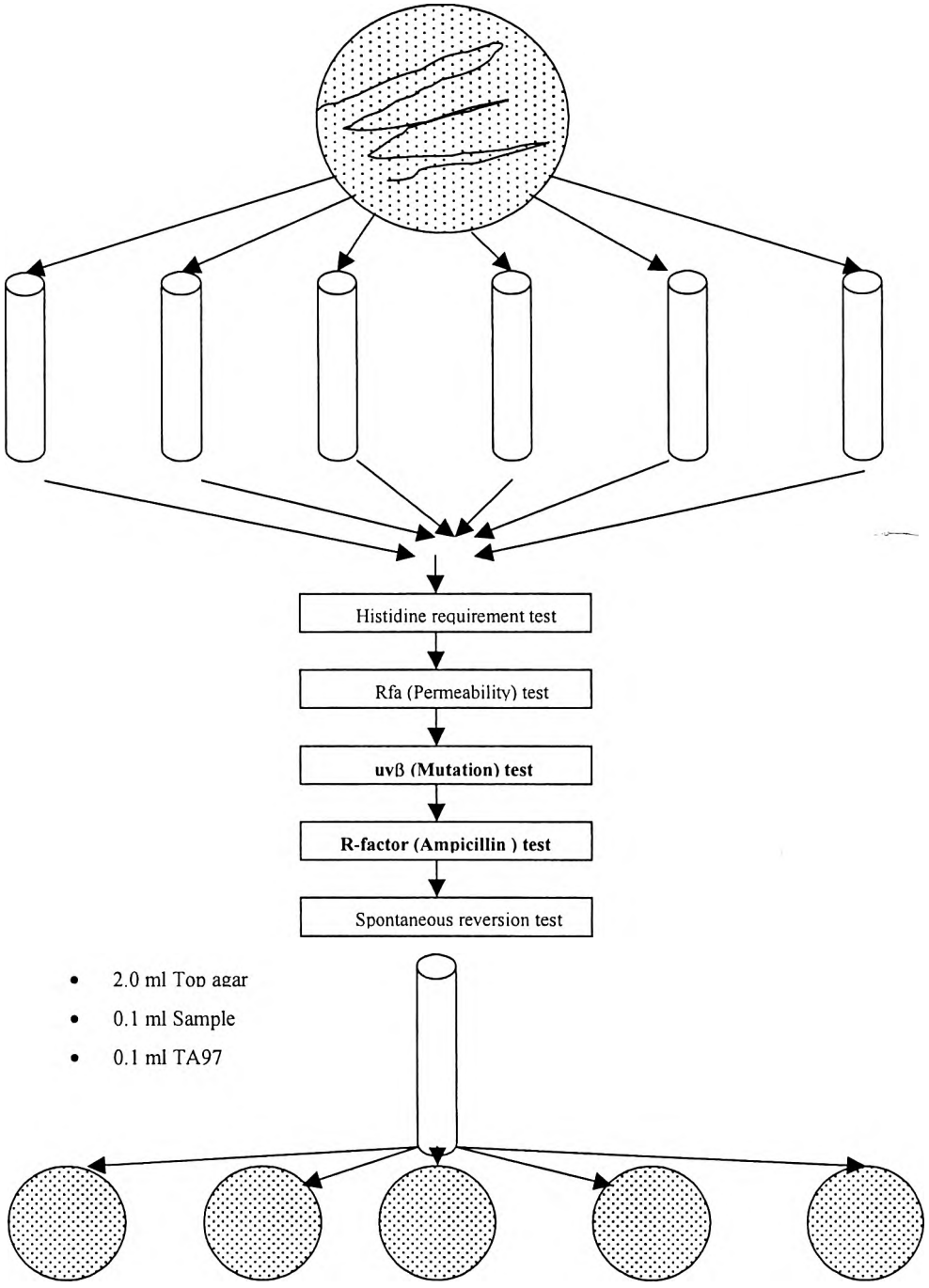

Figure 17 Summary of the steps involved in the characterization of the *Salmonella typhimurium* tester strains.

8.17 DETECTIONOF 8-OHdG IN RAT LIVER SECTIONS BY IMMUNO-HISTOCHEMICAL TECHNIQUES

8.17.1 Introduction

Free radical species have been shown to play a role in a variety of pathological and physiological processes. ROS, such as $O_2^{-\bullet}$, H_2O_2, $^{\bullet}OH$, $^1O_2$, can oxidize various tissue components leading to the formation of toxic metabolites. Methods have been developed to monitor oxidative damage in tissues, and these are based on the qualitative or quantitative detection of the secondary products of free radical reactions. Oxidative stress markers include oxidized proteins or DNA adducts, or peroxidized lipids. The advantage of detecting these secondary products is that, they are less reactive and more stable than the free radical species. They are therefore suitable markers for the assessment of the long-term effects of ROS.

8.17.2 Principle

A specific monoclonal antibody, N45.1 has been used in several immunohistological investigations to demonstrate the presence of increased levels of 8OHdG in various cell types (Hatori *et al.*, 1995; Toyokuni *et al.*, 1997, 1999). Direct photodyanamic activity (Kasai *et al.*, 1992), and the actions of $^1O_2$ (Devasagayam *et al.*, 1991) and $^{\bullet}OH$ (Kasai and Nishimura, 1984) have been implicated in the hydroxylation of the C8 position of 2-deoxyguanosine, to form 8OHdG. Methods have been developed to detect 8OHdG DNA adducts in paraffin sections.

8.17.3 Reagents

- Phosphate buffered saline (PBS), pH 7.4
- Xylene
- Ethanol
- Bovine serum albumin (BSA)
- Specific anti-8OHdG antibodies (rabbits)
- Biotinylated rabbit IgG (Sigma)
- ExtrAvidin peroxidase (Sigma)
- Diamino benzidine (DAB) substrate
- Mayer's haematoxylin solution
- Entellan mounting medium

8.17.4 Assay Procedure

Rat liver specimens were obtained from rats that were sacrificed at various time points after being fed various diet regimens. Paraffin embedded sections were prepared and picked up onto slides. Slides were placed in an oven at 56-60°C (but not more than 60°C) for 15 min, for antigen retrieval. Sections were immersed in two changes of xylene (5 min each) and then into two changes of absolute ethanol (3 min each). They were then rinsed briefly with water.

After incubation in PBS for 15 min sections were blocked, for monospecific binding of the antibody, by incubation in 5% BSA for 15 min at room temperature. They were then covered in a humidified chamber with 300-500 μl of the primary antibody,

([anti-8-OHdG] = 5 μg/ml) in PBS overnight at room temperature. PBS without primary antibody was used as negative control. Slides were then gently rinsed with PBS from a wash bottle, and left in the buffer for 5 min. 300 μl of biotinylated secondary antibody diluted in PBS (1/300) was applied onto the sections for at least 30 min at room temperature. Slides were washed with PBS as above.

Slides were allowed to drain and then covered with 300 μl of ExtrAvidin peroxidase diluted in PBS (1:100), and incubated for at least 30 min at room temperature. After rinsing briefly with PBS and shaking off excess fluid, the area around the sections was carefully wiped. Freshly prepared diaminobenzidine (DAB) substrate mixture was applied to cover the sections, and incubated for 5-10 min. Slides were gently rinsed under running tap water and after drying they were mounted with the aqueous medium Entellan. They were then observed microscopically using 10X and 40X objectives.

8.18 DETECTION OF 4-HNE IN RAT LIVER SECTIONS BY IMMUNOHISTO-CHEMICAL TECHNIQUES

8.18.1 Introduction

Selective biochemical methods have been used in qualitative and quantitative determination of free radical-induced oxidative stress in various pathophysiologic conditions. This has enabled detection of oxidative modifications in tissue homogenates, sub-cellular fractions and reconstituted systems. Application of immunohistochemical procedures in detecting various biomarkers of oxidative modifications has allowed

determination of the *in vivo* distribution of oxidative stress. These methods are based on the use of specific antibodies against secondary products of oxidative modification, lipids, proteins and DNA adducts formed by these products.

4-HNE is one of the major LPO products generated by free radical attack on ω-6 PUFAs. The toxic effects of 4-HNE are as a result of interactions with proteins. 4-HNE reacts with histidine, lysine or cystein residues of proteins resulting in the formation of stable *hemiacetal Michaelis* addition adducts (Uchida and Stadtman, 1992). 4-HNE protein adducts are relatively stable and have been used as markers of free radical-mediated damage. 4-HNE shows genotoxic as well as mutagenic effects on cell proliferation (Esterbauer and Cheeseman, 1990). Previous studies have demonstrated by immunohistochemical methods, the accumulation of 4-HNE-modified proteins in the cytoplasm of hepatocytes from the livers of Long-Evans Cinnamon rats (Ma *et al.*, 1997). Semi-quantitative analyses of 4-HNE-protein adduct and Fe intensities in histological sections have indicated significant positive correlation (Ohhira *et al.*, 1998). Also in the above-mentioned study, an increase in 4-HNE-protein adducts was demonstrated in sections of human alcoholic liver disease.

8.18.2 Reagents and Equipment

- Phosphate buffered saline (PBS), pH 7.4
- Xylene
- Ethanol
- Bovine serum albumin (BSA)

- Specific anti-HNE antibodies (rabbits)
- Biotinylated rabbit IgG (Sigma)
- ExtrAvidin peroxidase (Sigma)
- Diamino benzidine (DAB) substrate
- Mayer's haematoxylin solution
- Entellan mounting medium

8.18.3 Assay Procedure

The assay procedure is the same as that used for 8OHdG (see section 8.17.4). However, 2 μg/ml anti-HNE primary antibody was used instead.

8.19 LIVER IRON HISTOLOGY

Formalin-fixed liver specimens for histology were embedded in paraffin wax. 1 μm sections were stained with haematoxylin-eosin (H & E) and Perls' Prussian blue stain for iron. The degree of iron loading was assessed histologically in coded sections and graded on a scale of 0 - 4. Iron-free foci were confirmed by glutathione-sulfhydryl-transferase-π (GST-π stain).

8.20 ALPHA FETO PROTEIN (AFP)

AFP was determined using an auto-analyser (Advia Centaur) and kits from Bayer (Tarrytown, USA).

8.21 AST / ALT DETERMINATION

AST and ALT were determined using an auto-analyser (Cobas Integra 400) and kits from Roche Diagnostics (Indianapolis, USA).

8.22 SERUM COPPER DETERMINATION

8.22.1 Introduction

Cu is an essential trace element in human nutrition and a component of many metalloenzymes. Cu is important for the function of ceruloplasmin and for the synthesis of melanin and collagen. Cu deficiency is characterized by growth failure and hypochromic-microcytic anaemia. Acute Cu toxicity can cause gastroenteritis and acute renal failure.

8.22.2 Principle

At pH 4.7, Cu that bound to ceruloplasmin is released by a reducing agent. Cu then reacts with a specific colour reagent, 4-(-3,5-Dibromo-2-pyridylozo)-N-ethyl-N-(3-sulphopropyl)- analine, to form a stable colour chelate. The intensity of the colour is directly proportional to the amount of Cu in the sample.

8.22.3 Assay Procedure

Cu kit from Randox Laboratories was used. The manufacturer's instructions were followed accordingly.

8.23 STATISTICAL ANALYSES

The SAS statistical package was used. All data was expressed as ± SEM. Statistical analysis was performed by independent Student's *t* test at the level of 0.05 for paired and unpaired data. A probability value of $p<0.05$ was considered statistically significant. For multiple groups, analysis of variance was performed by Bonferroni (Dunn) Multiple comparison *t* Test. Pearson's correlation coefficient was determined within groups. Multiple regression analysis was performed to determine predictive indicators of oxidative stress.

9.0 RESULTS

Results of analyses are presented in Figures 18-54 (pages 226-246). Colour codes for curves in graphs represent the ff:



9.0.1 Serum Iron

Figure 18 shows serum iron levels of iron-overloaded Wistar rats. The curve for the control group remained the lowest with a maximum value of 56.8 ± 14.0 µmol/l at 8 mo and a minimum of 45.7 ± 10.3 µmol/l at 24 mo. Curves for all other groups increased and remained high with a minor peak at 4 mo followed by a decrease at 8 mo and a sharp increase from 8 mo to 16 mo. A plateau was observed after 16 mo. The curve of the Fe gp obtained a maximum serum iron concentration of 118.4 ± 13.3 µmol/l at 20 mo, the Fe + V gp was 123.9 ± 12.0 µmol/l at 24 mo, the Fe –V gp was 133.6 ± 14.2 µmol/l at 16 mo, the Fe + ASA gp was 134.4 ± 4.4 µmol at 24 mo and Fe + Cu gp was 129.5 ± 41.4 µmol/l at 20 mo. The minor peak at 4 mo was not statistically significant. However, the peak observed at 16 mo was statistically significant (p=0.05).

9.0.2 Superoxide free radical ($^{\bullet}O_2$)

Figure 19 shows superoxide radical ($^{\bullet}O_2$) levels in iron-overloaded Wistar rats. The curve of the control group showed little change and remained the lowest with a maximum of 0.402 mV at 2 mo. Thereafter it declined gradually until 20 mo with a minimum of 0.280 ± 0.110 mV. The curves of the Fe, Fe + V, Fe – V and Fe + ASA groups were more

prominent, having peak values of 0.944 ± 0.878 mV, 0.880 ± 730 mV, 1.220 ± 0.650 mV and 1.230mV, respectively, at 12 mo. The curve of the Fe + Cu gp on the other hand was different with an early peak at 2 mo (0.929mV) and a second peak at 16 mo (0.520 ± 0.31 mV). At 12 mo, the Fe + Cu gp had a low $^{\bullet-}O_2$ value of 0.200mV.

9.0.3 Glutathione peroxidase (GPx)

Figure 20 shows glutathione peroxidase levels of iron-overloaded Wistar rats. The curves of all the groups except the Fe – V gp had a similar undulating nature. The C and Fe + Cu curves remained the highest up to about 10 mo and later the C and Fe + V groups continued to be the highest from 14 mo to the end. Peak values occurred at 4 and 16 mo and declined between 8 and 12 mo. Differences between 2-4, 4-8 and 12-16 mo were statistically significant (p=0.05 ea). Peak GPx values in the various groups were as follows: C gp = 214 ± 11.9 U/g Hb (4 mo), Fe gp = 179.1 ± 16.1 U/g Hb (20 mo), Fe + V gp = 228.8 ± 17.6 U/g Hb (16 mo), Fe – V = 176.9 ± 24.9 U/g Hb (24 mo), Fe + ASA = 189.2 ± 30.8 U/g Hb (16 mo), Fe + Cu = 233.8 ± 39.6 U/g Hb (4 mo). GPx level of the Fe – V gp declined from 4 mo, reaching its the lowest at 12 mo and increased gradually to a maximum at 24 mo. However, it was the lowest at several time points.

9.0.4 SOD

Figure 21 shows SOD level of iron-overloaded Wistar rats. Curves for all the groups including the control group showed an undulating pattern. The C gp remained the highest throughout and the Fe – V gp, the lowest. SOD levels for the Fe + Cu and Fe + V gps were directly below the C gp until 16 mo when they declined and were below the Fe + ASA and

Fe gps. Peak values observed between 12 and 16 mo were as follows: C gp = 2165 ± 444 U/g Hb (12 mo), Fe gp = 1584 ± 360 U/g Hb (16 mo), Fe + V = 1626 ± 199 U/g Hb (12 mo), Fe – V = 1242 ± 201 U/g Hb (16 mo), Fe + ASA = 1546 ± 442 U/g Hb (12 mo), and Fe + Cu = 1747 ± 162 (12 mo). Significant differences were observed between 8 and 12 mo ($p=0.05$) and 12 and 20 mo ($p=0.05$). In addition, significant differences were observed between the control and the various groups.

9.0.5 Catalase

Figure 22 shows catalase levels of iron-overloaded Wistar rats. Generally, curves showed increased values at 2 and 8 mo followed by decreased values. The pattern was very close to the SOD curves in Figure 21. The control group was the highest throughout with the Fe + Cu and Fe – V gps the lowest. The levels of the Fe + V gp were below that of the C gp, and the Fe gp was in the middle of the levels of the other groups. Peak catalase levels were as follows: C gp = 66.9 ± 7.9 Units x 10^{3}/min (8 mo), Fe = 61.0 ± 3.7 Units x 10^{-3}/min (8 mo), Fe + V gp = 65.2 ± 10.7 Units x 10^{-3}/min (8 mo), Fe – V gp = 48.7 ± 4.4 Units x 10^{-3}/min (12 mo), Fe + ASA = 51.3 ± 2.2 Units x 10^{-3}/min (12 mo), Fe + Cu = 48.8 ± 4.8 Units x 10^{-3}/min (12 mo). The various groups were significantly different for the period 4 - 8 and 8 - 20 mo ($p=0.05$; $p=0.05$, respectively).

9.0.6 Vitamin C

Figure 23 shows vitamin C levels of iron-overloaded Wistar rats. There was a general increase from about 1 μmol/l to about 6.5 μmol/l over 24 mo. Vitamin C levels for the Fe and Fe + V gps were mostly the highest, and the Fe + Cu and Fe gps, the lowest. Vitamin

C levels of the other groups were in-between. These seemingly straight lines declined at 4, 12 and 20 mo but the decline was statistically insignificant. Significant differences were observed between the Fe + V gp & Fe gp, Fe + V gp & Fe – V gp and Fe + V gp & Fe + Cu gp with p=0.05 each.

9.0.7 TAS

Figure 24 shows Total Antioxidant Status (TAS) of iron-overloaded Wistar rats. TAS level for the control group remained the highest before 12 mo and well separated from the rest from 10 - 24 mo. This difference was statistically significant (p=0.05). Between 12 and 16 mo TAS levels for the Fe gp were below that of the C gp, however, between 16 and 24 mo, TAS levels for the Fe + V gp were below the C gp. Furthermore, between 2-4 and 8-16 mo TAS levels for the Fe + Cu gp were the lowest. At 24 mo the TAS level for the Fe – V gp was the lowest. Peak values for most groups occurred at 20 mo and were as follows: C gp = 0.87 $\pm$ 0.08 mmol/l, Fe gp = 0.67 $\pm$ 0.08 mmol/l (16 mo), Fe + V gp = 0.76 $\pm$ 0.07 mmol/l, Fe – V gp = 0.73 $\pm$ 0.03 mmol/l, Fe + ASA gp = 0.68 $\pm$ 0.04 mmol/l, Fe + Cu gp = 0.73 $\pm$ 0.05 mmol/l.

9.0.8 ORAC

Figure 25 shows ORAC of water- and lipid-soluble fractions of iron-overloaded Wister rat's liver homogenate. ORAC-A and ORAC-L were in the ratio of about 4:1. Curves for ORAC-A showed peaks at 12 mo whilst ORAC-L showed peaks at 20 mo. Differences between the various groups appeared after 12 mo. In both cases, the curve for the control group was the lowest and the Fe + Cu gp the highest except at 12 mo when the curve for

the Fe gp of the ORAC-A fraction was the highest. In addition, both curves (ORAC-A and ORAC-L) appeared to operate in an inverse relationship. When ORAC-A curves were at peak values, ORAC-L curves were low. Conversely when ORAC-L curves were at peak values, ORAC-A curves were low. The correlation analysis showed a negative correlation between ORAC-L and ORAC-A in the C and Fe + ASA groups ($r = -0.39$, $p=0.0412$; $r = -0.42$, $p=0.0235$, respectively).

9.0.9 MDA

Figure 26 shows MDA levels of iron-overloaded Wistar rats. Generally MDA values were low from 2-12 mo. All other groups apart from the C gp showed increases after 12 mo. MDA level for the C gp was the lowest and fairly straight with a maximum value of 6.1 ± 1.5 μM. The steepest curve was seen in the Fe gp with a maximum MDA value of 55.5 ± 39.8 μM (24 mo). Curves for the Fe + ASA and Fe + Cu gps clustered with maximum MDA values of 42.5 ± 23.5 μM and 39.5 ± 1.4 μM, respectively, at 24 mo. Similarly, the curves of the Fe + V and Fe - V gps also clustered with maximum values of 25.3 ± 8.0 μM and 28.4 ± 21.7 μM, respectively.

9.0.10 8-IP

Figure 27 shows 8-IP level of iron-overloaded Wistar rats. The curve for the C gp was the lowest and relatively straight. The maximum value for the C gp was 590 ± 194 ng/g liver wt. 8-IP levels for all other groups were well above the C gp. 8-IP levels of the Fe + Cu gp were far above the rest with a hyperbolic curve. A maximum value of 12940 ± 4173 ng/g liver wt was obtained at 16 mo. This value compared to the C gp was statistically

significant (p=0.05). 8-IP levels for the rest of the groups were between the two extremes with relatively no differences up to 12 mo and beyond 20 mo. Differences seen between 12 and 20 mo were statistically significant (p=0.05). Peak values of the Fe gp and Fe + ASA gp were 4102 ± 2464 ng/g and 2280 ± 1172 ng/g liver wt., respectively.

9.0.11 FADU

Figure 28 shows Fluorimetric Analysis of DNA Unwinding of liver homogenate of iron-overloaded Wistar rats. Generally there was relatively no difference amongst the various groups up to 12 mo. Thereafter the rate of DNA unwinding of the various groups increased sharply apart from the control group. The rate of DNA unwinding of the control group remained the lowest with a maximum value of 0.096 ± 0.062 units / min. DNA unwinding of the Fe + Cu gp was the highest with a maximum value of 0.268 ± 0.062 unit / min. The rate of DNA unwinding for all other groups were in-between with maximum values as follows: F gp = 0.210 ± 0.033 unit/min, V gp = 0.198 ± 0.071 unit/min, Fe – V gp = 0.178 ± 0.027 unit/min, Fe + ASA gp = 0.226 ± 0.069 unit/min. The rates of DNA unwinding between 12 and 20 mo for all groups were statistically significant (P=0.05).

9.0.12 LPO

Figure 29 shows Lipid hydroperoxides (LOOH) of iron-overloaded Wistar rats. There was virtually no difference in serum LOOH values amongst the various groups for the first twelve months. Thereafter LOOH levels for all groups apart from the C gp increased sharply and attained peak values at 20 mo. LOOH levels for the C gp were the lowest and did not show any peak value. The maximum LOOH value of the C gp was 44.8 ± 8.4 μM

(24 mo). The Fe + Cu gp was the highest with a peak value of 133.3 ± 33.2 μM. LOOH levels for the various groups were between the C and Fe + Cu gps with peak values as follows: Fe gp = 102.2 ± 34.3 μM, Fe + V gp = 95.2 ± 40.7 μM, Fe – V gp = 78.2 ± 17.9 μM, Fe + ASA gp = 113.9 ± 36.0 μM. Differences between the various groups compared to the C gp were statistically significant (p=0.05).

9.0.13 8OHdG

Figure 30 shows liver 8OHdG levels of iron- overloaded Wistar rats. The curves for all groups had a winding pattern with low values at 8 mo. 8OHdG level of the C gp was the lowest with a first peak at 4 mo. A second peak was seen at 12 mo with liver 8OHdG concentration of 170 ± 64.8 ng/g liver wt. The curve of the C gp was fairly flat after 16 mo. The curve of the Fe gp (immediately above that of the C gp) increased from 8 mo and attained a maximum value of 370 ± 32 ng/g liver wt at 24 mo. 8OHdG level for the Fe + V gp was high after 8 mo and had a peak value of 346 ± 117 ng/g wt at 20 mo. Curves for the Fe –V and Fe + ASA gps, clustered. However, the former showed a peak 8OHdG value at 16 mo (504 ± 25 ng/g wt) and the latter, at 20 mo (523 ± 208 ng/g wt). Both curves showed a sharp decline thereafter. 8OHdG levels of the Fe + Cu gp showed an early peak at 4 mo (8OHdG = 376 ± 70 ng/g wt). This declined sharply at 8 mo and increased again to a second peak value of 562 ± 180 ng/g wt at 20 mo and gradually declined until 24 mo. 8OHdG levels of most time-points between 12 and 20 mo were statistically significant (p=0.05).

9.0.14 AMES mutagenicity test

Figure 31 shows Ames mutagenesis test, using fractionated Wistar rat liver homogenate on *Salmonella typhimurium* strain TA 102. The level for the C gp was fairly straight with a maximum value of 365 revertant colonies. The curve for the Fe + Cu gp showed a steady increase from 2 mo to a peak value of 588 revertant colonies at 20 mo. The rest of the curves for the various groups clustered until 16mo, and showed peak values at 20 mo. Peak values were as follows: Fe = 662 - , Fe + V = 665 - , Fe – V = 643 – and Fe + ASA= 582 revertant colonies. Significant differences occurred between 16 and 24 mo (p=0.05).

9.0.15 AST

Figure 32 shows serum AST levels of Fe-overloaded Wister rats. AST levels of the C gp remained the lowest with values in the region of 100 IU. AST levels for the other groups showed a gradual increase after 12 mo. The curve for the Fe + V gp was next to that of the C gp with a maximum value of 117 $\pm$ 22 IU (20 mo). The Fe + Cu gp remained the highest with a maximum value of 537 $\pm$ 138 (20 mo). Curves for the Fe + ASA, Fe – V and Fe gps had maximum serum AST values of 364 $\pm$ 96 IU, 329 $\pm$ 49 IU, 310 $\pm$ 61 IU, respectively, and clustered in-between the curves of the Fe + Cu and Fe + V groups. Significant differences (p=0.05) occurred between 12 and 20 mo. The spotted data (Table 8y, Appendix F) show some AST (and ALT) values above 4000 IU.

9.0.16 ALT

Figure 33 shows serum ALT levels of Fe- overloaded Wistar rats. The curve for the C gp was fairly straight and the lowest with a maximum ALT value of 65 IU. ALT levels of the

other groups increased slightly until 12 mo, and thereafter increased sharply. ALT levels for the Fe + Cu and Fe + ASA gps continued to increase, whilst that of the rest of the groups showed a decline after 16 mo. The curve for the Fe + V gp, lying next and above to the C gp had a maximum ALT value of 163 ± 21 IU at 16 mo. ALT levels of the Fe + Cu gp were above that of the Fe + V gp. In addition, serum ALT value of the former was 250 ± 73 IU at 20 mo. ALT levels of the Fe gp declined sharply from a peak of 234 ± 114 IU (16 mo) to 140 ± 23 IU (20 mo). ALT level of the Fe + ASA gp increased to 235 ± 87 IU at 20 mo. From 8 to about 18 mo, ALT level of the Fe – V gp was the highest with a maximum value of 252 ± 45 IU at 16 mo and then declined to 202 ± 51 IU at 20 mo. Significant differences occurred after 12 mo ($p=0.05$).

9.0.17 Cu

Figure 34 shows serum Cu levels of iron-overloaded Wistar rats. All curves showed an initial increase in serum Cu from 2-4 mo, followed by a decline between 4 and 8 mo, and then another increase up to 16 mo. Thereafter, serum Cu values of all groups apart from the Fe + ASA gp remained relatively constant. The serum Cu level of the Fe + ASA gp continued to increase to 46.6 ± 7.3 μmol/l (24 mo). The curve for the C gp was initially in the middle of the other curves and attained a peak value of 30.4 ± 3.4 μmol/l (12 mo). However, the curve remained constant and the lowest after 16 mo (25.0 ± 11.2 μmol/l). The curve for the Fe – V gp was the lowest up to 16 mo (36.1 ± 4.0 μmol/l) and then showed increased values above the C gp. Peak Cu values of the other groups were as follows: Fe gp = 34.9 ± 4.6 μmol/l (16 mo), Fe – V gp = 33.9 ± 4.0 μmol/l (16 mo),

Fe + Cu gp = 34.1 ± 13.9 μmol/l (16 mo). Significant differences (p=0.05) occurred between 8 and 16 mo.

9.0.18 8OHdG Immunohistochemistry

Figures 35-39 on pages 229-233 are slides of 8OHdG immunohistochemistry. There was hardly any brown visible immuno-staining in the control livers [Figure 35 (*a*) & (*b*) to Figure 39 (*a*) & (*b*)]. Lots of brown stains indicating positive labelling of 8OHdG, were observed throughout the livers of the Fe + V gp. Intense labelling was observed in several aggregates found in these sections, and there was also granular labelling within the cells. Similar intense labelling in aggregates was observed in the livers of the Fe – V and Fe + Cu gps. This granular labelling was also observed within cells in the liver sections of the Fe + ASA gp. Immuno-staining was concentrated in the nuclei, appearing as dark brown spots in the liver sections of the Fe + ASA gp.

9.0.19 4-HNE Immunohistochemistry

In the liver sections of the control [Figure 40 (*a*) & (*b*) to Figure 44 (*a*) & (*b*), pages 234-238] there was hardly any brown labelling observed after exposure to the anti-HNE antibodies. Intense brown cytoplasmic granular immuno-staining was observed in the hepatocytes of the Fe + ASA, Fe and the Fe + Cu gps. Similar but less intense immuno-staining in the liver sections of the Fe – V gp was seen. Intense brown immuno-staining of 4-HNE aggregates was also seen in the liver sections of the Fe + V gp especially around the vessels.

9.0.20 Liver Iron Content (LIC) (see appendix F, spotted data)

LIC at 32 months was: C gp = 0.6 ± 0.2, F gp = 16.4 ± 5.6, Fe + V gp = 21.9 ± 6.9, Fe – V gp = 21.6 ± 8.4, Fe + ASA gp = 18.7 ± 7.5, Fe + Cu gp = 17.2 ± 6.8 (units = mg/g w.wt).

9.0.21 Liver Histology

Data presented in Table 46x (see appendix E) show a gradual hepatic Fe overload over 32 months. At 4 months, all Fe-loading groups had grade 1+ Fe overload. At 8, 12 and 16 months, this progressed into 2+, 2+ and 4+ respectively, and remained at 4+ until the end of the study (Figure 45, page 239). The control group had grade 0 Fe load throughout, except at 24-28 months when traces and 2+ of iron were seen in a few. Kupffer cell Fe on the other hand was 2+ at 16 months when hepatic Fe was 4+. Fe load in the Kupffer cells increased to 3+ at 20 months and most of them stained 4+ at 24 months. At 28 and 32 months, all Kupffer cells were 4+. The portal tract was also loaded with Fe but not the bile ductular cells. Early signs of iron-free foci (IFF) were seen after 20 months (Figure 46, page 240). Of the 25 (iron-overloaded) samples presented for histological examination at 20 months, 5 (20%) had IFF and 1 was indeterminate (borderline case). Two of the 5 occurred in the Fe group, 2 in the Fe – V group, and 1 in the Fe + V group. The borderline case IFF belonged to the Fe + V group. At 24 months, 4 out of 34 (12%) Fe-overloaded livers had IFF, with 2 from the Fe group being very prominent. The remaining 2 belonged to the Fe – V and Fe + V groups. Of the 54 iron-loaded samples presented for histological examination at 28 months, 16 had IFF (30%). Twelve out of 26 iron-overloaded samples (46%) submitted to histological examination at 32 months had IFF and 2 were borderline cases. Two livers with IFF were found in the Fe group, 5 in the Fe + V group, 5 in the

Fe + ASA group and the 2 borderline cases belonged to the Fe group. Out of the 144 Fe-overloaded samples examined between 20 and 32 months, 37 (26%) had IFF. The breakdown is as follows: F group = 10, Fe + V group = 12, Fe – V group = 6, Fe + ASA group = 8 and Fe + Cu group = 1. Inclusions resembling Mallory bodies (MB)(Figure 49, page 242) were first identified at 20 months in association with IFF in the Fe group and again at 28 months in association with IFF, fat and stem cells in the Fe + V group. Fat and fatty foci were also identified and mostly associated with IFF. Microsteatosis was present at 28 months in 4 samples. Of the 4 cases, 2 were found in the Fe + V group and 1 in the Fe group. However, this was not peculiar to the Fe-loaded groups as 1 case was seen in the control group. Hamartoma was found in one of the 12 Fe group livers taken at 28 months. Within the same sample size of 12, one liver had microsteatosis, and another, Gandy-Gamma bodies. An inconclusive adenoma was seen in one sample belonging to the Fe group at 32 months. Von Meyenburg complexes (VMCs) were also identified. Large liver cell dysplasia was also observed at 28 months in the Fe group (Figure 49, page 242). Hepatocellular adenoma (HCA) was seen in one sample from the Fe group at 28 months. HCC was a borderline case in one of the 6 samples from the Fe + V group at 32 months. However, HCC developed in one out of the 8 rats that survived up to 32 months in the Fe group. The HCC was 2 cm in diameter (Figures 51-54, pages 244-246). Of the remaining 7 rat livers, 3 with IFF were confirmed malignant by GST-π stain (Figure 48, page 241). In addition, fibrosis and cirrhosis were not present (Figure 52, page 245).

9.0.22 AFP and Comet assays

AFP values remained within the normal reference range with time-increasing trend

(see Table 8y, appendix F). The comet assay did not give satisfactory results.

9.1 CORRELATION ANALYSIS (Appendix A)

Letters used for the correlation analysis represents the ff groups: C=C group, F = Fe group, V = Fe + V group, N = Fe – V group, A = Fe + ASA group, Cu = Fe + Cu group.

9.2 CORRELATION ANALYSIS OF TEST PARAMETERS WITHIN GROUPS

9.2.1 Control Group (C gp)

9.2.1.1 ALT

The correlation analysis in the Table 20x shows that for group C, ALT and AST (r=0.53, p=0.0032), ALT and TAS (r=0.57, p=0012), ALT and LPO (r=0.64, p=0.0002), ALT and FADU (r=0.52, p=0.0041), ALT and Vit C (r=0.53, p=0.0029), ALT and 8-IP (r=0.49, p=0.0142) are significantly positively correlated.

9.2.1.2 AST

The correlation matrix in Table 20x shows that for group C, AST and TAS (r=0.56, p=0.0016), AST and LPO (r=0.59, p=0.0007), AST and ORAC-L (r=0.46, p=0.0225 are significantly positively correlated.

9.2.1.3 $^{\bullet}O_2$

The correlation analysis in Table 20x shows that for group C, $^{\bullet-}O_2$ and TAS (r= -0.44, p=0.0496), $^{\bullet-}O_2$ and FADU (r= - 0.45, p=0.0445) are significantly negatively correlated.

9.2.1.4 GPx

The correlation matrix in Table 20x shows that for the C group, GPx and LPO (r=0.45, p=0.0069) are significantly positively correlated. However, GPx and CAT (r= -0.45, p= 0.0082) are significantly negatively correlated.

9.2.1.5 TAS

The correlation matrix in Table 20x shows that for group C, TAS and LPO (r=0.67, p<0.0001), TAS and FADU (r=0.60, p=0.0002), TAS and Vit C (r=0.76, p<0.0001), TAS and MDA (r=0.73, p<0.0001), TAS and ORAC-L (r=0.77, p<0.0001), TAS and 8-IP (r=0.38, p=0.0405), TAS and Cu (r=0.50,p=0.0028) are significantly positively correlated.

9.2.1.6 CAT

The correlation matrix in Table 20x shows that for group C, CAT and ORAC-A (r=0.55, p=0.0018) are significantly positively correlated. However, CAT and LPO (r= -0.34, p=0.0490), are significantly negatively correlated.

9.2.1.7 LPO

The correlation matrix in Table 20x shows that for group C, LPO and FADU (r=0.50, p=0.0024), LPO and Vit C (r=0.65, p<0.0001), LPO and MDA (r=0.68, p<0.0001), LPO and 8_IP (r=0.59, p=0.0007), LPO and ORAC-L (r=0.55, p=0.0019), are significantly positively correlated. However, LPO and ORAC-A (r= -0.59, p=0.0008) are significantly negatively correlated.

9.2.1.8 8OHdG

The correlation matrix in table 10x shows that for group C, 8OHdG and Vit C (r=0.39, p=0.0211), 8OHdG and Cu (r=0.48, p=0.0038) are significantly positively correlated.

9.2.1.9 FADU

The correlation matrix in Table 10x shows that for group C, FADU and Vit C (r=0.54, p=0.0009), FADU and MDA (r=0.69, p<0.0001), FADU and ORAC-L (r=0.64, p=0.0002), FADU and 8-IP (r=0.65, p=0.0001), FADU and Cu (r=0.47, p=0.0051) are positively correlated. However, FADU and ORAC-A (r= -0.39, p=0.0381) are negatively correlated.

9.2.1.10 Vit C

The correlation matrix in Table 10x shows that for group C, Vit C and MDA (r=0.70, p<0.0001), Vit C and ORAC-L (r=0.52, p=0041), Vit C and 8-IP (r=0.56, p=0.0015), Vit C and Cu (r=0.37, p=0.0300) are significantly positively correlated.

9.2.1.11 MDA

The correlation matrix in Table 10x shows that for group C, MDA and ORAC-L (r=0.62, p=0.0012), MDA and 8-IP (r=0.66, p=0.0005) were significantly positively correlated.

9.2.1.12 ORAC-L

The correlation matrix in Table 10x also shows that for group C, ORAC-L and 8-IP (r=0.38, p=0.0412) are significantly positively correlated. However, ORAC-L and ORAC-A (r= -0.39, p=0.0391) are significantly negatively correlated.

9.2.1.13 ORAC-A

The correlation matrix in table 10x shows that for group C, ORAC-A and ORAC-L (r= -0.39, p=0.0391) are significantly negatively correlated.

9.2.2 F Group (Fe gp)

9.2.2.1 Fe

The correlation matrix in Table 22x shows that for group F, serum iron (Fe) and ALT (r=0.56, p=0.0014), Fe and AST (r=0.76, p<0.0001), Fe and GPx (r=0.44, p=0.0099), Fe and SOD (r=0.40, p=0.0178), Fe and LPO (r=0.78, p<0.0001), Fe and 8OHdG (r=0.62, p<0.0001), Fe and FADU (r=0.61, p=0.0001), Fe and Vit C (r=0.69, p<0.0001), Fe and MDA (r=0.62, p=0.0005), Fe and AMES test (r=0.55, p=0.0023), Fe and ORAC-L (r=0.72, p<0.0001), Fe and 8-IP (r=0.47, p=0101), Fe and Cu (r=0.69, p<0.0001) are significantly positively correlated.

9.2.2.2 ALT

The correlation matrix in Table 22x shows that for group F, ALT and AST (r=0.75, p<0.0001), ALT and GPx (r=0.44, p=0.0158), ALT and SOD (r=0.58, p=0.0009), ALT and TAS (r=0.36, p=0.0480), ALT and LPO (r=0.63, p=0.0002), ALT and FADU (r=0.52, p=0.0030), ALT and Vit C (r=0.57, p=0.0009), ALT and MDA (r=0.85, p<0.0001), ALT and ORAC-L (r=0.61, p=0.0012), ALT and Cu (r=0.53, p=0.0024) are significantly positively correlated.

9.2.2.3 AST

The correlation matrix in table 22x shows that for group F, AST and GPx (r=0.46, p=0.0113), AST and SOD (r=0.51, p=0.0042), AST and TAS (r=0.41, p=0.0229), AST and LPO (r=0.71, p<0.0001), AST and 8OHdG (r=0.41, p=0.0252), AST and FADU (r=0.70, p<0.0001), AST and Vit C (r=0.62, p=0.0003), AST and MDA (r=0.86, p<0.0001), AST and AMES test (r=0.49, p=0.0147), AST and ORAC-L (r=0.83, p<0.001), AST and CU (r=0.52, p=0.0032) are significantly positively correlated.

9.2.2.4 $^{\bullet}O_2$

The correlation matrix in table 22x shows that for group F, $^{\bullet-}O_2$ and ORAC-A (r=0.49, p=0.0277) are significantly positively correlated. However, $^{\bullet-}O_2$ GPx (r= -0.45, p=0.0488), $^{\bullet-}O_2$ and LPO (r= - 0.45, p=0.0466) are significantly negatively correlated.

9.2.2.5 GPx

The correlation matrix in the Table 22x shows that for group F, GPx and LPO (r=0,49, p=0.0030), GPx and 8OHdG (r=0.47, p=0.0046), GPx and FADU (r=0.44, p=0.0091), GPx and AMES test (r=0.39, p=0.0429), GPx and ORAC-L (r=0.49, p=0.0068), GPx and Cu (r= 0.57, p=0.0005) are significantly positively correlated. However, GPx and ORAC-A (r= -0.42, p=0.0242) are significantly negatively correlated.

9.2.2.6 SOD

The correlation matrix in table 22x shows that for group F, SOD and ORAC-L (r=0.57, p=0.0013), SOD and Cu (r=0.44, p=0.0093) are significantly positively correlated.

9.2.2.7 TAS

The correlation matrix in Table 22x shows that for group F, TAS and FADU (r=0.46, p=0.0058), TAS and Vit C (r=0.43, p=0.0115), TAS and ORAC-A (r=0.38, p=0.0402), TAS and Cu (r=0.35, p=0.0411) are significantly positively correlated.

9.2.2.8 CAT

The correlation matrix in Table 22x shows that for group F, CAT and ORAC-A (r=0.48, p=0.0078), are significantly positively correlated. However, CAT and LPO (r= -0.46, p=0.0059), CAT and FADU (r= -0.40, p=0.0178), CAT and ORAC-L (r= -0.51, p=0.0048), CAT and Cu (r= -0.49, p=0.0030) are significantly negatively correlated.

9.2.2.9 LPO

The correlation matrix in table 22x shows that for group F, LPO and 8OHdG (r=0.55, p=0.0008), LPO and FADU (r=0.57, p=0.0004), LPO and Vit C (r=0.71, p<0.0001, LPO and MDA (r=0.55, p=0.0024), LPO and AMES test (r=0.47, p=0.0120), LPO and ORAC-L (r=0.79, p<0.0001), LPO and 8-IP (r=0.50, p=0.0062), LPO and Cu (r=0.63, p<0.0001) are significantly positively correlated. However, LPO and ORAC-A (r= -0.50, p=0.0053) are significantly negatively correlated.

9.2.2.10 8OHdG

The correlation matrix in Table 22x shows that for group F, FADU and Vit C (r=0.71, p<0.0001), FADU and MDA (r=0.62, p=0.0005), FADU and AMES test (r=0.64, p=0.0002), FADU and ORAC-L (r=0.75, p<0.0001), FADU and Cu (r=0.64, p<0.0001) are

significantly positively correlated. However, FADU and ORAC-A (r= -0.40, p=0.0326) are significantly negatively correlated.

9.2.2.11 Vit C

The correlation matrix in Table 22x shows that for group F, Vit C and MDA (r=0.64, p=0.0002), Vit C and AMES test (r=0.44, p=0.0191), Vit C and ORAC-L (r=0.60, p=0.0006), Vit C and Cu (r=0.67, p<0.0001), are significantly positively correlated.

9.2.2.12 MDA

The correlation matix in Table 22x shows that for group F, MDA and AMES test (r=0.67, p=0.0004), MDA and ORAC-L r=0.44, p0.0316), MDA and 8-IP (r=0.64, p=0.0008), MDA and Cu (r=0.54, p=0.0030) are significantly positively correlated. However, MDA and ORAC-A (r= -0.41, p=0.0444) are significantly negatively correlated.

9.2.2.13 AMES

The correlation matrix in Table 22x shows that for group F, AMES test and ORAC-L (r=0.63, p=0.0004), AMES test and Cu (r=0.40, p=0.0326) are significantly positively correlated. However, AMES test and ORAC-A (r= -0.51, p=0.0057) are significantly negatively correlated.

9.2.2.14 ORAC-L

The correlation matrix in Table 22x shows that for group F, ORAC-L and Cu (r=0.60, p=0.0007) are significantly positively correlated.

9.2.2.15 ORAC-A

The correlation matrix in table 22x shows that for group F, ORAC-A and 8-IP (r= -0.39, p=0.0348) are significantly negatively correlated.

9.2.3 V group (Fe + V gp)

9.2.3.1 Fe

The correlation matrix in table 24x shows that for group V, Fe and ALT (r=0.61, p=0.0008), Fe and AST (r=0.61, p=0.0011), Fe and GPx (r=0.43, p=0.0191), Fe and TAS (r=0.48, p=0.0067), Fe and LPO (r=0.66, p<0.0001), Fe and 8OHdG (r=0.72, p<0.0001), Fe and FADU (r=0.66, p<0.0001), Fe and Vit C (r=0.60, p=0.0005), Fe and MDA (r=0.64, p=0.0005), Fe and AMES test (r=0.44, p=0.0207), Fe and ORAC-L (r=0.56, p=0020), Fe and Cu (r=0.57, p=0.0011) are significantly positively correlated.

9.2.3.2 ALT

The correlation matrix in Table 24x shows that for group V, ALT and AST (r=0.61, p=0.0008), ALT and GPx (r=0.69, p<0.0001), ALT and TAS (r=0.52, p=0.0053), ALT and LPO (r=0.82, p<0.0001), ALT and 8OHdG (r=0.67, p=0.0001), ALT and FADU (r=0.48, p=0.0105), ALT and Vit C (r=0.72, p<0.0001), ALT and MDA (r=0.85, p<0.0001), ALT and ORAC-L (r=0.70, p<0.0001), ALT and 8-IP (r=0.59, p=0.0019), ALT and Cu (r=0.61, p=0.0007) are significantly positively correlated.

9.2.3.3 AST

The correlation matrix in Table 24x shows that for group V, AST and GPx (r5=0.61,

p=0.0010), AST and TAS (r=0.75, p<0.0001), AST and LPO (r=0.58, p=0.0017), AST and 8OHdG (r=0.56, p=0.0023), AST and FADU (r=0.71, p<0.0001), AST and Vit C (r=0.64, p=0.0003), AST and MDA (r=0.71, p<0.0001), AST and ORAC-L (r=0.77, p<0.0001), AST and 8-IP (r=0.52, p=0.0078), AST and Cu (r=0.43, p=0.0271) are significantly positively correlated.

9.2.3.4 GPx

The correlation matrix in Table 24x shows that for group V, GPx and TAS (r=0.57, p=0.0011), GPx and LPO (r=0.65, p<0.0001), GPx and 8OHdG (r=0.48, p=0.0066), GPx and Vit C (r=0.38, p=0.0410), GPx and ORAC-L (r=0.64, p=0.0003), GPx and 8-IP (r=0.44, p=0.0184), GPx and Cu (r=0.47, p=0.0088) are significantly positively correlated. However, GPx and CAT (r= -0.52, p=0.0034) are significantly negatively correlated.

9.2.3.5 SOD

The correlation matrix in Table 24x shows that for group V, SOD and ORAC-A (r=0.42, p=0.0238), SOD and 8-IP (r=0.39, p=0.0361) are significantly positively correlated.

9.2.3.6 TAS

The correlation matrix in Table 24x shows that for group V, TAS and 8OHdG (r=0.36, p=0.0468), TAS and Vit C (r=0.36, p=0.0450), TAS and ORAC-L (r=0.63, p=0.0003), TAS and 8-IP (r=0.51, p=0047) are significantly positively correlated.

9.2.3.7 CAT

The correlation matrix in Table 24x shows that for group V, CAT and LPO (r= -0.64, p=0.0001), CAT and 8OHdG (r= -0.51, p=0.0031), CAT and FADU (r= -0.39, p=0.0293), CAT and Vit C (r= -0.37, p=0.0398), CAT and ORAC-L (r= -0.52, p=0.0036), CAT and Cu (r= -0.44, p=0124) are significantly negatively correlated.

9.2.3.8 LPO

The correlation matrix in Table 24x shows that for group V, LPO and 8OHdG (r=0.79, p<0.0001), LPO and FADU (r=0.56, p=0.0011), LPO and Vit C (r=0.53, p=0.0020), LPO and MDA (r=0.71, p<0.0001), LPO and ORAC-L (r=0.72, p<0.0001), LPO and Cu (r=0.70, p<0.0001) are significantly positively correlated.

9.2.3.9 8OHdG

The correlation matrix in Table 24x shows that for group V, 8OHdG and FADU (r=0.75, p<0.0001), 8OHdG and Vit C (r=0.60, p=0.0004), 8OHdG and MDA (r=0.89, p<0.0001), 8OHdG and AMES test (r=0.70, p<0.0001), 8OHdG and ORAC-L (r=0.77, p<0.0001), 8OHdG and 8-IP (r=0.40, p=0.0322), 8OHdG and Cu (r=0.69, p<0.0001) are significantly positively correlated.

9.2.3.10 FADU

The correlation matrix in Table 24x shows that for group V, FADU and Vit C (r=0.63, p=0.0001), FADU and MDA (r=0.85, p<0.0001), FADU and AMES test (r=0.78, p<0.0001), FADU and ORAC-L (r=0.70, p<0.0001), FADU and Cu (r=0.58, p=0.0007) are

significantly positively correlated.

9.2.3.11 Vit C

The correlation matrix in Table 24x shows that for group V, Vit C and MDA (r=0.70, p<0.0001), Vit C and AMES test (r=0.57, p=0.0012), Vit C and ORAC-L (r=0.52, p=0.0035), Vit C and Cu (r=0.40, p=0.0242) are significantly positively correlated.

9.2.3.12 MDA

The correlation matrix in table 24x shows that for group V, MDA and AMES test (r=0.75, p<0.001), MDA and ORAC-L (r=0.67, p=0.0004), MDA and Cu (r=0.74, p<0.0001) are significantly positively correlated.

9.2.3.13 AMES test

The correlation matrix in Table 24x shows that group V, AMES test and ORAC-L (r=0.59, p=0.0007), AMES test and 8-IP (r=0.42, p=0.0242), AMES test and Cu (r=0.44, p=0.0171) are significantly positively correlated. However, AMES test and ORAC-A (r= -0.39, p=0.0373) are significantly but weakly, negatively correlated.

9.2.3.14 ORAC-L

The correlation matrix in table 24x shows that for group V, ORAC-L and 8-IP (r=0.55, p=0.0019), ORAC-L and Cu (r=0.61, p=0.0005) are significantly positively correlated.

9.2.4 N Group (Fe-V)

9.2.4.1 Fe

The correlation matrix in Table 23x shows that for group N, Fe and ALT (r=0.89, p<0.0001), Fe and AST (r=0.85, p<0.0001), Fe and SOD (r=0.52, p=0.0017), Fe and TAS (r=0.49, p=0031), Fe and LPO (r=0.78, p<0.0001), Fe and 8OHdG (r=0.72, p<0.0001), Fe and FADU (r=0.75, p<0.0001), Fe and Vit C (r=0.76, p<0.0001), Fe and MDA (r=0.68, p0.0001), Fe and ORAC-L (r=0.81, p<0.0001), Fe and Cu (r=0.79, p<0.0001) are significantly positively correlated.

9.2.4.2 ALT

The correlation matrix in Table 23x shows that for group N, ALT and AST (r=0.84, p<0.0001), ALT and SOD (r=0.72, p<0.0001), ALT and TAS (r=0.57, p=0.0013) ALT and LPO (r=0.87, p<0.0001), ALT and 8OHdG (r=0.80, p<0.0001), ALT and FADU (r=0.72, p<0.0001), ALT and Vit C (r=0.74, p<0.0001), ALT and MDA (r=0.96, p<0.0001), ALT and ORAC-L (r=0.81, p<0.0001), ALT and Cu (r=0.84, p<0.0001) are significantly positive correlated. However, ALT and $^{\bullet-}O_2$ (r= -0.56, p=0.0128), ALT and CAT (r= -0.40, p=0.0319) are significantly negatively correlated.

9.2.4.3 AST

The correlation matrix in Table 23x shows that for group N, AST and SOD (r=0.67, p<0.0001), AST and TAS (r=0.64, p=0.0002), AST and LPO (r=0.71, p<0.0001), AST and 8OHdG (r=0.74, p<0.0001), AST and FADU (r=0.65, p=0.0001), AST and Vit C (r=0.76, p<0.0001), AST and MDA (r=0.81, p<0.0001), AST and Cu (r=0.75, p<0.0001) are

significantly positively correlated.

9.2.4.4 $^{\bullet}O_2^-$

The correlation matrix in Table 23x shows that for group N, $^{\bullet}O_2^-$ and CAT (r=0.68, p=0.0009), $^{\bullet}O_2^-$ and ORAC-A (r=0.60, p=0.0055) are significantly positively correlated. However, $^{\bullet}O_2^-$ and LPO (r= -0.64, p=0.0024), $^{\bullet}O_2^-$ and 8OHdG (r= -0.66, p=0.0015), $^{\bullet}O_2^-$ and FADU (r= -0.47, p=0.0350), $^{\bullet}O_2^-$ and AMES test (r= -0.45, p=0.0468), $^{\bullet}O_2^-$ and ORAC-L (r= -0.56, p=0.0096), $^{\bullet}O_2^-$ and Cu (r= -0.74, p=0.0002) are significantly negatively correlated.

9.2.4.5 GPx

The correlation matrix in the table 23x shows that for group N, GPx and CAT (r= -0.36, p=0.0390), GPx and ORAC-A (r= -0.41, p=0.0279) are significantly negatively correlated.

9.2.4.6 SOD

The correlation matrix in Table 23x shows that for group N, SOD and TAS (r=0.46, p=0.0059), SOD and LPO (r=0.34, p=0.0469), SOD and Vit C (r=0.39, p=0.0208), SOD and ORAC-L (r=0.49, p=0.0065), SOD and ORAC-A (r=0.039, p=0.0385), SOD and Cu (r=0.35, p=0.0400) are significantly positively correlated.

9.2.4.7 TAS

The correlation matrix in table 23x shows that for group N, TAS and LPO (r=0.36,

p=0.0385), TAS and 8OHdG (r=0.44, p=0.0090), TAS and Vit C (r=0.57, p=0.0005), TAS and ORAC-L (r=0.54, p=0.0024), TAS and ORAC-A (r=0.48, p=0.0091), TAS and Cu (r=0.34, p=0.0490) are significantly positively correlated.

9.2.4.8 CAT

The correlation matrix in Table 23x shows that for group N, CAT and ORAC-A (r=0.45, p=0.0152), are significantly positively correlated. However, CAT and LPO (r= -0.54, p=0.0010), CAT and 8OHdG (r= -0.46, p=0.0068), CAT and FADU (r= -0.40, p=0.0176), CAT and ORAC-L (r= -0.43, p=0.0215), CAT and Cu (r= -0.55, p=0.0007) are significantly negatively correlated.

9.2.4.9 LPO

The correlation matrix in Table 23x shows that for group N, LPO and 8OHdG (r=0.78, p<0.0001), LPO and FADU (r=0.77, p<0.0001), LPO and Vit C (r=0.69, p<0.0001), LPO and MDA (r=0.59, p=0.0007), LPO and AMES (r=0.38, p=0.0448), LPO and ORAC-L (r=0.79, p<0.0001), LPO and Cu (r=0.84, p<0.0001) are significantly positively correlated.

9.2.4.10 8OHdG

The correlation matrix in Table 23x shows that for group N, 8OHdG and FADU (r=0.59, p=0.0002), 8OHdG and Vit C (r=0.57, p=0.0004), 8OHdG and MDA (r=0.51, p=0.0050), 8OHdG and AMES test (r=0.53, p=0.0029), 8OHdG and ORAC-L (r=0.76, p<0.0001), 8OHdG and Cu (r=0.72, p<0.0001) are significantly positively correlated.

9.2.4.11 FADU

The correlation matrix in Table 23x shows that for group N, FADU and Vit C (r=0.75, p<0.0001), FADU and MDA (r=0.63, p=0.0003), FADU and AMES test (r=0.52, p=0.0038, FADU and ORAC-L (r=0.78, p<0.0001), FADU and 8-IP (r=0.52, p=0.0042), FADU and Cu (r=0.76, p<0.0001) are significantly positively correlated.

9.2.4.12 Vit C

The correlation matrix in Table 23x shows that for group N, Vit C and MDA (r=0.59, p=0.0008), Vit C and AMES test (r=0.48, p=0.0085), Vit C and ORAC-L (r=0.64, p=0.0002), Vit C and 8-IP (r=0.40, p0.0303), Vit C and Cu (r=0.73, p<0.0001) are significantly positively correlated.

9.2.4.13 MDA

The correlation matrix in Table 23x shows that for the group N, MDA and AMES test (r=0.74, p<0.0001), MDA and ORAC-L (r=0.54, p=0.0062). MDA and Cu (r=0.70, p<0.0001) are significantly positively correlated.

9.2.4.14 AMES test

The correlation matrix in Table 23x shows that for group N, AMES test and ORAC-L (r=0.52, p=0.0037), AMES test and 8-IP (r=0.57, p=0.0012), AMES test and Cu (r=0.54, p=0.0025) are significantly positively correlated. However, AMES test and ORAC-A (r= -0.51, p=0.0050) are significantly negatively correlated.

9.2.4.15 ORAC-L

The correlation matrix in Table 23x shows that for group N, ORAC-L and Cu (r=0.76, p<0.0001) are significantly positively correlated.

9.2.4.16 ORAC-A

The correlation matrix in Table 23x shows that for group N, ORAC-A and 8-IP (r= -0.50, p=0.0053), ORAC-A and Cu (r= -0.51, p=0.0049) are significantly negatively correlated.

9.2.5 A Group (Fe+ASA gp)

9.2.5.1 Fe

The correlation matrix in Table 19x shows that for group A, Fe and ALT (r=0.69, p<0.0001) Fe and AST (r=0.60, p=0.0008), Fe and TAS (r=0.43, p=0.0150), Fe and LPO (r=0.71, p<0.0001), Fe and 8OHdG (r=0.63, p=0.0001), Fe and FADU (r=0.68, p<0.0001), Fe and Vit C (r=0.79, p<0.0001), Fe and MDA (r=0.64, p=0.0003), Fe and AMES test (r=0.39, p=0.0417), Fe and ORAC-L (r=0.57, p=0.0016), Fe and Cu (r=0.68, p<0.0001) are significantly positively correlated.

9.2.5.2 ALT

The correlation matrix in Table 19x shows that for group A, ALT and AST (r=0.66, p=0.0001), ALT and TAS (r=0.48, p=0084), ALT and LPO (r=0.84, p<0.0001), ALT and 8OHdG (r=0.78, p<0.0001), ALT and FADU (r=0.79, p<0.001), ALT and Vit C (r=0.74, p<0.0001), ALT and MDA (r=0.89, p<0.0001), ALT and AMES test (r=0.46, p=0.0200), ALT and ORAC-L (r=0.86, p<0.0001), ALT and 8-IP (r=0.47, p=0.0187), ALT and Cu

(r=0.63, p=0.0003) are significantly positively correlated. However, ALT and CAT (r= -0.48, p=0.0085), ALT and ORAC-A (r= -0.41, p=0.0395), are significantly negatively correlated.

9.2.5.3 AST

The correlation matrix in Table 19x shows that for group A, AST and TAS (r=0.63, p=0.0002), AST and LPO (r=0.70, p<0.0001), AST and 8OHdG (r=0.83, p<0.0001), AST and FADU (r=0.84, p<0.0001), AST and Vit C (r=0.76, p<0.0001), AST and MDA (r=0.69, p=0.0002), AST and AMES test (r=0.77, p<0.0001), AST and ORAC-L (r=0.86, p<0.0001), AST and CU (r=0.59, p=0.0007) are significantly positively correlated.

9.2.5.4 $^{\bullet}O_2$

The correlation matrix in Table 19x shows that for group A, $^{\bullet-}O_2$ and CAT (r=0.57, p=0.0089), $^{\bullet-}O_2$ and ORAC-A (r=0.65, p=0.0020), are significantly positively correlated. However, $^{\bullet-}O_2$ and LPO (r= -0.51,p=0.0214), $^{\bullet-}O_2$ and 8OHdG (r=0.52, p=0.0174), $^{\bullet-}O_2$ and FADU (r= -0.53, p=0.0159), $^{\bullet-}O_2$ and AMES test (r= -0.48, p=0.0315), $^{\bullet-}O_2$ and ORAC-L (r= -0.49, p=0.0280) are significantly negatively correlated.

9.2.5.5 GPx

The correlation matrix in Table 19x shows that for group A, GPx and TAS (r=0.41, p=0.0186), GPx and LPO (r=0.40, p=0.0216), are significantly positively correlated.

9.2.5.6 TAS

The correlation matrix in table 19x shows that for group A, TAS and LPO (r=0.42, p=0.0151), TAS and 8OHdG (r=0.39, p=0.0236), TAS and FADU (r=0.37, p=0.0356), TAS and Vit C (r=0.55, p=0.0009), TAS and ORAC-L (r=0.40, p=0312) are significantly positively correlated.

9.2.5.7 CAT

The correlation matrix in table 19x shows that for group A, CAT and ORAC-A (r=0.84, p<0.0001) are significantly positively correlated. However, CAT and LPO (r= -0.54, p=0.0013), CAT and 8OHdG (r= -0.39, p=0.0236), CAT and FADU (r= -0.45, p=0.0080), CAT and ORAC-L (r= -0.42, p=0.0245), CAT and Cu (r= -0.42, p=0.016) are significantly negatively correlated.

9.2.5.8 LPO

The correlation matrix in table 19x shows that for group A, LPO and 8OHdG (r=0.77, p<0.0001), LPO and FADU (r=0.75, p<0.0001), LPO and Vit C (r=0.69, p<0.0001), LPO and MDA (r=0.69, p<0.0001), LPO and AMES test (r=0.53, p=0.0024), LPO and ORAC-L (r=0.81, p<0.0001), LPO and 8-IP (r=0.45, p=0.0140), LPO and Cu (r=0.65, p<0.0001) are significantly positive correlated. However, LPO and ORAC-A (r= -0.59, p=0.0007) are significantly negatively correlated.

9.2.5.9 FADU

The correlation matrix in table 19x shows that for group A, FADU and Vit C (r=0.73, p<0.0001), FADU and MDA (r=0.77, p<0.0001), FADU and AMES test (r=0.83, p<0.0001), FADU and ORAC-L (r=0.75, p<0.0001), FADU and Cu (r=0.68, p<0.0001) are significantly positively correlated. However, FADU and ORAC-A (r= -0.56, p=0.0016) are significantly negatively correlated.

9.2.5.10 Vit C

The correlation matrix in table 19x shows that for group A, Vit C and MDA (p=0.67, p=0.0001), Vit C and AMES test (r=0.57, p=0.0014), Vit C and ORAC-L (r=0.59, p=0.0007, Vit C and 8-IP (0.56, p=0.0016), Vit C and Cu (r=0.64, p<0.0001) are significantly negatively correlated.

9.2.5.11 MDA

The correlation matrix in table 19x shows that for group A, MDA and AMES test (r=0.84, p<0.0001), MDA and ORAC-L (r=0.48, p=0.0180). MDA and Cu (r=0.73, p<0.0001), are significantly positively correlated. However, MDA and ORAC-A (r= -0.47, p=0.0210) are significantly negatively correlated.

9.2.5.12 AMES test

The correlation matrix in table 19x shows that for group A, AMES test and ORAC-L (r=0.64, p=0.0005), AMES test and Cu (r=0.63, p=0.0002) are significantly positively correlated. However, AMES test and ORAC-A (r= -0.47, p=0.0101) are significantly

negatively correlated.

9.2.5.13 ORAC-L

The correlation matrix in table 19x shows that for group A, ORAC-L and Cu (r=0.51, p=0.0047) are significantly positively correlated. However, ORAC-L and ORAC-A (r= -0.42, p=0.0235) are significantly negatively correlated.

9.2.5.14 ORAC-A

The correlation matrix in table 19x shows that for group A, ORAC-A and Cu (r= -0.52, p=0.0034) were significantly negatively correlated.

9.2.6 Cu Group (Fe + Cu gp)

9.2.6.1 Fe

The correlation matrix in Table 21x shows that for group Cu, Fe and ALT (r=0.57, p=0.0014), Fe and AST (r=0.48, p=0.0086), Fe and TAS (r=0.49, p=0.0037), Fe and LPO (r=0.62, p=0.0001), Fe and 8OHdG (r=0.53, p=0.0015), Fe and FADU (r=0.68, p<0.0001), Fe and Vit C (r=0.62, p=0.0001), Fe and MDA (r=0.56, p=0.0019). Fe and AMES test (r=0.63, p=0.0003), Fe and ORAC-L (r=0.66, p=0.0001), Fe and 8-IP (r=0.52, p=0.0046), Fe and Cu (r=0.47, p=0.0058) are significantly positively correlated. However, Fe and $^{\bullet-}O_2$ (r= -0.46, p=0.0490) are significantly negatively correlated.

9.2.6.2 ALT

The correlation matrix in Table 21x shows that for group Cu, ALT and AST

(r=0.84, p<0.0001), ALT and TAS (r=0.56, p=0.0012), ALT and LPO (r=0.86, p<0.0001), ALT and 8OHdG (r=0.70, p<0.0001), ALT and FADU (r=0.83, p<0.0001), ALT and Vit C (r=0.77, p<0.0001), ALT and MDA (r=0.92, p<0.0001), AST and AMES test (r=0.55, p=0.0043), ALT and ORAC-L (r=0.91, p<0.0001), ALT and 8-IP (r=0.56, p=0.0035), ALT and Cu (r=0.49, p=0.0061), are significantly positively correlated.

9.2.6.3 AST

The correlation matrix in Table 21x shows that for group Cu, AST and TAS (r=0.55, p=0.0018), AST and LPO (r=0.65, p<0.0001), AST and 8OHdG (r=0.62, p=0.0003), AST and FADU (r=0.66, p<0.0001), AST and Vit C (r=0.54, p=0.0021), AST and MDA (r=0.58, p=0.0026), AST and AMES test (r=0.56, p=0.0034), AST and ORAC-L (r=0.84, p<0.0001), AST and Cu (r=0.42, p=0.0195), are significantly positively correlated. However, AST and ORAC-A (r= -0.45, p=0240) are significantly negatively correlated.

9.2.6.4 $^{\bullet}O_2$

The correlation matrix in Table 21x shows that for group Cu, $^{\bullet-}O_2$ and GPx (r=0.63, p=0.0036) are significantly positively correlated. However, $^{\bullet-}O_2$ and TAS (r= -0.60, p=0.0049), $^{\bullet-}O_2$ and Vit C (r= -0.51, p=0.0202), $^{\bullet-}O_2$ and AMES test (r= -0.53, p=0.0152), $^{\bullet-}O_2$ and 8-IP (r= -0.49, p=0.0271) are significantly negatively correlated.

9.2.6.5 GPx

The correlation matrix in Table 21x shows that for group Cu, GPx and LPO (r=0.34, p=0.0493), GPx and 8OHdG (r=0.47, p=0053), GPx and Cu (r=0.38, p=0.0298) were

significantly positively correlated. However, GPx and SOD (r= -0.34, p=0.0499), GPx and CAT (r= -0.34, p=0.0493), GPx and ORAC-A (r= -0.48, p=0.0095) are significantly negatively correlated.

9.2.6.6 SOD

The correlation matrix in Table 21x shows that for group Cu, SOD and CAT (r=0.40, p=0.0200), SOD and ORAC-A (r=0.51, p=0.0044), SOD and 8-IP (r=0.59, p=0.0007) are significantly positively correlated.

9.2.6.7 TAS

The correlation matrix in Table 21x shows that for group Cu, TAS and LPO (r=0.53, p=0.0012), TAS and 8OHdG (r=0.42, p=0.0127), TAS and FADU (r=0.49, p=0.0032), TAS and Vit C (r=0.55, p=0.0007), TAS and AMES test (r=0.41, p=0.0257), TAS and ORAC-L (r=0.67, p<0.0001), TAS and 8-IP (r=0.38, p=0.0432), TAS and Cu (r=0.56, p=0.0006) are significantly positively correlated.

9.2.6.8 CAT

The correlation matrix in Table 19x shows that for group Cu, CAT and ORAC-A (r=0.80, p<0.0001) are significantly positively correlated. However, CAT and LPO (r= -0.35, p=0.0395), CAT and 8OHdG (r= -0.37, p=0.0295), CAT and FADU (r= -0.37, p=0.0331), CAT and MDA (r= -0.49, p=0061) are significantly negatively correlated.

9.2.6.9 LPO

The correlation matrix in Table 19x shows that for group Cu, LPO and 8OHdG (r=0.87, p<0.0001), LPO and FADU (r=0.82, p<0.0001), LPO and Vit C (r=0.75, p<0.0001), LPO and MDA (r=0.81, p<0.0001), LPO and AMES test (r=0.46, p=0.0115), LPO and ORAC-L (r=0.81, p<0.0001), LPO and 8-IP (r=0.40, p=0.0338), LPO and Cu (r=0.64, p<0.0001), are significantly positive correlated. However, LPO and ORAC-A (r= -0.57, p=0.0013) are significantly negatively correlated.

9.2.6.10 8OHdG

The correlation matrix in Table 19x shows that for group Cu, 8OHdG and FADU (r=0.70, p<0.0001), 8OHdG and Vit C (r=0.62, p<0.0001), 8OHdG and MDA (r=0.79, p<0.0001), 8OHdG and ORAC-L (r=0.68, p<0.0001), 8OHdG and Cu (r=0.64, p<0.0001) are significantly positively correlated. However, 8OHdG and ORAC-A (r= - 0.69, p<0.0001) are significantly negatively correlated.

9.2.6.11 FADU

The correlation matrix in Table 19x shows that for group Cu, FADU and Vit C (r=0.76, p<0.0001), FADU and MDA (r=0.87, p<0.0001), FADU and AMES test (r=0.69, p<0.0001), FADU and ORAC-L (r=0.73, p<0.0001), FADU and Cu (r=0.68, p<0.0001) are significantly positively correlated. However, FADU and ORAC-A (r= -0.49, p=0.0076) were significantly negatively correlated.

9.2.6.12 Vit C

The correlation matrix in Table 19x shows that for group Cu, Vit C and MDA (r=0.81, p<0.0001), Vit C and AMES test (r=0.58, p=0.0010), Vit C and ORAC-L (r=0.58, p=0.0011), Vit C and 8-IP (r=0.45, p=0.0137), Vit C and Cu (r=0.53, p=0.0014), are significantly positively correlated.

9.2.6.13 MDA

The correlation matrix in Table 19x shows that for group Cu, MDA and AMES test (r=0.54, p=0.0059), MDA and ORAC-L (r=0.54, p=0.0059), MDA and Cu (r=0.54, p=0.0023), are significantly positively correlated. However, MDA and ORAC-A (r= -0.62, p=0.0014) are significantly negatively correlated.

9.2.6.14 AMES test

The correlation matrix in Table 19x shows that for group Cu, AMES test and ORAC-L (r=0.58, p=0.0009), AMES test and 8-IP (r=0.40, p=0.325), AMES test and Cu (r=0.39, p=0.0368) are significantly positively correlated.

9.2.6.15 ORAC-L

The correlation matrix in Table 19x shows that for group Cu, ORAC-L and 8-IP (r=0.52, p=0.0042), ORAC-L and Cu (r=0.59, p=0.0007) are significantly positively correlated.

9.2.6.16 ORAC-A

The correlation matrix in Table 19x shows that for group Cu, ORAC-A and Cu (r= - 0.41, p=0.0272) are significantly negatively correlated.

9.3 ANALYSIS OF VARIANCE (ANOVA)

9.3.1 Group and Time effect on Iron

Table 25x shows that both time and treatment and their interaction had significant effects on serum iron ($p<0.0001$, $p<0.0001$, respectively). The multiple comparison test results in Table 26x show that:

i) Significant differences ($p<0.0001$) are as a result of experiments carried out for 12 months and less and those that lasted 16 months and above.

ii) With regard to treatment differences, it is noticed in Table 26x that significant differences ($p<0.0001$) occurred between the control group and all other groups. Groups other than the control group had significantly higher mean values than the control group.

9.3.2 Group and Time effect on ALT

Table 25x shows that both time and treatment and their interaction had significant effects on ALT ($p<0.0001$, $p<0.0001$, respectively). The multiple comparison test results in Table 27x show that:

i) Significant differences ($p<0.0001$) are as a result of experiments carried out for 4-16 months. This time frame showed maximum differences between the means of the various groups.

ii) With regard to treatment differences, it is noticed in Table 27x that significant differences ($p<0.0001$) occurred between the control group and all other groups. Groups other than the control group had significantly higher mean values than the control group.

9.3.3 Group and Time effect on AST

Table 25x shows that both time and treatment and their interaction had significant effects on AST ($p<0.0001$, $p<0.0001$, respectively). The multiple comparison test results in Table 28x show that:

i) Significant differences ($p<0.0001$) are as a result of experiments carried out from 2-20 months.

ii) With regard to treatment differences, it is noticed in Table 28x that significant differences ($p<0.0001$) occurred between the control group and all other groups. Groups other than the control group had significantly higher mean values than the control group. In addition, significant differences ($p<0.0001$) occurred between Cu & V and Cu & F.

9.3.4 Group and Time effect on $^{\bullet}O_2$

Table 25x shows that time had significant effects on blood $^{\bullet-}O_2$ ($p<0.0001$). There was no significant difference as a result of the diverse treatment to the various groups ($p=0.4203$). However, it was noticed that a combination of time and treatment type had significant differences between the groups ($p<0.0001$). The multiple comparison test results in Table 29x show that:

i) Significant differences ($p<0.0001$) are as a result of experiments carried out for 12 and 20 months. This time frame had the highest difference between means.

9.3.5 Group and Time effect on GPx

Table 25x shows that both time and treatment and their interaction had significant effects on GPx ($p<0.0001$, $p<0.0001$, respectively). The multiple comparison test results in Table 30x show that:

i) Significant differences ($p<0.0001$) are as a result of experiments carried out for 4-12 and 12-20 months.

ii) With regard to treatment differences, it is noticed in Table 30x that significant differences ($p<0.0001$) occurred between groups C & F, and C & N. V & N, Cu & N, and A & N also showed significant differences at $p=0.05$ level. Groups other than the control group had significantly higher mean values than the control group.

9.3.6 Group and Time effect on SOD

Table 25x shows that both time and treatment had significant effects on SOD ($p<0.0001$, $p<0.0001$, respectively). However, the interaction of both did not have any significant effect ($p=0.4125$). The multiple comparison test results in Table 31x show that:

i) Significant difference between means ($p<0.0001$) is maximum between12 and 24 months.

ii) With regard to treatment differences, it is noticed in Table 31x that significant differences ($p<0.0001$) occurred between the control group and all other groups.

In addition, significant differences occurred between Cu & N and V & N ($p<0.05$). Groups other than the control group had significantly higher mean values than the control group.

9.3.7 Group and Time effect on TAS

Table 25x shows that both time and treatment and their interaction had significant effects on TAS ($p<0.0001$, $p<0.0001$, respectively). The multiple comparison test results in Table 32x show that:

i) Significant differences ($p<0.0001$) are as a result of experiments carried out for 24 months at almost all time points.

ii) With regard to treatment differences, it is noticed in Table 32x that significant differences ($p<0.0001$) occurred between the control group and all other groups except the V group. In addition, V & N & V & Cu groups, were significantly different. Groups other than the control group had significantly higher mean values than the control group.

9.3.8 Group and Time effect on CAT

Table 25x shows that both time and treatment had significant effects on CAT ($p<0.0001$, $p<0.0001$, respectively) and the interaction of the two was also significant ($p=0.0228$). The multiple comparison test results in Table 33x show that:

i) Significant differences ($p<0.05$) are as a result of experiments carried out for 8 months and above.

ii) With regard to treatment differences, it is noticed in Table 33x that significant differences ($p<0.05$) occurred between the control group and all other groups. In addition, V & F, V & N, V & A, V & Cu and F & Cu groups were significantly different at the $p=0.05$ level. Groups other than the control group had significantly higher mean values than the control group.

9.3.9 Group and Time effect on Vitamin C

Table 25x shows that both time and treatment had significant effects on Vitamin C ($p<0.0001$, $p<0.0167$, respectively). However, their interaction showed no significant effect ($p=0.9598$). The multiple comparison test results in Table 34x show that:

i) Significant differences ($p<0.05$) are observed at all time-points except 16-20 months, 8-12 months and 2-4 months.

ii) With regard to treatment differences, it is noticed in Table 34x that significant differences ($p<0.05$) occurred between V & F, V & N and V & Cu groups. Groups other than the control group had significantly higher mean values than the control group.

9.3.10 Group and Time effect on LPO

Table 25x shows that both time and treatment and their interaction had significant effects on LPO ($p<0.0001$, $p<0.0001$, respectively). The multiple comparison test results in Table 36x show that:

i) Significant differences ($p<0.05$) are as a result of experiments carried out after 12 months and less and those that lasted 20months.

ii) With regard to treatment differences, it is noticed in Table 36x that significant differences ($p<0.05$) occurred between the control group and all other groups. In addition, significant differences ($p=0.05$) occurred between V & N, A & N, Cu & F, Cu & N and Cu & V groups. Groups other than the control group had significantly higher mean values than the control group.

9.3.11 Group and Time effect on Cu

Table 25x shows that both time and treatment had significant effects serum Cu ($p<0.0001$, $p<0.0001$, respectively). In addition, the interaction of both parameters was also significant ($p=0.0002$). The multiple comparison test results in Table 35x show that:

i) Significant differences ($p<0.05$) are as a result of experiments carried out for 24 months and can be seen for most time-points.

ii) With regard to treatment differences, it is noticed in Table 35x that significant differences ($p<0.05$) occurred between C & N, V & N, F & N, A & N and Cu & N groups. Groups other than the control group had significantly higher mean values than the control group.

9.3.12 Group and Time effect on FADU

Table 25x shows that both time and treatment had significant effects on FADU ($p<0.0001$, $p<0.0001$, respectively). In addition, the interactive effect of both parameters was also significant ($p=0.0033$). The multiple comparison test results in Table 37x show that:

i) Significant differences ($p<0.05$) are as a result of experiments carried out for 24 months can be seen for most time-points after 12 months.

ii) With regard to treatment differences, it is noticed in Table 37x that significant differences ($p<0.05$) occurred between C & F, C & N, C & A, and C & Cu groups. There was no significant difference between C & V groups. However, there was significant difference between V & Cu ($p=0.05$).

9.3.13 Group and Time effect on MDA

Table 25x shows that both time and treatment had significant effects on MDA ($p<0.0001$, $p<0.0001$ respectively) and the interaction of both parameters was also significant ($p<0.0001$). The multiple comparison test results in 38x show that:

i) Significant differences ($p<0.05$) are as a result of experiments carried out for 24 months can only be seen after 12 months.

ii) It is noticed in Table 38x that significant differences ($p<0.05$) occurred between C & F, C & A and C & Cu groups but not C & V and C & N groups.

9.3.14 Group and Time effect on AMES test

Table 25x shows that both time and treatment had significant effects on mutagenicity as determined by the AMES test ($p<0.0001$, $p<0.0001$, respectively) In addition the interaction of both parameters was also significant ($p<0.0001$). The multiple comparison test results in Table 39x show that:

i) Significant differences ($p<0.05$) are as a result of experiments carried out for longer periods i.e. 4-20 months or 4-24months. Shorter periods before 16

months did no have any significant effect.

ii) With regard to treatment differences, it is noticed in Table 39x that significant differences ($p<0.05$) occurred between the control group and all other groups.

9.3.15 Group and Time effect on 8OHdG

Table 25x shows that both time and treatment had significant effects 8OHdG ($p<0.0001$, $p<0.0001$, respectively) and the interaction of both parameters was also significant ($p<0.0001$). The multiple comparison test results in Table 40x show that:

i) Significant differences ($p<0.05$) are as a result of experiments carried out for 24 months. These differences were significant at most time-points.

ii) With regard to treatment differences it is noticed in 40x that significant differences ($p<0.05$) occurred between the control group and all other groups. In addition, Cu & F, Cu & N, Cu & A, Cu & V, N & F, N & V as well as A & V groups, were significantly different at $p=0.05$ level. Groups other than the control group had significantly higher mean values than the control group.

9.3.16 Group and Time effect on ORAC-L

Table 25x shows that both time and treatment had significant effects on ORAC-L ($p<0.0001$, $p<0.0001$, respectively). In addition, the interaction of both parameters was also significant ($p<0.0001$). The multiple comparison test results in Table 41x show that:

i) Significant differences ($p<0.05$) are as a result of experiments carried out for 24 months. These differences were significant at most time-points.

ii) With regard to treatment differences, it is noticed in Table 41x that significant differences ($p<0.05$) occurred between the control group and all other groups. In addition, groups A & N were significantly different ($p<0.05$).

9.3.17 Group and Time effect on ORAC-A

Table 25x shows that both time and treatment had significant effects on ORAC-A ($p<0.0001$, $p<0.0001$, respectively). In addition, the interaction of both parameters was also significant ($p<0.0001$). The multiple comparison test results in Table 42x show that:

i) Significant differences ($p<0.05$) are as a result of experiments carried out for 24 months. These differences were significant at most time-points.

ii) It is noticed in Table 42x that significant differences ($p<0.05$) occurred between the control group and all other groups except V. In addition, V & A, V & F, V & N and V & Cu were significantly different ($p<0.05$).

9.3.18 Group and Time effect on 8-IP

Table 25x shows that both time and treatment had significant effects on 8-IP ($p<0.0001$, $p<0.0001$, respectively). In addition, the interaction of both parameters was also significant ($p<0.0001$). The multiple comparison test results in Table 43x show that:

i) Significant differences ($p<0.05$) are as a result of experiments carried out for 24 months. These differences were significant for intervals after 4 months.

ii) It is noticed in Table 43x that significant differences ($p<0.05$) occurred between the control group and all other groups. In addition, Cu & A, Cu & F, Cu & N and Cu & V groups were significantly different ($p<0.05$).

9.4 REGRESSION ANALYSIS

A summary of the regression analysis is shown in the Table 44x. For the Fe group, Fe and $^{\bullet-}O_2$ significantly affected lipid and DNA destruction. Subsequently, MDA, 8-IP and 8OHdG adducts that were formed significantly contributed to liver damage. For the Fe + V group, $^{\bullet-}O_2$ and Cu significantly influence LPO. Lipid-soluble antioxidants and MDA influenced the formation of DNA adducts. In addition, 8-IP significantly affected the Ames mutagenicity test. The lipid-soluble antioxidants and DNA adducts affected liver damage. For the Fe – V group, Cu significantly influenced $^{\bullet-}O_2$ production. Furthermore, Cu and Fe affected LPO and MDA, respectively. LPO and the lipid-soluble antioxidants significantly influenced 8OHdG production. For the Fe + ASA group, Cu and $^{\bullet-}O_2$ significantly influenced LPO. Fe and $^{\bullet-}O_2$ influenced MDA production. Furthermore, MDA and ORAC-L significantly influenced 8OHdG formation and this significantly affected mutagenesis. For the Fe + Cu group, Fe influenced $^{\bullet-}O_2$ production, and both Fe and $^{\bullet-}O_2$ significantly influenced DNA destruction and 8OHdG production. Mutagenesis was significantly influenced by GPx and FADU. ALT levels were influenced by Cu, ORAC-L and MDA.

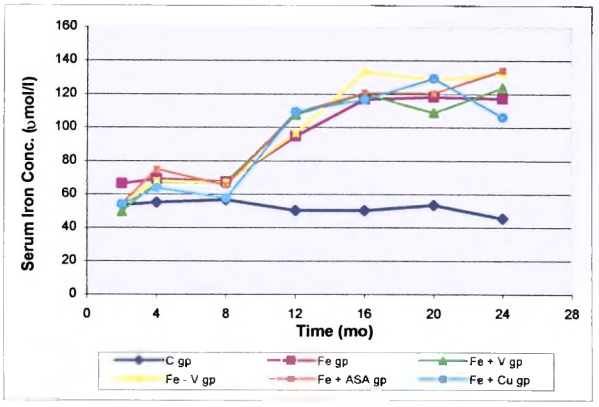

Figure 18. Interaction Plot of Time and Group: Serum Iron levels of iron over-loaded Wistar rats.

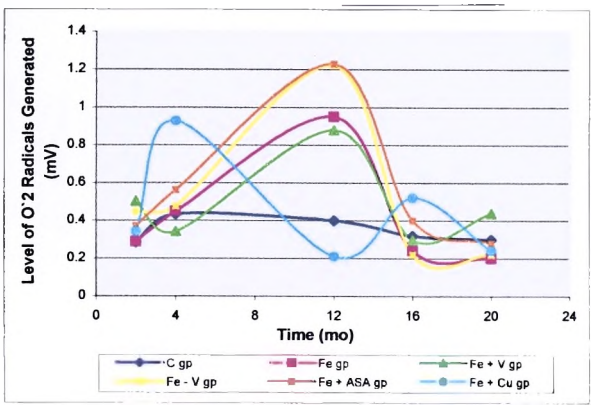

Figure 19. Interaction Plot of Time and Group: Super Oxide radical levels of iron-overloaded Wistar rats.

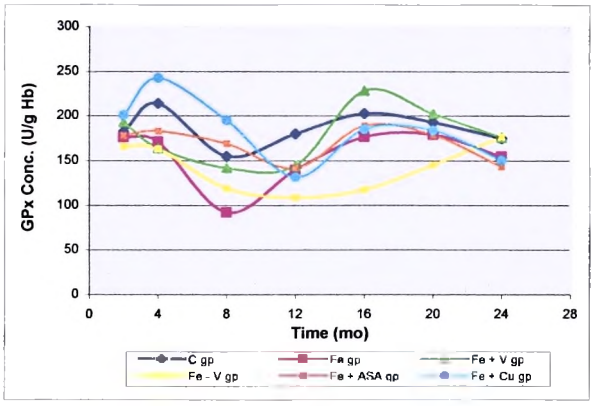

Figure 20. Interaction Plot of Time and Group: Glutathione Peroxidase levels of iron-overloaded Wistar rats.

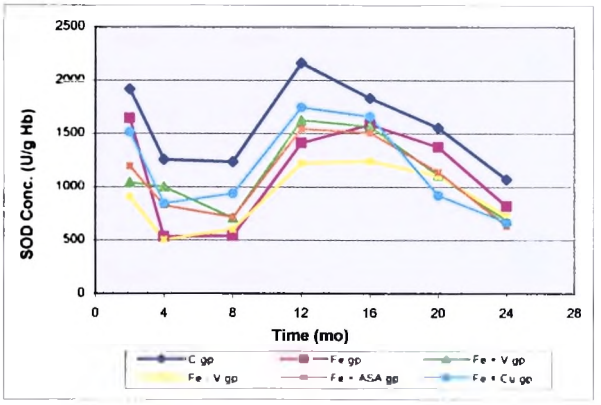

Figure 21. Interaction Plot of Time and Group: SOD levels of iron-overloaded Wistar rats.

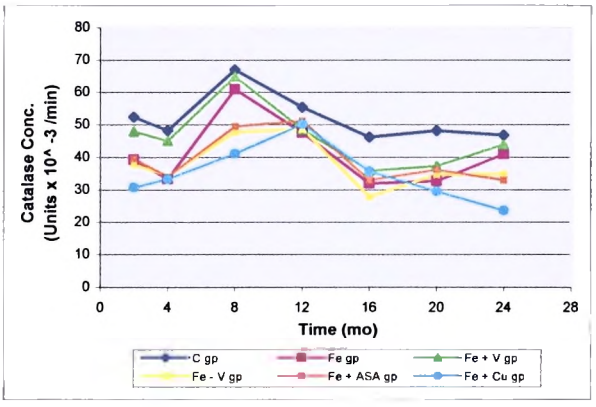

Figure 22. Interaction Plot of Time and Group: Blood Catalase levels of iron-overloaded Wistar rats.

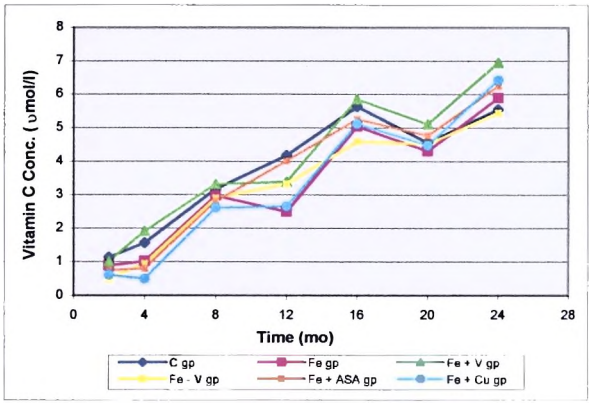

Figure 23. Interaction Plot of Time and Group: Serum Vitamin C levels of iron-overloaded Wistar rats.

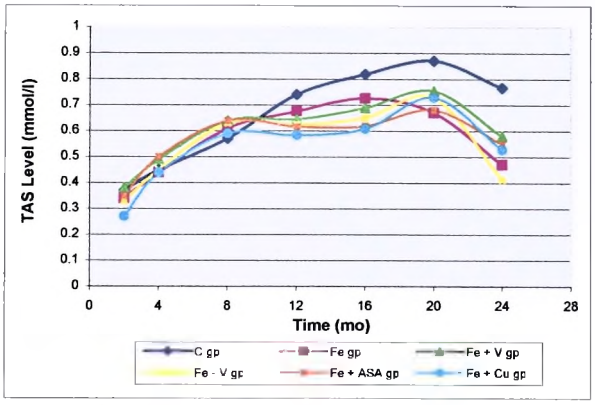

Figure 24 Interaction plot of Time and Group: Sreum Total Antioxidant Status of iron-overloaded Wistar rats

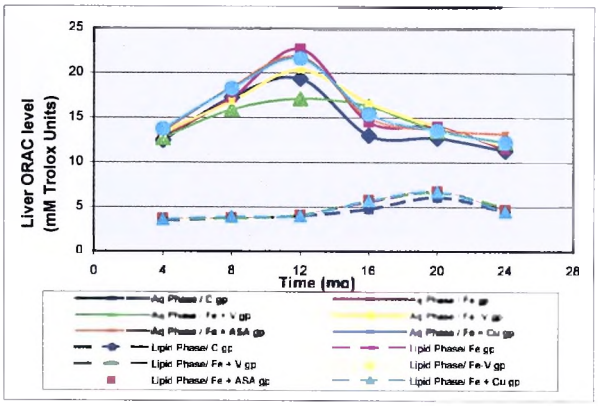

Figure 25. Interaction Plot of Tome and Group: ORAC of aqueous- and lipid-soluble fractions of iron-overloaded Wistar rat liver homogenate.

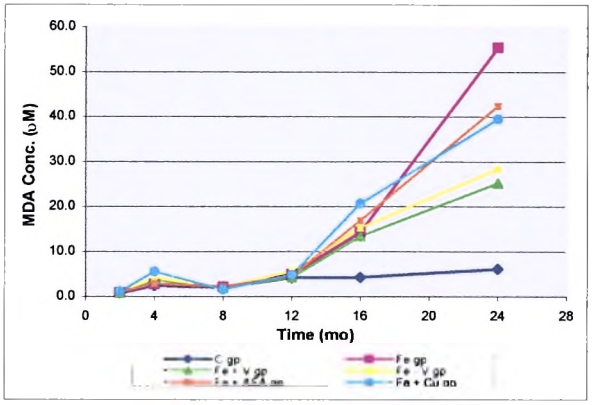

Figure 26. Interaction Plot of Time and Group: Serum MDA levels of iron-overloaded Wistar rats.

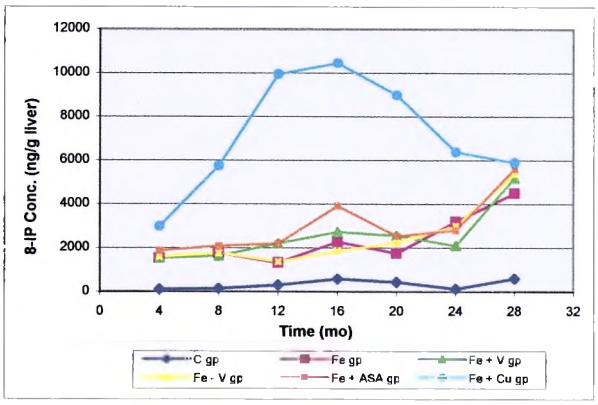

Figure 27. Interaction Plot of Time and Group: Liver 8-isoprostane levels of iron-overloaded Wistar rats.

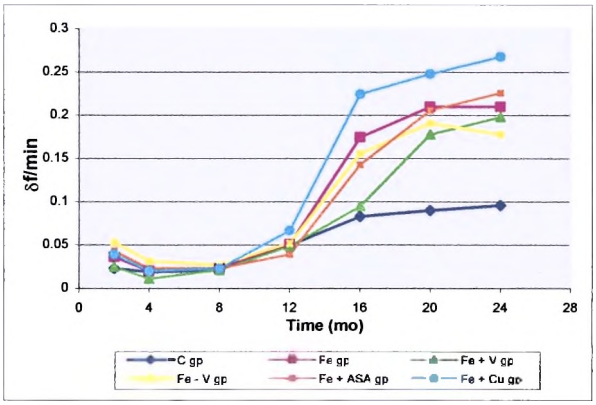

Figure 28. Interaction Plot of Time and Group: Fluorimetric Analysis of DNA Unwinding, of iron-overloaded Wistar rat liver homogenate.

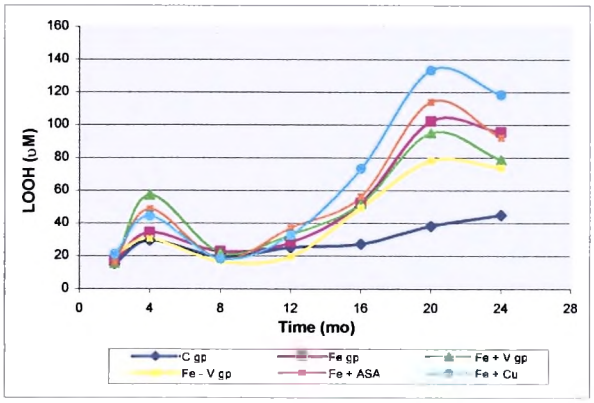

Figure 29. Interaction Plot of Time and Group: Serum Lipid hydroperoxides levels of iron-overloaded Wistar rats using the FOX II assay.

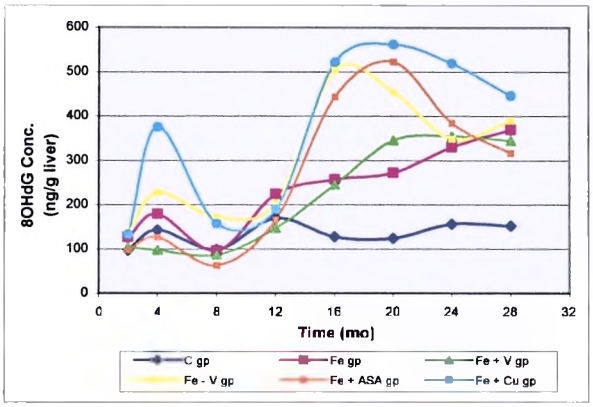

Figure 30. Interaction Plot of Time and Group: Liver 8OHdG levels of iron-overloaded Wistar rats.

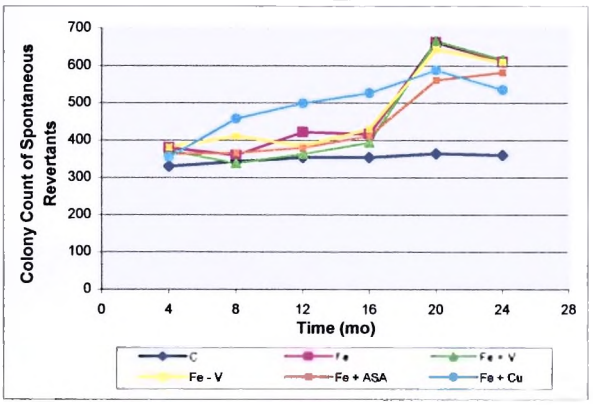

Figure 31. Interaction Plot of Time and Group: AMES mutagenicity test using *Salmonella typhimurium strain* TA 102 on iron-overloaded Wister rat liver homogenate.

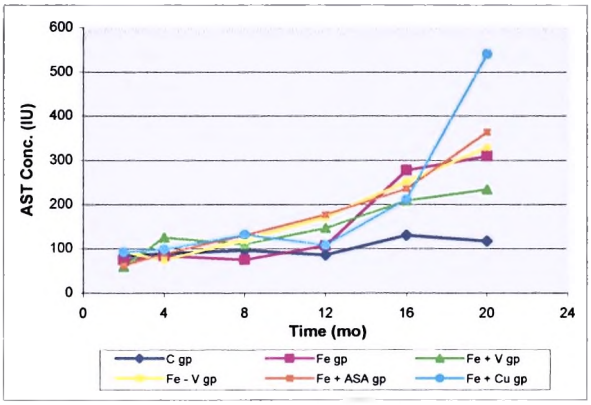

Figure 32. Interaction Plot of Time and Group: AST levels of iron-overloaded Wistar rats.

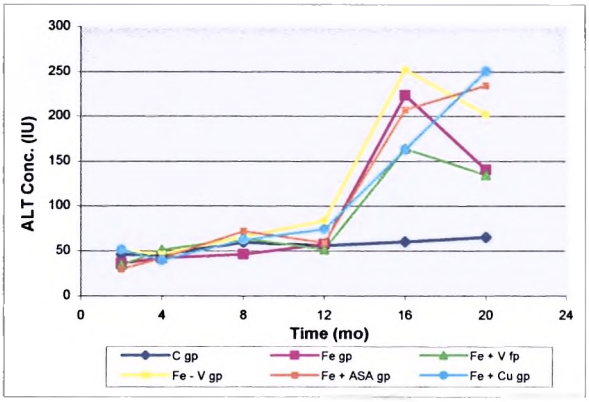

Figure 33. Interaction Plot of Time and Group: ALT levels of iron-overloaded Wistar rats.

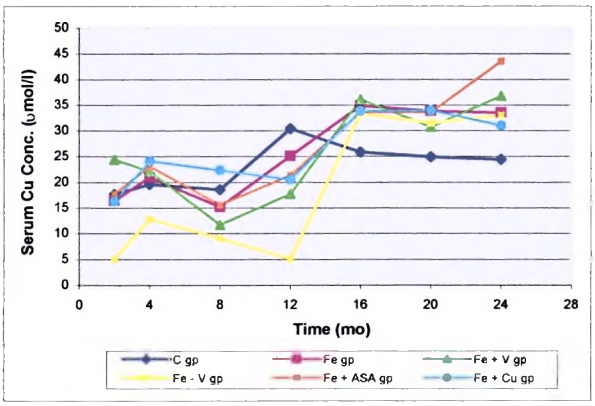

Figure 34. Interaction Plot of Time and Group: Serum copper levels of iron-overloaded Wistar rats.

Figure 35

RatLiv C3.4 anti8-OHdG 10c

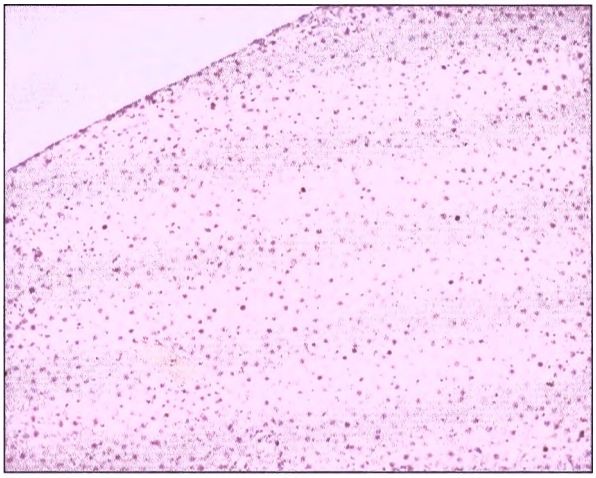

a

RatLiv C3.4 anti8-OHdG 40b

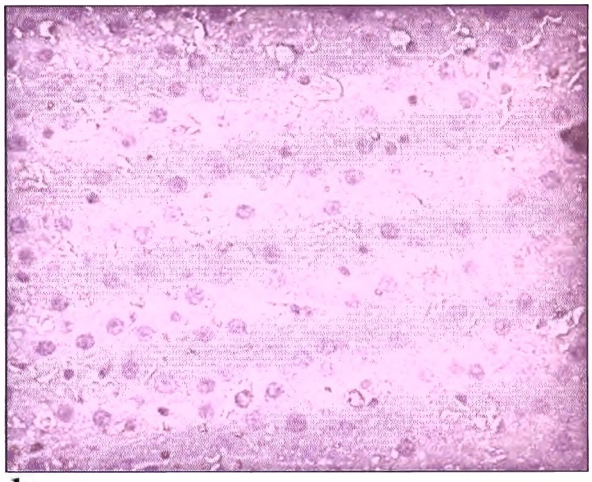

b

RatLiv F3.3 anti8-OHdG 10a

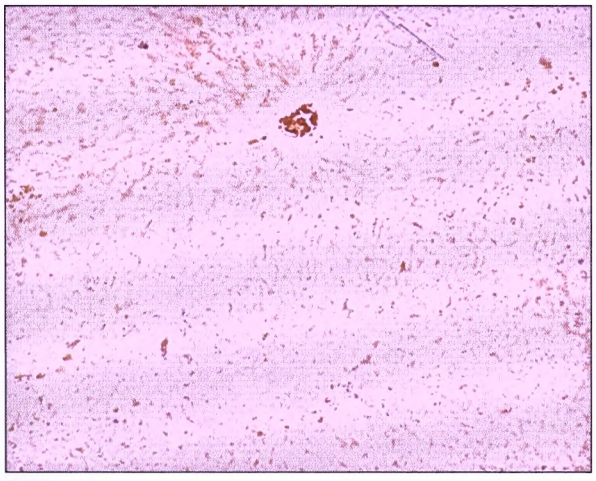

c

RatLiv F3.3 anti 8-OHdG 40a

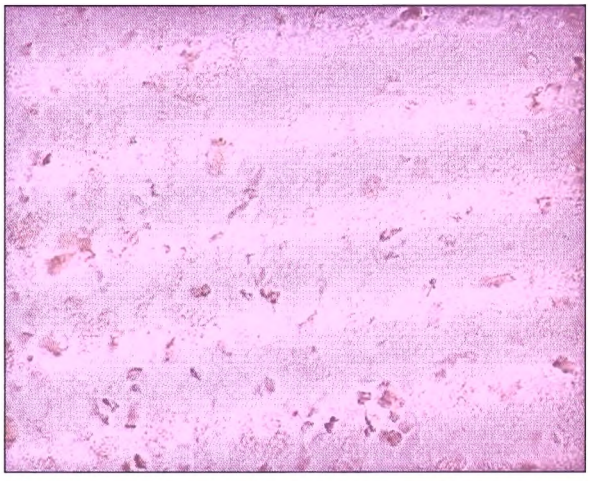

d

Immunohistochemical detection of 8OHdG adducts in normal and iron-overloaded livers. Photomicrographs (*a*) and (*b*) are negative for 8OHdG (control group, normal liver); (*c*) and (*d*) are positive (Fe group, iron-overloaded liver).

Figure 36

RatLiv C3.4 anti8-OHdG 10c

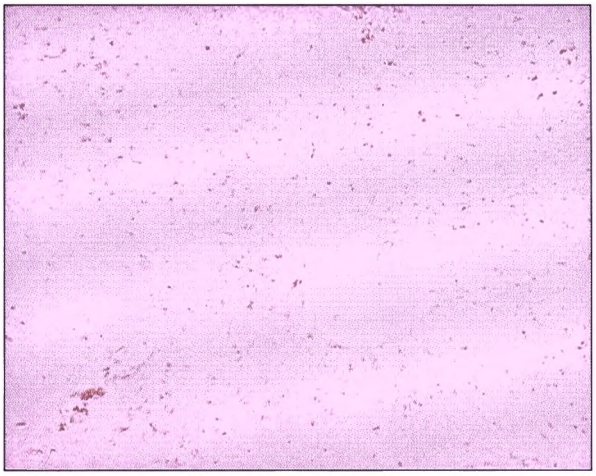

a

RatLiv C3.4 anti8-OHdG 40b

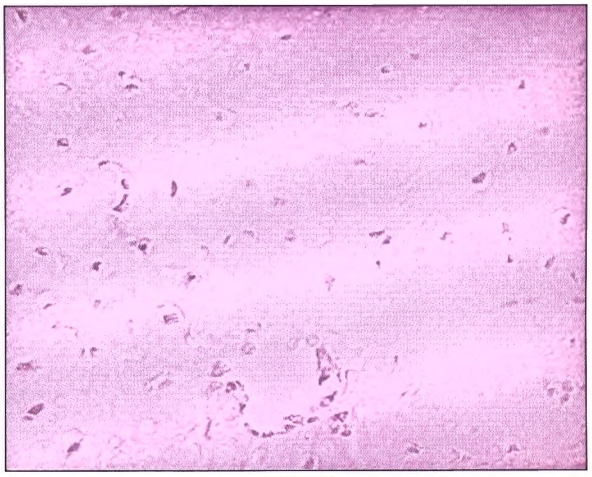

b

RatLiv V3.6 anti8-OHdG 10b

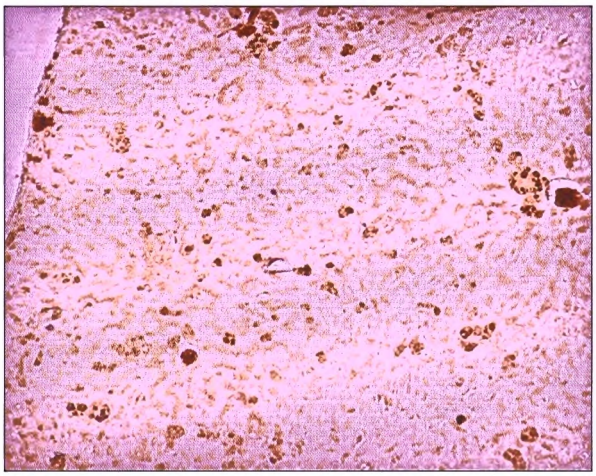

c

RatLiv V3.6 anti8-OHdG 40b

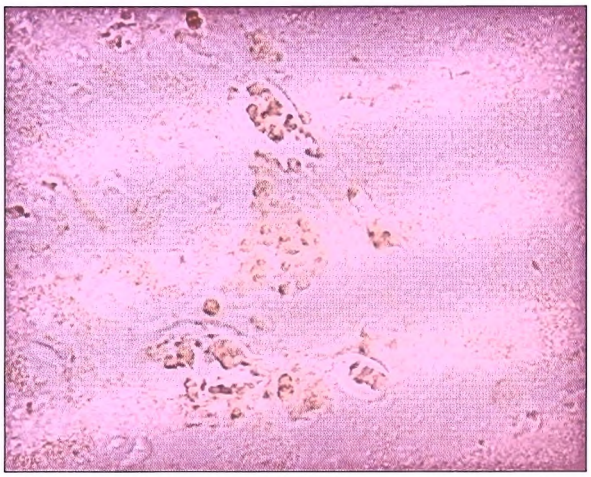

d

Immunohistochemical detection of 8OHdG adducts in normal and iron-overloaded livers. Photomicrographs (*a*) and (*b*) are negative for 8OHdG (control group, normal liver); (*c*) and (*d*) are positive (Fe + V group, iron-overloaded liver).

Figure 37

RatLiv C3.4 anti8-OHdG 10c



a

RatLiv C3.4 anti8-OHdG 40b

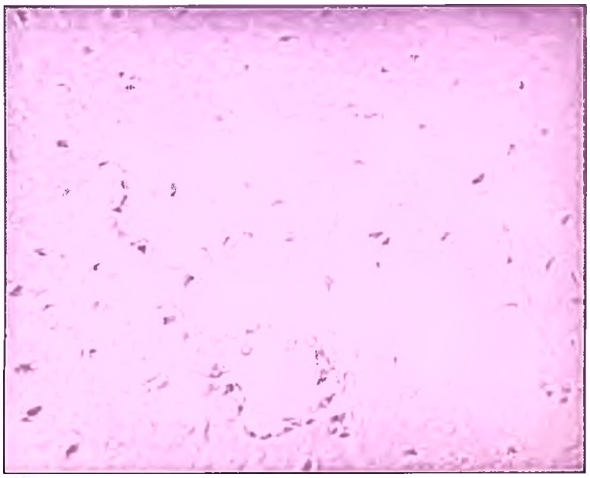

b

RatLiv N3.1 anti8-OHdG 10a

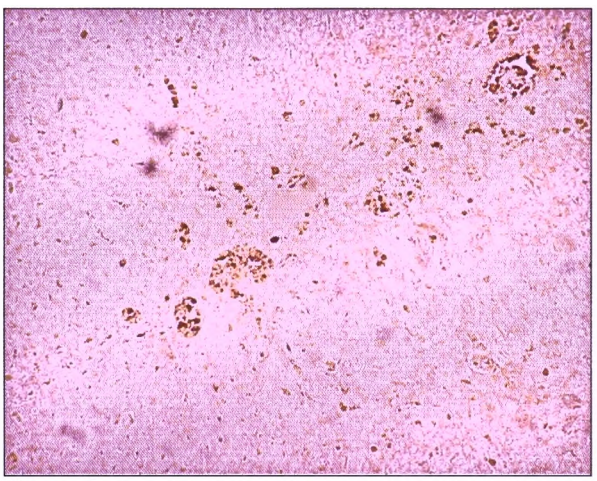

c

RatLiv N3.1 anti8-OHdG 40a

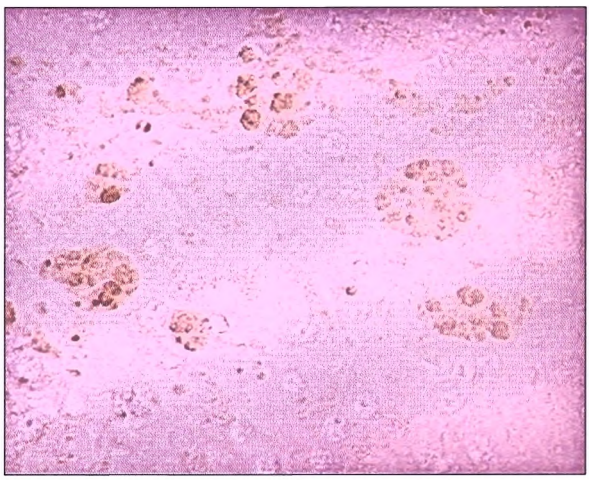

d

Immunohistochemical detection of 8OHdG adducts in normal and iron-overloaded livers. Photomicrographs (*a*) and (*b*) are negative for 8OHdG (control group, normal liver); (*c*) and (*d*) are positive (Fe - V group, iron-overloaded liver).

Figure 38

RatLiv C3.4 anti8-OHdG 10c

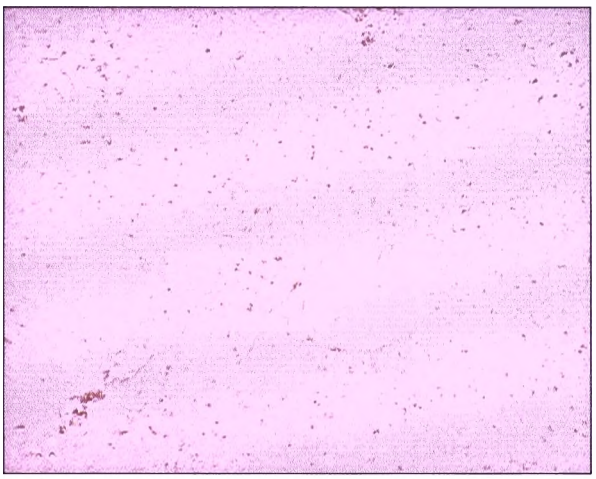

a

RatLiv C3.4 anti8-OHdG 40b

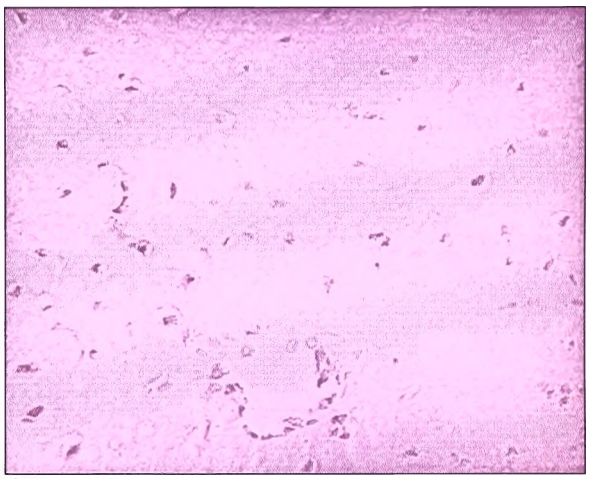

b

RatLiv A3.5 anti8-OHdG 10b

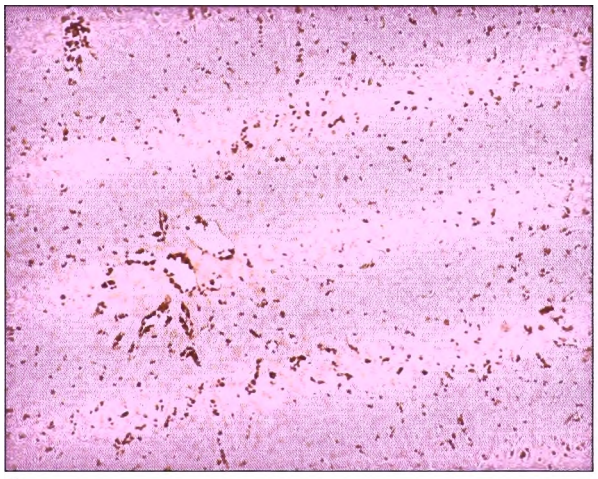

c

RatLiv A3.5 anti8-OHdG 40a

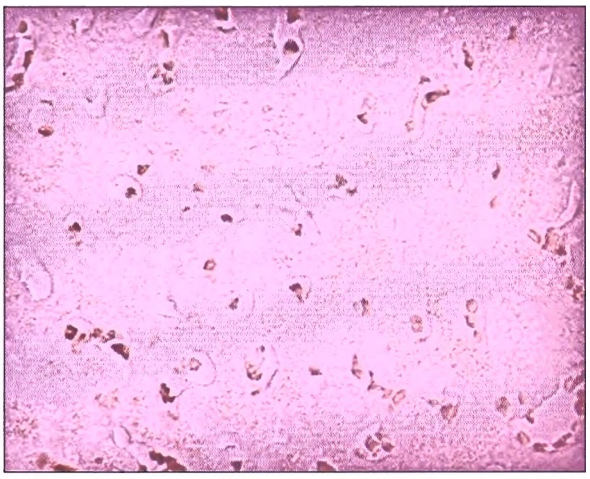

d

Immunohistochemical detection of 8OHdG adducts in normal and iron-overloaded livers. Photomicrographs (*a*) and (*b*) are negative for 8OHdG (control group, normal liver); (*c*) and (*d*) are positive (Fe + ASA group, iron-overloaded liver).

Figure 39

RatLiv C3.4 anti8-OHdG 10c

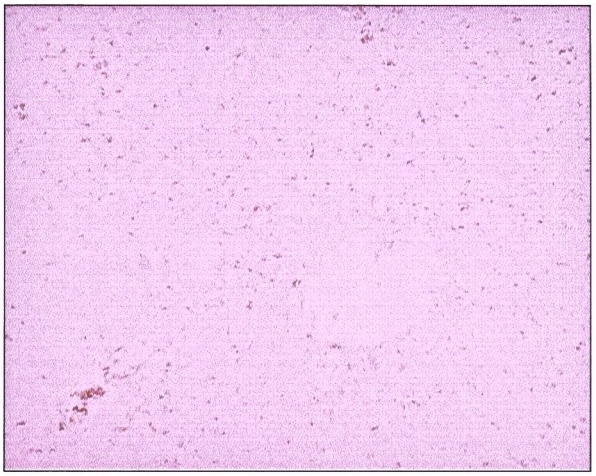

a

RatLiv C3.4 anti8-OHdG 40b

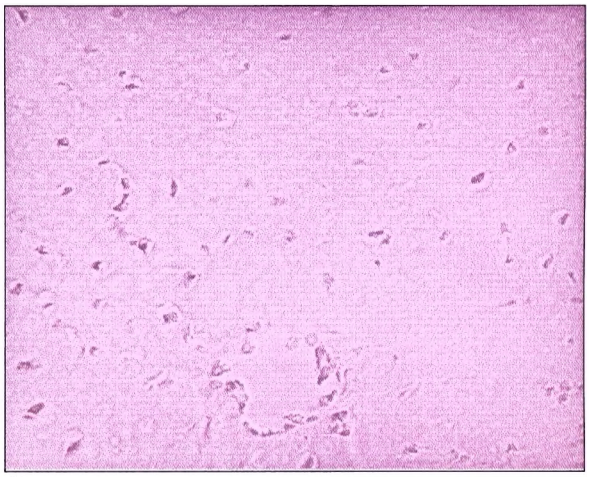

b

RatLiv Cu3.1 anti8-OHdG 10c

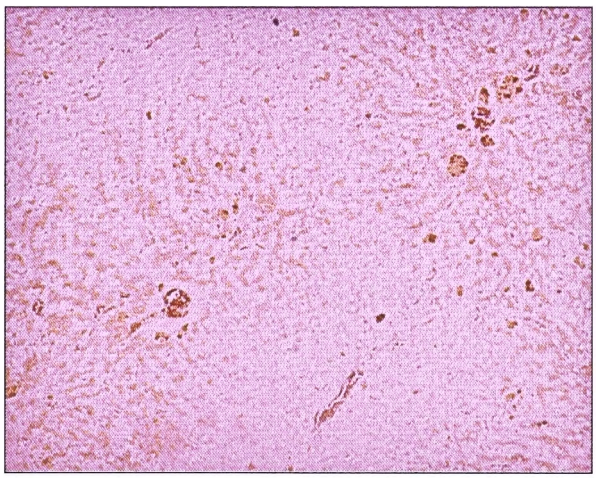

c

RatLiv Cu3.1 anti8-OHdG 40c

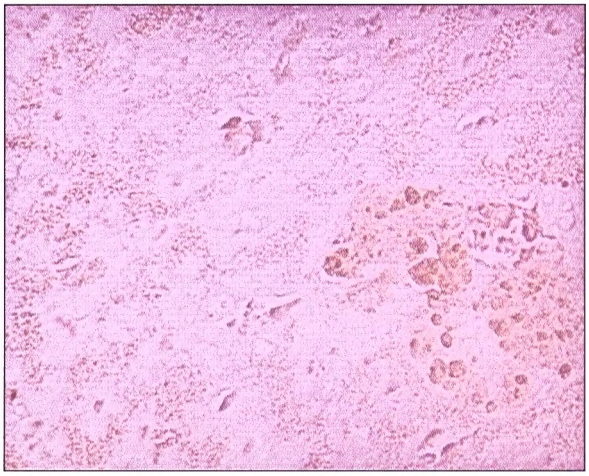

d

Immunohistochemical detection of 8OHdG adducts in normal and iron-overloaded livers. Photomicrographs (*a*) and (*b*) are negative for 8OHdG (control group, normal liver); (*c*) and (*d*) are positive (Fe + Cu group, iron-overloaded liver).

Figure 40

RatLiv Anti-HNE 3 C.7

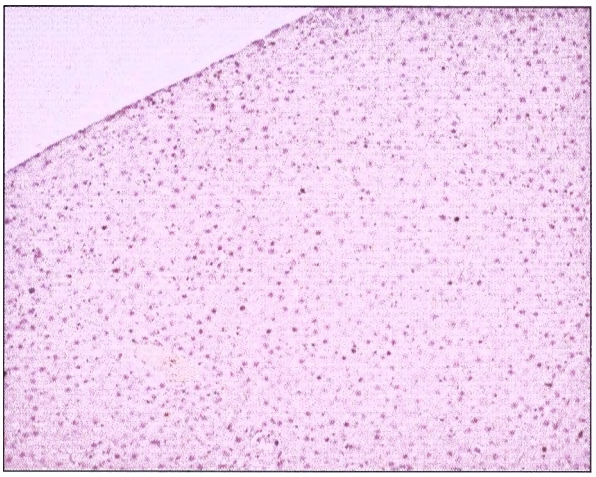

a

RatLiv Anti-HNE 3 C.7.1 40b

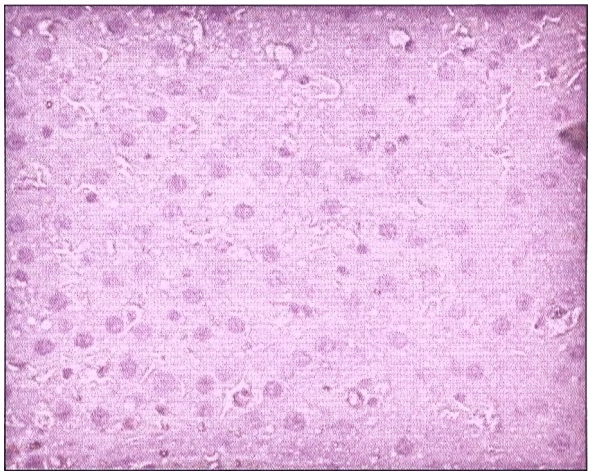

b

RatLiv Anti-HNE 3 F.7.10 10c

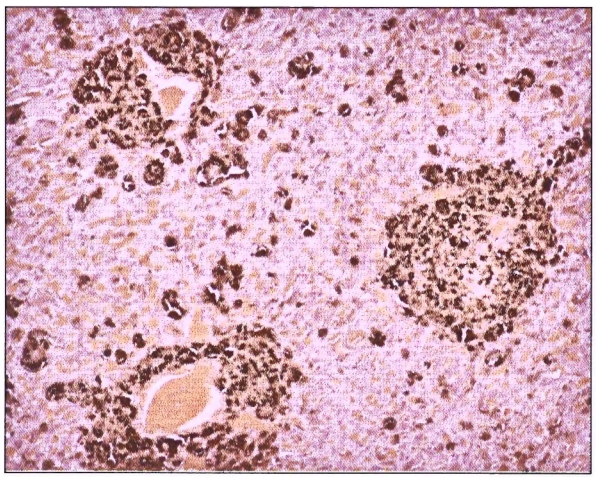

c

RatLiv Anti-HNE 3 F.7.10 40a

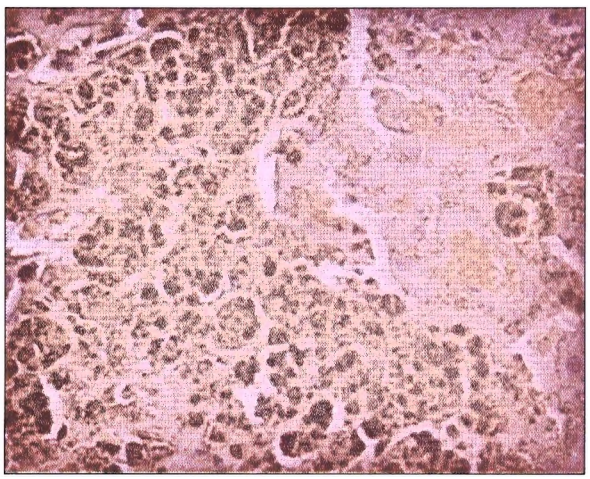

d

Immunohistochemical detection of 4-HNE adducts in normal and iron-overloaded livers. Photomicrographs (*a*) and (*b*) are negative for 4-HNE (control group, normal liver); (*c*) and (*d*) are positive (Fe group, iron-overloaded liver).

Figure 41

RatLiv Anti-HNE 3 C.7

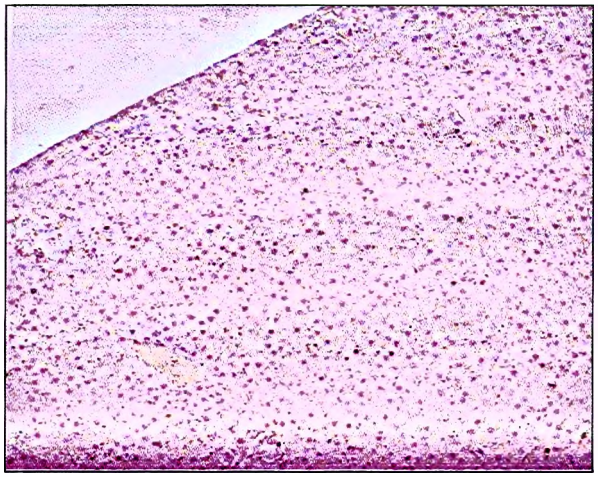

a

RatLiv Anti-HNE 3 C.7.1 40b

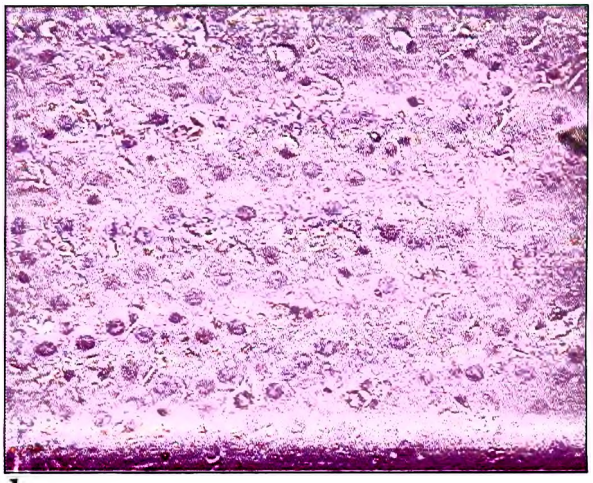

b

RatLiv Anti-HNE 3 V.7.8 10c

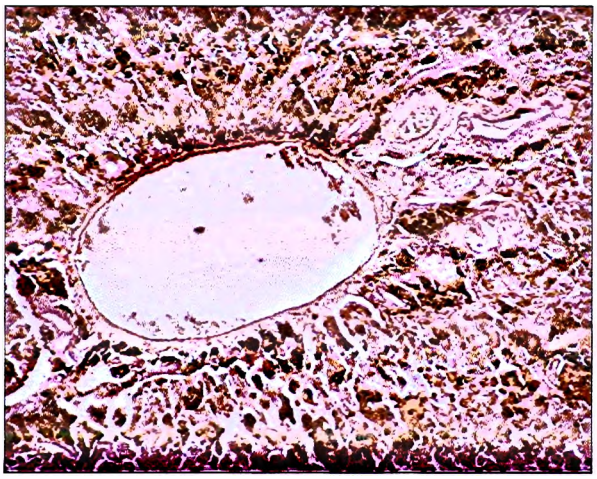

c

RatLiv Anti-HNE 3 V.7.8 40c

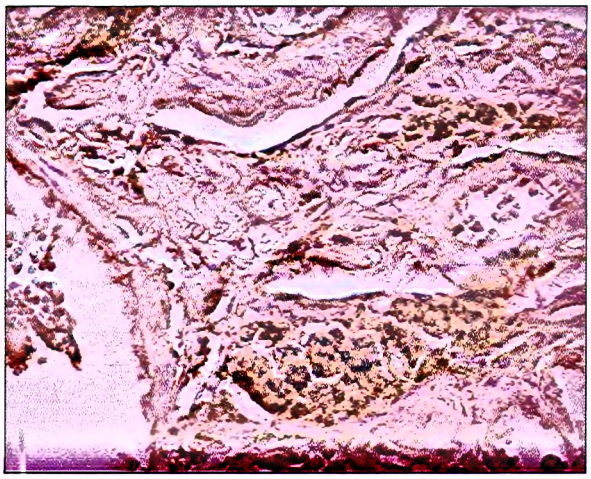

d

Immunohistochemical detection of 4-HNE adducts in normal and iron-overloaded livers. Photomicrographs (*a*) and (*b*) are negative for 4-HNE (control group, normal liver); (*c*) and (*d*) are positive (Fe + V group, iron-overloaded liver).

Figure 42

RatLiv Anti-HNE 3 C.7

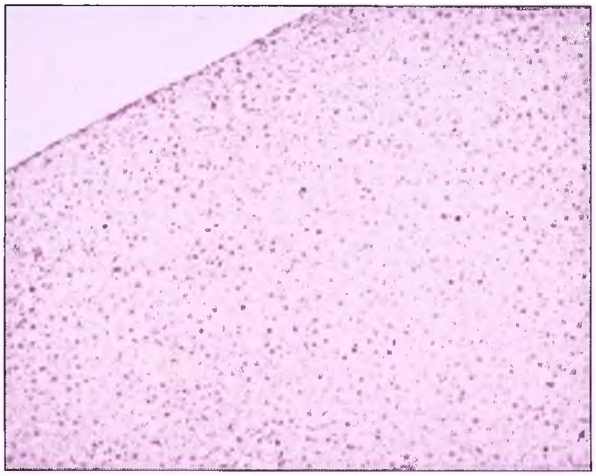

a

RatLiv AntiHNE 3 C.7.1 40b

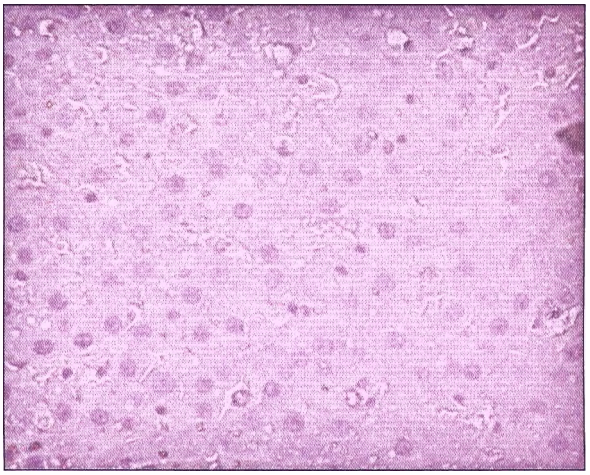

b

RatLiv Anti-HNE 3 N.7.1 10d

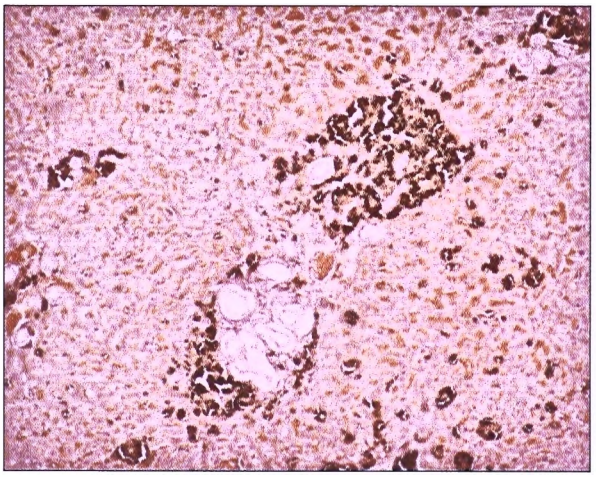

c

RatLivAnti-HNE 3N.7.1 40a

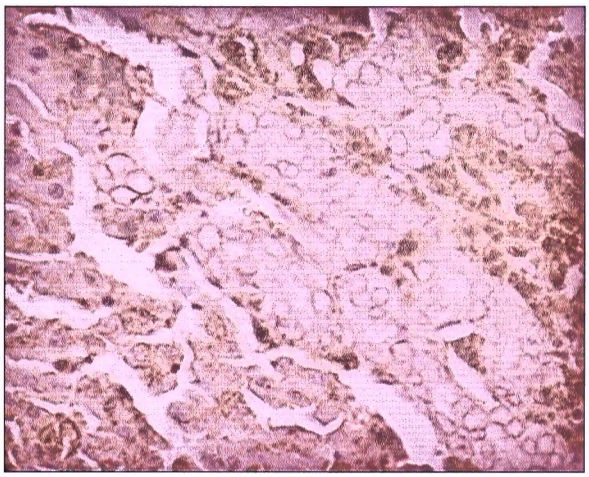

d

Immunohistochemical detection of 4-HNE adducts in normal and iron-overloaded livers. Photomicrographs (*a*) and (*b*) are negative for 4-HNE (control group, normal liver); (*c*) and (*d*) are positive (Fe - V group, iron-overloaded liver).

Figure 43

RatLiv Anti-HNE 3 C.7

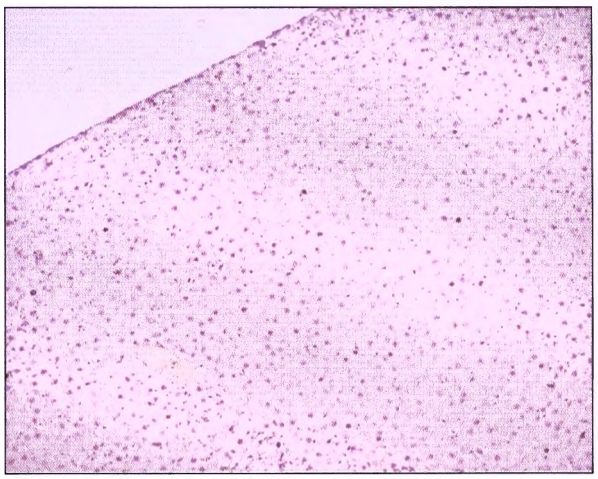

a

RatLiv Anti-HNE 3 C.7.1 40b

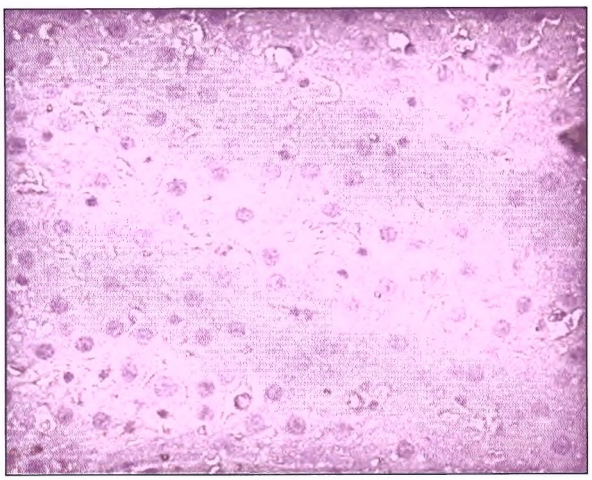

b

RatLiv Anti-HNE 3 A.7.9 10a

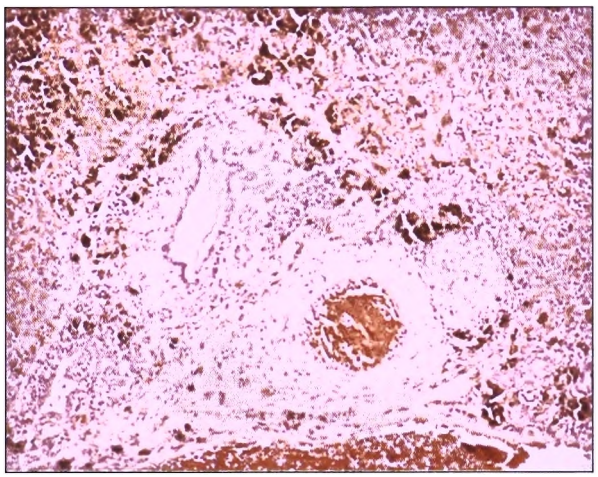

c

RatLiv Anti-HNE 3 A.7.9 40b

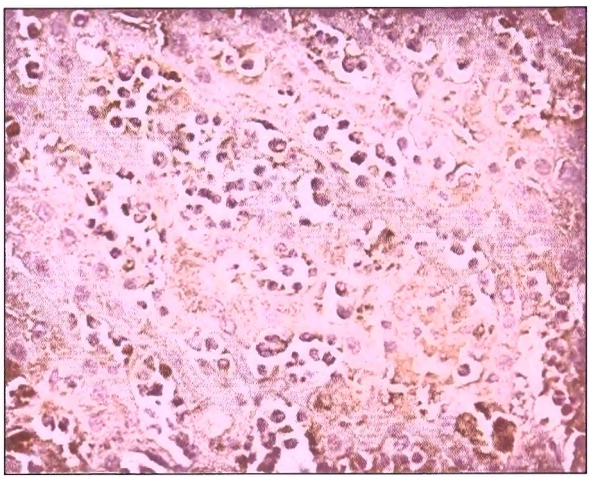

d

Immunohistochemical detection of 4-HNE adducts in normal and iron-overloaded livers. Photomicrographs (*a*) and (*b*) are negative for 4-HNE (control group, normal liver); (*c*) and (*d*) are positive (Fe + ASA group, iron-overloaded liver).

Figure 44

RatLiv Anti-HNE 3 C.7

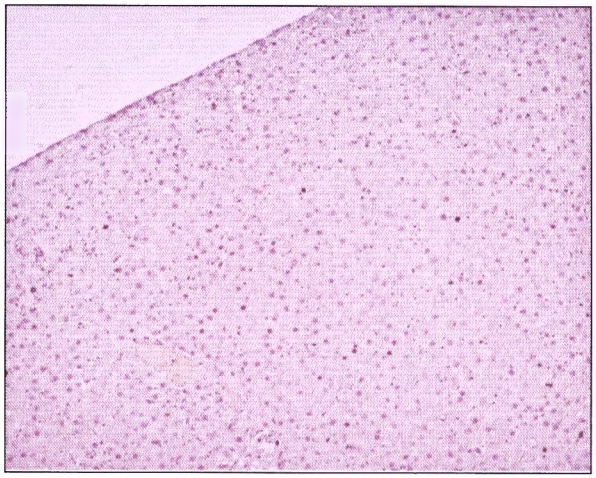

a

RatLiv Anti-HNE 3 C.7.1 40b

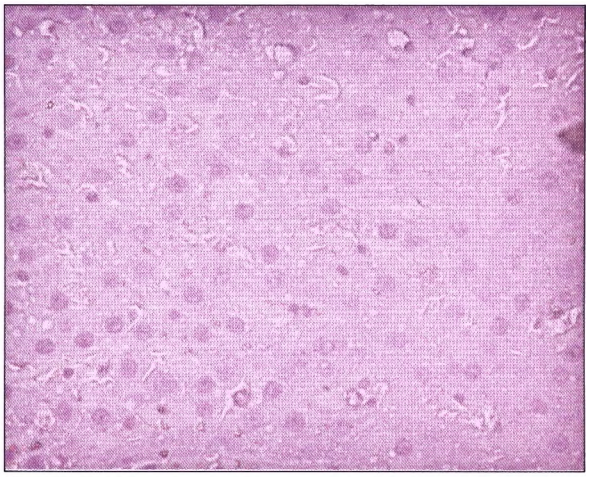

b

RatLiv Anti-HNE 3 Cu.7.5 10b

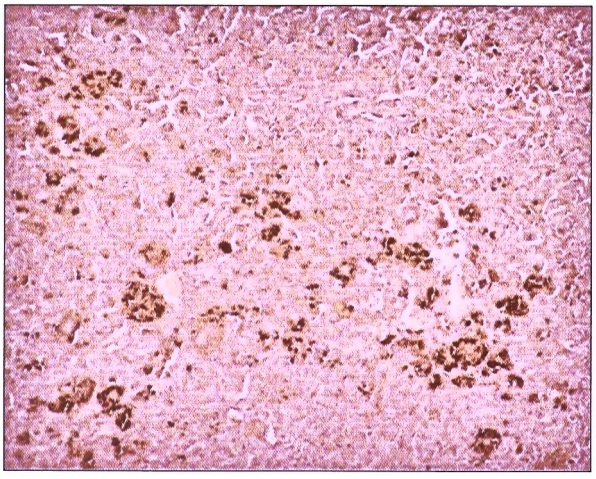

c

RatLiv Anti-HNE 3 Cu.7.5 40b

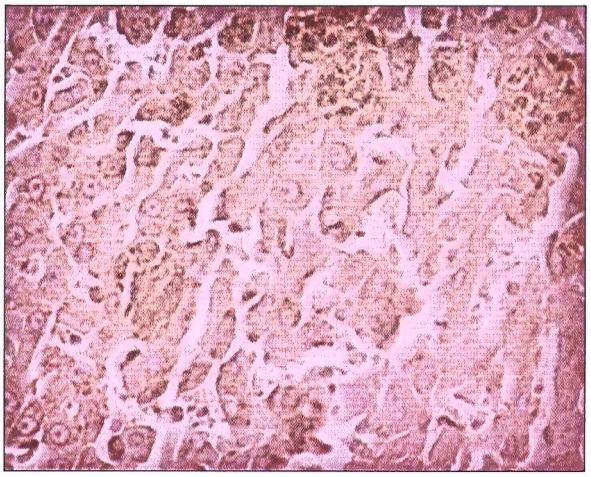

d

Immunohistochemical detection of 4-HNE adducts in normal and iron-overloaded livers. Photomicrographs (*a*) and (*b*) are negative for 4-HNE (control group, normal liver); (*c*) and (*d*) are positive (Fe + Cu group, iron-overloaded liver).

Figure 45a : F2.3 Rat Perls' Grade I

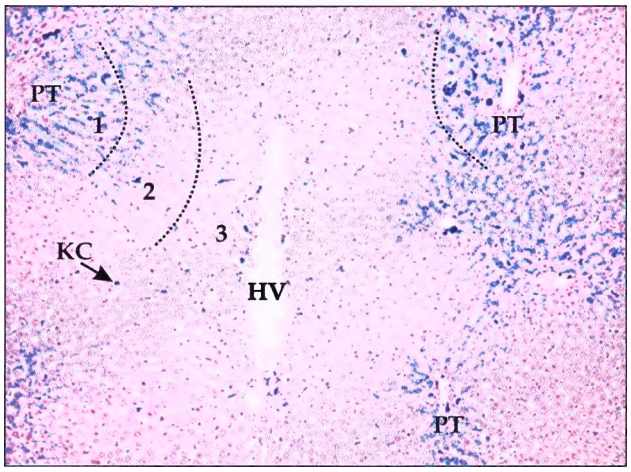

Figure 45b : F3.1 Rat Perls' Grade II

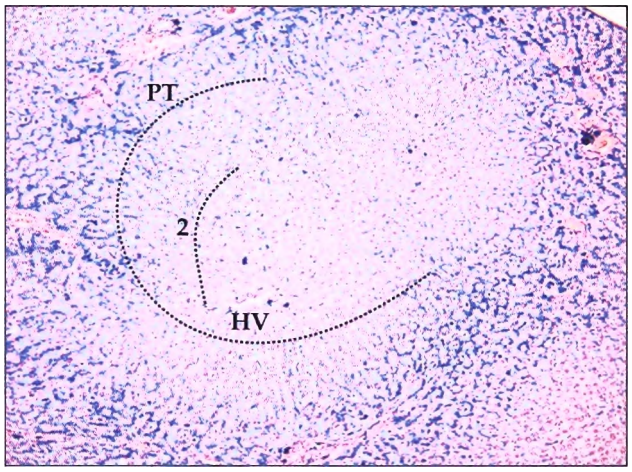

Figure 45c : F7.11 Rat Perls' Grade IV

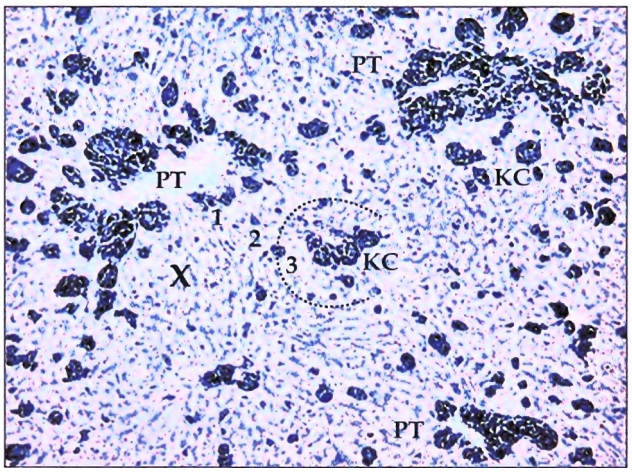

Figure 45: The photomicrographs show hepatic iron deposition as a result of dietary iron overload indicated by Perls ' Prussian blue stain. (a) Demonstrates iron deposition confined to periportal (zone 1) hepatocytes at 8 months, but subsequently progressed to zone 2 at 12 months and by 28 months, no gradient was observed (c). Iron deposition was massive with grade 4 hepatic iron (c). Kupffer cell iron storage also progressed with time. [**1** = zone 1, **2** = zone 2, **3** = zone 3, **PT** = Portal Tract, **HV** = Hepatic Vein, **KC** = Kupffer cell, **X** = Pericanalicular Iron]

Figure 46a : F7.3 Rat IFF H&E

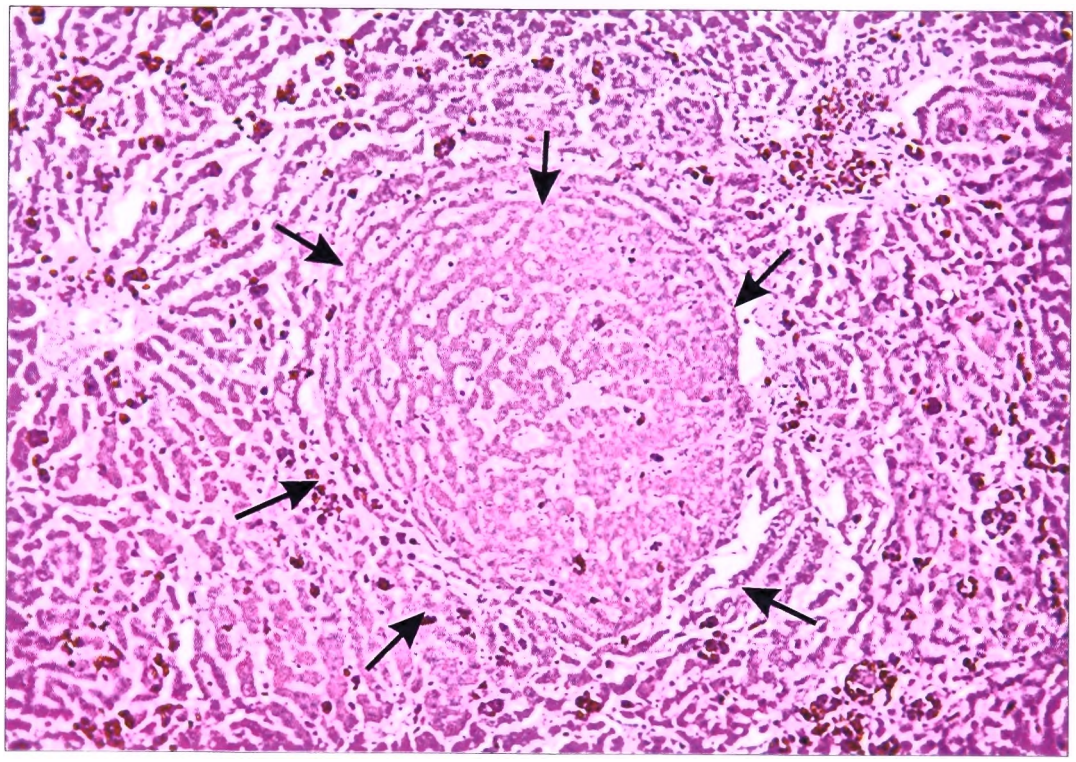

Figure 46b : F7.3 Rat IFF Perls'

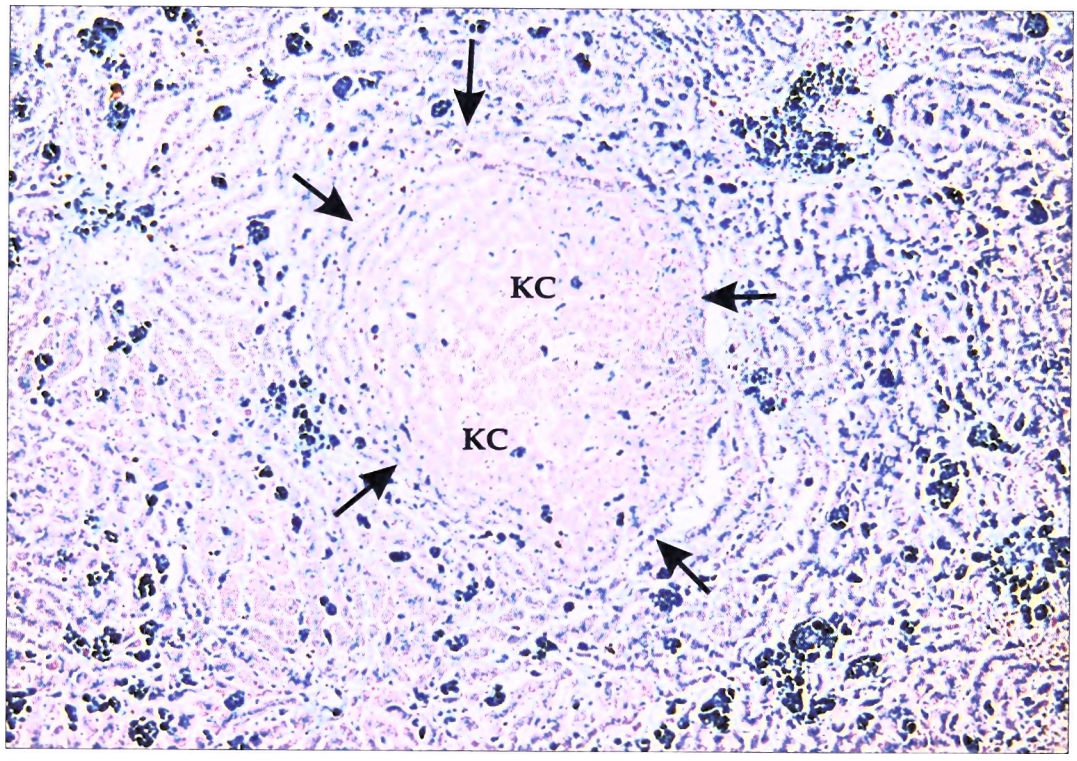

Figure 46 : This figure shows dietary iron overload in the liver with an iron-free focus (arrowed). Photomicrograph (**a**) shows the nodule and surrounding hepatic parenchyma on an H & E stain. In photomicrograph (**b**) iron deposition is indicated by Perls' Prussian blue stain. The iron free nodule with no or very little iron and iron in scattered Kupffer cells is evident and contrasts with the remaining hepatocytes that contain large amounts of iron. [Arrows surround iron free focus, **KC** = Kupffer cells]

Figure 47 : V7.1 Rat IFF H&E

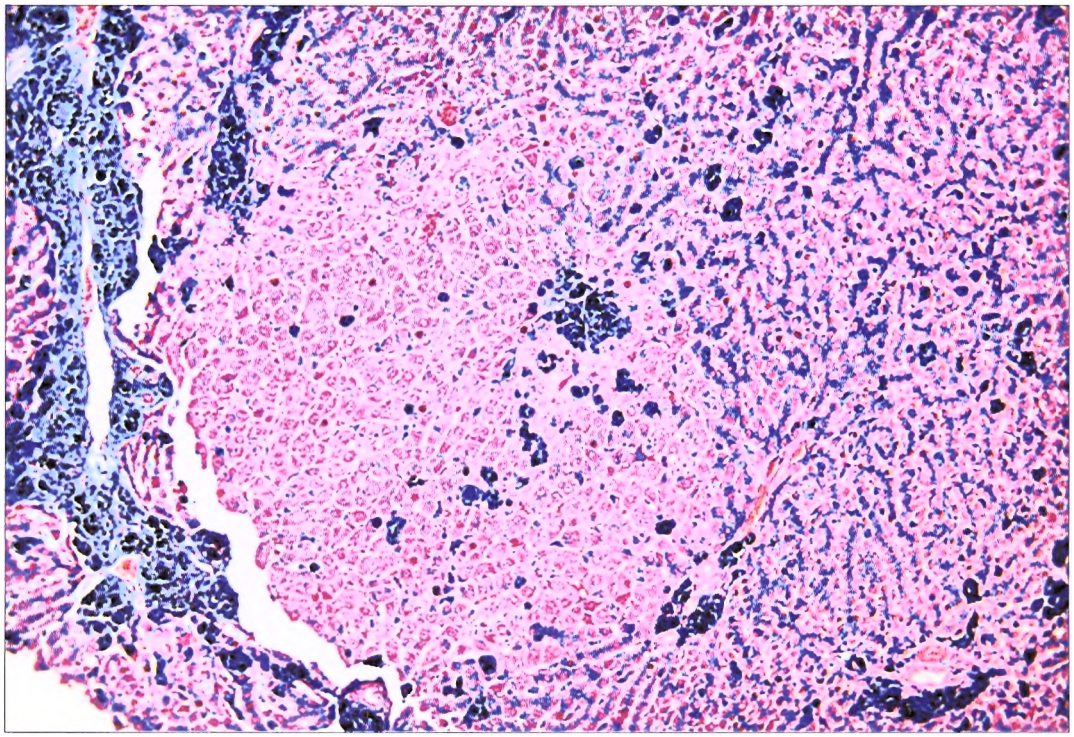

Figure 47 : Another example of the contrast between the heavily iron laden hepatocytes at 28 months in an iron-free focus showing little if any iron in the hepatocytes (H & E stain)

Figure 48 : V7.7 Rat GST-π



Figure 48 : Counterstaining with GST-π shows the iron-free foci to be positive for this stain, indicating (pre)neoplasia. [Arrows denote iron-free foci]

Figure 49a : ZV7.1 Rat IFF MB H&E

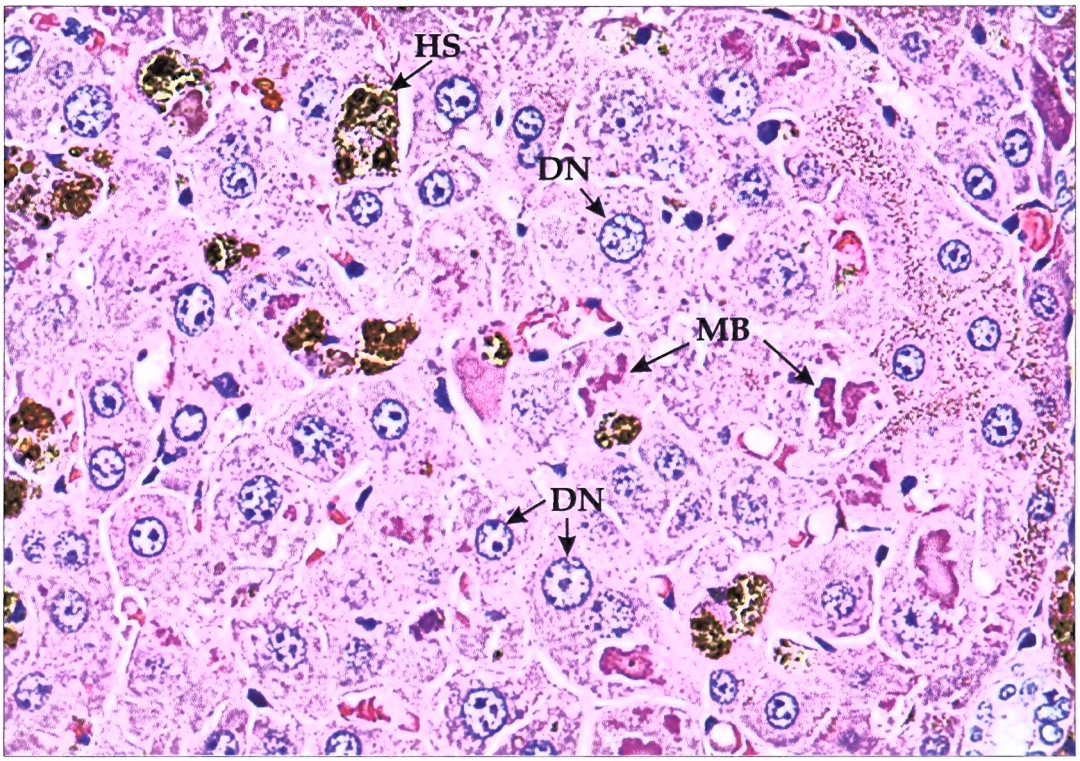

Figure 49b : ZV7.1 Rat IFF MB Perls'

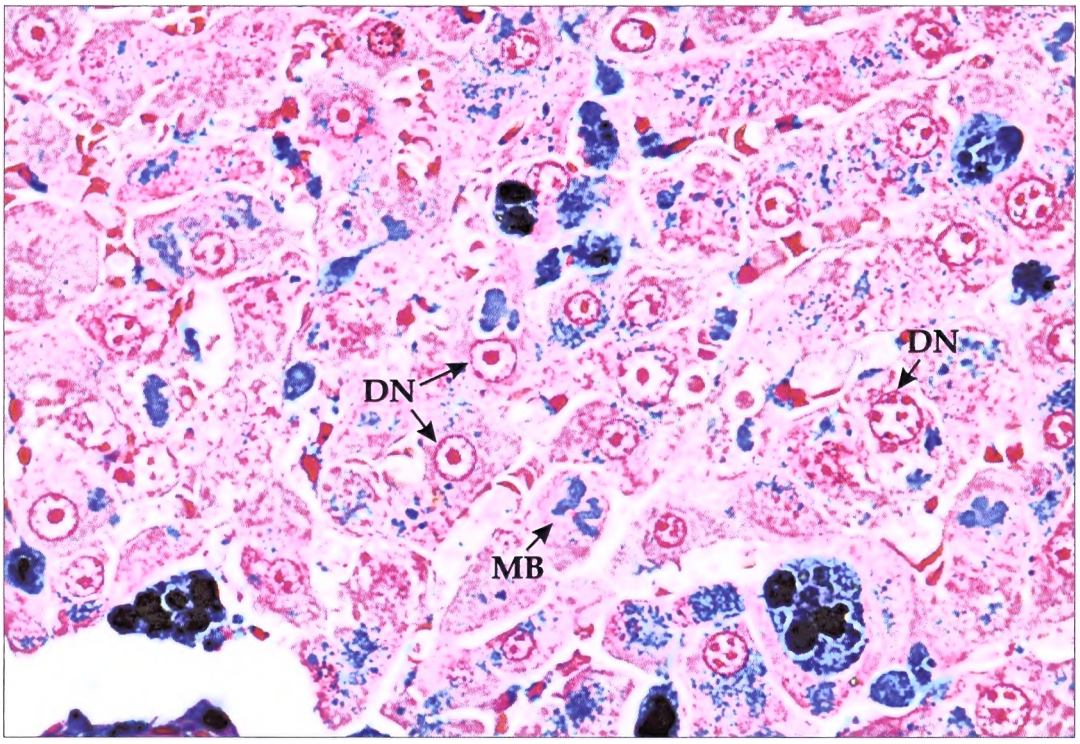

Figure 49: This figure shows a higher power view of an iron-free focus. Amphophilic (purple) intracytoplasmic 'rope-like' inclusions resembling Mallory bodies (**MB**) are evident (arrowed). Large dysplastic nuclei (**DN**) are also seen (arrowed) [H & E stain (**a**), Perls' Prussian blue stain (**b**), **HS** = Aggregates of haemosiderin in Kupffer Cells]

Figure 50a : ZF7.5 Rat IFF Globules H&E

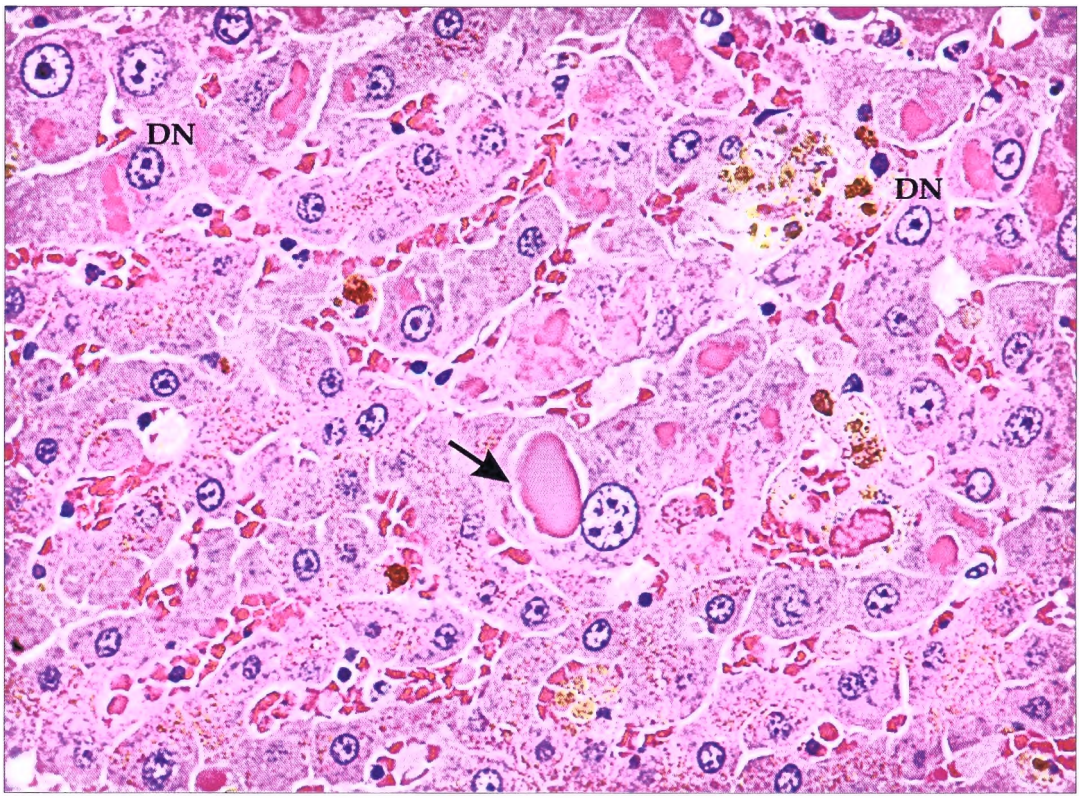

Figure 50b : ZF7.5 Rat IFF Globules Perls'

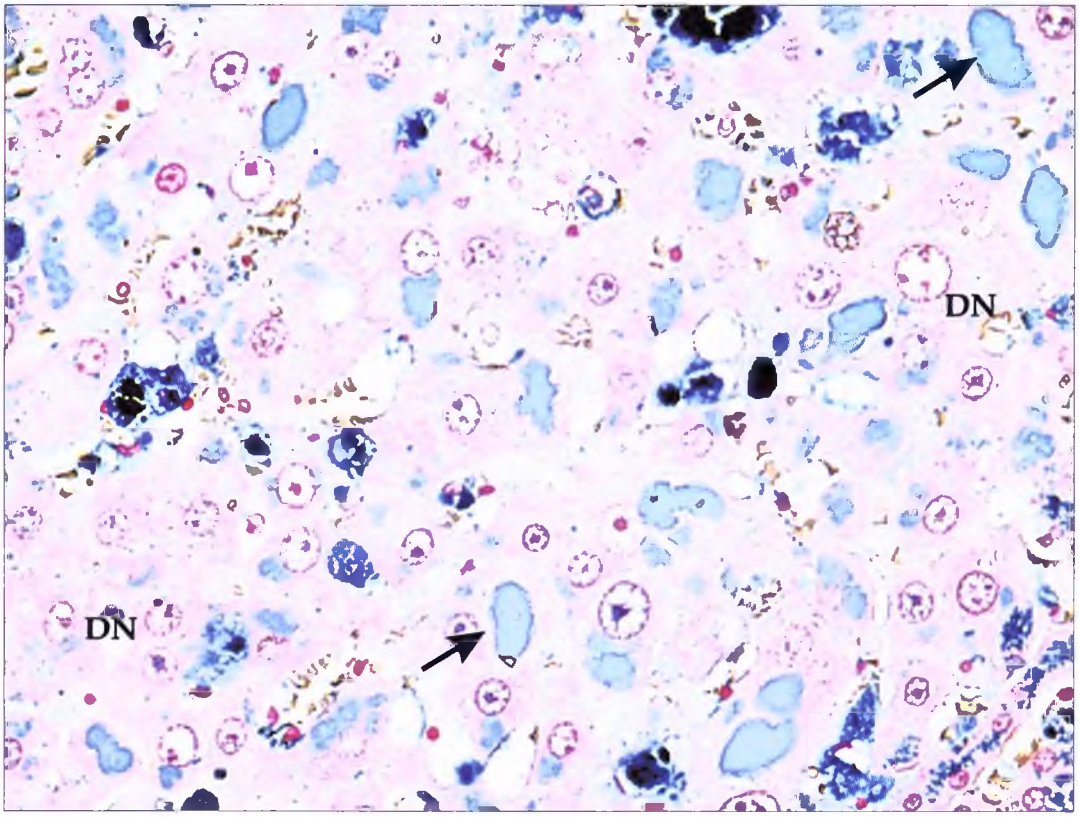

Figure 50: Photomicrograph (H & E stain) demonstrates the presence of globules (arrowed) within hepatocytes of the iron-free focus (a). Similarly, globules are relieved by Perls' Prussian blue stain (b). [DN = Large Dysplastic Nuclei]

Figure 51a : F8.8 Rat HCC wholemount H&E

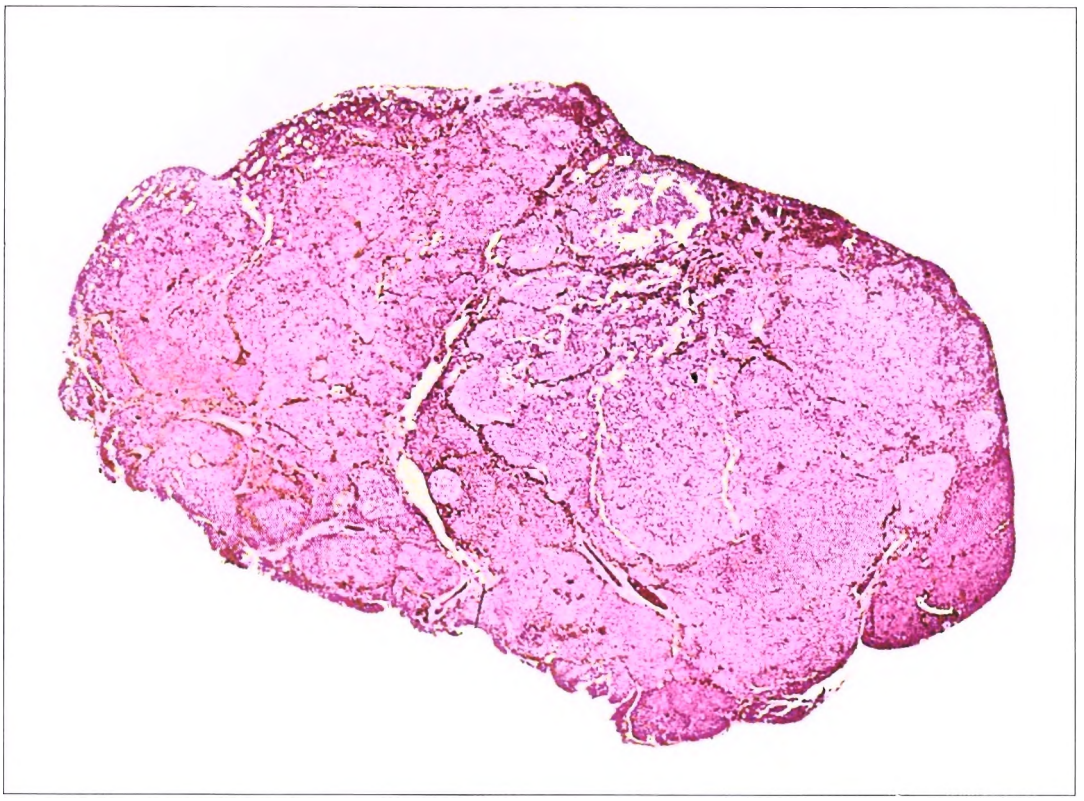

Figure 51b : F8.8 Rat HCC wholemount Perls'

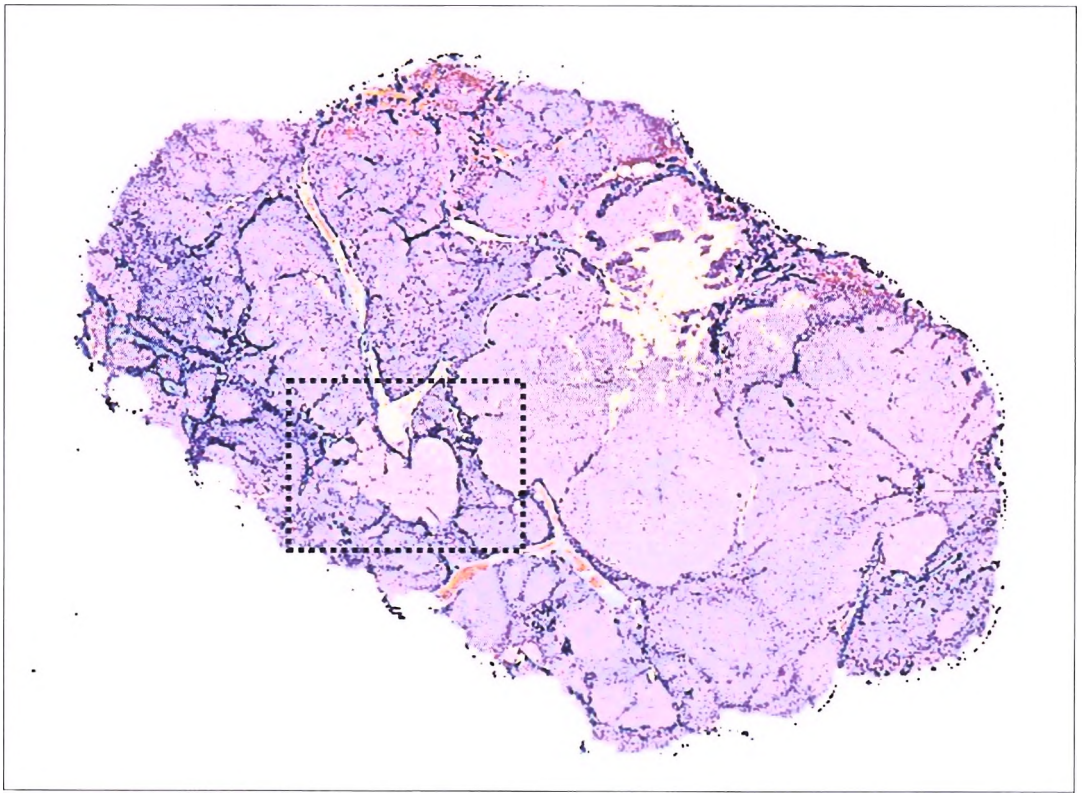

Figure 51: Hepatocellular carcinoma (2cm wholemount) arising in a rat's liver and seen at 32 months [H & E stain (a) and Perls' Prussian blue stain (b)].

Figure 52 : F8.8 Rat HCC Perls'

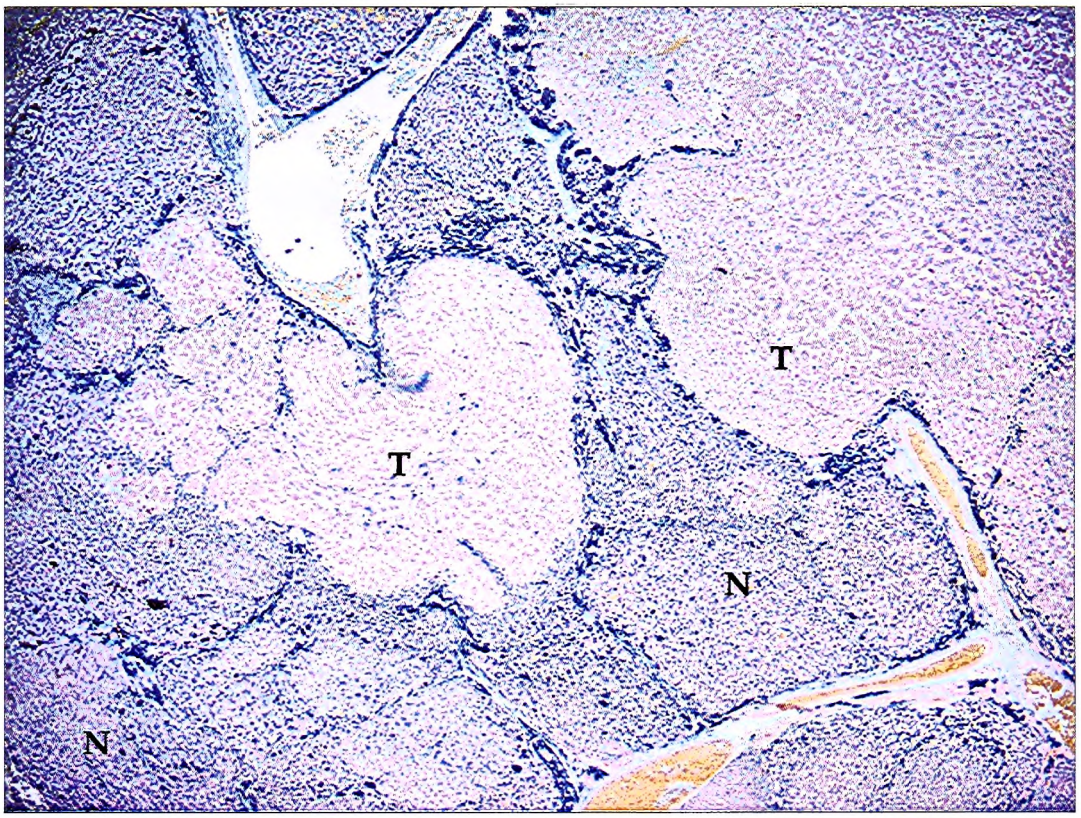

Figure 52 : This figure shows a higher power view of the area blocked in Fig 51b demonstrating small areas of normal liver tissue (N), seen contiguous with the tumours (T). Additionally, there was no fibrosis or cirrhosis (Perls' Prussian blue stain).

Figure 53 : F8.8 Rat HCC (pseudoglandular) H & E

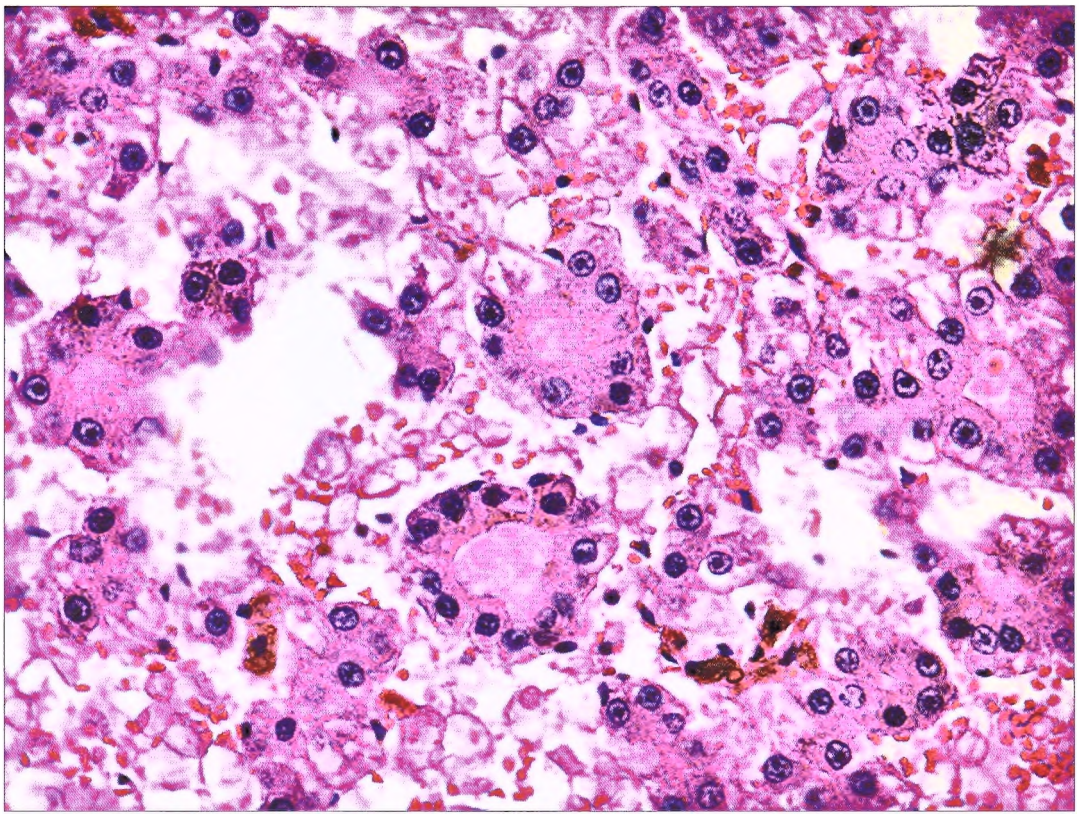

Figure 53 : Photomicrograph (H & E stain) showing pseudoglandular HCC after 32 months of iron loading.

Figure 54 : F8.8 Rat HCC (pseudoglandular) Perls'

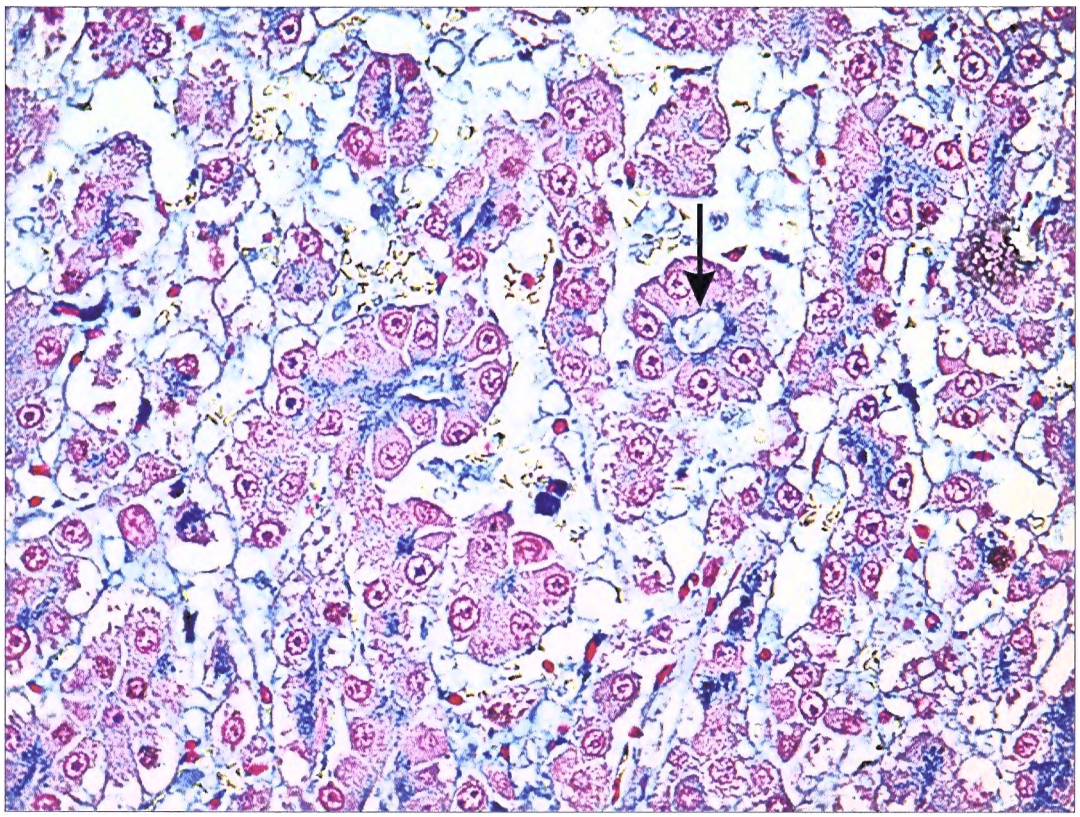

Figure 54 : Perls' Prussian blue stain of photomicrograph shows pseudoglandular HCC with iron at the canalicular pole (arrowed).



Figure 55. Pulsed Field Gel Electrophoresis (PFGE). Lane 1 = 50 kb marker, Lanes 3 & 4 = C group DNA, lanes 6 & 7 = Fe group DNA, lanes 8 & 9 = Fe + V group DNA, lanes 10 & 11 = Fe – V group DNA, lanes 12 & 13 = Fe + ASA group DNA, lanes 14 & 15 = Fe + Cu group DNA. PFGE was run for 17 hrs under the following conditions: 0.9% agarose gel, v = 4.5V, initial switch time = 0.1s, final switch time = 200s, current = 180 mA, pump rate = 75, temp ≈ 20°C. DNA was obtained from Wistar rats after 4 months iron loading. The figure demonstrates that DNA strand breaks occur as an early event of iron-overloaded-induced oxidative stress.

10.0 DISCUSSION

10.1 AN ANIMAL MODEL FOR DIETARY IRON OVERLOAD

Animal models of dietary iron overload have been studied repeatedly but not systematically. To date, no study has been done on different species of a particular animal using one type of dietary iron. Conversely, different types of dietary iron on one particular species of animal have also not been studied. The different animal models and different iron preparations, as well as different routes of drug administration, have yielded various histological representations of haemochromatosis. Nevertheless, animal models of dietary iron administration have provided important information about the mechanisms involved in pathophysiology of excess iron.

Park *et al.* (1987) achieved mild fibrosis and histological iron grading of 3 - 4 after feeding SD rats with 3% carbonyl iron (CI) for 12 months. Iancu *et al.* (1987) fed SD rats 2% CI for 15 months. A hepatic iron concentration of 1060 μg/g dry wt. was attained, in contrast to 8000 μg/g reported by Park *et al.* (1987). Plummer *et al.* (1997) fed Poton rats 2% CI and by 32 weeks, grade 3 - 4 hepatic iron concentration had been achieved. No fibrosis was apparent in any of the livers. Olynyk *et al.* (1995) fed lactating Wistar Furth rats 3% carbonyl iron. Pups continued on a 0.6% CI liquid diet. By 26 weeks all rats had grade 4 siderosis. Focal fibrosis was seen around Fe-laden periportal macrophages only. Oates *et al.* (2000) studied excretion in Fe-loaded rats following the change from an Fe-loaded to an Fe deficient diet. Wistar rats were fed 3% CI for 9 weeks. This resulted in a 20-fold increase in liver non-haem Fe (2110 ± 0.32 μg/g dry wt.). Fe-loading of hepatocytes was most prominent in the periportal region (zone I and II). Pietrangelo *et al.* (1990) analysed

the level of gene expression in Wistar albino rats during chronic Fe overload. Rats were fed 3% CI for 30 weeks. The liver Fe content was 2110 ± 345 μg/g dry wt. No histological signs of liver damage were evident.

Recent reports of the use of a more organic iron, ferrocene, to feed Wistar albino rats show promise of an experimental approach to characterizing the histopathological similarities to chronic hepatic Fe overload observed in humans. For example, Ward *et al.* (1991) fed Wistar rats 5 mg/day ferrocene for 6 weeks. Histologically, there were striking similarities to the livers of HH patients with grade 3 Fe overload. Dullman *et al.* (1992) also reported mild signs of fibrosis after 34 weeks of feeding Wistar rats 0.5% ferrocene. Stainable hepatic Fe at 39 weeks was grade 3 - 4. Nielsen *et al.* (1993) observed necrosis and mild fibrosis when Wistar rats were fed 0.5% ferrocene. The liver Fe concentration was 14.7 ± 1.4 mg /g dry wt. at 39 weeks. In the present study, the Wistar albino rat attained a maximum of grade 2 hepatic iron overload after 12 months on 2.5% CI. After switching over to 0.5% ferrocene (w/w) hepatic Fe reached grade 4 within 4 months. The serum Fe level of the control group was lowest and remained fairly unchanged until 20 months when it declined. Mean liver iron concentration of all Fe-loaded groups was 19.8 ± 6.9 mg/g w. wt (33 times above control value) at 32 months.

Ahluwalia *et al.* (2000) reported a decline of serum Fe in Lewis rats after 22 months. The reduced level of serum Fe in older rats therefore, may be a normal event. In the present study, all other groups remained prominently high after 8 months (Figure 18, page 226). Furthermore, the initial poor Fe loading up to 8 months could be the result of the 2% CI

administered at that time, although Olynyk *et al.* (1995) reported 3-4+ hepatic iron grading after feeding Wistar Furth rats on a 0.6% CI liquid diet for 8 weeks (after weaning from mothers that were fed 3% CI supplemented diet). In the present study, when CI was increased to 2.5%, a sharp increase in serum Fe was observed up to 12 months. Nevertheless, hepatic Fe was still grade 2. Although other researchers reported good initial hepatic Fe loading with 2-3% CI, this may be attributed to the different rats species used (Plummer *et al.*, 1997; Park *et al.*, 1987; Iancu *et al.*, 1987).

In the present study, 0.5% ferrocene was introduced after 12 months to replace the 2.5% CI. The increase between 12 and 16 months resulted largely from ferrocene administration and not the effect of ferrocene superimposed on CI. This was proved by feeding two new sets of Wistar rats with 2.5% CI and 0.5% ferrocene, respectively, for 17 months. The serum Fe concentration of the CI-fed group was almost the same as that obtained at 12 months in the previous experiment, but slightly below levels at 16 months. The ferrocene-fed group however, had higher values corresponding to that obtained at 16 months in the initial experiment. In addition, the histological grading of hepatic Fe was still 2+ in the CI-fed group and 4+ in the ferrocene-fed group. The plateau seen after 16 months could be the result of Tf saturation. The Fe groups obtained a maximum serum Fe concentration from 118 to 134 μmol/l between 16 and 24 months. The minor peak at 4 months was not statistically significant. Moreover, hepatic Fe loading was 1+ at that time-point. The peak seen at 16 months was statistically significant ($p=0.05$), however. The sharp decrease in serum Fe concentration of the Fe + Cu group between 20 and 24 months cannot be explained.

Furthermore, the analysis of variance shows that both time and treatment and their joint interaction had significant effects on serum iron (see section 9.3.1, page 216). It was noted that significant differences ($p<0.0001$) across the groups resulted from experiments carried out for periods <12 and >16 month. Hepatic Fe that was 4+ at 16 months and beyond also accompanied this significant difference after 16 months. In the Fe group, serum iron concentration was a predictive indicator of LPO and its by-product MDA (Table 44x). In the Fe – V and Fe + ASA groups, serum Fe was a predictive indicator of MDA concentration. In the Fe + Cu group, serum iron significantly predicted $^{\bullet-}O_2$ production and 8OHdG formation.

Although Fe overload diseases are generally regarded as examples of diseases involving oxidative stress, one study has suggested that Fe deficiency is associated with increased production of ROS. Rao and Jagadeesen (1996) showed that on feeding rats carcinogens, Fe deficiency rendered the rat more susceptible to tumourigenesis by a mechanism involving oxidative stress. On the contrary, Lemmer *et al.* (1999) reported that dietary Fe loading appeared to offer protection against the cancer-promoting properties of the mycotoxin fumonisin B_1.

In the published animal studies on haemochromatosis by other researchers, successful Fe loading was variously achieved. However, the Fe overload never resulted in HCC. The present study is the first to produce an animal model of haemochromatosis that progressed to the development of HCC. In addition and, of great significance, hepatic Fe loading of grade 4 and HCC developed in the absence of cirrhosis or fibrosis.

Fe may act as a genotoxic substance (Deugnier *et al.*, 1992), as a mitostimulatory agent (Crane *et al.*, 1985), as a promoter (Fellows *et al.*, 1988) or as a cofactor that enhances tumour formation induced by other carcinogens (Blumberg *et al.*, 1988). Furthermore, Fe stimulates growth of preneoplastic cells *in vitro* (Rotstein *et al.*, 1986), and Fe deprivation decreases cell growth of cultured hepatoma cells (Solt and Farber, 1976). On the contrary, studies conducted by Stal *et al.* (1995, 1999) suggest that Fe does not promote growth of initiated cells, and does not enhance progression of these into HCC. However, the present study has shown that Fe was involved in the initiation, promotion and progression of liver cells into HCC.

10.2 DIETARY IRON OVERLOAD AND HCC

An animal model of dietary Fe overload leading to HCC has hitherto not been produced. Attempts made by several researchers have resulted in haemochromatosis without HCC (Bacon *et al.*, 1983; Goddard and Sweeney, 1983; Park *et al.*, 1987; Iancu *et al.*, 1987,1988; Ward *et al.*, 1991; Pietrangelo *et al.*, 1995a, 1995b; Onylyk *et al.*, 1995; Plummer *et al.*, 1997; Valerio and Peterson, 2000; Arezzini *et al.*, 2003). The present study is the first in which dietary exposure to iron has produced Fe overload that was complicated by HCC development. Data presented in Table 46x (see appendix E) show a gradual hepatic Fe overload over 32 months. At 4 months, all Fe-loading groups had grade 1+ Fe overload. At 8, 12 and 16 months, this progressed into 2+, 2+ and 4+ respectively, and remained at 4+ until the end of the study (Figure 45, page 239). The control group had grade 0 Fe load throughout, except at 24-28 months when traces of iron were seen in a few, and surprisingly at 32 months about half of the surviving control rats had hepatocyte Fe

grade 2+ and the other half, 0. Kupffer cell Fe on the other hand was 2+ at 16 months when hepatic Fe was 4+. Fe load in the Kupffer cells increased to 3+ at 20 months and most of them stained 4+ at 24 months. At 28 and 32 months, all Kupffer cells were 4+. The portal tract was also loaded with Fe but not the bile ductular cells.

The main cellular elements of the liver involved in Fe uptake are the hepatocytes, Kupffer cells and sinus-lining endothelial cells. The distribution of Fe in these cells depends on the mode of application. Intravenously administered Fe is first taken up and stored by the Kupffer and sinus-lining endothelial cells and accumulates in parenchymal cells at a later stage only (Kuchta *et al.*, 1982). In contrast, orally given compounds at first induce a predominantly hepatocellular Fe accumulation. The distribution seen in the present study was predominantly hepatocellular at first, followed by Kupffer cell Fe loading. This preferential location is similar to that described by Park *et al.* (1987) and Iancu *et al.* (1987). In HH, the excess Fe reaches the liver via the enteral route, which leads to primary parenchymal Fe deposition (Stal *et al.*, 1990), in contrast to the reticuloendothelial (Kupffer) cells Fe overload seen after parenteral injections with Fe-dextran (Carthew *et al.*, 1991). In the present study, antioxidant vitamins and Cu did not interfere with the level of hepatic Fe loading or with the pattern of preferential Fe loading, mainly in the hepatocytes and Kupffer cells at first, and then fully saturated in the hepatocytes at 16 months, followed by saturation in the Kupffer cells between 24 and 28 months.

Early signs of iron-free foci (IFF), which are nodules of hepatocytes found in HH (Williams and Yamamoto, 1972; Powell and Kerr, 1975; Deugnier *et al.*, 1993a), with

significantly less or no Fe in the foci compared with the surrounding parenchyma, were seen after 20 months (Figure 46, page 240). IFF may be single or multiple, and are considered to be preneoplastic in nature. Of the 25 (iron-overloaded) samples presented for histological examination at 20 months, 5 (20%) had IFF and 1 was indeterminate (borderline case). Two of the 5 occurred in the Fe group, 2 in the Fe – V group, and 1 in the Fe + V group. The borderline case IFF belonged to the Fe + V group. At 24 months, 4 out of 34 (12%) Fe-overloaded livers had IFF, with 2 from the Fe group being very prominent. The remaining 2 belonged to the Fe – V and Fe + V groups. However, the number of samples with borderline IFF increased to 7. Furthermore, none of the samples (at 24 months) from the Fe + ASA and Fe + Cu groups showed signs of IFF. IFF were only noticed in those groups after 28 months. Of the 54 iron-loaded samples presented for histological examination at 28 months, 16 had IFF (30%). Twelve out of 26 iron-overloaded samples (46%) submitted to histological examination at 32 months had IFF and 2 were borderline cases. Two livers with IFF were found in the Fe group, 5 in the Fe + V group, 5 in the Fe + ASA group and the 2 borderline cases belonged to the Fe group. Out of the 144 Fe-overloaded samples examined between 20 and 32 months, 37 (26%) had IFF. The breakdown is as follows: F group = 10, Fe + V group = 12, Fe – V group = 6, Fe + ASA group = 8 and Fe + Cu group = 1. In comparison, Deugnier *et al.* (1993a) reported that 7.6% of 185 patients with uncomplicated HH had IFF in their livers. A later study by (Deugnier *et al.*, 1993b) revealed that IFF were present in 83% of the livers of HH patients with HCC. In this study, multiple IFF occurred in one sample from the Fe + V group and both small and large IFF were observed (Figure 48, page 241). Multiple IFF have been reported in HH (Deugnier *et al.*, 1993a). In their study IFF found in patients with untreated

HH and HCC, were always numerous and ranged in size from 1 to 7/cm^2. It was also observed that the distribution of IFF in HH was similar to that of foci with altered hepatocytes in chemically induced cancer, suggesting that IFF are proliferative lesions that may progress to HCC, as hypothesized in experimental carcinogenesis (Terada and Nakanuma, 1989a, 1989b; Deugnier *et al.*, 1993b). In HH patients with IFF studied by Deugnier *et al.* (1993b), more than 50% developed HCC compared with 8% of control patients without IFF. IFF in the livers in the present study appear to be a preneoplastic change. Furthermore, it has been shown that in iron-overloaded rats with chemically induced liver cancer, early nodules of altered hepatocytes thought to be involved in cancer development did not stain for iron (Stal *et al.*, 1995, 1999). Iron depletion was regarded as one of the earliest criteria for the identification of putative preneoplastic foci (Williams and Yamamoto, 1972; Hirota *et al.*, 1979). A later review by Williams (1989) suggested that only a few of these foci developed into neoplasms. Furthermore, the author reported that the rate of transformation from foci to cancer nodules has been estimated to be 1 in 1,000 to 1 in 2,500.

Inclusions resembling Mallory bodies (MB) [an accumulation of intermediate filaments of prekeratin (cytokeratin) in the cytoplasm of some damaged hepatocytes, seen in association with microtubular failure, vitamin A deficiency or as a marker of preneoplasia] were observed. MB was first identified at 20 months in association with IFF in the Fe group and again at 28 months in association with IFF, fat and stem cells in the Fe + V group (Figure 49, page 242). MBs are characteristically associated with alcoholic and non-alcoholic steatohepatitis (NASH), but are also present in benign and malignant hepatocellular

neoplasms, and a diversity of metabolic, toxic and chronic cholestatic liver disorders. MB formation in animal models of alcoholic steatohepatitis (ASH) and NASH has been demonstrated repeatedly (Denk *et al.*, 1979; Tsunoo *et al.*, 1987; Lieber *et al.*, 1989). In the present study, the presence of MB was thought to be an indication of preneoplasia. Fat and fatty foci were also identified and mostly associated with IFF. Fat accumulation may have resulted from defective fat metabolism. Microsteatosis was present at 28 months in 4 samples. Of the 4 cases, 2 were found in the Fe + V group and 1 in the Fe group. However, this was not peculiar to the Fe-loaded groups as 1 case was seen in the control group.

Hamartoma (a tumour-like but non-neoplastic aggregation of cells) was found in one of the 12 Fe group livers taken at 28 months. Within the same sample size of 12, one liver had microsteatosis, Gandy-Gamma bodies (deposits of hemosiderin and calcium) and an inconclusive adenoma was seen in one sample belonging to the Fe group at 32 months. Liver tissue frequently showed bile duct proliferation and occasional Von Meyenburg complexes (VMCs) were also identified. As reported in isolated cases in literature (Yaziji *et al.*, 1997; Balnc *et al.*, 2000; Morcos *et al.*, 2001), VMCs (and to lesser extent bile duct adenomas) are relatively common in liver diseases of people with HH. Although it has been suggested that a putative carcinogenic effect of iron on biliary cells may explain the occurrence of cholangiocarcinoma (Morcos *et al.*, 2001; Jain *et al.*, 2000), no such observation was seen in the present study. Furthermore, VMCs also occurred in 2 samples from the control group. The bile ductules did not show any accumulation of iron throughout.

Liver cell dysplasia was also observed at 28 months in the Fe group (Figure 49, page 242). Anthony *et al.* (1973), who first described liver cell dysplasia, suggested a possible chronological progression from cirrhosis to dysplasia to HCC. The progression is similar to the cellular evolution from initiated preneoplastic hepatocytes to HCC seen in experimental carcinogenesis. In another study, however, it was reported that the frequency of dysplasia in southern African HCC patients was high whether cirrhosis was present or not, implying that this progression was not constant (Cohen *et al.*, 1979). Furthermore, Kew *et al.* (1980) showed no statistically significant difference in the frequency of liver cell dysplasia between cirrhotic and noncirrhotic patients with HCC. However, the frequency of liver cell dysplasia in patients with HCC is 49.7% in Uganda (Anthony *et al.*, 1973), 19.4% and 23% in Japan (Sakuria, 1978; Nakashima *et al.*, 1983), 80% and 48% in southern Africa (Kew *et al.*, 1980; Cohen *et al.*, 1979). This suggests that liver cell dysplasia is a major risk factor for HCC (Paterson *et al.*, 1989; Borzio *et al.*, 1995). Liver cell dysplasia could be large or small. Large liver cell dysplasia (LLCD) refers to the presence of groups of hepatocytes with nuclear and cellular enlargement, normal nucleocytoplasmic ratio, nuclear pleomorphism, multinucleation and prominent nucleoli (Anthony *et al.*, 1973; Anthony, 1976, 1979). Small liver cell dysplasia (SLCD) was defined according to Watanabe *et al.* (1983) as groups of hepatocytes with decreased cytoplasm, slight nuclear pleomorphism and an increased nucleocytoplasmic ratio, leading to the impression of nuclear crowding. Previous studies have shown the LLCD is a risk factor for HCC in patients with cirrhosis of various and unknown aetiology (Borzio *et al.*, 1995; Ganne-Carrie *et al.*, 1996). Furthermore, Libbrecht *et al.* (2000) have shown that the presence of LLCD in patients with non-cirrhotic chronic viral hepatitis is an important

independent factor for the development of HCC. In addition, a study by Grand-Lemaire *et al.* (1999) showed that patients with HCC in the absence of cirrhosis had pathological changes, especially iron overload and LLCD in the non-tumourous liver tissue. The researchers suggested that HCC could originate even in non-cirrhotic livers. Deugnier *et al.* (1993a) reported of 10 patients with LLCD in IFF and of the 10, 50% developed HCC. In the present study, LLCD was seen at 28 months in the absence of cirrhosis and was associated with IFF.

Hepatocellular adenoma (HCA) was seen in one sample from the Fe group at 28 months. Benign hepatic tumours, such as HCA and adenomatous hyperplasia (AH), result from a variety of neoplastic and regenerative proliferative processes. HCA is an uncommon benign tumour of the liver, most frequently occurring in women with longstanding contraceptive steroid use. HCA in men is usually associated with glycogen storage disease, diabetics, and the use of androgenic anabolic steroids. Malignant transformation of HCA is rare, but it may be difficult to differentiate a benign tumour from a well-differentiated HCC (Brunt, 2001). The frequent occurrence of HCA in liver may lead to hepatocellular adenomatosis, which is a rare disease (Radhi *et al.,* 2000). However, HCA in a young woman with β-thalassemia associated and secondary iron overload has been reported (Cannon *et al.*, 1981). In addition, HCA in a non-cirrhotic HBV-related chronic liver disease has recently been reported (Hsu *et al.*, 2003). HCA in experimental iron overload, apart from the present study, has so far not been reported.

HCC was a borderline case in one of the 6 samples from the Fe + V group at 32 months. However, HCC developed in one out of the 8 rats that survived up to 32 months in the Fe group. The HCC was 2 cm in diameter (Figures 51, page 244). Of the remaining 7 rats, 3 with IFF were confirmed malignant by glutathione-sulfhydryl-transferase-π (GST-π) stain (Figure 48, page 241). This is the first time HCC has been shown in an experimental rat model of haemochromatosis (Figures 53 & 54, page 246). In addition, fibrosis and cirrhosis, which are often present when HCC develops in HH, were not present (Figure 52, page 245). Other Fe overload animal studies did not observe fibrosis (Iancu *et al.*, 1987; Plummer *et al.*, 1997; Pigeon *et al.*, 1999) while others reported mild fibrosis (Park *et al.*, 1987; Valerio *et al.*, 2000; Arezzini *et al.*, 2003). The link between oxidative stress and experimental animal models of fibrogenesis has not been firmly established (Pietrangelo, 1996). It is argued that during experimental Fe overload in rats, levels of oxidative damage remain below a theoretical threshold at which stimulation of fibrosis occurs. Data from Brown *et al.* (2003) suggests that Fe induced oxidative stress elicits an adaptive response involving thiol metabolism that effectively limits the accumulation of oxidative (lipid) damage and that may protect against fibrosis. Similarly, HCC occurring in non-fibrotic livers have been reported in humans (Bralet *et al.*, 2000).

Cirrhosis originally was thought to be the cause of HCC in patients with HH. However, patients with HH are also at high risk for developing HCC in the absence of cirrhosis. Furthermore, a number of studies have confirmed that cirrhosis is not an absolute prerequisite for the development of HCC in the haemochromatotic liver (Deugnier *et al.*, 1993a; Fellows, 1990; Blumberg *et al.*, 1988). It has recently been reported that the C282Y

and H63D mutations found in HH do not appear to be associated with an increased risk of HCC in patients with cirrhosis (Boige *et al.*, 2003). In addition, HCC associated with secondary haemochromatosis in a non-cirrhotic liver of a 40-year-old multiply transfused patient, has been reported (Chung *et al.*, 2003). This is similar to the present finding of HCC in a non-cirrhotic animal model of haemochromatosis. Furthermore, HCC has been reported to be more aggressive in Fe-overloaded patients without cirrhosis than in those with cirrhosis (Choong *et al.*, 2003). In the present study, AFP levels were within the normal range up to 24 months, although values increased with time as shown in the dotted data (see Table 8y, Appendix F).

The major risk factors for the development of HCC are now well recognised and models of neoplastic transformation have been used to identify a multiple step pathway. Three stages involved in hepatocarcinogenesis have been identified in a number of animal studies including initiation, promotion and progression (Dragan and Pitot, 1992). Studies of age-dependent tumour formation in rats suggest that as many 5 or 6 steps may be involved (Okuda, 1992). Initiation of cellular transformation involves the formation of abnormal cells containing an irreversible genetic change, occurring either spontaneously or as a result of exposure to chemical or biological agents. During the promotion stage, selected cells clonally expand into foci of altered hepatocytes. This promotion step may be reversible (Solt *et al.*, 1980); it is greatly influenced by the continuous presence of a promoter agent and for an extended period (Laconi *et al.*, 1993). In the progression stage, subsets (1% to 5%) of these foci eventually progress through a process of neoplastic transformation into frank malignancy. Androgens and estrogens, the ornithine

decarboxylase activity and growth factors are thought to influence tumour-promotion. This process involves additional genetic alterations that include activation of oncogenes and/ or inactivation of tumour suppressor genes (Cote *at al.*, 1985; Hsu *et al.*, 1991). The way in which the possible mechanisms of hepatic oncogenesis operate at the molecular level is still incompletely understood. However, possible biochemical explanation for the role of Fe and oxidative stress in the development of HCC in the present study is further discussed.

10.3 DIETARY IRON OVERLOAD AND OXIDATIVE STRESS

Cellular damage arising from an imbalance between ROS- generating and -scavenging systems has been implicated in the pathogenesis of a diverse range of human disorders, including liver diseases. With regard to the latter, the most widely studied areas include the toxic reactions to acute and chronic ethanol ingestion. The involvement of ROS in alcoholic liver disease is not, of course, exclusive in terms of tissue damaging agents. Free radicals are also thought to play a role in liver damage caused by viral hepatitis, Wilson disease, drug-induced liver damage and haemochromatosis, to mention just a few.

10.3.1 $^{\bullet-}O_2$ Production

The level of involvement of the $^{\bullet-}O_2$ radical in the Fe-induced liver damage in the present study was investigated. Superoxide radical ($^{\bullet-}O_2$) levels in Fe-overloaded rats are shown in Figure 19 (page 226). The control group showed little change, and had the lowest $^{\bullet-}O_2$ level. This steady state suggests that other agents of oxidative stress did not exacerbate the effect of the Fenton reaction. The Fe, Fe + V, Fe – V and Fe + ASA groups showed more

impressive changes, having peak values at 12 months. However, differences between the Fe-supplemented groups and the control group were not statistically significant. Although the Fe + Cu group had an early peak at 4 months, the pattern of the curve did not correlate with the others and was not significantly different. A significantly positive correlation was found between the Fe and Fe + ASA, Fe and Fe – V, Fe – V and Fe + ASA, Fe – V and Fe + V groups. The analysis of variance on $^{\bullet-}O_2$ in this study showed that treatment type (i.e. the addition or omission of antioxidants) did not have any significant effect on $^{\bullet-}O_2$ production (see section 9.3.4). However, the regression analyses of the various animal models showed that in the Fe, Fe + V and Fe + ASA groups, the $^{\bullet-}O_2$ levels significantly predicted LPO. In the Fe – V group, Cu was significantly predictive of $^{\bullet-}O_2$ production ($p=0.0002$) and in the Fe + Cu group, serum Fe influenced $^{\bullet-}O_2$ production.

Aruoma *et al.* (1991) examined the production of $^{\bullet}OH$ during oxidative stress by confirming the pattern of damage to the purine and pyrimidine bases of DNA exposed to Cu ions and H_2O_2, and showing that the pattern was characteristic of $^{\bullet}OH$ attack. Kamp *et al.* (1995) also demonstrated that asbestos-induced alveolar epithelial cell injury *in vitro* is the result of Fe-catalyzed $^{\bullet}OH$-like free radical generation, which in turn causes DNA strand breaks. Furthermore, cell-associated reactive Fe is more prone than extracellular Fe to induce $^{\bullet}OH$ generation (Demougeot *et al.*, 2000). In addition, Bruck *et al.* (2001) prevented cirrhosis in rats by $^{\bullet}OH$ scavengers. Although *in vitro* studies have demonstrated the production and quenching of $^{\bullet-}O_2$ by antioxidants (Jovanovic *et al.*, 2000), $^{\bullet-}O_2$ was not the ultimate reactive free radical produced in the present study because the levels

generated were not significant. Thus, the $^{\bullet}OH$ free radical remains the more likely ROS produced during Fe-induced oxidative stress.

10.4 DIETARY IRON OVERLOAD AND ANTIOXIDANTS

Primary and secondary Fe overload disorders are characterized by, the accumulation of Fe in mononuclear phygocytes and parenchymal cells of the liver and other organs. Fe is a catalyst in the Habar-Weiss reaction and is involved in the initiation and propagation of LPO. Considering the role of Fe in Fe reactions, the question is whether antioxidant compounds may have additional therapeutic value in supporting the antioxidant defence at the cellular level and, if so, which antioxidants are of importance in haemochromatosis.

10.4.1 GPx

Glutathione peroxidase (GPx) reduces GSH (reduced glutathione) to GSSG (oxidized glutathione) and in the process converts H_2O_2 to H_2O and O_2, and LPO into lipid alcohol. GPx levels of Fe-overloaded rats are shown in Figure 20. All groups except Fe – V group had a similar undulating nature. The curves of the control and Fe + Cu groups remained the highest up to 10 months. The control and Fe + V groups continued to be above the others from 14 months to the end. In the case of the control group, the absence of oxidative stress did not pose a challenge to the antioxidant defence system in the normal rat, hence the high GPx values. Similarly, Vitamins A and E reduced the impact of ROS on GPx. Hence the high GPx level in the Fe + V group, especially in the second half of the Wistar rat's life, even though hepatic Fe overload was 4+. Similarly, Hamilton *et al.* (2000) showed that

vitamin E supplementation increased GPx activity and the authors suggested a homeostatic control of antioxidants. The reverse is seen in the Fe – V group where GPx was low throughout. In this same group, GPx & catalase and GPx & ORAC-A, were significantly negatively correlated (see section 9.2.4.5, page 205). Thus, catalase, which plays a similar role in breaking down H_2O_2 to H_2O and O_2, may have augmented the function of GPx. In the regression analysis, GPx was not predictive of most of the other parameters. Because H_2O_2 itself is a minor ROS with less potency in liver oxidative stress, GPx may not be an important antioxidant in Fe-induced oxidative stress. Fletcher *et al.* (1989) measured the activity of GPx in the livers of iron-loaded rats fed 1.0% - 2.5% CI, and reported no significant differences in the GSH and GPx activity, although there was a trend of increased GPx activity in the rats receiving 2.5% CI. Similarly, other researchers (Selden *et al.*, 1980; Young *et al.*, 1994) found no statistical difference between hepatic GPx concentration of HH patients and controls. These results also suggest that GPx may not be an important antioxidant in Fe-induced oxidative stress. However, significant differences were found between GPx of the control group and the Fe group, as well as the control and Fe-V groups in the present study, suggesting some importance of GPx in oxidative stress. Furthermore, in the Fe group only, GPx significantly affected 8OHdG levels ($p=0.0121$). The discrepancy between this GPx levels in this study and that of others, may be attributed to the particular period when GPx was measured in any of the above experiments. For example GPx levels of the control and Fe groups were statistically significant between 12 and 16 months, but not 16 and 20 months (Table 30x).

10.4.2 SOD

SOD (a CuZn- or Mn- containing enzyme) removes $^{\bullet-}O_2$ by converting it into H_2O_2 that is then removed by GPx. During this process the Fe-transporting protein, Tf, is normally kept around 30% Fe saturation to ensure that no Fe is available to catalyse the formation of dangerous radicals such as $^{\bullet}OH$ (Halliwell and Gutteridge, 1992).

SOD levels of Fe-overloaded Wistar rats are given in Figure 21. All the groups including the control exhibit an undulating pattern. The control group remained the highest and the Fe – V group the lowest, implying that oxidative stress reduces the level of SOD in Fe loading conditions. This observation is contrary to that of Broide *et al.* (2000) (who noted a significant increase in liver SOD activities in children with cholestastic liver disease), but similar to that of Irshad *et al.* (2002), who observed a reduction in SOD in various forms of liver diseases. Significant differences were observed between 8 and 12 months ($p=0.05$) and, 12 and 20 months ($p=0.05$). This may be attributed to the period when CI was increased from 2 to 2.5% (after 8 months) and when ferrocene was introduced (after 12 months). SOD levels in all groups declined after 12 months. This decline is normal and associated with age (Glass and Gershon, 1981). In addition, significant differences were observed between the control and the various groups. Comparison between the control and the Fe groups (8-12 months) shows that dietary iron reduced the erythrocyte SOD concentration by about 60%. Contrary to the observations of Yasa *et al.* (1999) and Cristol *et al.* (1999), in the present study oxidative stress reduced SOD activity at all time points throughout the study (Figure 21, page 226).

Fletcher *et al.* (1989) reported a 75% reduction in liver SOD level after feeding rats with CI for 28 days. The researchers speculated that the loss of antioxidant protection provided by SOD relatively early in the process of hepatic Fe deposition, may be an important factor contributing to LPO, which was later observed in that work as well as in the present study. However, a different observation between SOD and LPO (measured as TBARs) was made by Cristol *et al.* (1999), who noted that the antioxidant defence mechanism in elderly women was impaired without markers of oxidative stress, when compared with healthy volunteers. SOD activity was significantly decreased. However, no corresponding increase in TBARs levels was observed. Similarly, Yasa *et al.* (1999) also noted SOD differences were statistically significant in cirrhotic patients and controls, but not TBARs. Furthermore, no correlation between SOD and TBARs was found in that study. In the present study, a weak correlation between SOD and the products of LPO was found, except in the Fe + Cu group where a strong correlation occurred between SOD and 8-IP ($r=0.59$, $p=0.0007$) (Table 21x). This association cannot be explained. In conclusion, SOD is an important enzyme in Fe-induced hepatic oxidative stress, but may not directly influence LPO.

10.4.3 Catalase

Catalase and GPx in the erythrocyte are not compartmentalized and therefore studies performed on the hemolysate are a reflection of similar conditions within the erythrocyte. Furthermore, catalase is the major H_2O_2 decomposing enzyme in normal erythrocyte. It decomposes H_2O_2 without generation of free radicals by minimizing one-electron-transfers. Hence, the protective role against free radicals may be its main physiological

function within the cell.

Catalase levels of Fe-overloaded Wistar rats are shown in Figure 22 (page 226). Generally, an increase was observed at 2 and 8 months. The control group remained the highest throughout with the Fe – V group the lowest. The pattern seen here is very close to the SOD curve in Figure 21. This suggests that the intracellular antioxidant enzymes play an important role in cellular antioxidant defences.

Soltys *et al.* (2001) observed that the administration of 100 units of vitamin E/kg by gavage for 2 days before sacrifice, improved the catalase activity in oxidatively stressed obese rats compared with the level seen in lean rats. In this study, catalase decreased from the 8 month peak to its lowest at 16 months, when liver Fe had attained a maximum of 4+. It is believed that there is interplay of the lipid-soluble antioxidants and water-soluble antioxidants in maintaining the overall antioxidant balance in the host. For example, in Figures 20-24 the values of the control group were higher than the other groups at almost all time-points. This was closely followed by the Fe + V group, whiles the Fe - V group was almost always the lowest. However, in Figure 25, the control group is the lowest (12-24 months) and the Fe - V group the highest as seen in the curves of aqueous-soluble phase (ORAC-A) between 14 and 22 months.

10.4.4 Vitamin C

Vitamin C is considered as one of the most important and least toxic of the natural antioxidants (Weber *et al.*, 1996). It is water-soluble and found in high concentrations in

many tissues. Additionally, vitamin C accounts for 10-15% of the antioxidant capacity in fasting plasma (Benzie and Strain, 1997).

Vitamin C levels of Fe-overloaded Wistar rats are shown in Figure 23 (page 226). There was a general increase from about 1 μmol/l to about 6.5 μmol/l over 24 months. The control and Fe + V groups were mostly the highest, with the Fe + Cu and Fe groups being the lowest. All other groups were in between. The increase in vitamin C status after supplementation with α-tocopherol might be linked to increased absorption and or decreased plasma clearance of ascorbic acid. This rate of increase depicted in Figure 23 decreased at 4, 12 and 20 months. However, these decreases were statistically insignificant. A study conducted by Hamilton *et al.* (2000) showed that supplementation with α-tocopherol (7.35mg/d) in humans (for 6 weeks) was associated with increased plasma ascorbic acid concentration, as well as improved vitamin E status, even though the latter was relatively small. Lenton *et al.* (2000) demonstrated that seasonal changes account for the undulating nature of curves of vitamin C concentration with time in humans. Furthermore, this undulating nature was also associated with age. Under the experimental conditions of controlled daylight, humidity and temperature in this study, this was not expected in the Wistar rats, unless the animal has its own body clock irrespective of its immediate environmental factors.

Zolch and Ginter (1995) showed that in guinea pigs deficient in vitamin C, ethanol administration caused greater depletion in vitamin C. However, in rats, daily consumption of ethanol resulted in an increase in the body stores of vitamin C as a result of its enhanced

biosynthesis. Suresh *et al.* (1999) obtained similar results of a lower hepatic but a higher plasma vitamin C level upon ethanol administration. Ethanol administration creates oxidative stress, and perhaps the increase in oxidative stress in this study may account for the rise in vitamin C levels.

Significant differences in vitamin C levels were observed between the Fe + V and Fe groups, Fe + V and Fe – V groups, and, Fe + V and Fe + Cu groups (Table 34x). Thus, antioxidant supplementation significantly affected vitamin C levels in the Fe-fed groups. However, there was no significant difference between vitamin C in the control group and other groups. Similarly, Solty *et al.* (2001) working with Zucker rats under oxidative stress noted that the liver vitamin C level of the obese rats (oxidatively stressed group) was not significantly different from those of the lean group (without oxidative stress). Furthermore, Figure 23 shows an increase in vitamin C throughout the period with little differences in rate of increase between the groups. One possible reason for this unexpected behaviour might be related to the ability of the adult rat to easily synthesize vitamin C and thus resist the effect of scorbutic conditions (Meister, 1994).

It is noted from Figure 23 that between 16 and 24 months vitamin C in the control group did not increase above 5.6 μmol/l. However, at 24 months all other groups were above this value. It is assumed that oxidative stress was maximal after 16 months when hepatic iron was 4+. Under such conditions, plasma vitamin C increased whereas hepatic vitamin C decreased, as inferred from ORAC studies in Figure 25 (page 227), where the water-soluble antioxidants decreased after 12 months and declined further between 16 and 24

months. This apparently low vitamin C level in the control group (Figure 23) may have contributed to an increase in lipid peroxidation, as observed later (Figure 29, page 227) and also suggested by Halliwell and Gutteridge (1989). The interaction of vitamin C with other parameters was examined by correlation analysis. A strong positive correlation between vitamin C and DNA damage (estimated by 8OHdG measurements) for all Fe-fed groups was observed. However, the weakest correlation between vitamin C and 8OHdG was found in the control group. It is possible that vitamin C in the Wistar rat seems to have a pro-oxidant tendency that is aggravated under oxidative stress.

The present study showed that a decrease in dietary vitamins in the Fe – V group did not affect serum vitamin C levels (Figure 23, page 226). Furthermore, no correlation between GPx and vitamin C was observed in all groups except for a weak correlation seen in the Fe + V group. On the contrary, Lykkesfeldt *et al.*, (1998) demonstrated that the increase in the antioxidant glutathione was accompanied by increased vitamin C after the injection of lipoic acid. Lastly, there was no correlation between vitamin C and FADU in all groups.

10.4.5 TAS/ORAC

Figures 24 and 25 (page 227) relate to the total antioxidant status of the plasma and liver, respectively. The trolox equivalent antioxidant capacity (TEAC) assay of Miller *et al.* (1993) is based on the inhibition of the absorbance of the radical cation, 2,2'-azinobis(3-ethylbenzthiazoline 6-sulphonate) [$ABTS^{(+)}$], by antioxidants (Figure 24). ORAC (Figure 25) on the other hand depends on the unique properties of phycoerythrin (PE). It relates a lag phase or a rate constant of PE florescence decay to antioxidant capacity of an added

antioxidant sample. To date, it is the only method that takes the reactive species to completion and uses an "area under the curve" technique for quantification, thus combining both inhibition time and inhibition percentage of the reactive species action by antioxidants into a single quantity.

In Figure 24, the control group is the lowest before 12 months. Similar observations were made by Irshad *et al.* (2002), who noted that TAS was in some cases higher in patients with liver diseases than in matching controls. The high TAS level in the various test groups compared to the control group suggests that oxidative stress in various tissues leads to an enhanced expression of antioxidant enzymes, as observed by Venkatraman *et al.* (1994). However, the control group in the present attained the highest level, well separated from the rest between 10 and 24 months. This is an indication of a compromised antioxidant defence system in the Fe-fed groups after 12 months, when hepatic Fe increased significantly.

Whereas Figure 24 is a reflection of plasma total antioxidant capacity, Figure 25 is a refection of the total antioxidant capacity in the liver assessed by a different method. In Figure 24, the peak occurred at 20 months whereas in Figure 25, it occurred at 12 months. Thus, the antioxidant capacity of the liver was long saturated before it became evident in the plasma. This correlates well with the immunohistological findings that as early as 12 months LPO and DNA oxidative damage could not be attenuated by antioxidants in the liver. Khan *et al.* (2002) also observed the presence of HNE and MDA adducts in the liver, after 6 weeks of feeding SD rats 2.5% CI. In Figure 25, the control group is the highest up

to 8 months and thereafter falls below the rest of the groups. However, in Figure 24 the control group is the highest after 8 months with all other groups below the control group. An inverse relationship between the plasma and liver total antioxidant capacities appear to exist.

The analysis of variance shows that both time and treatment had significant effects on TAS ($p<0.0001$, $p<0.0001$, respectively). The interaction of time and treatment also had a significant effect on TAS ($p=0.0002$) (Table 25x). The multiple comparison test results in Table 32x show that significant differences ($p<0.0001$) resulted from experiments carried out for 24 months at almost all time points. With regard to treatment differences it is noted in Table 32x that significant differences ($p<0.0001$) occurred between the control group and all other groups except the V group. Thus, the addition of antioxidant vitamins to the diet of the Fe + V group, appeared to have cancelled out the effects of oxidative stress on the antioxidant defense system of that group to some extent, which closely resembled that of the control group.

In Figure 25, the total antioxidant capacity is separated into two groups. The upper part of the graph relates to the water-soluble liver antioxidants and the lower part, the lipid-soluble liver antioxidants. Notably, the amount of lipid-soluble antioxidant was about 4-5 times less than the amount of water-soluble antioxidants (Figure 25). The lipid- and water-soluble antioxidants operated in an inverse relationship until 20 months. At 12 months the water-soluble antioxidants attained a peak level. However, this level declined between 16 and 20 months. On the contrary, the level of the lipid-soluble antioxidants was lowest at 12

months and peaked between 16 and 20 months. There was virtually no difference at all time points between the antioxidant levels of the various groups. However, the water-soluble antioxidants showed significant differences between 8 and 16 months.

Figure 25 suggests that a possible inverse relationship exist between the water- and the lipid-soluble antioxidants. Between 8 and 16 months, the water-soluble antioxidants in the liver were at a peak. Over the same period, the lipid-soluble antioxidants were low. At 12 months the Fe + V group had the lowest level of water-soluble antioxidants compared to the rest. This again is suggestive of the operation of a compensatory mechanism of water- and lipid-soluble antioxidants, perhaps in an attempt to maintain equilibrium. This concept of a compensatory mechanism amongst the various antioxidants can be seen when Figures 20-23 are examined. GPx peak values occurred at 4 months (Figure 20), catalase peak values at 8 months (Figure 22), SOD at 12 months (Figure 21), GPx again at 16 months, TAS at 20 months, and vitamin C at 24 months (Figure 23). It is believed that the dynamics of the various antioxidants was an attempt to "scavenge" the continuous production of free radicals in the rat liver. In addition, Brown *et al.* (2003) have shown an up-regulation of antioxidant defences involving thiol metabolism in hepatic iron overload.

In a clinical study of SOD, TAS and liver diseases, a similar conclusion was drawn. In that study, SOD was found to be significantly lower in all patients compared to the control group (Irshad *et al.*, 2002). Moreover, the degree of reduction was found to be nearly the same in all types of liver diseases. However, TAS was found to be comparable to that of the control group and independent of the type and aetiology of liver disease. In several cases, the TAS level was higher in patients than the matched control. The view of the

possibility of some adaptive or compensatory rise in some other antioxidants that were not measured was postulated and the concept tested. A rise in uric acid was observed in all types of liver diseases, irrespective of their aetiology (Irshad *et al.*, 2002).

In conclusion, even though the liver has ample resources to dispose of ROS, i.e. SOD, catalase, glutathione, and vitamin E, these ROS scavenging systems are mainly compartmentalized in specific organelles like peroxisomes (catalase) and mitochondria (MnSOD) and can not effectively scavenge ROS in hepatocytes.

10.5 DIETARY IRON OVERLOAD AND BIO-MARKERS OF LIPID PEROXIDATION.

In Fe overload diseases such as HH, organ damage has been attributed mostly to Fe-induced peroxidation of PUFAs of membrane lipids, which can lead to the breakdown of biomembrane functions and finally cell death. Fe is involved in the initiation of this free radical chain reaction (LPO) by decomposition of hydrogen peroxide to form the highly reactive $^{\bullet}OH$ in the Fenton reaction and by activation of oxygen by ferrous and ferric complexes. LPO processes may be studied by monitoring the resulting secondary reaction products, which include lipid LOOH, MDA, 4-HNE and 8-IP.

10.5.1 Lipid Hydroperoxides (LOOH)

LOOH of Fe-overloaded Wistar rats is seen in Figure 29 (page 227). There was virtually no difference in serum LOOH among the various groups for the first 12 months. Thereafter

LOOH in all groups, apart from the control group, increased sharply, attaining a peak at 20 months. Thus, little or no LPO took place within the first 12 months. This can be attributed to poor Fe loading over the same period. In Figure 29, the control group has the lowest serum LOOH and does not show any peak value. It is inferred that in the absence of iron overload, oxidative stress is virtually absent and LPO is minimal and insignificant. In Figure 29, differences between the various groups compared to the control group were statistically significant. Furthermore, the analysis of variance indicated that both time and treatment and their interaction had significant effects on LPO ($p<0.0001$, $p<0.0001$, respectively). The multiple comparison test results in Table 25x show that significant differences resulted from experiments carried out between 12 and 20 months. With regard to treatment differences, Table 36x shows that significant differences occurred between the control group and all other groups.

From the afore-mentioned and Figure 29, all other groups receiving Fe supplementation showed significant signs of LPO. The greatest effect was seen in the Fe + Cu group. The presence of a possible co-carcinogen may be attributed to this as seen in the Long Evans Cinnamon rat an animal model of Wilson disease (Kato *et al.*, 1996; Ebara *et al.*, 1999). Multiple regression analysis showed that serum Cu levels in the Fe + V, Fe – V, Fe + ASA groups significantly predicted LPO ($p=0.0001$; $p=0.0002$; $p=0.0046$, respectively). Serum Fe also predicted LPO in the Fe group. However, there was no group in which both serum Fe and Cu could predict LPO.

In Figure 29, the Fe – V group is the lowest suggesting the presence of less LPO. This was unexpected and contrary to what other researchers observed (Huang *et al.*, 2002).

However, Meagher *et al.* (2001) administered α-tocopherol supplements at doses of 200, 400, 800, 1200, or 2000 IU to healthy persons for 8 weeks and found no benefit of α-tocopherol on LPO. In Figure 29, the curve for the Fe + V group lies above the Fe – V group, suggesting that more LOOH was produced as a result of vitamin supplementation. This was again unexpected. It is possible that the high LPO observed in the vitamin-supplemented group (Fe + V) may be attributed to vitamin A (50mg/kg diet). Vitamin A may have behaved as a pro-oxidant more than an antioxidant. For example, a recent report by Graffin *et al.* (2002) showed that β-carotene (pro-vitamin A) induced hepatic fibrosis in a 66-yr-old woman. In this study, vitamin antioxidants did not make a significant impact in reducing LOOH, as seen in Figure 29. Similarly, acetyl salicylic acid (ASA), used as an antioxidant, made less impact in reducing LPO (Figure 29). In Figure 29, the decline in LOOH in all the iron-supplemented groups after 20 months is an indication of a decline in LPO, although the by-products (i.e. 4-HNE) were detected immunohistochemically in the livers at that time-point. Benedetti *et al.* (1984) demonstrated in rats that the loss of cellular capacity to undergo LPO may be an early event in hepatocarcinogenesis and may therefore represent an early preneoplastic marker. In this study, histopathological evidence of neoplastic transformation commenced at 28 months. Unfortunately, immunohistochemistry of LPO by-products was not performed after 20 months as a result of technical difficulties.

10.5.2 MDA

Increased LPO is an important expression of both chronic and acute Fe toxicity. Evidence supporting increased LPO in chronic Fe overload includes the demonstration of increased concentrations of MDA (a by-product of LPO) in organs obtained from thalassaemic

patients and Fe-loaded experimental animals (Bacon *et al.,* 1983).

MDA levels of iron-overloaded rats are shown in Figure 26 (page 227). There was relatively no activity among the various groups from 2-12 months. This is attributed to the poor Fe loading using CI over that period. All other groups, apart from the control group, show an increase after 12 months. The control group remained a roughly straight line but at a low level with a maximum value of 6.1 μM. Thus, LPO resulting from oxidative stress did not occur in the control group. At 24 months, MDA in the Fe group was 9 times higher than the value in the control group. Brown *et al.* (1997) studied fibrogenesis in 2.5-3% CI-fed SD rats and observed a 3- 5 fold increase in TBARs of the CI-fed rats over the controls at all time points over 14 months. A 2.5-5 fold MDA increase in the Fe-fed groups was observed in the present study at 14 months and this increased to 4-9 fold at the end of 24 months. Furthermore, Valerio and Petersen (2000) examined whether DBA/2Ibg mice fed a ferrocene-enriched diet for 16 weeks would develop hepatic LPO and if liver microsomes would contain adducts of MDA. Chronic Fe feeding of the mice resulted in a severe hepatic Fe overload with hepatic stores 12-fold greater than those measured in control mice and a 3-fold increase in hepatic MDA concentrations. In addition, 10 liver microsomal MDA adducts conjugated to proteins in Fe-overloaded mice were detected. Similarly, Sochaski *et al.* (2002) studied LPO and protein modification in a mouse model of chronic Fe overload and observed a 2-3 fold plasma increase in aldehydes and a 6-fold increase in MDA after 3 weeks of intraperitoneal administration of Fe dextran. Furthermore, Arezzini *et al.* (2003) fed C3H male mice 3% CI for 12 weeks and observed a 3-fold increase in MDA levels in the livers of the mice. A significant increase in MDA was observed in mice

receiving Fe and those treated with Fe and CCl_4. On the contrary, no significant difference with respect to controls was observed in mice treated with CCl_4 alone. These results support the observation in the present study that MDA production was mainly the result of excess hepatic Fe.

Lastly, the association between excess hepatic Fe, hepatic TBARs and the co-localization of MDA-lysine adducts in selected hepatocytes of 3% CI-fed SD rats also suggests that intracellular LPO is enhanced by excess Fe, leading to the formation of aldehydes (Houglum *et al.*, 1990). In support of a hepatocellular origin for aldehyde protein adducts, the stable presence of 4-HNE and MDA protein adducts found in the circulation of animals did not disappear despite the withdrawal of the 3% CI diet (Houglum *et al.*, 1990). These observations provide direct evidence of the contribution of ROS, LPO and reactive carbonyl intermediates to the pathogenesis of Fe-overload diseases. In the present study, MDA levels in the Fe + V group, statistically did not differ significantly from the control group, suggesting some degree of intervention by vitamins in LPO (Table 38x). Similar results were obtained by Brown *et al.* (1997). Aspirin however, was not as effective as vitamin E in reducing the MDA levels in the Fe + ASA group. The Fe – V group also had MDA levels that were statistically different compared to the control group. LPO appears therefore to be a key step in the hepatocarcinogenic process.

10.5.3 8-IP

Enzymatic oxidation of arachidonic acid by way of the cyclooxygenase pathway leads to the formation of prostaglandins (Samuelsson *et al.*, 1975). Several pro-inhibitory stimuli

induce cyclooxygenase-2, an isoform of cyclooxygenase, in macrophages, epithelial cells and fibroblasts leading to the release of prostaglandins. Major metabolites of the primary prostaglandin $F_{2\alpha}$, 15-keto-13,14-dihydro-prostaglandin $F_{2\alpha}$ (15-K-DH-PGF $_{2\alpha}$), and 8-IP can be used as an index of inflammation and enzymatic LPO via cyclooxygenase-catalyzed oxidation of arachidonic acid. In addition, levels of both 8-IP and 15-K-DH-$PGF_{2\alpha}$ in plasma and urine have been shown to increase in an animal model of CCl_4-induced hepatotoxicity (Basu, 1999).

Liver 8-IP levels of Fe-overloaded Wistar rats are shown in Figure 27. The control group has the lowest level in a relatively straight line. Thus, oxidative stress was virtually absent in the control group and neither did 8-IP increase with time. The maximum value for the control group was 590 ng/g liver wt. This value is 4-8x less that of the groups receiving iron, except the Fe + Cu group. All other groups were significantly higher than the control group. 8-IP in the Fe + Cu group increased in a hyperbolic manner, significantly higher than the rest and reaching a maximum value of 12940 $\pm$ 4173 ng/g liver wt at 16 months. This value was 22x that of the control and statistically significant. 8-IP levels for the rest of the groups were in between the two extremes, with relatively no difference up to 12 months and beyond 20 months.

The effect of antioxidant vitamins and aspirin on liver 8-IP was minimal. In fact, aspirins seem to have increased 8-IP levels between 12 and 20 months. This increase was however, statistically insignificant when compared to the control group [$p<0.05$ (12-20 months), Table 43x]. Similarly, Meagher *et al.* (1999) investigating alcohol-induced generation of

LPO products in humans observed that vitamin C, but not aspirin, reduced urinary isoprostanes. The difference between the control group and the Fe + V group was statistically significant. However, the difference between the Fe group and the Fe + V group was not statistically significant. Vitamins A and E were therefore not effective in lowering the level of liver 8-IP. Similarly, when Van den Berg *et al.* (2001) fed 22 male smokers on a high fruit and vegetable concentrate diet with high antioxidant capacity for 3 weeks, no effect of 8-IP as a marker of oxidative lipid damage was observed. On the contrary, Södergren *et al.* (2001), reported that rats supplemented with vitamin E prior to CCl_4-induced oxidative injury had lower levels of urinary 8-IP compared with rats treated with CCl_4 alone. Hepatic levels of 8-IP were also lower in the vitamin E-supplemented CCl_4-treated rats compared to rats treated with CCl_4 alone. However, plasma 8-IP levels did not differ between CCl_4-treated rats with or without vitamin E supplementation. The present study, however, showed that vitamin or vitamin-free diet (in combination with iron) did not affect liver 8-IP (Table 43x). However, it cannot be explained why serum vitamin C correlated positively with 8-IP in the groups that were not supplemented with antioxidant (i.e. the C, Fe, Fe-V and Fe + Cu groups), which is different from the negative correlation observed between vitamin C and 8-IP by Meagher *et al.* (1999) in a study on alcohol-induced oxidative stress.

A positive correlation was observed between 8-IP and ALT in the following groups: Fe + ASA, Fe + Cu and Fe + V. Thus, LPO of arachidonic acid by way of the cyclooxygenase pathway contributed to liver damage after 12 months when ALT levels were significantly raised in these groups. In the multiple regression analysis, Fe in the Fe group significantly

predicted 8-IP (p=0.0084). In the Fe + V group 8-IP significantly predicted mutagenicity by the Ames mutagenicity test (p=0.0292). Finally, in the Fe + Cu group 8-IP predicted 8OHdG levels. It can be explained for the Fe + Cu group that in the presence of two possible carcinogens (Fe, Cu), oxidative stress led to increased 8-IP levels. However, it is difficult to explain why this was not applicable to all the other Fe-receiving groups. 8-IP as a marker of oxidative stress may be far more complex than it is now known. Other studies attempting to correlate antioxidant levels (ascorbate, tocopherols, β-carotene, etc.) with plasma or urinary 8-IP are not available. This may indicate that none of the isoprostanes correlate with antioxidant insufficiency, or that simply, the isoprostane responsible for LPO is another untested isomer.

10.5.4 4-HNE Immunohistochemistry

In the 3C.7 sections (control group) there was hardly any brown immuno-labelling observed after exposure to the anti-HNE antibodies [Figures 40 (*a*) & (*b*) – 44 (*a*) & (*b*), pages 234-238]. Intense brown cytoplasmic granular immuno-staining was observed in the hepatocytes in the Fe + ASA [Figure 43 (*c*) & (*d*)], Fe + V [Figure 41 (*c*) & (*d*)], Fe [Figure 40 (*c*) & (*d*)], and Fe + Cu [Figure 44 (*c*) & (*d*)] groups of the rat liver. Similar but less intense immuno-staining in the Fe – V group liver sections, was observed [Figure 42 (*c*) & (*d*)]. Intense immuno-staining of brown aggregates was also observed in the 3V7.8 sections, especially around the vessels (Figure 41).

From the afore-mentioned, it may be concluded that there was virtually no LPO activity in the livers of the control group. Thus, with the normal RDA of Fe, little "free Fe" was

available to generate substantial amounts of free radicals. However, the small amount of free radicals produced was effectively scavenged by the body's antioxidant system with virtually little left for LPO. Alternatively, because LPO, a free radical-mediated mechanism, leads to oxidative destruction of PUFAs constitutive of cellular membranes, the process of LPO in the control group was effectively abolished by antioxidants with very little or no 4-HNE formed. On the other hand, the intense brown immuno-staining of 4-HNE was observed in all the Fe-overloaded groups irrespective of vitamin levels. In addition, Cu supplementation in the Fe + Cu group did not increase the intensity of 4-HNE microscopically. Similar findings of 4-HNE adducts have been reported in liver tissues from patients with different chronic liver diseases, including alcoholic liver injury (Paradis *et al.,* 1997a) chronic viral hepatitis (Paradis *et al.,* 1997b) and HH (Niemela *et al.,* 1999). Furthermore, 4-HNE adducts were mainly found in the cytoplasm of all iron-overloaded groups. Similar findings of cytoplasmic localization of 4-HNE adducts resulting from iron overload was observed by Seki *et al.* (2002).

Immunohistochemical staining for 4-HNE was not examined before 12 months. However, by 12 months, liver samples already had 4-HNE deposits. Biochemical results (Figures 26 and 27) of MDA and 8-IP, respectively, showed very little activity at 12 months. LOOH determined by the FOX II assay showed that LPO was just beginning at 12 months (Figure 29). Although serum Fe levels at 12 months were fairly raised, hepatic Fe was still mild (2+) at this time-point. LPO on the other hand was adequately detectable at 12 months. LPO may therefore occur as an early event in the hepatocarcinogenic process induced by excess Fe and has profound effects on the liver, although it may not be adequately detected

at the serum level. In addition, it is likely that the process of LPO commences from within the liver, and the spill over of adducts is then evident in the serum. Finally, it was noted that low hepatic Fe levels are adequate to commence this chain reaction, which was never attenuated by high doses of vitamin and aspirin antioxidants.

Although it still remains to be clarified whether LPO is the cause or consequences of liver damage, ALT and AST values of all Fe-loaded groups obtained at 12 months were not statistically significant when compared to the control group. Therefore, if LPO is part of the hepatocarcinogenic process it does so in the absence of overt hepatic damage as evidenced by significantly raised serum transaminase levels.

10.6 DIETARY IRON OVERLOAD AND OXIDATIVE DNA DAMAGE

Apart from lipids, nucleic acids and proteins are also targets for ROS attack. For example, DNA is attacked by $^{\bullet}OH$, which results in increased 8OHdG production, and can be adequately quantified in urine, serum and tissue. Although enzyme repair mechanisms operate, it is possible that in the long term, protein expression is impaired following such DNA damage. ROS-induced oxidative damage to proteins resulted in a variety of chemical modifications, particularly in the introduction of carbonyl groups into amino acid residues (especially proline, arginine, lysine and threonine). Kuchino *et al.* (1987) observed that the formation of 8OHdG leads to mutations by inducing misreading of the base itself and its adjacent bases. The presence of such mutagens can be detected by the Ames mutatgenicity test. Furthermore, Hagen *et al.* (1994) demonstrated that HCC developed as a result of sustained accumulation of 8OHdG in the hepatic nuclear DNA of hepatitis B virus transgenic mice.

10.6.1 Hepatic 8OHdG levels

Hepatic 8OHdG levels of Fe-overloaded Wistar rats are shown in Figure 30. All groups have winding curves that relate to the level of 8OHdG in the liver. The control group is the lowest with a first peak at 4 months and a second at 12 months. Although minor peaks occurred, the general pattern of the control group's curve especially from 12 months was 'fairly' flat, as expected of the control group that received the normal chow diet. In Figure 30 all curves after 20 months were attenuated and this may be attributed to an adaptive mechanism (Radak *et al.*, 2000).

Both time and treatment had significant effects on hepatic 8OHdG levels in this study ($p<0.0001$, $p<0.0001$, respectively). In addition, the interactive effect of both parameters was significant ($p<0.0001$)(Table 40x). The control group in this study did not show any net 8OHdG change at the end of 28 months (Figure 30). Similarly, increase in 8OHdG in the liver has been reported not to be time dependent (Fraga *et al.*, 1990; Hirano *et al.*, 1996; Nakae *et al.*, 2000). In summary, 2.5% CI supplementation made little impact before 12 months. Thereafter, supplementation with 0.5% ferrocene caused a drastic increase in liver 8OHdG production. The analysis of variance between 2 and 8 months was not statistically significant. However, significant differences amongst the various groups occurred at 24 months ($p<0.05$). On the contrary, Kang *et al.* (1998) fed SD male rats on 3% CI for 8 weeks and obtained 8OHdG levels that were statistically significant compared to the control group. The Fe + V group had lower 8OHdG levels than the other groups except for the period 16 to 24 months. The antioxidant vitamins given to the Fe + V group appear to have scavenged free radicals generated to by ferrocene and reduced oxidative DNA damage up to 16 months.

The present study shows that vitamins and aspirin antioxidants reduced liver 8OHdG by 17% and 22%, respectively, within the first two months. However, the absence of antioxidants led to 34% increase in 8OHdG level in the Fe –V group when compared with that of the Fe + V group and 10% increase when compared with the Fe group. Similarly, Haegele *et al.* (2000) showed that in a 14-day fruit and vegetable intervention trial, plasma β-cryptoxanthine (a xanthophyll carotenoid) inversely correlated with 8OHdG in the lymphocyte DNA. Thompson *et al.* (1999) reported that the concentration of 8OHdG in lymphocyte DNA was reduced by 21.5% by a 2-week vitamin intervention. Thus, in the absence of vitamin antioxidants, the DNA is more prone to oxidative damage by ROS. However, not all vitamin intervention studies had corresponding decreases in 8OHdG levels (Huang *et al.*, 2000).

In Figure 30, aspirin as an antioxidant (Fe + ASA group) was only effective within the first 12 months. For example aspirin led to 22% reduction in hepatic 8OHdG within the first two months. However, under increased oxidative stress with time, this antioxidant was no longer effective. The hydroxylation of aspirin has been shown in *in vitro* studies as an $^{\bullet}OH$ scavenger (Richmond *et al.*, 1981). However, *in vivo* application of aspirin in the present study showed efficacy only under low oxidative stress (i.e. up to 12 months). Multiple regression analysis in groups receiving antioxidants (Fe + V and Fe + ASA groups) showed that ORAC-L or lipid antioxidants in those groups significantly affected 8OHdG levels ($p=0.0000$)(Table 44x). Denda *et al.* (1994) fed male Fischer 344 rats a choline-deficient, L-amino acid-reactive (CDAA) diets for 30 weeks and reported that aspirin at concentrations >0.2% prevented the development of both cirrhosis and preneoplastic

nodules. Aspirin also prevented hepatocyte proliferation as well as the generation of TBARS and 8OHdG. In the present study, 20 mg/kg/d aspirin was used. This comes to about one-third of the 0.2% Denda (1994) used to prevent 8OHdG generation. The inability of aspirin to reduce liver 8OHdG after 12 months could be related to the high oxidative stress (after 12 months as seen in figures 26, 28, 29, 30, 32 and 33) and perhaps the low aspirin dose administered.

The administration of Cu induced high hepatic levels of 8OHdG from the onset. The correlation analysis (in section 9.1.13, page 191) shows that the Fe + Cu group correlated very well with all the other groups apart from the control group. The nature of the curve can therefore be attributed to the generation of ROS and its oxidative damage to DNA. In the present study, a correlation was also established in the Fe + Cu group between 8OHdG and FADU ($r=0.70$, $p<0.0001$)(Table 21x). Similarly, Toyokuni and Sagripanti (1996) observed this kind of association. The multiple regression analysis indicates that Fe, O_2, TAS, ORAC-A, LPO and 8-IP in the Fe + Cu group, significantly predicted 8OHdG production in this group rather than any other group. The presence of 8OHdG has been shown in other liver diseases as well (Farinati *et al.*, 1999; Cardin *et al.*, 2001; Ichiba *et al.*, 2003).

10.6.2 8OHdG Immunohistochemistry

8OHdG, a DNA base modified product generated by ROS, can induce G-C to T-A transversion at DNA replication (Shebutani *et al.*, 1991). It has been demonstrated that

8OHdG is a good marker of oxidative DNA damage (Kasai, 1997). Previous studies have shown that various carcinogens including aflatoxin B_1, psychological stress and ionising radiation, increase hepatic 8OHdG content. Although increased 8OHdG levels in tissue extracts from patients with chronic viral hepatitis has been reported (Shimoda *et al.*, 1994), little is known about the *in situ* localization of 8OHdG in Fe-overloaded livers.

Photomicrographs of 8OHdG immunohistochemistry can be seen on pages 229-233. The intrahepatic localization of 8OHdG differed from group to group, which may be attributed to the differences in the various diet regimens and target(s) of oxidative stress among the various groups. The slides show that there was hardly any visible brown immuno-staining in the control group liver sections, suggesting that insignificant amounts of 8OHdG adducts were present in those livers [Figures 35 (*a*) & (*b*) – 39 (*a*) & (*b*)]. A great deal of brown immuno-staining, indicating positive labelling of 8OHdG, was observed throughout the liver sections of the Fe + V group [Figure 36 (*c*) & (*d*)]. Intense labelling was observed in several aggregates found in these sections, as well as granular labelling within cells. Similar intense labelling in aggregates was observed in the liver sections of the Fe – V and Fe + Cu groups [Figure 37 (*c*) & (*d*), and 39 (*c*) & (*d*) respectively]. This granular labelling was also observed within cells in the liver sections of the Fe + ASA group, especially around blood vessels. In addition, the immuno-staining was concentrated in nuclei, appearing as dark brown spots in this group [Figure 38 (*c*) & (*d*)]. 8OHdG has also been demonstrated to be present in chronic human liver diseases such as hepatitis B and C, autoimmune hepatitis, alcoholic liver disease, and primary biliary cirrhosis. Kitada *et al.* (2001) and Ichiba *et al.* (2003) have suggested a possible link between 8OHdG and active

inflammation and hepatocarcinogenesis. Seki *et al.* (2002) also demonstrated the presence of 8OHdG in non-alcoholic steatohepatitis (NASH). In that study, 65% of the cases examined exhibited nuclear expression of 8OHdG in hepatocytes and sinusoidal cells in areas of active inflammation. Quantitative analysis revealed that 8OHdG expression significantly correlated with the grade of necro-inflammation but not with the severity of steatosis. The association between body Fe stores and 8OHdG, was demonstrated by Kato *et al.* (2001). Normalization of elevated hepatic 8OHdG levels in chronic hepatitis C was achieved in patients by phlebotomy and low Fe diet (Kato *et al.*, 2001).

10.6.3 FADU

Different methods have been used for measuring DNA damage and repair activities. The FADU assay which is one of the common methods, is based on the fact that the rate of unwinding of large DNA molecules exposed to alkaline is related to increases in strand breaks and conversely, strand breaks are responsible for the rate of DNA unwinding (Birnboim and Jevcak, 1981).

In the present study, the FADU (in the liver cells) of Fe-overloaded Wistar rats is seen in Figure 28. The absence of substantial differences between the various groups up to 12 months is suggestive of insignificant DNA strand breaks resulting from low ROS attack on the DNA. However, FADU values of all groups apart from the control group and the Fe + V group increased sharply between 12 and 16 months. Furthermore, at most of the time points the rate of DNA unwinding in the control group was lower than that of other groups. Similarly, Edling *et al.* (1990) observed that the unwinding of hepatic double stranded

DNA (dsDNA) was greater at all time-points in Fe-loaded rats compared to the control after 22 weeks of feeding Wistar rats 2.5-3.0% CI.

In the present study, DNA unwinding of the Fe + V group increased steeply from 16-20 months. The interaction plot of time and group in Figure 28 (page 227) suggests that the level of DNA strand-breaks in the Fe + V group was lower than the other groups between 12 and 20 months, further suggesting that ROS release from the neutrophils in the Fe + V group was suppressed or delayed compared to the other groups. This effect was also noticed during $^{\bullet-}O_2$ measurement by chemiluminescence. Apart from vitamins suppressing the release of ROS they also lowered the level of DNA strand breaks and unwinding by scavenging the ROS produced. The Fe + V group's curve was almost always the lowest of all the Fe-receiving groups. The analysis of variance shows that there was no significant difference between group C and Fe + V (see section 9.3.12, page 222). Vitamin supplementation therefore significantly reduced the rate of DNA unwinding.

The oxidative DNA damage led to DNA strand breaks and unwinding and the subsequent formation of adducts, such as 8OHdG. This is seen by the strong positive correlation ($p < 0.0001$- 0.0007) that exists between FADU and 8OHdG in all the groups except the control group. Toyokuni and Sagripanti (1996) obtained similar results and suggested that DNA strand breaks and 8OHdG are possibly related through a common chemical mechanism. In the present study, the correlation analysis showed that all the groups were significantly positively correlated (section 9.1.14, page 192). The analysis of variance showed that both time and treatment had significant effects on the rate of liver DNA

unwinding (section 9.3.12, page 222). Furthermore, the absence of vitamins increased the rate of DNA unwinding in the Fe - V group compared to the Fe + V group and antioxidant vitamins were more effective than aspirin in reducing DNA strand breaks and unwinding by scavenging peroxyl radicals (Niki, 1996). Similarly, Navasumrit *et al.* (2000) demonstrated that the administration of vitamin C or E (400 mg/kg, i.p., 100 mg/kg, i.p., respectively, daily for 5 days) prior to administration of ethanol to male Wistar rats inhibited the generation of 1-hydroxyethyl-POBN a free radical adduct by 30 and 50% respectively, and both agents prevented the increased frequency of DNA single strand breaks caused by ethanol. [POBN = α-(4-pyridyl-1-oxide)-n-tert-butylnitrone, is a spin-trapper]. In HH, unwinding of hepatic double stranded DNA and the risk of HCC has been associated with chronic Fe overload (Nidereau *et al.,* 1985).

In the present study, DNA unwinding in the Fe + Cu group was higher than other groups at all time-points after 8 months. Cu, a possible co-carcinogen, may have caused greater DNA strand breaks and unwinding and greater hepatic damage (Ebara *et al.,* 1999; 1991; Klein *et al.*, 2000) as seen in the Long-Evans cinnamon rat (Hatano *et al.,* 2000).

10.7 DIETARY IRON OVERLOAD AND MUTAGENESIS

Damage to the DNA is likely to be a major cause of cancer. The Ames mutagenicity test has been used extensively to screen a variety of substances for mutagenic activity. This test measures back-mutation in several specially constructed mutants of *Salmonella typhimurium*. The test strain *Salmonella typhimurium* TA 102 contains A-T base pairs at the site of the mutation (determined by DNA sequence anaylsis) in contrast to the other

Salmonella tester strains that detect mutagens damaging G-C base pairs. This strain differs from previous tester strains in that the mutation has been introduced into a multi-copy plasmid, so that ≈ 30 copies of the mutant gene are available for back-mutation. This strain detects a variety of oxidative mutagens, including hydrogen peroxide and other hydroperoxides, X-rays, a variety of aldehydes (MDA), bleomycin, UV light etc. (Levin *et al.*, 1982).

The results of the Ames mutagenicity test, showing the interaction of time with the various treatment types and, using fractionated liver homogenate on *Salmonella typhimurium* strain TA 102 are shown in Figure 31 (page 228). In this figure, the curve of the control group is fairly straight with a maximum value of 365 'revertant' colonies. Using the established cut-off point of 360 'revertant' colonies for *Salmonella typhimurium* TA 102, the liver homogenate of the control group was considered negative throughout for the Ames mutagenicity test. Colony counts of 'revertants' for the negative control ranged from 310-330 'revertants' during the same period. The positive control, daunorubicin hydrochloride (daunomycin) had colony counts of 510-520 'revertants'.

In the Ames mutagenicity test, the control group also showed increase in 'revertant' colonies. However, this increase was minimal. Spontaneous mutagenesis and aging may be accountable for this. Mutation frequencies in the liver have been reported to increase with aging (Dollé *et al.*, 1997). The accumulation with age of spontaneous mutation has long been considered to play key roles in senescence in experimental animals (Vijg and van Steeg, 1998). Thirty to 40% of mutations that occur are detected in the brain and kidney,

whereas 10 - 20% are in the liver, lung and spleen (Boerrigter, 1998). About one-third of such spontaneous mutations arise before birth; about one-third during the growth period of youth; and the remainder during the rest of the animal's life (Paashuis-Lew and Heddle, 1998).

In the present study, colony counts for the Fe + Cu group increased steadily from 2 months until 20 months where it attained a peak value of 588 'revertant' colonies and then decreased slightly. Mutagenic activity in the Fe + Cu group appears to be the synergetic effect of Fe and Cu. By 8 months this group was moderately positive for the AMES mutagenicity test. Although liver homogenate was not analysed to determine the active mutagenic compound, it is believed that mutagenicity in the liver fractions was caused by MDA and 8OHdG. These two compounds have been implicated in mutagenesis caused by oxidative stress (Niedernhofer *et al.*, 2003; Cheng *et al.*, 1992).

Niedernhofer *et al.* (2003) reacted MDA with pSP189 shuttle vector DNA and then transfected them into human fibroblasts for replication. MDA induced up to 15-fold increase in mutation frequency in the supF reporter gene compared to untreated DNA. Sequence analysis revealed that the majority of MDA-induced mutations occurred at GC base pairs. These experiments provide biological and biochemical evidence for the existence of MDA-induced DNA inter-strand cross-links that could result from endogenous oxidative stress and are likely to have potent biological effects. Cheng *et al.* (1992) showed that 8OHdG is pro-mutagenic. However, it requires DNA replication without repair in order to cause mutation by specifically inducing GC-to-TA transversion.

In Figure 31 (Ames mutagenicity test), values after 16 months were statistically significant compared to those before (p=0.05). MDA and 8OHdG products at 16 months were also statistically significant (Figures 26 and 30, respectively). However, at 16 months, only the Fe + Cu group showed very high increases in the Ames test. From Figure 31, colony counts as high as 660 'revertant' where noted in the Fe, Fe + V and Fe – V groups, and ≈ 600 in the Fe + ASA group at 20 months. Therefore, antioxidant vitamins (A and E) and aspirin were unable to prevent the formation of mutagens in the Fe + V and Fe + ASA groups, respectively. It appears that once excess Fe accumulates in the liver, the process of MDA and 8OHdG formation to mutagenic levels is inevitable.

Detailed data on the Ames mutagenicity test are shown in Table z (appendix G). It is seen from the Table z that mutagens were strongly present in the microsomes and this increased with time. In addition, more liver homogenate fractions became positive for the Ames mutagenicity test with time. From what has been mentioned previously, it appears that the mutagenic levels 8OHdG and MDA originated from the microsomes and spread to other parts of the liver. Similar observations were made by Levin *et al.* (1982). Finally, from Table z (appendix G), it is noted that by 24 months almost all liver fraction (S9, nucleosomes, cytosol, microsomes and whole homogenate) were strongly positive for mutagenesis in all groups except the control group.

Mutation frequencies in the liver of a recently developed *lac*1 transgenic rat were substantially lower than those of the transgenic mice previously developed, and mutation

patterns induced by aflatoxin B1 were clearly different in those two animal models (de Boer *et al.*, 1996). Mutation events, either spontaneous or induced, are therefore species-dependent. In addition, GC-to-AT transitions are the most frequent class among spontaneous mutations (Vijg and van Steeg, 1998), and 8OHdG specifically induces GC-to-TA transversion (Cheng *et al.*, 1992). Furthermore, different forms of oxidative DNA damage can induce different types of mutations, including point mutations, transitions, deletions, additions, frameshifts or chromosomal translocation (Gille *et al.*, 1994). Moreover, environmental toxins may alter the methylation status of DNA. These events may lead to potential mutagenic effects (Pogribny *et al.*, 1995) and activation of oncogenes and inactivation of tumour suppressor genes.

Tumour suppressor genes suppress malignant transformation. In some types of tumours, inactivation of suppressor genes may occur by methylation (Vorce *et al.*, 1989) and may be a molecular mechanism underlying cell proliferation that contributes to carcinogenesis (Goodman and Counts, 1993). The p53 protein is a multifunctional transcriptional factor that orchestrates cellular responses to DNA damage and thus conserves genetic stability. Induction of DNA damage activates p53, which in turn induces either cell growth arrest or programmed cell death, depending on the cell type or experimental system. Bressac *et al.* (1995) and Hsu *et al.* (1991) found G:C to T:A mutations in codon 249 of the p53 gene leading to a substitution of arginine to serine in tumours and HCC from southern Africa and the Qidong area of China, respectively. The mutation frequency of the p53 tumour suppressor gene in HH was studied recently. In one study, 60% A:T to G:C and 40% A:T to T:A mutations were observed (Vautier *et al.*, 1999). However, 45% G:C to C:G, 33%

A:T to C:G, 11% G:C to T:A mutations were observed in another (Marrogi *et al.*, 2001). This mutation spectrum suggests that etheno-deoxyguanine or etheno-deoxyadenine DNA adducts may be responsible for the DNA damage. These DNA modifications are produced by the reaction with lipid peroxidation products in the livers of HH patients (Nair *et al.*, 1998).

11.0 CONCLUSION

An animal model of dietary Fe overload leading to HCC has hitherto not been produced. Attempts made by several researchers have resulted in haemochromatosis without HCC (Bacon *et al.*, 1983; Goddard *et al.*, 1983; Park *et al.*, 1987; Iancu *et al.*, 1987, 1988; Ward *et al.*, 1991; Pietrangelo *et al.*, 1995b; Onylyk *et al.*, 1995; Plummer *et al.*, 1997; Valerio *et al.*, 2000; Arezzini *et al.*, 2003). The present study is the first in which dietary exposure to iron has produced Fe overload that was complicated by HCC development. Furthermore, HCC occurred in the absence of cirrhosis and fibrosis. A biochemical explanation for the pathogenesis of HCC has been shown to involve oxidative stress. Iron overload led to the generation of ROS. Although $^{\bullet-}O_2$ free radical was 2-2.5 times higher in the iron-fed groups compared to the control, it was not statistically significant. Thus, the $^{\bullet}OH$ free radical remains the most likely free radical generated during dietary iron overload.

Antioxidant enzymes operate in a dynamic equilibrium and with a compensatory mechanism. The total lipid-soluble antioxidant within the antioxidant defence system was 25% the total hepatic antioxidants. This explains the ineffectiveness of the antioxidant vitamins to attenuate the consequences of oxidative stress such as oxidative lipid and DNA damage. LPO occurred as an early event of oxidative stress generating adducts such as MDA and 4-HNE of which the latter was massively deposited in the liver at 12 months of Fe-loading. DNA modifications such as 8OHdG were produced by reactions with LPO products in the livers of the Fe-overloaded Wistar rats as seen in HH patients (Nair *et al.*, 1998). The level of such mutations in the Fe-fed groups was statistically significant

compared to the control group. Such mutations were accompanied by DNA strand breaks and unwinding, and were confirmed by PFGE (Figure 55) and FADU as early events in the carcinogenic process. Liver damage estimated by AST and ALT occurred after 16 months of Fe loading although this was not histologically visible. However, signs of carcinogenesis were histologically noticeable at 20 months when IFF was first noticed. IFFs developed to dysplastic nodules by 28 months and progressed to frank HCC in one sample from the Fe group. Dietary Fe alone may be carcinogenic through a mechanism that involves the generation of ROS, LPO, oxidative DNA damage, DNA strand breaks and unwinding, and mutagenesis.

LIST OF ABBREVIATIONS

$^{\bullet-}O_2$	Superoxide radical
γ-GT	Gamma-glutamytranspeptidase
$^{\bullet}OH$	hydroxyl radical
$^1O_2$	Singlet oxygen
4-HNE	4-hydroxy-2'-nonenal
8-IP	8-isoprostane
8OHdG	8-hydroxy-2'-deoxyguanosine
AAPH	2,2'-azobis(2-methylpropionamide)-dihydrochloride
ACP	Acid phosphatase
ADP	Adinosine diphosphate
AFP	Alpha-feto protein
AIN	American Institute of Nutrition
ALT	Alanine aminotransferase
ASA	Acetylsalicylic acid
AST	Aspartate amonotransferase
ATP	Adenosine triphosphate
C gp	Control group
CI	Carbonyl iron
Cu	Copper
DNA	Deoxyribonucleic acid
dsDNA	Double stranded deoxyribonucleic acid
FADU	Fluorimetric Analysis of DNA Unwinding
Fe	Iron
Fe – V gp	Iron, minus vitamin group
Fe + ASA gp	Iron, plus acetyl salicylic acid
Fe + Cu gp	Iron, plus copper

Fe + V gp	Iron, plus vitamins
Fe gp	Iron group
FeNTA	Iron nitriloacetate
FOX	Ferrous Oxidation with Xylenol
GC/MS	Gas Chromatography / Mass Spectroscopy
GPx	Glutathione peroxidase
GSH	Glutathione
GST-π	Glutathione-sulfhydryl-transferase-π
HCA	Hepatocellular adenoma
HCC	Hepatocellular carcinoma
HH	Hereditary haemochromatosis
HLA	Human Lymphocyte Antigen
HMdU	5-hydroxymethyl-2'-deoxyuridine
IFF	Iron free focus (iron free foci)
LEC	Long Evans Cinnamon
LIC	Liver iron content
LLCD	Large liver cell dysplasia
$LO^{\bullet}$	Alkoxyl radical
$LOO^{\bullet}$	Peroxyl radical
LOOH	Lipid hydroperoxide
LPO	Lipid peroxidation
MDA	Malondialdehyde
NADP	Nicotinamide adenine dinucleotide phosphate
NADPH	Reduced nicotinamide adenine dinucleotide phosphate
NAGA	N-acetylglucosamine
$NO^{\bullet}$	Nitric oxide radical
ORAC	Oxygen radical absorbance capacity
ORAC_A	Aqueous phase Oxygen radical absorbance capacity
ORAC_L	Lipid phase Oxygen radical absorbance capacity

PFGE	Pulse Field Gel Electrophoresis
PUFA	Poly Unsaturated Fatty Acid
ROI	Reactive Oxygen Intermediate
$ROO^{\bullet}$	Peroxyl free radical
ROS	Reactive Oxygen Species
SLCD	Small liver cell dysplasia
SD	Sprague-Dawley
SeGPx	Selenium dependent glutathione peroxidase
SeiGPx	Selenium independent glutathione peroxidase
SOD	Superoxide dismutase
TAS	Total Antioxidant Status
TBARs	Thiobarbituric Acid Reactive Substances
Tf	Transferrin
TfR	Transferrin Receptor
WD	Wilson disease

(ABCPS) The α-tocopherol-Tocopherol, Beta Carotene Cancer Prevention Study Group (1994). The effect of vitamin E and beta carotene on the incidence of lung cancers in male smokers. *N Eng J Med.* 330:1029-1035.

Ahluwalia N, Gordon MA, Gordon H, Mahlon M, Li N-Q *et al.*, (2000). Iron status and stores decline with age in Lewis rats. *J Nutr* 130:2378-2383.

Albanes D (1999). Beta carotene and lung cancer: a study. *Am J Clin Nutr* 69(Suppl): 1345S-1530S.

Allard JP, Royall D, Kurian R, Muggli R and Jeejeebhoy KN (1994). Effects of beta-carotene supplementation on lipid peroxidation in humans. *Am J Clin Nutr* 59:884-890.

Anderson GJ and Powell LW (2000). Of metals, mice, and men: what animal models can teach us about body iron loading. *The J Clin Invest* May 105 (9): 1185-86.

Anderson GJ (2001). Ironing out diseases: inherited disorders of iron homeostasis. *IUBMB Life* 51:11-17.

Anon (1991). Copper-glutathione: a key intermediate in cellular copper metabolism. *Nutr Rev*, 49:95.

Anthony PP, Vogel CL and Barker LF (1973). Liver cell dysplasia: a premalignant condition. *J Clin Pathol.* 26:217-223.

Anthony PP (1976). Precancerous lesions for liver cancer in humans. *Cancer Res*, 36: 2579- 2582.

Anthony PP (1979). Precancerous changes in the human liver. *J Toxicol Env Health.* 5: 301-313.

Arezzini B, Lunghi B, Lungarella G and Concetta G (2003). Iron overload enhances the development of experimental liver cirrhosis in mice. *Int J Bioch and Cell Biol* 35: 486-495.

Aruoma OI, Halliwell B, Gajewski E and Dizdaroglu M (1991). Copper ion-dependent, damage to the bases in DNA in the presence of hydrogen peroxide. *Biochem J* 273:601-4.

Aruoma OI (1996). Characterization of drugs as antioxidant prophylactics. *Free Rad Biol & Med.* 20: 675-705.

Aruoma OI (1998). Free radicals, oxidants and antioxidants: trends toward the year 2000. In: Aruoma OI and Halliwell B, eds. Molecular Biology of Free Radicals in Human Diseases. Saint Lucia, London: OICA International, pp 2-3.

Babior BM and Woodman RC (1990). Chronic granulomatous disease. *Seminars Haematology* 27: 247-257.

Bacon BR, Tavill AS, Brittenham GM, Park CH and Recknagel RO (1983). Hepatic lipid peroxidation in rats with chronic iron overload. *J Clin Invest* 71:429-39.

Bacon BR, Healey JF, Brittenham GM, Park CH, Nunnari J and Tavill AS *et al.*, (1986). Hepatic microsomal function in rats with chronic dietary iron overload. *Gastroenterology* 90:1844-53.

Badway JA and Karnovsky ML (1980). Active oxygen species and the functions of phagocytic leukocytes. *Annu Rev Biochem* 49: 695-726.

Bagdon RE, Zbinden G and Studer A (1960). Chronic toxicity studies of beta-carotene. *Toxicol Appl Pharmacol* 2: 225-36.

Basu S (1999). Oxidative injury induced cyclooxygenase activation in experimental hepatotoxicity. *Biochem Biophys Res Commun* 254:764-767.

Beers J, Glerum DM and Tzagoloff A (1997). Purification, characterization and localization of yeast Cox17p: a mitochondria copper shuttle. *J Biol Chem* 272:33191-33196.

Benedetti A, Malvaldi G, Fulceri R and Comporti M (1984). Loss of lipid peroxidation as a histochemical marker of preneoplastic hepatocellular foci of rats. *Cancer Research* 44, 5712-5717.

Benzie IFF and Strain JJ (1997). Simultaneous automated measurement of total antioxidant (reducing) capacity and ascorbic acid concentration. *Redox Report* 3, 322-328.

Bergeron R, Streiff R and Elliot G (1985). Influence of iron on *in vivo* proliferation and lithality of L1210 cells. *J Nutr* 115: 369-374

Birnboim HC and Jevcak JJ (1981). Fluorimetric method for rapid detection of DNA strand breaks in human WBC produced by low doses of radiation. *Cancer Res* May 41.1889-1892.

Blanc JF, Bernard PH, Carles J, Le Bail B, Balabaud C and Bioulac-Saga (2000). Cholangiocarcinoma arising in von Meyenburg complexes associated with hepatocellular carcinoma in genetic haemochromatosis. *Eur J Gastroenterol Hepatol* 12:233-237.

Blot WJ, Li J-Y, Taylor PR, Guo W, Dawsen S *et al.,* (1993). Nutrition intervention trials in Linxian, China: Supplementation with specific vitamin/mineral combinations, cancer incidence, and disease specific mortality in the general population. *J Natl Cancer Inst* 85: (18) 1483-1492.

Blumberg RS, Chopra S, Ibrahim R, Crawford J, Farraye FA *et al.*, (1988). Primary hepatocellular carcinoma in idiopathic haemochromatosis after reversal of cirrhosis. *Gastroenterology* 95:1399-1402.

Boerrigter M (1998). High sensitivity for color mutants in Lac Z plasmid-based transgenic mice, as detected by positive selection. *Environ Mol Mutagen* 32:148-154.

Boige V, Castera L, de Roux N, Ganne-Carrie, Ducot B *et al.,* (2003). Lack of association between *HFE* gene mutations and hepatocellular carcinoma in patients with cirrhosis. *Gut* 52:1178-1181.

Bonkovsky HL, Mitchell WJ and Healey JF (1984). Effects of haemochromatosis on hepatic cytochrome P-450 and antipyrine metabolism in humans. *Clin Chem* 30:1430-1431.

Borjigin J, Payne AS, Deng J, Li X, Wang MM *et al.*, (1999). A novel pineal night-specific ATPase encoded by the Wilson disease gene. *J Neurosci* 19: 1019-1026.

Borzio M, Bruno S, Roncalli M, Mels GC, Ramella G, Borzio F *et al.,* (1995). Liver cell dysplasia is a major risk factor for hepatocellular carcinoma in cirrhosis: a prospective study. *Gastroenterology* 108:812-817.

Bothwell TH and Brandlow BA (1960). Siderosis in the Bantu. A combined histopathological and chemical study. *Arch Pathol* 70:279-292.

Bothwell TH and Isaacson C (1962). Siderosis in the Bantu. A comparison of incidence in males and females. *Br Med J* 1:522.

Bothwell TH, Seftel H, Jacobs P, Torrance JD and Baumslag N (1964). Iron overload in Bantu subjects. Studies on the availability of iron in Bantu beer. *Am J Clin Nutr* 14:47-51.

Bothwell T, Abrahams C, Bradlow BA and Charlton RW (1965). Idiopathic and Bantu haemochromatosis. *Arch Path* 79:163.

Bralet M-P, Regimbeau J-M, Pineau P, Dubois S, Loas G *et al.*, (2000). Hepatocellular carcinoma occurring in nonfibrotic liver: epidemiological and histopathological analysis of 80 French cases. *Hepatology* 32:200-204.

Brennan P and O'Neill LAJ (1995). Effects of oxidants and antioxidants on nuclear factor κB activation in three different cell lines: evidence against a universal hypothesis involving oxygen radcals. *Biochemica et Biophysica Acta* 1260: 167-175.

Bressac B, Kew M, Wands J and Ozturk M (1995). Selective G to T mutations of p53 gene in hepatocellular cercinoma. *Cancer* 75: 2420-2426.

Britton RS, O'Neill R and Bacon BR (1990). Chronic dietary overload in rats. *Hepatology* 11:789-804.

Britton RS, O'Neill R and Bacon BR (1991). Chronic dietary iron overload in rats results in impaired calcium sequestration by hepatic mitochondria and microsomes. *Gastroenterology* 101: 806-11.

Britton RS, Tavill AS and Bacon BR (1994). Mechanisms of iron toxicity. In: Brock JH, Halliday JW, Pippard MJ, Powell LW, eds. Iron Metabolism in Health and Disease. London: WB Saunders Company Ltd, pp 311-51.

Britton RS (1996): Metal-induced hepatotoxicity. *Seminars in liver disease*: Vol 16. No. 1: 3-12.

Broide E, Klinowski E, Koukoulis G, Hadzic N, Portmann B *et al.*, (2000). Superoxide dismutase activity in children with chronic liver diseases. *J Hepatology* 32:188-192.

Brown KE, Poulos JE, Li L, Soweid AM, Ramm GA *et al.,* (1997). Effect of vitamin E supplementation on hepatic fibrogenesis in chronic dietary iron overload. *Am J Physiol* 272 (*Gastrointest. Liver Physiol.* 35): G116-G123.

Brown KE, Dennery PA, Ridnour LA, Fimmel CJ, Kladney ED *et al.*, (2003). Effect of iron overload and dietary fat on indices of oxidative stress and hepatic fibrogenesis in rats. *Liver International* 23, 232-42.

Bruck R, Shirin H, Aeed H, Matas Z, Hochman A *et al.*, (2001). Prevention of hepatic cirrhosis in rats by hydroxyl radical scavengers. *J Hepatology* 35: 457-464.

Brunt EM (2001). Benign tumours of the liver. *Clin Liver Dis*, 5:1-15.

Buchanan WM (1966). Siderosis in Rhodesian Africans. *Central Afr J Med* 12:199.

Buchanan WM (1967). Bantu siderosis with special reference to Rhodesian Africans. *University College of Rhodesia Faculty of Medicine Research Series*. Vol 1. Salisbury: University College of Rhodesia, 5-30.

Buchanan WM (1969). Bantu siderosis- A review. *Central Afr J Med* 15:105.

Buckley GB (1994). Reactive oxygen metabolites and reperfusion injury: aberrant triggering of reticuloendothelial function. *Lancet* 344: 934-936.

Buege JA and Aust SD (1978). Microsomal lipid peroxidation. *Methods Enzymol.* 302-310.

Bull PC and Cox DW (1993b). Long range restriction mapping of 13q14.3 focused on the Wilson disease region. *Genomics* Jun 16(3): 593-8.

Bull PC, Thomas GR, Rommens JM, Forbe JR and Cox DW (1993a). The Wilson's disease gene is a putative copper transporting P-type ATPase similar to the Menke's gene. *Nat Genet* 5: 327-337.

Burkitt MJ and Mason RP (1991). Direct evidence for *in vivo* hydroxyl radical generation in experimental iron overload: An ESR spin-trapping investigation. *Proc Natl Acad Sci USA* 88: 8440-4.

Burton GW, Foster DO, Perly B, Staler TF and Smith ICP (1985). Biological antioxidants. *Phil Trans R Soc Lond* B311: 565-578.

Campbell TC, Allison RG and Carr CJ (1980). Feasibility of identifying adverse health Effects of vitamins and essential minerals in man. Life Science Research Office, Federation of American Societies for Experimental Biology. Bethesda, MD, pp. 76

Cannon RO III, Dusheiko GM, Long JA Jr, Ishak KG, Kapur S *et al.*, (1981). Hepatocellular adenoma in a young woman with β-thalassemia and secondary iron overload. *Gastroenterology* 81:352-5.

Cao G and Prior RL (1999). Measurement of oxygen radical absorbance capacity in biological samples. *Methods in Enzymology* Vol. 299; 50-62.

Cao G, Alessio HM, and Cutler RG (1993). Oxygen-radical absorbance capacity assay for antioxidants. *Free Radic Biol Med* 14:303-311.

Cardin R, Saccoccio G, Masutti F, Bellentani S, Farinati F and Tiribelli C (2001). DNA oxidative damage in leukocytes correlates with the severity of HCV-related liver disease: validation in an open population study. *J Hepatology* 34: 587-92.

Carmichael PL, Hewer A, Osborn MR, Strain AJ and Phillips DH (1995). Detection of bulk DNA lesions in the liver of patients with Wilson's disease and primary haemochromatosis. *Mutation Res* 326:235-43.

Carthew P, Smith AG, Edwards RE, Dorman BM, and Francis JE (1991). Rapid induction of hepatic fibrosis in the gerbil after the parenteral administration of iron-dextran complex. *Hepatology* 13, 534-539.

Casareno RL, Waggoner D and Gitlin JD (1998). The copper chaperon CCS directly interacts with copper/zinc superoxide dismutase. *J Biol Chem* 273: 23625-23628.

Ceriotti F and Ceriotti G (1980). Improved direct specific determination of serum iron. *Clin Chem* 26/2, 327-331.

Cerutti PA (1985). Prooxidant states and tumour production. *Science* 227: 375-381.

Cheeseman KH (1993). Lipid peroxidation and cancer. In: Halliwell B and Aruoma OI, eds. DNA and Free Radicals, London: Ellis Horwood, pp. 109-144.

Chelly J, Tumer Z, Tonnesen T, Petterson A, Ishikawa-Brush Y *et al.*, (1993). Isolation of a candidate gene for Menke's disease that encodes a potentially heavy metal binding protein. *Nat Genet* 3:14-19.

Cheng KC, Cahill DS, Kasai H, Nishimura S, and Loeb LA (1992). 8-hydroxyguanine, an abundant form of oxidative DNA damage, causes G-->T and A-->C substitutions. *J Biol Chem* 267:166-172.

Cheng W, BA Valentine and XG Lei (1999). High levels of dietary vitamin E do not replace cellular glutathione peroxidase (GPX1) in protecting mice from acute oxidative stress. *J Nutr* 129:1951- 1957.

Chevion M, Laing Y, Hae-El R, Berenshtein E, Urettzky G and Kitrossky N (1993). Copper and iron are mobilized following myocardial ischemia: possible productive criteria for tissue injury. *Proc Natl Acad Sci USA* 90: 1102-1106.

Chisolm GM (1991). Cytotoxicity of oxidized lipoproteins. *Current Opinions In Lipidology* 2: 311-316.

Choong NW, Brandhagen DJ and Roberts LR (2003). Characteristics of hepatocellular carcinoma in hepatic iron overload without cirrhosis. *J Invest Med.* Vol 51. Supp 2 Mar. S336 (Abstract).

Chung H, Kudo M, Kawasaki T, Kitano M, Minami Y *et al.*, (2003). Hepatocellular carcinoma associated with secondary haemochromatosis in non-cirrhotic liver: a case report. *Hepatol Res* Jul; 26(3): 254-258.

Cohen C, Berson SD and Geddes EW (1979). Liver cell dysplasia: Association with hepatocellular carcinoma, cirrhosis and hepatitis B antigen carrier status. *Cancer* 44:1671-1676.

Cohen LS (1976). Clinical pharmacology of acetylsalicylic acid. *Semin Thromb Hemost.* 2:146-75.

Collins AR, Duthie SJ, and Dobson VL (1993). Direct enzymatic detection of endogenous oxidative base damage in human lymphocyte DNA. *Carcinogenesis* 14: 1733-1735.

Collins T (1993). Endothelial nuclear factor κB and the initiation of the atherosclerotic lesion. *Lab Invest* 68:499-508.

Cook JD, Watson SS, Simpson KH, Lipschitz DA and Skikne BS. (1984). The effect of high ascorbic acid supplementation on body iron stores. *Blood* 64:721-6.

Cote GJ, Lastra BA, Cook JR, Huang DP and Chiu JF (1985). Oncogene expression in rat hepatoma and during hepatocarcinogenesis. *Cancer Lett* 26: 121-127.

Crane FL, Sun IL, Clark MG, Grebing C and Low H (1985). Transplasma membrane redox systems in growth and development. *Biochim Biophys Acta* 811:233-364.

Cristol JP, Abderrazick M, Favier F, Michel F, Castel J *et al.*, (1999). Impairment of antioxidant defense mechanisms in elderly women without increase in oxidative stress markers: "A weak equilibrium". *Lipids* 34, S289.

Curnutte JT and Babior BM (1987). Chronic granulomatous disease. *Advances in Human Genetics*. 16: 229-245.

Dabbagh AJ, Marian J, Lynch SM and Frei B (1994). The effect of iron overload on rat plasma and liver oxidant status *in vivo*. *Biochem J.* 300: 799-803.

Dallman PR (1990). Iron. In: Brown ML, ed. Present Knowledge in Nutrition. 6th ed. Washington, DC: International Life Sciences Institute-Nutrition Foundation. pp 251-260.

de Boer JG, Erfle H, Holcroft J, Walsh D, Dycaico M *et al.*, (1996). Spontaneous mutants recovered from liver and germ cell tissue of low copy number *lacI* transgenic rats. *Mutat Res* 352:73-78.

Del Maestro RF (1980). An approach to free radicals in medicine and biology. *Acta Physiol Scand* Suppl. 492: 153-168.

Delanty N, Reilly M, Pratico D, Fitzgerald DJ, Lawson JA *et al.*, (1996). 8-epiPGF2$_\alpha$ specific analysis of an isoeicosanoid as an index of oxidant stress *in vivo*. *Br J Clin Pharmacol* 42 (1) :15-19.

DeLuca LM and Ross SA (1996). Beta-carotene increases lung cancer in cigarette smokers. *Nutr Rev* 54:178-180.

Demopoulos HB (1973). Control of free radicals in biologic systems. *Fed Proc* 32: 1903-1908.

Demopoulos HB, Flamm ES, Pietronigro D and Seligman ML (1980). The free radical pathology and the microcirculation in the major central nervous system disorders. *Acta Physiol Scand* Suppl 492:91-119.

Demougeot C, Marie C and Beley A (2000). Importance of iron location in iron-induced hydroxyl radical production by brain slices. *Life Sciences* 67; 399-410.

Denda A, Tang Q, Endoh T, Tsujiuchi T, Horiguchi K *et al.*, (1994). Prevention by acetylsalicylic acid of liver cirrhosis and carcinogenesis as well as generation of 8-hydroxydeoxyguanosine and thiobarbituric acid-reactive substances caused by a choline-deficient, L-amino acid-defined diet in rats. *Carcinogenesis* Jun; 15(6): 1279-83.

Denk H, Franke WW, Erjaschki D and Eckersdorfer R (1979). Mallory bodies in experimental animals and man. *Int Rev Exp Pathol* 20:77-121.

Deugnier YM, Loreal O, Turlin B, Guyader D, Jouanolle H *et al.*, (1992). Liver pathology in genetic haemochromatosis: a review of 135 homozygous cases and their bioclinical correlations. *Gastroenterology* 1992; 102:2050-2059.

Deugnier YM, Charalambous P, Quilleuc D, Turlin B, Searle J *et al.*, (1993a). preneoplastic significance of hepatic iron-free foci in genetic haemochromatosis: a study of 185 patients. *Hepatology*, 18:1363-1369.

Deugnier Y, Guyander D, Crantock L, Lopez J, Turlin B *et al.*, (1993b). Primary liver cancer in genetic haemochromatosis: a clinical, pathological and pathogenic study of 54 cases. *Gastroenterology* 104:228-234.

Devasagayam TP, Di Mascio P, Kasai S and Sies H (1991). Singlet oxygen induced single-strand breaks in plasmid pBR322 DNA: the enhancing effect of thiols. *Biochem Biophy Acta* Mar 26; 1088(3): 409-12.

Diplock AT (1995). Safty of antioxidant vitamins and beta-carotene. *Am J Clin Nutr* 62 (suppl): 1510S–6S.

Dix TA and Aitkens J (1993). Mechanisms and biological relevance of lipid peroxidation. *Chemical Research In Toxicology* 6: 2-18.

Dixon ZR, Shie FS, Warden BA, Burri BJ and Neidlinger TR (1998). The effect of low carotenoid diet on malondialdehyde-thiobarbituric acid (MDA-TBA) concentrations in women: a placebo-controlled double-blind study. *J Am Coll Nutr* 17:54-58.

Dollé MET, Giese H, Hopkins CL, Martus H-J, Hausdorff JM and Vijg J (1997). Rapid accumulation of genome rearrangements in liver but not in brain of old mice. *Nat Genet* 17:431-434.

Domarle O, Blampain G, Agnaniet H, Nzadiyabi T, Brocard J *et al.*, (1998). *In vitro* antimalaral activity of a new organometallic analogue, ferrocene-chloroquine. *Antimicrob Agents Chemother* 42 (3) 540-544.

Dormandy TL (1983). An approach to free radicals. *Lancet* ii: 1010–1014.

Dougherty JJ, Croft WA, Hoekstra WG (1981). Effect of ferrous chloride and iron dextran on lipid peroxidation *in vivo* in vitamin E and selenium adequate and deficient rats. *J Nutr* Oct 111(10): 1784-96.

Dragan YP and Pitot HC (1992). The role of the stages of initiation and promotion in phenotype diversity during hepatocarcinogenesis in the rat. *Carcinogenesis* 13: 739-750.

Dresow B, Albert C, Zimmermann I and Nielsen P (1995). Ethane exhalation and vitamin E/Ubiquinol status as markers of LPO in ferrocene iron-loaded rats. *Hepatol* Apr 21(4): 1099-105.

Driscoll B, Buckley S, Barsky L, Weinberg K, Anderson KD *et al.*, (1999). Abrogation of cyclin D1 expression predisposes lung cells to serum deprivation-induced apoptosis. *A J Physiol* 276(4 Pt 1): L679-89.

Dullman J, Wulfhekel U, Nielsen P and Heinrich HC (1992). Iron overload of the liver by trimethylhexanoylferrocene in rats. *Acta Anatomica* 143, 96-108.

Ebara M, Watanabe S, Kita K, Yoshikawa M, Suguira N *et al.*, (1991). MR imaging of the small hepatocellular carcinoma: effect of intratumoral copper content on signal intensity. *Radiology* 180:617-621.

Ebara M, Fukuda H, Kojima Y, Morimoto N, Yoshkawa M *et al.*, (1999). Small hepatocellular carcinoma: Relationship of signal intensity to histopatolologic findings and metal content of the tumour and surrounding hepatic parenchyma. *Radiology* 210:81-8.

Edling JE, Britton RS, Grisham MB and Bacon BR (1990). Increased unwinding of hepatic double-stranded DNA in rats with chronic dietary iron overload (Abstract). *Gastroenterology* 98:A585.

Esterbauer H and Cheeseman KH (1990). Determination of aldehydic lipid peroxidation products: malondialdehyde and 4-hydroxynonenal. *Methods of Enzymol* 186:407-21.

Esterbaur H, Wag G and Puhl H (1993). Lipid peroxidation and its role in atherosclerosis. *Br Med Bull* 49: 566-567.

Eze MO, Hunting DJ and Ogan AU (1993). Reactive oxygen associated with parasitic and other tropical infections: carcinogenic potential. In: Aruoma OI, ed. Free Radical in Tropical Diseases. Harwood Academic Publishers: London. pp 111-136.

Fantone JC, Ward PA (1982). Role of oxygen-derived free radicals and metabolites in leukocyte dependent inflammatory reactions. *Am J Pathol* 107:397- 418.

Farber E (1976). On the pathogenesis of experimental hepatocellular carcinoma. In: Okuda K, Peters RL, eds. Hepatocellular Carcinoma. New York: John Wiley, pp 3-26.

Farinati F, Cardin R, Degan P, De Maria N, Floyd RA *et al.*, (1999). Oxidative DNA damage in circulating leukocytes occurs as an early event in chronic HCV infection. *Free Radic Biol Med* 27:1284-1291.

Faux SP, Francis JE, Smith AG, Chipman JK (1992). Introduction of 8-hydroxydeoxyguanosine in *Ah*-responsive mouse liver by iron and Aroclor 1254. *Carcinogenesis* 13:247-50.

Feder JN, Gnirke A, Thomas W, Tsuchihashi Z, Ruddy DA *et al.*, (1996). A novel MHC class 1-like gene is mutated in patients with hereditary haemochromatosis. *Nat Genet* 13: 399-408.

Fellows IW, Stewart M, Jeffcoate WJ, Smith PG and Toghill PJ (1988). Hepatocellular carcinoma primary haemochromatosis in the absence of cirrhosis. *Gut* 29:1603-1606.

Fellows IW (1990). Hereditary (primary) haemochromatosis. *BMJ* Sep 22; 301 (6752): 609.

Finch CA and Huebers H (1982). Perspectives in iron metabolism. *N Eng J Med* Jun 1520-27.

Fleming MD, Trenor CC, Su MA, Foemzler D, Beier DR *et al.*, (1997). Microcytic anaemia mice have a mutation in Nramp2, a candidate iron transporter gene. *Nat Genet.* Aug 16(4): 383-6.

Fletcher LM, Roberts FD, Irving MG, Powell LW and Halliday JW (1989). Effects of iron loading on free radical scavenging enzymes and lipid peroxidation in rat liver. *Gastroenterology* 97:1011-8.

Fracanzani AL, Conte D, Fraquelli M, Taioli E, Mattioli M *et al.*, (2001). Increased cancer risk in a cohort of 230 patients with hereditary haemochromatosis in comparison to matched control patients with non-iron related liver disease. *Hepatology* 33:647-651.

Fraga GC, Shigenaga MK, Park-JW, Degan P and Ames BN (1990). Oxidative damage to DNA during aging. 8-Hydroxy-2'-deoxyguanosine in rat organ DNA and urine. *Proc Natl Acad Sci USA* 87:4533-4537.

Freeman BA and Crapo JD (1982). Biology of disease: free radicals and tissue injury. *Lab Invest* 47: 412- 426.

Frei B, Stocker R, and Ames BN (1989). Ascorbate is an outstanding antioxidant in human blood plasma. *Proc Natl Acad Sci USA* 86: 6377–6381.

Frenkel K, Karkoszka J, Glassman T, Dubin N, Toniolo P *et al.*, (1998). Serum auto-antibodies recognizing 5-hydroxymethyl-2'-deoxyuridine, an oxidized DNA base, as biomarkers of cancer risk in women. *Cancer Epidemiol Biomarkers Prev* 7: 49-57.

Fridovich I (1983). Superoxide radical: an endogenous toxicant. *Annu Rev Pharmacol Toxical* 23: 239-257.

Fridovich I (1989). Superoxide Dismutases. An adoptation to paramagnetic gas. *J Biol Chem* 264:7761-7764.

Friedman BM, Baynes RD, Bothwell TH, Gordeuk VR, Macfalane BJ *et al.*, (1990). Dietary iron overload in southern African rural blacks. *S Afr Med J* 78:301-305.

Frigerio R, Mela Q, Passiu G, Cacace E, La Nasa G *et al*; (1984). Iron overload and lysosomal stability in β-thalassaemia intermedia and trait: correlation between serum ferritin and serun N-acetyl-β-D - glucosaminidase levels. *Scand J Haematol* 33:252-5.

Ganne-Carrie, Chastang C, Chapel F, Munz C, Pateron D *et al.*, (1996). Predictive score for the development of hepatocellular carcinoma and additional value of liver large cell dysplasia in Western patients with cirrhosis. *Hepatol* 23: 1112-1118.

Gardner PR and Fridovich I (1991). Superoxide sensitivity to Escherichia coli aconitase. *J Biol Chem* 266:19328-33.

Gaziano JM, Hatta A, Flynn M, Johnson EJ, Krinsky NI *et al.*, (1995). Supplementation with beta-carotene *in vivo* and *in vitro* does not inhibit low density lipoprotein oxidation. *Atherosclerosis* 112:187-195.

Geubel AP, de Galocsy C, Alves N, Rahier J and Dive C (1991). Liver damage caused by therapeutic vitamin A administration: Estimate of dose related toxicity in 41 cases. *Gastroenterology* 100: 1701.

Gille JJP, van Berkel CGM and Joenje H (1994). Mutagenecity of metabolic oxygen radicals in mammalian cell cultures. *Carcinogenesis* 15:2695-2699.

Gillman J and Gillman T (1951). Perspectives in Human Malnutrition; A contribution to the biology of disease from a clinical and pathological study of chronic malnutrition and pellagra in the African. New York, NY: Grune and Stratton.

Glass GA and Gershon D (1981). Enzymatic changes in rat erythrocytes with increasing cell and donor age: loss of superoxide dismutase activity associated with increased catalytically defective forms. *Biochem Biophys Res Commun* 103:1245-53.

Goddard JG and Sweeney GD (1983). Ferric nitroliacetate a potent stimulant of *in vivo* lipid peroxidation in mice. *Biochem Pharmacol.* Dec 15; 32(24): 3879-82.

Goodman GE, Metch BJ and Omenn GS (1994). The effect of long-term beta-carotene and vitamin A administration on serum concentrations of alpha-tocopherol. *Cancer Epidemiol Biomarkers Prev* 3:429-32.

Goodman JI and Counts JL (1993). Hypomethylation of DNA: a possible nongeneotoxic mechanism underlying the role of cell proliferation in carcinogenesis. *Environ Health Perspect* 5: 169-172.

Gordeuk VR, Boyd RD and Brittenham GM (1986). Dietary iron overload persists in rural sub-Saharan Africa. *Lancet* 1:1310.

Gordeuk VR, Mukiibi J, Hasstedt SJ, Samowitz W, Edwards CQ *et al.*, (1992a). Iron overload in Africa: an interaction between a gene and dietary content. *N Eng J Med* 326:95-100.

Gordeuk VK (1992b). Hereditary and nutritional iron overload. *Bailliere's Clin Haematol* 5:169-186.

Gordeuk VR, McLaren CE, MacPhail AP, Deichsel G and Bothwell TH (1996). Association of iron overload in Africa with hepatocellular carcinoma and tuberculosis: Strachan's 1929 thesis revisited. *Blood* Vol 87, No 8, 3470-3476.

Graffin B, Genty I, Cretel E Jean R and Durand JM (2002). β-carotene-induced hepatic fibrosis. *Dig Dis and Sci* Vol. 47, No. 4 Apr, 793.

Grando-Lemaire V, Guettier C, Chevret S, Beaugrand M and Trinchet JC (1999). Hepatocellular carcinoma without cirrhosis in the West: epidemiological factors and histopathology of the non-tumourous liver. Groupe d'Etude et de Traitement du Carcinome hepatocellulaire. *J Hepatol* Sep; 31(3): 508-13.

Granger DN (1988). Role of xanthine oxidase and granulocytes in ischaemia reperfusion injury. *Am J Physiol* 255: H1269-H1275.

Greenberg ER, Baron JA, Tosteson TD, Freeman DH Jr, Beck GJ *et al.*, (1994). A clinical trial of antioxidant vitamins to prevent colorectal adenoma. Polyp Prevention Study Group *N Engl J Med* 331:141-147.

Grootveld M and Halliwell B. (1986). Aromatic hydroxylation as apotential measure of hydroxyl-radical formation *in vivo*. Identifications of hydroxylated derivatives of salicylate in human body fluids. *Biochem J* 237, 499-504.

Gunther T, Vormann J, Hollriegl V and Gossrau R. (1991). Effect of magnesium deficiency and salicylate on lipid peroxidation *in vivo*. *Magnesium-Bull* 13:26-29.

Gutteridge JMC (1984). Reactivity of hydroxyl and hydroxyl-like radicals discriminated by release of thiobarbituric acid-derivative metal from deoxy sugars, nucleotides and benzoate. *Biochem J* 224,761-767.

Haegele AD, Gillette C, O'Neill C, Wolfe P, Heimendinger J *et al.*, (2000). Plasma xanthophylls carotenoids correlate inversely with indices of oxidative DNA damage and lipid peroxidation. *Cancer Epidemoil Biomarkers Prev* 9:421-425

Hagen TM, Huang S, Curnuttle J, Fowler P, Martinez V *et al.,* (1994). Extensive oxidative DNA damage in hepatocytes of transgenic mice with chronic active hepatitis destined to develop hepatocellular carcinoma. *Proc Natl Acad Sci USA* 91:12808-12.

Halliwell B and Gutteridge JMC (1989). Lipid peroxidation: a radical chain reaction. In: Free radicals in biology and medicine. Oxford: Clarendon Press; pp. 188-276.

Halliwell B and Gutteridge JMC (1990). Role of free radicals and catalytic metal ions in human disease: an overview. *Methods Enzymol* 186:1-85.

Halliwell B and Gutteridge JM (1992). Biologically relevant metal ion-dependent hydroxyl radical generation. An update. *FEBS Lett* Jul 27; 307(1): 108-12.

Hamberg M, Svensson J, and Samuelson B (1975). Thromboxane: a new group of biologically active compounds derived from prostaglandin endoperoxides. *Pro Natn Acad Sci USA* 72: 2994.

Hamilton IMJ, Gilmore WS, Benzie IFF, Mulholland CW and Strain JJ (2000). Interactions between vitamin C and E in human subjects. *British J Nutr* 84, 261-267.

Hanck A (1982). Tolerance and effect of high doses of ascorbic acid. *Dosis facit venenum. Int J Vitam Nutr Res* Suppl. 23:221-38.

Handelman GJ and Pryor WA (1999). Evaluation of antioxidant status in humans. In: Papas AM, ed. Antioxidant status, diet, nutrition and health. CRC Press: Boca Raton, FL pp 37-62.

Harlan, UK (2000). Price list 2000. pg 11

Harris DA, Klomp LW and Giltin JD (1998). Aceruloplasminemia: an inherited neurodegerative disease with impairment of iron homeostasis. *Am J Clin Nutr* 67: 972S-977S.

Hartley JA, Gibson NW, Zwelling LA and Yuspa SH (1985). Association of DNA strand breaks with accelerated terminal differentiation in mouse epithelial cells exposed to tumour promoters. *Cancer Res* 45:4864-70.

Hatano R, Ebara M, Fukuda H, Yoshkawa M, Sugiura N *et al.*, (2000). Fatty liver, chronic hepatitis C and hepatocellular carcinoma: accumulation of copper in the liver and hepatic injury in chronic hepatitis C. *J Gastroenterology and Hepatology* 15, 786-791.

Hatori M, Klatte KJ, Teixeira CC and Shapiro IM (1995). End labeling studies of fragmented DNA in the avian growth plate: evidence of apoptosis in terminally differentiated chondrocytes. *J Bone Miner Res* Dec; 10(2): 1960-8.

Hennekens CH, Buring JE, Manson JE *et al.*, (1996). Lack of effect of long-term supplementation with beta-carotene on the incidence of malignant neoplasms and cardiovascular disease. *N Engl J Med* 334:1145-1149.

Heywood R, Palmer AK, Gregson RL and Hummler H (1985). The toxicity of beta carotene. *Toxiclogy* 36:91-100.

Higginson J, Gerritsen T and Walker ARP (1953). Siderosis in the Bantu of southern Africa. *Am J Pathol* 29:779.

Hirano T, Yamaguchi R, Asami S, Iwamoto N and Kasai H (1996). 8OHdG levels in nuclear DNA and its repair activity in rat organs associated with age. *J Gerontol* 51A:B303-B307.

Hirayama T (1979). Diet and Cancer. *Nutr Cancer* 1:67-81.

Hirota N and Williams G (1979). The sensitivity and hetrogenicity of histochemical markers for altered foci involved in liver carcinogenesis. *Am J Pathol* 95: 317-328.

Holland MK, Alvarez JG and Story BT (1982). Production of superoxide and activity of superoxide dismutase in rabbit epididymal spermatozoa. *Biol Reprod* 27: 1109-1118.

Hornsby PJ and Crivello JF (1983). The role of lipid peroxidation and biological antioxidants in the function of the adrenal cortex. Part 1. A background review. *Mol Cell Endocrinol.* 30: 1-20.

Houglum K, Filip M, Witztum JL and Chojkier M (1990). Malondialdehyde and 4-Hydroxynonal protein adducts in plasma and liver of rats with iron overload. *J Clin Invest* 86:1991-1998.

Hruszkewycz AM (1988). Evidence of mitochondrial DNA damage by lipid peroxidation. *Biochem Biophys Res Commun* 153: 191-7.

Hsu C-Y, Chu C-H, Lin S-C, Yang F-S, Yang T-L *et al.,* (2003). Concomitant hepatocellular adenoma and adenomateous hyperplasia in a patient without cirrhosis. *World J Gastroenterol* 9 (3): 627-630.

Hsu K, Metcalf RA, Sun T *et al.*, (1991). Mutational hotspot in the p53 gene in human hepatocellular carcinomas. *Nature* 350: 427-428.

Hu JJ, Chi CX, Frenkel K, Smith BN, Henfelt JJ *et al.*, (1999). Alpha-tocopherol dietary supplement decreases titers of antibodies against 5-hydroxymethyl-2'-deoxyuridine (HmdU). *Cancer Epidemiol Biomarkers Prev* 8:693-698.

Huang H-Y, Helzlsouer KJ, and Appel LJ (2000). The effects of vitamin C and vitamin E on oxidative DNA damage: results from a randomised controlled trial. *Cancer Epidemiol Biomarkers Prev* 9: 647-652.

Huang H-Y, Appel LJ, Croft KD, Miller III ER, Mori TA and Puddey IB (2002). Effects of vitamin C and vitamin E on *in vivo* lipid peroxidation: results of a randomised control trial. *Am J Clin Nutr* 76:549-55.

Hye-Sung L and Csallany AS (1994). The Influence of Vitamin E and selenium on lipid peroxidation and aldehyde dehydrogenase activity in rat liver and tissue. *Lipids,* Vol. 29, no 5.

Iancu TC, Ward RJ and Peters TJ (1987). Ultrastructural observation in the carbonyl iron-fed rat; an animal model for haemochromatosis. *Virchows Arch B* 53:208-217.

Iancu TC and Shiloh H (1988). Experimental iron overload. Ultra structural studies. *Ann NY Acad Sci* 526: 164-78.

Iancu TC and Shiloh H (1994). Morphological observations in iron overload: an update. *Adv Exp Med Biol* 356: 255-65.

Ibrahim W, Lee US, Yeh CC, Szabo J, Bruckner G *et al.*, (1997). Oxidative stress and antioxidant status in mouse liver: effects of dietary lipid, vitamin E and iron. *J Nutr* 127:1401-1406.

Ichiba M, Maeta Y, Mukoyama T, Saeki T, Yasui S *et al.*, (2003). Expression of 8-hydroxy-2'-deoxyguanosine in chronic liver disease and hepatocellular carcinoma. *Liver International* 23, 338-345.

Imlay JA, Chin SM and Linn S (1988). Toxic DNA damage by hydrogen peroxide through the Fenton reaction *in vivo* and *in vitro*. *Science* 240:640-2.

Inan C, Kilinc K, Kotilogu E, Akman HO, Kilic I *et al,* (1998). Antioxidant therapy of cobalt and Vitamin E in hemosiderosis. *J Lab Clin Med* Aug 132 (2): 157-65.

Irshad M, Chaudhuri PS and Joshi YK (2002). Superoxide dismutase and the total anti-oxidant levels in various forms of liver diseases. *Hepatology Research* 23; 178-184.

Itoh T, Shirakama S, Ishida N, Yamashita Y, Yoshida T *et al.*, (2000). Synthesis of novel ferrocenyl sugars and their antimalarial activities. *Bioorg Med Chem Lett* Aug 7; 10(15): 1657-9.

Jain D, Sarode VR, Abdul-Karim FW, Homer R, Robert ME *et al.*, (2000). Evidence of the neoplastic transformation of von-Meyenburg complexes. *Am J Surg Pathol* 24:1131-1139.

Jazwinska EC, Cullen LM, Busfield F, Pyper WR, Webb SI *et al.*, (1996). Haemochromatosis and HLA-H. *Nat Genet* 14: 249-51.

Jialal I, Fuller CJ and Huet BA (1995). Effect of alpha-tocopherol supplementation on LDL oxidation. *Arterioscler Thromb Vasc Biol.* Feb; 15(2) 190-8.

Johnson PE and Milne DB (1991). Effects of age and sex on copper absorption, turnover and status. *F.A.S.E.B.J* 5: A1076.

Jovanovic SV and Simic MG (2000). Antioxidants in nutrition. *Ann NY Acad Sci,* 899:326-34.

Kadiiska MB, Hanna PM, Hernandez L and Mason RP (1992). *In vivo* evidence of hydroxyl radical formation after acute copper and ascorbic acid intake: electron spin resonance spin-trapping investigations. *Mol Pharmacol* 42: 723-9.

Kadiiska MB, Burkitt MJ, Xiang Q-U and Mason RP (1995). Iron supplementation generates hydroxyl radicals *in vivo*. An ESR spin-trapping study. *J Clin Invest* 96: 1653-7.

Kamp DW, Israbian VA, Preusen SE, Zhang CX and Weitzman SA (1995). Asbestos causes DNA strand breaks in cultured pulmonary epithelial cells: role of iron-catalyzed free radicals. *Lung Cell Mol Physiol* 12: L471-L480.

Kang JO, Jones C and Brothwell B (1998). Toxicity associated with iron overload found in haemochromatosis: possible mechanism in a rat model. *Clin Lab Sci* 11 (6): 350-354.

Kasai H and Nishimura S (1984). DNA damage induced by asbestos in the presence of hydrogen peroxide. *Gann* Oct, 75(10): 841-4.

Kasai H, Chung MH, Jones DS, Inoue H, Ishikawa H *et al.*, (1992). 8-hydroxyguanine, a DNA adduct formed by oxygen radicals: its implication on oxygen radical-involved mutagenesis/ carcinogenesis. *J Toxicol Sci* Feb 16 Suppl 1:95-105.

Kasai H (1997). Analysis of a form of oxidative DNA damage 8-hydroxy-2'-deoxyguanosine, a marker of cellular oxidative stress during carcinogenesis. *Mutat Res* 387:147-163.

Kato J, Kobune M, Kohgo Y, Sugawara N, Hisai H *et al.*, (1996). Hepatic iron deprivation prevents spontaneous development of fulminant hepatitis and liver cancer in Long Evans Cinnamon rats. *J Clin Invest* Aug 15; 98(4): 923-9.

Kato J, Kobune M, Nakamura T, Kuriowa G, Takada K *et al.*, (2001). Normalization of elevated hepatic 8-hydroxy-2'-deoxyguanosine levels in chronic hepatitis C patients by phlebotomy and low iron diet. *Cancer Res* Dec 15: 61(24) 8697-702.

Kew MC, Ray MB, Desmet VJ and Desmyter J (1980). Hepatitis-B surface antigen in tumour tissue and nontumourous liver in black patients with hepatocullular carcinoma. *Br J Cancer* 41:399-406.

Kew MC (1981). Clinical pathologic and etiologic hetrogenecity in hepatocellular carcinoma: evidence from southern Africa. *Hepatology* 1:366-369.

Kew MC (1992). Chronic hepatitis B virus infection and hepatocellular carcinoma. *S Afr J Sci* 88:524.

Kew MC (1994). Epidemiology of hepatocellular Carcinoma. *Viral hepatitis and Liver Diseases* 681-684.

Khan MF, Wu X, Tipnis UR, Ansari GAS and Boor PJ (2002). Protein adducts of malondialdehyde and 4-Hydroxynonenal in livers of iron loaded rats: quantitation and localization. *Toxicology* 173, 193-201.

Kirkova M, Kassabova T and Russanov E (1992). *In vivo* effects of indomethacin. I. Activity of antioxidant enzyme and lipid peroxidation. *Gen Pharmac* 23: 503-507.

Kirkova M, Ivancheva E and Russannov E (1995). Lipid peroxidation and antioxidant enzyme activity in aspirin treated rats. *Gen Pharm* Vol 26 No 3, 613-617.

Kitada T, Seki S, Iwai S, Yamada T, Sakaguchi H and Wakasa K (2001). In situ detection of oxidative DNA damage, 8-hydroxydeoxyguanosine, in chronic human liver disease. *J Hepatology* 35: 613-618.

Klebanoff SJ (1980). Oxygen metabolism and the toxic properties of phagocytes. *Ann Inter Med* 93:480-489.

Klein D, Lichtmannegger J, Heinzman and Summer KH (2000). Dissolution of copper-rich granules in hepatic lysosomes by D-penicillamine prevents the development of fulminant hepatitis in Long Evans cinnamon rats. *J Hepatology* 32:193-201.

Knekt P (1991). Role of vitamin E in the prophylaxis of cancer. *Ann Med* 23:3-12.

Knekt P, Aromaa A, Maatela J, Aran RK, Nikkari T *et al.*, (1991). Vitamin E and Cancer Prevention. *Am J Clin Nutr* 53: 283S-286S.

Knutson MD, Handelman GY and Viteri FE (2000). Methods for measuring ethane and pentane in expired air from rats and humans. *Free Radic Biol Med* 28:514-519.

Kovjazin R, Eldar T, Patya M, Vanichkin A, Lander HM and Novogrodsky A (2003). Ferrocene-induced lymphocyte activation and antitumor activity is mediated by redox-sensitive signalling. *The FASEB J* Vol 17 (3) Mar, 467-9.

Kraus RJ and Ganther HE. Reaction of Cyanide with glutathione peroxidase (1980). *Biochem & Biophys Res Comm* 96(3): 1116-2.

Kristina Elmendorff-Dreikorn, Chauvin C, Slor H, Kutzner J, Batel R *et al.*, (1999). Assessment of DNA damage and repair in human peripheral blood mononuclear cells (PBMC) using a novel unwinding technique. *Cellular and Molecular Biol.* 45(20) 211-218.

Kuchino Y, Mori F, Kasai H, Inoue H, Iwai S *et al.*, (1987). Misreading of DNA templates containing 8-hydroxydeoxyguanosine at the modified base and at adjacent residues. *Nature* 327 :77-9.

Kuchta B, Wulfhekel U and Dullman J (1982). Experimental siderosis of the liver sinusoidal cells in the rat: The role of Kupffer cells for transformation and utilization of colloidal iron. In: Knook DL, Wisse E, eds. Sinusoidal Liver Cells. Amsterdam, Elsevier Biomedical Press, pp 223-230.

Laconi E, Denda A, Rao PM, Rajalakshmi S, Pani P and Sarma DS (1993). Studies on liver tumour promotion in the rat by orotic acid: dose and minimum exposure time required for dietary orotic acid to promote hepatocarcinogenesis. *Carcinogenesis* 14: 1771-1775.

LaRusso NF (1989). Hepatic lysosomes in intracellular digestion and biliary secretion. In: Forte JG, ed. Handbook of physiology. The gastrointestinal system III. Bethesda: *American Physiological Society*, pp. 677-91.

Lemmer ER, Gelderblom WC, Shephard EG, Abel S, Seymour BL *et al.*, (1999). The effects of dietary iron overload on fumonisin B1-induced cancer promotion in the rat liver. *Cancer Lett.* Nov 15; 146(2): 207-15.

Lenton KJ, Therriault H, Cantin AM, Fülöp T, Payette H and Wagner RJ (2000). Direct correlation of glutathione and ascorbate and their dependence on age and season in human lymphocytes. *Am J Clin Nutr* 71:1194-200.

Leone N, Volpes R, Carrera M, Pellicano R, De Paolis P *et al.*, (2000). Hepatocellular carcinoma in a non-cirrhotic liver. Two case reports and literature review. *Panminerva Med* Jun; 42(2): 151-4.

Levin DE, Hollstein M, Christman MF, Schwiers E and Ames BN (1982). A new *Salmonella* tester strain (TA 102) with A-T base pairs at the site of mutation detects oxidative mutagens. *Proc Natl Acad Sci USA* Dec. Vol 79, 7445-7449.

Levine RL, Garland D, Oliver CN, Amici A, Climent I *et al.*, (1990). Determination of carbonyl content in oxidatively modified proteins. *Methods Enzymol* 186:464-478.

Levy G (1967). Effect of bed rest on the distribution and elimination of drugs. *J Pharm Sci* 56:928-29.

Levy JE, Montross LK, and Andrew NC (2000). Genes that modify the haemochromatosis phenotype in mice. *J Clin Invest* 105: 1209-1216.

Libbrecht L, Craninx M, Nevens F, Desmet V and Roskams T (2001). Predictive value of liver cell dysplasia for development of hepatocellular carcinoma in patients with non-cirrhotic and cirrhotic chronic viral hepatitis. *Hepatol* 39: 66-73.

Lieber CS, DeCarli LM, Sorrell MF (1989). Experimental methods of ethanol administration. *Hepatology* 10; 501-10.

Linder MC (1991). Biochemistry of copper. In: Freiden E ed. Biochemistry of elements. New York: Plenum Press, pp. 1-13.

Linder MC and Hazegh-Azam M (1996). Copper biochemistry and molecular biology. *Am J Clin Nutr* 63:797S-811S.

Link G, Pinson A and Hershko C (1994). Ability of the orally effective iron chelators dimethyl- and diethyl-hydroxypyrid-4-one and of deferoxamine to restore sarcolemmal thiolic enzyme activity in iron loaded heart cells. *Blood* 83:2692-7.

Loft S, Astrup A, Buemann B and Poulsen HE (1994). Oxidative DNA damage correlates with oxygen consumption in humans. *FASEB J* 8:534-537.

Lykkesfeldt J, Hagen TM, Vinarsky V and Ames BN (1998). Age-associated decline in ascorbic acid concentration, recycling and biosynthesis in rat hepatocyte - reversal with (R)- α-lipoic acid supplementation. *FASEB J* 12: 1183-9.

Ma Y, Zhang D, Kawabata T, Kiriu T, Toyokuni S *et al.*, (1997). Copper and iron-induced oxidative damage in non-tumour bearing LEC rats. *Pathol Int* Apr 47(4): 203-8.

Mackinnon M, Clayton C, Plummer J, Ahem M, Cmielewski P *et al.*, (1995). Iron overload facilitates hepatic fibrosis in the rat alcohol/low dose carbon tetrachloride model. *Hepatology* 21: 1083-1088.

MacLennan R, Da Costa J, Day NE, Law CH, Ng YK and Shanmugaratnam K (1977). Risk factors for lung cancer in Singapore Chinese, a population with high female incidence rates. *Int J Cancer* 20:854-860.

MacPhail AP, Derman DP, Bothwell TH, Torrance JD, Charlton RW *et al.*, (1979a). Serum ferritin concentrations in black miners. *S Afr Med J* 55: 758.

MacPhail AP, Simon MO, Torrance JD, Bothwell TH and Isaacson C (1979b). Changing patterns of dietary iron overload in black South Africans. *Am J Clin Nutr* 32: 1272.

Madinaveitia JL (1965). Ferrocenes as haematinics. *Bri J Pharmacol* Apr vol 24, 352-359.

Mallory MA and Kowdley KV (2001). Hereditary haemochromatosis and cancer risk: more fuel to the fire? *Gastroenterology* Vol.121, No. 5, 1253-1254.

Mandishona E, MacPhail AP, Gordeuk VR, Kedda MA, Paterson AC *et al.*, (1998). Dietary iron overload as a risk factor for hepatocellular carcinoma in Black Africans. *Hepatology* 27:1563.

Marangon K, Devaraj S, Tirosh O, Packer L and Jialal I (1999). Comparison of the effect of alpha-lipoic acid and alpha-tocopherol supplementation on measurements of oxidative stress. *Free Radic Biol Med* 27:1114-1121.

Marcus AJ (1995). Aspirin as prophylaxis against colorectal cancer. *The New Eng J Med* Sept Vol 333 (10): 656-8.

Marklund SL (1984). Extracellular superoxide dismutase in human tissues and human cell lines. *J Clin Invest* 74: 1398-1403.

Marmunti M and Catalá A (1998). Non-enzymatic lipid peroxidation of rat liver nuclei and chromatin fractions. *The Int J Biochem & cell Biol* 30: 967-72.

Maron DM and Ames BN (1983). Revised methods for the *Salmonella* mutagenicity test. *Mutat Research* May; 113 (3-4): 173 –215.

Marrogi AJ, Khan MA, van Gijssel GH, Welsh JA, Rahim H *et al.*, (2001). Oxidative stress and p53 mutations in the carcinogenesis of iron overload-associated hepatocellular carcinoma. *J Natl Cancer Inst* 93: 1652-1655.

Masuda R, Yoshida MC, Sasaki M, Dempo K and Mori M (1988). High susceptibility to hepatocellular carcinoma development in LEC rats with hereditary hepatitis. *Jpn J Cancer Res* 79:828-35.

McCay PB (1985). Vitamin E: Interactions with free radicals and ascorbate. *Annu Rev Nutr* 5: 323-340.

McCord JM and Fridovich I (1978). The biology and pathology of oxygen radicals. *Ann Intern Med* 89:122-127.

McKie AT, Marciani P, Rolfs A, Brennan K, Wehr K *et al.*, (2000). A novel duodenal iron-regulated transporter, IREG1, implicated in the basolateral transfer of iron to the circulation. *Mol Cell* 5(2): 299-309.

Meagher EA, Barry OP, Burke A, Lucey MR, Lawson *et al.*, (1999). Alcohol-induced generation of lipid peroxidation products in humans. *J Clin Invest* 104:805-813.

Meagher EA, Barry OP, Lawson JA, Rokach J and FitzGerald GA (2001). Effects of vitamin E on lipid peroxidation in healthy persons. *JAMA* March 7, Vol 285, No.9.

Mehta SW and Eikam R (1989). Effect of estrogen on serum and tissue levels of copper and zinc. *Adv Exp Med Biol.* 258:155-62.

Meister A. Glutathione-ascorbate acid antioxidant system in animals. *J Biol Chem* 1994; 269:9397-400.

Mello Filho AC and Meneghini R (1984). *In vivo* formation of single strand breaks in DNA by hydrogen peroxide is mediated by the Haber-Weiss reaction. *Biochem Biophys Acta* 781:56-63.

Miller SA, Dykes DD and Polesky HF (1988). A simple salting out procedure for extracting DNA from human nucleated cells. *Nucleic Acid Research* Feb 11; 16(3):1215.

Miller DM, Buettner GR and Aust SD (1990). Transition metals as catalyst of autooxidation reactions. *Free Rad Biol & Med* 8: 95-108.

Miller NJ, Rice-Evans C, Davis MJ, Gopinathan V and Milner A (1993). A novel method for measuring antioxidant capacity and its application to monitoring the antioxidant status of premature neonates. *Clin Sci* 84: 407-412.

Moody CS and Hassan HM (1982). Mutagenicity of oxygen free radicals. *Proc Natl Acad Sci USA* 79: 2855-2859.

Morcos M, Dubois S, Bralet MP, Belghiti J, Degott C and Terris B (2001). Primary liver carcinoma in genetic haemochromatosis reveals a broad histologic spectrum. *Am J Clin Path* Nov 116(5) 738-43.

Morrow DJ, Hill EK, Burk RF, Nammour TM, Badr KF and Roberts LJ (1990). A series of prostaglandin F2-like compounds are produced *in vivo* in humans by a non-cyclooxygenase, free radical-catalyzed mechanism. *Proc Natl Acad Sci USA* 87:9383-9387.

Morrow JD and Roberts LJ (1996). The isoprostanes: current knowledge and direction for future research. *Biochemical Pharmacology* 51: 1-9.

Moyo VM, Makunike R, Gangaidzo IT, Gordeuk VR, McLaren CE *et al.*, (1998). African iron overload and hepatocellular carcinoma (HA-7-0-080). *Eur J Haematol* 60:28-34.

Mure K and Rossman TG (2001). Reduction of spontaneous mutagenesis in mismatch repair-deficient and proficient cells by dietary antioxidants. *Mutat Res* Sep 1; 480-481: 85-95.

Murrell GAC, Francis MJO and Bromley L (1990). Modulation of fibroblast proliferation by oxygen free radicals. *Biochem J* 265:659-65.

Myers BM, Prendergast FG, Holman R, Kuntz SM and La Rosso NF (1991). Alterations in the structure, physicochemical properties, and pH of hepatocyte lysosomes in experimental iron overload. *J Clin Invest* 88:1207-15.

Nair J, Carmichael P, Fernando R, Philips D, Strain A and Bartsch H (1998). Lipid peroxidation-induced etheno-DNA adducts in the liver of patients with the genetic metal storage disorders Wilson's disease and primary haemochromatosis. *Epidemiol Biomarkers Prev* 7: 435-440.

Nakae D, Akai H, Kishida H, Kusuoka O, Tsutsumi M and Konishi Y (2000). Age and organ dependent spontaneous generation of nuclear 8-hydroxydeoxyguanosine in male Fischer 344 rats. *Lab Invest* 80:249-261.

Nakashima T, Okuda K, Kojiro M, Jimi A, Yamaguchi R *et al.*, (1983). Pathology of hepatocellular carcinoma in Japan: 232 consecutive cases autopsied in ten years. *Cancer* 51: 863-877.

Nakayama T, Kodama M and Nagata C (1984). Free radical formation in DNA by lipid peroxidation. *Agric Biol Chem* 48: 571-572.

National Research Council (1989). Committee on Dietary Allowances: Recommended Dietary Allowances. 10th revised ed. Washington, DC, *National Academy of Sciences*.

Navasumrit P, H-Ward T, Dodd NJF and O'Connor JO (2000). Ethanol-induced free radicals and hepatic DNA strand breaks are prevented *in vivo* by antioxidants: effects of acute and chronic ethanol exposure. *Carcinogenesis* vol.21 no. 1, 93-99.

Niederau C, Fischer R, Sonnenberg A, Stremmel W, Trampisch HJ and Stromeyer MD (1985). Survival and causes of death in cirrhotic and non-cirrhotic patients with primary haemochromatosis. *N Engl J Med* 313:1256-1262.

Niedernhofer LJ, Daniels JS, Rouzer CA, Greene RE and Marnett LJ (2003). Malondialdehyde, a product of lipid peroxidation, is mutagenic in human cells. *J Biol Chem*. May 29.

Nielsen P and Heinrich HC (1993). Metabolism of iron from (3,3,5-trimethylhexanoyl) ferocene in rats. A dietary model for severe iron overload. *Biochemical Pharmacology* Vol 45 No 2, 385-391.

Nielsen P, Heinelt S and Dullman J (1993). Chronic feeding of carbonyl iron and TMH-ferrocene in rats. Comparison of two iron-loaded models with different iron absorption. *Comp Biochem Physiol* Vol. 106C, No 2, 429-436.

Niemela O, Pakkila S, Brunt E, Janney C and Bacon B (1999). Hepatic lipid peroxidation in hereditary haemochromatosis and alcoholic liver injury. *J Lab Clin Med* 133:451-460.

Niki E (1987). Interaction of ascorbic and α-tocopherol. In: Burns, JJ, Rivers JM, Machlin LJ, eds. The third conference on vitamin C. Ann NY Acad Sci Vol. 498. New York: Academy of Sciences; pp 186-199.

Niki E (1990). Free radical initiators as source of water- or lipid soluble peroxyl radicals. In: Packer L and Glazer AN, eds. *Methods in Enzymology* vol 186, New York: Academic Press, pp. 100-108.

Niki E (1996). α-Tocopherol. In: Cadenas E and Packer, eds. Handbook of Antioxidants. USA: Marcel Dekker Inc., pp. 3-25.

Nourooz-Zadeh J, Tajaddini-Sarma DI and Wolff SP (1994). Measurement of plasma hydroperoxide concentration by the ferrous oxidation - xylenol assay in conjuction with triphenylphosphine. *Analytical Biochemistry* 220, 403-409.

Nourooz-Zadeh J, Gopaul NK, Barrow S, Mallet AI and Anggard EE (1995). Analysis of F_2-isoprostanes as indicators of non-enzymatic lipid peroxidation *in vivo* by gas chromatography-mass spectroscopy: development of a solid phase extraction procedure. *J Chromatogr Biomed Appl* 19; 667: 199-208.

Oates PS, Jeffry GP, Basciain KA, Thomas C and Morgan EH (2000). Iron excretion in iron-overloaded rats following the change from an iron-overload to an iron-deficient diet. *J Gastroenterology Hepatol* Jun; 15(6): 665-75.

O' Connell MJ, Ward RJ, Baum H and Peters TJ (1985). The role of iron in ferritin and haemosiderin mediated lipid peroxidation in lysosomes. *Biochem J* 229:135-9.

O' Connell M, Halliwell B, Moorhouse CP, Aruoma OI, Baum H and Peters TJ (1986). Formation of hydroxyl radicals in the presence of ferritin and haemosiderin. Is haemosiderin formation a biological protective mechanism? *Biochem J* 234:727-31.

Ohhira M, Ohtake T, Matsumoto A, Saito H, Ikuta K *et al.*, (1998). Immunohistochemical detection of 4-hydroxy-2-nonenal-modified-protein adducts in human alcoholic liver diseases. *Alcohol Clin Exp Res.* May; 22(3 Suppl): 145S-149S.

Okada S, Hamazaki S, Ebina Y (1983). Nephrotoxicity and induction of the renal adenocarcinoma by ferric-nitrilotriacetate (Fe-NTA) in rats. In Urushizaki I, Aisen P, Listowsky I, Drysdale JW, eds. Structure and function of iron storage and transport proteins. New York: Elsevier, pp. 473-8.

Okuda K (1992). Hepatocellular carcinoma: a recent progress. *Hepatology* 15: 948-963.

Olaso E and Friedman SL (1998). Molecular regulation of hepatic fibrogenesis. *J Hepatol* 29: 836-47.

Olynyk J, Hall P, Reed W, Williams P, Kerr R and Mackinnon M (1995). A long-term study of the interaction between iron and alcohol in an animal model of iron overload. *J Hepatol* 22; 671-676.

Omenn GS, Goodman GE, Thornquest MD, Balmes J, Cullen MR *et al.*, (1996). Risk factors for lung cancer and for intervention effects in CARET, the beta-carotene and retinol efficiency trial. *N Engl J Med* 334: 1550-1559.

Omer B, Pernur Oner, Kemay Baysal and Hikmet OZ (1990). Effect of acetylsalicylic acid in liver plasma membrane. Ca^{2+} ATPase activity. *Pol J Pharmacol Pharm* 42: 441-44.

Owen CA Jr (1973). Effects of iron on copper metabolism and copper on iron metabolism in rats. *Am J Physiol* Vol 224, No 3, Mar 224 (3): 682-6.

Owen CA (1982). Biochemical aspects of copper. Copper proteins, ceruloplasmin and copper protein binding. NJ: Noyes Park Ridge, pp. 9-17, 75-111, 128-176.

Paashuis-Lew YR and Heddle JA (1998). Spontaneous mutation during fetal development and post-natal growth. *Mutagenesis* 13:613-617.

Paglia DE and Valentine WN (1967). Studies on the quantitative and qualitative characterization of the erythrocyte glutathione peroxidase. *J Lab Clin Med* Jul 70:158-169.

Paradis V, Kollinger M, Fabre M, Holstege A, Poynard T and Bedossa P. (1997a). In situ detection of lipid-peroxidation by-products in chronic liver diseases. *Hepatology* 26:135-142.

Paradis V, Mathurin P, Kollinger M, Imbert-Bismut F, Charlotte F *et al.*, (1997b). In situ detection of lipid determination in chronic hepatitis C: correlation with pathological features. *J Clin Pathol* 50:401-406.

Park CH, Bacon BR, Brittenham GM and Tavill AS (1987). Pathology of dietary carbonyl iron overload in rats. *Lab Invest* 57, 555-563.

Park J-W and Floyd RA (1992). Lipid peroxidation products mediate the formation of 8-hydroxydeoxyguanosine in DNA. *Free Rad Biol Med* 12:245-50.

Parthasarathy S and Rankin S (1992). The role of oxidized low density lipoprotein in atherogenesis. *Progress In Lipid Research* 31: 127-143.

Paterson AC, Kew MC, Herman AAB, Becker PJ, Hodkinson J and Isaacson C (1985). Liver morphology in southern African blacks with hepatocelular carcinoma. A study within the urban environment. *Hepatology* 5:72.

Paterson AC, Kew MC, Dusheiko GM and Isaacson C (1989). Liver cell dysplasia accompanying hepatocellular carcinoma in southern Africa. *J Hepatol* 8: 241-248.

Pellise M, Gonzalez-Abraldes J, Navasa M, Miquel M and Bruguera M (2001). Hepatocellular carcinoma in a patient with hereditary haemochromatosis without cirrhosis. *Gastroenterol Hepatol* Mar; 24(3): 132-4.

Pena MMO, Lee J and Thiele DJ (1999). A delicate balance: Homeostatic control of copper uptake and distribution. *J Nutr* 129:1251-1260.

Peters TJ and Seymour CA (1976). Acid hydrolase activities and lysosomal integrity in liver biopsies from patients with iron overload. *Clin Sci Mol Med* 50: 75-8.

Peters TJ, O' Connel MJ and Ward RJ (1985). Role of free radical mediated lipid peroxidation in the pathogenesis of hepatic damage by lysosomal disruption. In: Poli G, Cheeseman KH, Dianzani MU, Slater TF, eds. Free radicals in liver injury. Oxford: IRL Press, pp 107-15.

Petkai A (1980). Radiation carcinogenesis from a membrane perspective. In: Free radicals - medicine and biology. *Acta Physiol Scand.* Suppl 492:81-90.

Peto R, Doll R, Buckley JD and Sporn MB (1981). Can dietary beta-carotene materially reduce human cancer rates? *Cancer* 290: 201-208.

Pietrangelo A, Rocchi E, Schiaffonati L, Ventura E and Cairo G (1990). Liver gene expression during chronic dietary iron overload in rats. *Hepatology* 11:798-804.

Pietrangelo A, Borella F, Casalgrandi G, Montosi G, Ceccarelli D *et al.*, (1995b). Antioxidant activity of silybin *in vivo* during long-term iron overload in rats. *Gastroenterology* 109:1941-9.

Pietrangelo A, Gualdi R, Casalgrandi G, Montosi G and Ventura E (1995a). Molecular and cellular aspects of iron-induced cirrhosis in rodents. *J Clin Invest* 1995; 95:1824-31.

Pietrangelo A (1996). Metals, oxidative stress and hepatic fibrogenesis. *Semin Liver Dis* 16:13-30.

Pigeon C, Turlin B, Iancu TC, Leroyer P, Le Lan J *et al.*, (1999). Carbonyl iron supplementation induces hepatocyte nuclear changes in BALB/CJ male mice. *J Hepatology* 30: 926-934.

Plummer JL, Mackinnon M, Cmielewski PL, Williams P, Ahern MJ *et al.*, (1997). Dose related effects of dietary iron supplementation in producing hepatic iron overload in rats. *J Gastroenter and Hepatol* 12, 839-84.

Pogribny IP, Poirier LA and James SJ (1995). Differential sensitivity to loss of cytosine methyl groups within the hepatic p53 gene of folate/methyl deficient rats. *Carcinogenesis* 16: 2863-2867.

Pool-Zobel BL, Bub A, Muller H, Wollowski I and Rechkemmer G (1997). Consumption of vegetables reduce genetic damage in humans: first results of a human intervention trial with carotenoid-rich foods. *Carcinogenesis* 18:1847-1850.

Pottathil R, Chandrabose KA, Chatrecasas P and Lang DJ (1981). Establishment of the interferon medicated antiviral state: possible role of superoxide dismutase. *Proc Natl Acad Sci* USA 78: 3343-3347.

Powell JW and Kerr J (1975). The pathology of the liver in hae mochromatosis. *Pathobiol Annu* 317-337.

Powell LW (2002). Hereditary haemochromatosis and iron overload diseases. *J Gastroenter and Hepatol* 17:S191-S195.

Preddki PF and Sarkar B (1992). Effect of replacement of "zinc finger" zinc on oestrogen receptor DNA interactions. *J Biol Chem* 267: 5842-5846.

Pryor WA (1982). Free radical biology: xenobiotics, cancer and aging. *Ann NY Acad Sci.* 293:1-22.

Radak Z, Pucsuk J, Boros S, Josfai L and Taylor AW (2000). Changes in urinary 8OHdG levels of super-marathon runners during a four-day race period. Life Sci *Mar 24; 66 (18)1763-7.*

Radhi JM and Loewy J (2000). Hepatocellular adenomatosis associated with hereditary haemochromatosis. *Postgrad Med J* Feb; 76(892): 100-2.

Rafter GW (1994). Plasma thiols, copper and rheumatoid arthritis. *Med Hypothesis* July 43 (1): 59-61.

Rainsford KD, Schweitzer A and Brune K (1983). Distribution of the acetyl compared with the acetyl moiety of acetylsalicylic acid. *Biochem Pharmacol.* 32: 1301-308.

Ramos CL, Pou S, Britigan BE, Cohen MS and Rosen GM (1992). Spin trapping evidence for myeloperoxidase-dependent hydroxyl radical formation by human neutrophils and monocytes. *J Biol Chem* 267: 8307-8312.

Ramos CL, Pou S and Rosen GM (1995). Effects of antiinflamatory drugs on myoloperoxidase-dependent hydroxyl radical generation by human neutrophils. *Biochem Pharmacol* 19:1079-1084.

Rang HP and Dale MM (1987). Drugs used to suppress inflammatory and immune reactions. In: Pharmacology. Edinburg: Churchill Livingstone, pp. 204-213.

Rao J and Jagadeesen V (1996). Lipid peroxidation and activities of antioxidant enzymes in iron deficiency and effect of carcinogen feeding. *Free Radical Biology and Medicine* 21, 103-108.

Reeves PG, Nielsen FH and Fahey GC Jr. (1993). AIN-93 Purified Diets for Laboratory Rodents: Final Report of the American Institute of Nutrition Ad Hoc Committee on the Reformulation of the AIN-76A Rodent Diet. *J Nutr* 123: 1939-1951.

Reilly M, Delanty N, Lawson JA and FitzGerald GA (1996). Modulation of oxidant stress *in vivo* in chronic cigarette smokers. *Circulation* 94: 19-25.

Reilly MP, Barry P, Lawson *et al.*, (1997). Urinary 8-epiPGF2α an index of oxidative stress *in vivo*. *Fibrinolysis and Roteolysis* 11:81-84.

Reinberg A, Clench J, Ghata J, Halberg F, Abulker C *et al.* (1975). Circadian rhythms in the urinary excretion of salicylate (chronopharmacokinetics) in healthy adults. *CR Seances Acad Sci [III].* 280:1697-18.

Richmond R, Halliwell B, Chauhan J and Darbre A (1981). Superoxide-dependent formation of hydroxyl radicals: Detection of hydroxyl radicals by the hydroxylation of aromatic compounds. *Anal Biochem* 118: 328-335.

Richter C, Azzi A, Weser U and Wendel A (1977). The action of Cu-(tyrosine)2 as a superoxide dismutase model of hepatic microsomaldemethylation. In: Michelson AM, McCord J, Fridovich I, eds. Superoxide and Superoxide Dismutases. NY: Academic Press, pp 375-385.

Rivers JM (1989). Safety of high-level vitamin C ingestion. *Int J Vitam Nutr Res* Suppl 30:95-102.

Roberts FD, Charalambous P, Fletcher L, Powell LW and Halliday JW (1993). Effect of chronic iron overload on procollagen gene expression. *Hepatol* 18:950-5.

Roberts LJ and Morrow JD (1997). The generation and actions of isoprostanes. *Biochim Biophys Acta* 1345:121-135.

Rojas LK, McDowell LR, Cousins RJ, Martin FG, Wilkinson NS *et al.*, (1996). Interactions of different organic and inorganic zinc and copper sources fed rats. *J Trace Elements in Med and Biol* 10:139-144.

Rossi F, Bianca VD and de Tongi P (1985). Mechanisms and functions of the oxygen radicals producing respiration and phagocytes. *Comp Immuno and Micro Infect Dis* 8: 187-204.

Rotstein J, Sarma DSR and Farber E (1986). Sequential alterations in growth control and cell dynamics of rat hepatocytes in early precancerous steps in hepatocarcinogenesis. *Cancer Res* 46:2377-2385.

Sagone AL Jr, Greenwald J, Kraut F, Bianchine J and Singh D (1983). Glucose: a role as a free radical scavenger in biological systems. *J Lab Clin Med.* 101: 97-104.

Sakurai M (1978). Liver cell dysplasia and hepatitis B surface and core antigens in cirrhosis and hepatocellular carcinoma of autopsy cases. *Acta Pathol Jap* 28:705-719.

Salganik R. Paper presented at: American Society for Cell Biology Annual Meeting; Dec.15, 1999: Washington DC.

Slater TF (1984). Review article: Free-radical mechanisms of tissue injury. *Biochem J* Aug 15; 222(1): 1-15.

Samuelsson B, Granström E, Green K, Hamberg M and Hammarström S (1975). Prostaglandins. *Annu Rev Biochem* 44:669-695.

Santella RM (1999). Immunological methods for detection of carcinogen-DNA damage in humans. *Cancer Epidemiol. Biomarkers Prev.* 8:733-739.

Sato M and Gitlin JD (1991). Mechanisms of copper incorporation during the biosynthesis of human ceruloplamin. *J Biol Chem* 266: 5128-5134.

Sato K, Niki E and Shimasaki H (1990). Free radical-mediated chain oxidation of low density lipoprotein and its synergistic inhibition by vitamin E and vitamin C. *Arch Biochem Biophy* 279:402-405.

Schreck R, Albermann KAJ and Baeuerle PA (1992). Nuclear factor κB: An oxidative stress response transcription factor of eukaryotic cells. *Free Rad Res Comm* 17:221-237.

Seki S, Kitada T, Yamada T, Sakaguchi H, Nakatani K and Wakasa K (2002). In-situ detection of lipid peroxidation and oxidative DNA damage in non-alcoholic fatty liver diseases. *J Hepatology 37: 56-62.*

Selden C, Seymour CA and Peters TJ (1980). Activities of some free-radical scavenging enzymes and glutathione concentrations in human and rat liver and their relationship to the pathogenesis of tissue damage in iron overload. *Clin Sci* 58:211-219.

Seymour CA and Peters TJ (1978). Organelle pathology in primary and secondary haemochromatosis with special reference to lysosomal changes. *Br J Haematol* 40: 239-59.

Shibutani S, Takeshita M and Grollman AP (1991). Insertion of specific bases during DNA synthesis past the oxidation-damaged base 8-oxodG. *Nature* 349:431-434.

Shimoda R, Nagashima M, Sakamoto M, Yamaguchi N, Hirohashi S *et al.* (1994). Increased formation of oxidative DNA damage 8-hydroxydeoxyguanosine, in human livers with chronic hepatitis. *Cancer Res* 54:3171-3172.

Smith PK, Gleason HL, Stoll CG and Ogorzalek S (1946). Studies on pharmacology of salicylates. *J Pharmacol Exp Ther.* 87: 237-55.

Sochaski MA, Bartfay WJ, Thorpe SR., Baynes JW, Bartfay E *et al.*, (2002). Lipid peroxidation and protein modification of a mouse model of chronic iron overload. *Metabolism* May 51 (5): 645-51.

Sodergren E, Cederberg J, Basu S and Vessby B (2000). Vitamin E supplementation decreases basal levels of F(2)-isoprostanes and prostaglandins F(2alpha) in rats. *J Nutr* 130:10-14.

Sodergren E, Cederberg J, Vessby B and Basu S (2001). Vitamin E reduces lipid peroxidation in experimental hepatotoxicity in rats. *Eur J Nutr* 40:10-16.

Sokol RJ, Devereaux MW, O'Brien K, Khandwala RA and Loehr JP (1993). Abnormal hepatic mitochondrial respiration and cytochrome c oxidase activity in rats with long-term copper overload. *Gastroenterol* 105:178-187.

Solt DB and Farber E (1976). New principle for the analysis of chemical carcinogenesis. *Nature* 263:702-703.

Solt DB, Cayama E, Sarma DS and Farber E (1980). Persistence of resistant putative preneoplastic hepatocytes induced by N-nitrosodiethylamine or *N*-methyl-*N*-nitrosourea. *Cancer Res* 40: 1112-1118.

Soltys K, Dikdan G and Koneru B (2001). Oxidative stress in fatty livers of obese Zucker rats: rapid amelioration and improved tolerance to warm ischemia with tocopherol. *Hepatol* Jul, 34(1) 13-18.

Spector AA and Yosek MA (1985). Membrane lipid composition and cellular function. *J Lipid Res* 26:1015-1035.

Stadtman ER and Beriett BS (1998). Reactive-oxygen mediated protein oxidation in aging and disease. *Drug Metab Rev* 30:225-243.

Stadtman TC (1990). Selenium Biochemistry. *Ann Rev Biochem* 59:111.

Stål P, Glaumann H and Hultcrantz R (1990). Liver cell damage and lysosomal iron storage in patients with idiopathic haemochromatosis. A light and electron microscopic study. *J Hepatol* 11: 172-80.

Stål P, Hultcrantz R, Möller L and Eriksson LC (1995). The effect of dietary iron on initiation and promotion in chemical carcinogenesis. *Hepatol* 21:521-528.

Stål P, Wang G-S, Olsson JM and Eriksson LC (1999). Effects of dietary iron overload on progression in chemical hepatocarcinogenesis. *Liver* 19:326-334.

Sternlieb I (1980). Copper and the liver. *Gastroenterology* 78:1615-1628.

Strachan AS (1929). Haemochromatosis and Haemochromatosis in southern African Natives with a Comment on the Etiology of Haemochromatosis. MD Thesis. Glasgow, UK, University of Glasgow.

Strain JJ (1994). Newer aspects of micronutrients in chronic disease: copper. *Proc of the Nutr Soc* 53: 583-598.

Suresh MV, Lal JJ, Kumar S and Indira M (1999). Ascorbic acid metabolism in rats and guinea pigs after the administration of ethanol. *Comparative Biochem and Physio* Part C 124; 175-179.

Takahashi M, Tsuchiya J, Niki E and Urano S. (1988). Action of vitamin E as an antioxidant in phospholipid liposomal membranes as studied by spin label technique. *J Nutr Sci Vitaminol* 34:25–34.

Takahashi M, Tsuchiya J and Niki E (1989). Scavenging of radicals by vitamin E in the membranes as studied by spin labeling. *J Am Chem Soc* 111: 6350–6353.

Takashi T, Takanobu K, Yoshihiro H *et al.*, (1998). Primary changes in liver damage by Aspirin in rats. *Acta Paed Japonica* 40, 593-596.

Tappel AL (1973). Lipid peroxidation damage to cell components. *Fed Proc* 32: 1870-1874.

Tector AJ, Olynyk JK, Britton RS, Janney CG, O'Neill R and Bacon BR (1995). Hepatic mitochondrial oxidative metabolism and lipid peroxidation in iron loaded rats fed ethanol. *J Lab Clin Med* 126: 597-602.

Terada T and Nakanuma Y (1989a). Iron-negative foci in siderotic macroregenerative nodules in human cirrhotic livers. *Arch Pathol Lab Med* 113:916-20.

Terada T and Nakanuma Y (1989b). Survey of iron accumulative macroregenerative nodules in cirrhotic livers. *Hepathol* 10:851-4.

Thompson H, Kennedy K, Witt M and Juzefyk J (1991). Effect of dietary iron deficiency or excess on the induction of mammary carcinogenesis by 1-methyl-1-nitrosurea. *Carcinogenesis* 12: 111-114.

Thompson HJ, Heimendinger J, Haegele A, Sedlacek SM, Gillette C *et al.*, (1999). Effect of increased vegetable and fruit consumption on markers of oxidative cellular damage. *Carcinogenesis* Vol. 20, No. 12, Dec 2261-2266.

Tomoda T, Takeda K, Kurashige T, Enzan H and Miyahara M (1992). Experimental study on Reye's syndrome: Inhibitory effect of interferon α on acetylsalicylate induced injury to rat liver mitochondria. *Metabolism* 41:887-92.

Torrance JD and Bothwell TH (1968). A simple technique for measuring storage iron concentrations in formalinized liver samples. *S. Afr J Med* 33,9-11.

Toyokuni S and Sagripanti J-L (1996). Association between 8-hydroxy-2'-deoxyguanosine formation and DNA strand breaks mediated by copper and iron. *Free Rad Biol & Med* Vol 20, No 6, 859-864.

Toyokuni S, Tanaka T, Hattori Y, Nishiyama Y, Yoshida *et al.* (1997). Quantitative immunohistochemical determination of 8-hydroxy-2'-deoxyguanosine by monoclonal N45.1: its application to ferric nitrilotriacetate-induced renal carcinogenesis model. *Lab Invest* Mar 76(3): 365-74.

Toyokuni S, Iwasa Y, Kondo S, Tanaka T, Ochi H, *et al.*, (1999). Intranuclear distribution of 8-hydroxy-2'-deoxyguanosine. An immunohistochemical study. *J Histochem Cytochem* Jun: 47(6):833-6.

Tsuchiya T and Levy G (1972). Biotransformation of salicylic acid to its acetyl and phenolic glucuronides in man. *J Pharm Sci* 61:800-801.

Tsunoo C, Harwood TR, Arak S and Yokoo H (1987). Cytoskeletal alterations leading to Mallory body formation in livers of mice fed 3,5-diethoxycarbonyl-1,4-dihydro-collidine. *J Hepatol* 5:85-97.

Uchida K and Stadtman (1992). Modification of histidine residues in proteins by reaction with 4-hydroxynonenal. *Proc Natl Acad Sci USA* May 15; 89(10): 4544-8.

Valerio LG Jr and Petersen DR (1998). Formation of liver microsomal MDA-protein adducts in mice with chronic iron overload. *Toxicol Lett* Sep 1; 98 (1-2): 31-9.

Valerio LG Jr and Petersen DR (2000). Characterization of hepatic iron overload following dietary administration of dicyclopentadienyl iron (ferrocene) to mice: cellular, biochemical and molecular aspects. *Exp and Mol Path* 68, 1-12.

Van den Berg R, van Vliet T, Broekmans WMR, Cnubben NHP, Vaes WHJ *et al.*, (2001). A vegetable/ fruit concentrate with high antioxidant capacity has no effect on biomarkers of antioxidant status in male smokers. *J Nutr* 131:1714-1722.

Vautier G, Bomford A, Portmann B, Metivier E, Williams R and Ryder S (1999). p53 mutations in British patients with hepatocellular carcinoma: clustering in genetic haemochromatosis. *Gastroenterology* 117: 154-160.

Venkatraman JT, Chandrase B, Kim JD and Fernandes G (1994). Effects of n-3 and n-6 fatty acids on the activities and expression of hepatic antioxidant enzymes in autoimmune-prone NZB*NZW F1 mice. *Lipids* 29: 561-568.

Vijg J and van Steeg H. (1998). Transgenic assays for mutation and cancer: current status and future perspective. *Mutat Res* 400:337-354.

Vistness AI, Henrikson T, Nicolaissen B and Armstrong D (1983). Free radicals and aging. Elecron spin resonance studies on neuronal lipopigments and cell grown *in vitro*. *Mech Aging Develop* 22: 335-345.

Vorce RL and Goodman JL (1989). Altered methylation of *ras* oncogenes in benzidine-induced B6C3F1 mouse liver tumours. *Toxicol Appl Pharmacol* 100: 398-410.

Vulpe CD, Kuo YM, Murphy TC, Cowley L, Askwill C *et al.*, (1999). Hephaestin, a ceruplasmin homologue implicated in intestinal iron transport, is defective in the *sla* mouse. *Nat Genet* Feb 21(2): 195-9.

Waeg G, Demsity G and Esterbauer H (1996). Monoclonal antibodies for detection of 4-hydroxynonenal modified proteins. *Free Rad Res* 25: 149-159.

Walker ARP and Arvidsson UB (1953). Iron 'overload' in the South African Bantu. *Trans Roy Soc Trop Med Hyg* 47:536.

Waller RL, Glende EA Jr. and Recknagel RO (1983). Carbon tetrachloride and bromotrichloromethane toxicity. Dual role of covalent binding of metabolic cleavage products and lipid peroxidation in depression of microsomal calcium sequestration. *Biochem Pharmacol* 32:1613-7.

Walles SAS and Erixson K (1984). Single strand-breaks in DNA of various organs of mice induced by methyl methanesulfoxide determined by the alkaline unwinding technique. *Carcinogenesis* 5: 319-22.

Wang XD and Russell RM (1999). Procarcinogenic and anticarcinogenic effects of beta-carotene. *Nutr Rev* 57:263-272.

Ward RJ, Florence AL, Baldwin D, Abiaka C, Roland F *et al.*, (1991). Biochemical and biophysical investigations of the ferrocene-iron-loaded rat. An animal model of primary haemochromatosis. *Eur J Biochem* 202, 405-410.

Watanabe S, Okita K, Harada T *et al.*, (1983). Morphologic studies of the liver cell dysplasia. *Cancer* 51: 2197-2205.

Wayner DD, Burton GW, Ingold KU and Locke S (1985). Quantitative measurement of the total peroxyl radical-trapping antioxidant capacity of human blood plasma by controlled peroxidation. The important contribution made by plasma proteins. *FEBS Lett* 187:33-37.

Weber P, Bendich A and Schalch (1996). Vitamin C and Human health - a review of recent data relevant to human requirement. *Int J Vit and Nutr Res* 66, 19-30.

Weiss SJ (1989). Tissue destruction by neutrophils. *N Eng J Med* 320: 365-376.

Wheeler MD, Katuna M, Smutney OM, Froh M, Dikalova A *et al.*, (2001). Comparison of the effect of adenoviral delivery of three superoxide dismutase genes against hepatic ischemia-reperfusion injury. *Hum Gene Ther* 12:2167-2177.

Williams G and Yamamoto R (1972). Absence of stainable iron from preneoplastic and neoplastic lesions in rat liver with 8-hydroxyquinoline-induced siderosis. *Natl Cancer Inst* 49:685-692.

William G (1989). The significance of chemically-induced hepatocellular altered foci in rat liver and application to carcinogen detection. *Toxicol Pathol* 17:663-672.

Wilson JD (1991). Disorders of vitamins: Deficiency, excess and errors of metabolism. In: Petersdorf RG, Adams RD, Braunwald E, *et al.*, eds. Harrison's Principle of Internal Medicine. 12th ed. New York: McGraw-Hill, pp 434-445.

Windorfer A, Kanitzky D, Gasteiger U and Stehr K (1978). Investigations on salicylate protein binding in newborns and infants. *Eur J Pediatr.* 127:163-72.

Winterbourn CC and Buss IH (1999). Protein carbonyl measurement by enzyme-linked immunosorbent assay. *Methods Enzymol* 300:106-111.

Wolff SP (1994). Ferrous ion oxidation in presence of ferric ion indicator xylenol orange for measurement of hydroperoxides. *Methods in Enzymol* 233:182-288.

Wong SH, Knight JA, Hopfer SM, Zaharia Q, Leach CN Jr., and Sunderman FW Jr. (1987). Lipoperoxides in plasma as measured by liquid-chromatographic separation of malondialdehyde-thiobarbituric acid adducts. *Clin Chem* 33:214-220.

Wood ML, Dizdaroglu M, Gajewski E and Essigmann JM (1990). Mechanistic studies of ionizing radiation and oxidative mutagenesis: genetic effects of a single 8-hydroxyguanosine (7-hydro-8-oxoguanine) residue inserted at a unique site in a viral genome. *Biochem* 29:7024-32.

Wosilait WD (1976). Theoretical analysis of the binding of salicylate to human serum albumin. *Eur J Clin Pharmacol* 9:285-90.

Yamada M, Awai M and Okigaki T (1990). Rapid *in vitro* transformation system for liver epithelial cells by iron chelate, Fe-NTA. *Cytotechnology* 3:149-56.

Yasa HM, Kacmaz M, Ozturk SH and Durak I (1999). Antioxidant status of erythrocytes from patients with cirrhosis. *Hepato-Gastro* 46:2460-2463.

Yaziji N, Martin L, Hillon P, Favre JP, Henninger JF, *et al.*, (1997). Cholangiocarcinoma arising from biliary micro-haratomas in a man suffering from haemochromatosis. *Ann Pathol* 17:346-349.

Younes M and Siegers CP (1984). Interrelation between lipid peroxidation and other hepatotoxic events. *Biochem Pharmacol* 33: 2001-2003.

Young IS, Trouton TG, Torney JJ, McMaster D, Callender ME and Trimble E (1994). Antioxidant status and lipid peroxidation in hereditary haemochromatosis. *Free Rad Biol Med* Vol. 16. No 3. 393-397.

Zolch Z and Ginter E (1995). Moderate alcohol consumption and vitamin C status in the guinea pig and the rat. *Physiol Res* 44:173-8.

Zs-Nagy I and Floyd RA (1984). Hyroxyl free radical reactions with amino acids and protein studies by electron spin resonance spectroscopy and spin trapping. *Biochem Biophys Acta* 790: 238-250.